
BRIGHTON AND SUSSEX MEDICAL SCHOOL

FRANCESCA CAVICCHIOLI

**Epigenetic regulation of amino acids metabolic genes
defines targets of synthetic lethality in breast cancer**

A thesis submitted in partial fulfilment of the requirements of the University of
Brighton and the University of Sussex for the degree of Doctor of Philosophy.

June 2014

Abstract

Breast cancer is the second most common cause of death after lung cancer in developing countries. There is a great need to expand the range of biomarkers to identify patients that can be treated using new therapies. Epigenetic silencing of amino acid regulatory genes have been postulated as a predictive biomarker in breast cancer and treatment based on modulating amino acid levels have been shown to be effective in other cancers. In this study, I have examined how the amino acid regulatory genes for glutamine (Glutamine synthetase, *GLUL*) and arginine (Arginino-succinate synthetase, *ASSI*) synthesis are silenced via methylation in a panel of breast cancer cell lines.

Using methylation array, bisulphite sequencing, pyrosequencing and chromatin immuno-precipitation, it was determined that *GLUL* is silenced by DNA methylation and loss of histone acetylation. Methylated breast cancer cells not expressing *GLUL* were found to be highly sensitive to glutamine depletion. In a cohort of primary breast cancer patients, 68% of patients were determined to be methylated and showed a trend towards worse survival compared to non-methylated patients. Further *in vitro* work confirmed that glutamine depletion was sufficient to induce tumour cell death.

Using a similar method for *ASSI*, no cell line in our panel was found to be methylated. However, in a cohort of breast cancer patients, 21% was determined to be methylated. When *ASSI* was silenced, depletion therapy using Arginine Deiminase (ADI-PEG20) was sufficient to induce cell death.

Silencing of amino acid regulatory genes via epigenetic modifications causes the tumours to be auxotrophic for the amino acid. Depletion of that amino acid is sufficient to induce cell death. Therefore, *GLUL* and *ASS1* have been identified as therapeutic targets for synthetic lethality in breast cancer.

Table of Contents

1	INTRODUCTION.....	18
1.1	Introduction to Breast cancer	18
1.1.1	Breast cancer incidence and mortality	18
1.1.2	Risks factors	21
1.1.3	Breast cancer staging system.....	24
1.1.4	Breast cancer development.....	25
1.1.5	Breast cancer classification	28
1.1.5.1	Atypical hyperplasia	28
1.1.5.2	<i>In situ</i> carcinoma.....	28
1.1.5.3	Invasive carcinoma	29
1.1.6	Molecular profiling	32
1.1.7	Breast cancer screening, diagnosis and treatment	34
1.1.7.1	Breast cancer screening.....	34
1.1.7.2	Breast cancer diagnosis	34
1.1.7.3	Breast cancer treatment	35
1.1.8	New biomarker for breast cancer.....	37
1.2	Epigenetics and cancer.....	39
1.2.1	DNA methylation.....	39
1.2.2	Histone modifications	43
1.2.3	Chromatin structure.....	44
1.2.4	Alteration in DNA methylation as a biomarker.....	49
1.3	Synthetic lethality	51
1.4	Cancer metabolism.....	53
2	MATERIALS AND METHODS	58
2.1	Work with immortalised cell lines	58
2.1.1	Cell lines and culture conditions.....	58
2.1.2	Glutamine deprivation.....	60
2.1.3	Survival analysis	60
2.1.4	Autophagy analysis	61
2.1.5	Chloroquine treatment.....	61
2.1.6	Arginine deprivation	62
2.1.7	Arginine Deiminase (ADI-PEG20) administration	62
2.1.8	De-methylation and pro-acetylation treatment	63
2.1.9	shRNA transfection.....	63
2.1.10	Plasmid transfection	67
2.2	DNA and RNA extraction and analysis	69
2.2.1	DNA extraction from formalin-fixed paraffin-embedded (FFPE) tissues and cell lines ...	69
2.2.2	DNA bisulphite modification	70
2.2.3	450k Methylation array	72
2.2.4	Bisulphite sequencing	72
2.2.5	Pyrosequencing analysis.....	77
2.2.6	Chromatin Immuno-Precipitation (ChIP).....	80
2.3	RNA and protein extraction and analysis	83
2.3.1	RNA extraction from cell lines	83
2.3.2	Gene expression analysis.....	83

2.3.3	Protein analysis	84
2.3.3.1	SDS-PAGE electro-blotting in reducing conditions	84
2.3.3.2	Native gel separation.....	88
2.4	Clinical samples	89
2.4.1	Cuneo's cohort.....	89
2.4.2	Tissue Micro-Array.....	89
2.4.3	<i>In silico</i> dataset	89
2.5	Statistical analysis	91
2.5.1	Survival analysis	91
2.5.2	<i>In vitro</i> data statistical analysis.....	92
3	GLUTAMINE SYNTHETASE.....	93
3.1	Introduction.....	93
3.2	Epigenetic regulation.....	96
3.2.1	Methylation analysis	96
3.2.1.1	450k methylation array	96
3.2.1.2	Bisulphite sequencing validation.....	100
3.2.1.3	Pyrosequencing analysis	102
3.2.2	Expression analysis	104
3.2.2.1	<i>GLUL</i> expression level in breast cancer cell lines.....	104
3.2.2.2	Glutamine synthetase protein (GS) level in breast cancer cell lines	107
3.2.2.3	Correlation between methylation gene expression and protein level	111
3.2.3	De-methylation effects on <i>GLUL</i> expression	113
3.2.4	Histone acetylation analysis	118
3.3	Functional analysis of Glutamine synthetase	123
3.3.1	Glutamine deprivation.....	123
3.3.2	Autophagy induction.....	128
3.3.2.1	Autophagy response to gln deprivation	128
3.3.2.2	Autophagy repression effects on glutamine deprivation.....	131
3.3.3	<i>GLUL</i> re-expression	135
3.4	Methylation analysis of <i>GLUL</i> in primary breast cancer tissues.....	137
3.4.1	Primary tissue cohort.....	137
3.4.1.1	Methylation analysis	137
3.4.1.2	Tissue Micro-Array analysis	143
3.4.1.3	TMA and methylation combined analysis	146
3.4.2	TCGA dataset	149
3.5	Discussion	151
3.5.1	<i>GLUL</i> promoter region is epigenetically silenced in breast cancer cell lines	152
3.5.2	<i>GLUL</i> methylation influences response to glutamine deprivation treatment	156
3.5.3	Glutamine synthetase epigenetic regulation and breast cancer patients	161
4	ARGININO-SUCCINATE SYNTHETASE	165
4.1	Introduction.....	165
4.2	Epigenetic regulation.....	167
4.2.1	Methylation analysis	167
4.2.1.1	450k methylation array	167
4.2.1.2	Pyrosequencing analysis	170
4.2.2	Gene expression analysis.....	172

4.3	Functional analysis of <i>ASS1</i>	175
4.3.1	Arginine deprivation	177
4.3.2	ADI-PEG20 administration	180
4.4	Methylation analysis of <i>ASS1</i> in primary breast cancer tissues	183
4.4.1	Cuneo's cohort	183
4.4.2	TCGA dataset	188
4.5	Discussion	192
4.5.1	<i>ASS1</i> is not methylated in the breast cancer cell line panel	193
4.5.2	<i>ASS1</i> hyper-methylation relevance in breast cancer	195
5	FINAL REMARKS	197
6	REFERENCES	199
7	SUPPLEMENTARY TABLES AND FIGURES	228

List of figures

Figure 1-1. Breast cancer incidence and mortality.....	20
Figure 1-2. Breast anatomy.	26
Figure 1-3. Breast cancer development.....	27
Figure 1-4. Histological images of breast cancer.....	31
Figure 1-5. DNA methylation pattern in normal and cancer cells.	42
Figure 1-6. Chromatin structure.....	48
Figure 1-7. Metabolic network.....	57
Figure 2-1. pSilencer plasmid.	66
Figure 2-2. pcDNA3.1 (+) plasmid map.	68
Figure 2-3. Bisulphite conversion reaction.	71
Figure 2-4. <i>GLUL</i> CpG island.....	74
Figure 2-5. pGEM®-T vector map and reference points.	76
Figure 2-6. Pyrograms from methylated and unmethylated DNA.	79
Figure 3-1. Methylation array analysis for Glutamine synthetase.	99
Figure 3-2. <i>GLUL</i> CpG Island bisulphite sequencing.....	101
Figure 3-3. Screening of cell lines for <i>GLUL</i> by pyrosequencing.	103
Figure 3-4. <i>GLUL</i> expression level analysis.....	106
Figure 3-5. Glutamine synthetase protein analysis.	109
Figure 3-6. 3D scatter blot of <i>GLUL</i> methylation and expression levels.....	112
Figure 3-7. <i>GLUL</i> re-expression analysis.	117
Figure 3-8. Histone acetylation analysis by ChIP.....	122
Figure 3-9. Effects of Gln deprivation on breast cancer cell lines.....	127
Figure 3-10. Induction of autophagy in response to gln deprivation.	130

Figure 3-11. Effect of Chloroquine administration on survival and autophagy induction during gln deprivation.....	134
Figure 3-12. <i>GLUL</i> re-expression and gln deprivation.....	136
Figure 3-13. Pyrosequencing analysis of <i>GLUL</i> promoter region of primary tissue cohort.....	139
Figure 3-14. Methylation analysis of normal and tumour samples.....	140
Figure 3-15. Overall survival of primary tissue cohort based on methylation status.	142
Figure 3-16. Primary tissue cohort survival based on TMA analysis.....	145
Figure 3-17. Survival analysis on primary tissue cohort based on TMA and methylation status.....	148
Figure 3-18. Array analysis of the methylation status of the TCGA dataset.	150
Figure 3-19. <i>GLUL</i> modulation in low glutamine conditions.....	160
Figure 4-1. Results of 450k Methylation array for Arginino-succinate synthetase.	169
Figure 4-2. Pyrosequencing analysis of <i>ASS1</i> in breast cancer cell lines.	171
Figure 4-3. Analysis of Arginino-succinate synthetase expression in breast cancer cell lines.	174
Figure 4-4. <i>ASS1</i> silencing by shRNA in Hs 578T and SKBR3.....	176
Figure 4-5. Effects of <i>ASS1</i> knock-down on arginine deprivation in Hs 578T.....	178
Figure 4-6. Effects of <i>ASS1</i> knock-down on arginine deprivation in SKBR3.	179
Figure 4-7. IC ₅₀ analysis in shRNA transfected Hs 578T.....	181
Figure 4-8. IC ₅₀ analysis in shRNA transfected SKBR3.	182
Figure 4-9. Pyrosequencing analysis of <i>ASS1</i> promoter region in primary breast cancer cohort.....	184
Figure 4-10. Methylation analysis of normal and tumour samples.....	185

Figure 4-11. Survival of primary tissue cohort based on methylation status.....	187
Figure 4-12. 450k Methylation array analysis of TCGA's dataset.	189
Figure 4-13. TCGA cohort survival based on methylation status.....	191
Figure 7-1. <i>GLUL</i> methylation array in a bigger breast cancer cell line panel.	228
Figure 7-2. Correlation of mRNA, protein and methylation level for Glutamine synthetase.	229
Figure 7-3. Enrichment of acetylated Histone3 and Histone4 across each tested gene promoter region in various cell lines.....	232
Figure 7-4. Modulation of <i>GLUL</i> during glutamine deprivation treatment.	233
Figure 7-5. Percentage of samples in each subset of primary breast cancer tissues.	234
Figure 7-6. Liner regression between Arginino-succinate mRNA and protein level.	235
Figure 7-7. Example images of SDS-PAGE electro-blotting analysis of Glutamine synthetase.	236
Figure 7-8. Example images of SDS-PAGE analysis of Arginino-succinate synthetase.	237

List of Tables

Table 2-1. Panel of Breast cancer cell lines.	59
Table 2-2. <i>ASS1</i> shRNA constructs.....	65
Table 2-3. Bisulphite sequencing PCR primer sets.....	75
Table 2-4. Pyrosequencing primer sets.	78
Table 2-5. ChIP qPCR primer set.	82
Table 2-6. Antibodies used in SDS-PAGE electro-blotting.....	87
Table 3-1. Methylation status of the <i>GLUL</i> promoter region after the epigenetic treatments.	115
Table 3-2. Clinical characteristics of hypo- and hyper-methylated primary breast cancer tissue samples.	141
Table 3-3. Clinical characteristics of GS-positive and GS-negative primary breast cancer tissue samples.	144
Table 3-4. Clinical characteristics of hypo-methylated, hyper-methylated GS-positive and hyper-methylated GS-negative primary breast cancer tissue samples.	147
Table 4-1. Clinical characteristics of hypo- and hyper-methylated primary breast cancer tissue samples.	186
Table 4-2. Clinical characteristics of hypo- and hyper-methylated in the TCGA dataset.....	190

List of Abbreviations

2D:	two dimensional
3D:	three dimensional
3'UTR:	untranslated region at 3' of the mRNA or trailer sequence
5'UTR:	untranslated region at 5' of the mRNA or leader sequence
ADI-PEG20:	Arginine Deiminase, ADI, with polyethylene glycol of 20 kilo-Daltons, PEG 20
AI:	Aromatase inhibitor
AKT:	Alpha serine/threonine-protein kinase
arg:	L-arginine
ASS1:	Arginino-succinate synthetase
ATM:	Ataxia telangiectasia mutated
ATP:	Adenosine triphosphate
aza:	5-aza-2'-deoxycytidine
bp:	base pair in a nucleotide sequence
BRCA1/2:	Breast cancer gene1 and 2
BSA:	bovine serum albumin
BTN:	biotinylated
C.I.:	Confidence Interval
cDNA:	complementary DNA
ChIP:	Chromatin immuno-precipitation
citr:	L-citrulline
c-Myc:	Myelocytomatosis Viral Oncogene Homolog
CQ:	Chloroquine

Ct:	threshold cycle
ct:	control
DCIS:	Ductal carcinoma in situ
DIC:	Ductal invasive carcinoma
DMEM:	Dulbecco`s modification of Eagle`s medium
DMSO:	Dimethyl Sulfoxide
DNA:	Deoxyribonucleic acid
DNA:	deoxyribonucleic acid
DNMTs:	DNA Methyl-transferases
ECL:	Enhanced chemiluminescence
EDTA:	Ethylene-diaminetetra-acetic acid
EGFR:	Epidermal growth factor receptor 1
EMT:	Epithelial-mesenchymal transition
eNOS:	endothelial Nitric oxide synthases
ER:	Oestrogen receptor
F/U:	follow up
FBS:	Foetal Bovine Serum
FFPE:	Formaldehyde Fixed-Paraffin Embedded Tissue
FISH:	Fluorescence in situ hybridization
FOXO:	Forkhead box O
FOXO3A:	Forkhead box O3A
GAPDH:	Glyceraldehyde 3-phosphate dehydrogenase
GATA3:	GATA binding protein 3
gln:	L-glutamine or glutamine
GLS1:	Glutaminase 1

GLUL:	Glutamine synthetase gene
GS:	Glutamine synthetase protein
H&E:	Haematoxylin and Eosin stain
H.R.:	Hazard Ratio
h:	hour
H1:	Histone 1
H2A:	Histone 2A
H2B:	Histone 2B
H3:	Histone 3
H4:	Histone 4
H5:	Histone 5
HATs:	Histone acetyl-transferases
HBA2:	Haemoglobin A2
HDACs:	Histone deacetylases
HEPES:	4-(2-hydroxyethyl)-1-piperazineethanesulfonic acid
Her2:	Epidermal growth factor receptor 2
HIF1 α :	Hypoxia inducible factor 1 alpha
HKII:	Hexokinase 2
IC50:	half maximal inhibitory concentration
IHC:	Immune-histochemistry
IPTG:	Isopropyl- β -D-1-thiogalactopyranoside
IUPAC:	International Union of Pure and Applied Chemistry
kb:	kilo-base pair in a nucleotide sequence
LCIS:	Lobular carcinoma in situ
LIC:	Lobular invasive carcinoma

LSD:	Lysine-Specific histone Demethylase
MDB:	Methyl binding protein
MeCP2:	methyl CpG binding protein 2
MGMT:	O6-methylguanine DNA methyltransferase
min:	min
mRNA:	messenger RNA
mTOR:	Mammalian target of Rapamycin
MTT:	3-[4,5-dimethylthiazol-2-yl]-2,5 diphenyl tetrazolium bromide
NH ₄ :	ammonium
NO:	nitric oxide
PARP:	Adenosine diphosphate (ADP) ribose polymerase
PBS:	Phosphate buffered saline
PCR:	Polymerase chain reaction
PCR:	polymerase chain reaction
PI3K:	Phosphatidyl-inositide 3-kinases
PR:	Progesterone receptor
PTEN:	Phosphatase and tensin homolog
PVDF:	polyvinylidene difluoride
qPCR:	real-time PCR
R:	correlation coefficient
RFTA:	radio-frequency thermal ablation
RNA:	Ribonucleic acid
RNA:	ribonucleic acid
ROC:	Receiver Operating Characteristic
RPLP0:	ribosomal protein large P0

RPMI:	Roswell Park Memorial Institute medium
SDS:	Sodium Dodecyl Sulphate
sec:	sec
shRNA:	short hairpin RNA
siRNA:	short interfering RNA
SNPs:	Single nucleotide polymorphisms
T:	temperature
TBS-T:	Tris-Buffered Saline and Tween 20
TCA cycle:	Tricarboxylic acid cycle
TCGA:	The Cancer Genome Atlas
TDLU:	terminal ductal lobular unit
TE:	Tris-EDTA
TKI:	Tyrosine Kinase inhibitor
TMA:	Tissue Micro-array
TNB:	Triple negative breast cancer
TNM:	Tumour-nodal-metastatic staging
tsa:	Trichostatin A
TSS:	Transcriptional start site
VEC:	empty vector/plasmid
X-Gal:	5-bromo-4-chloro-3-indolyl-X-D-galactopyranoside

Acknowledgments

First and foremost I want to thank my supervisor, Prof. Peter Schmid, and his great team, in particular Dr Alice Shia and PhD Karen O’Leary. It has been an honour to exchange ideas with them, even if it mostly consisted of never-ending discussions with no final agreement. We share the joy and enthusiasm for research, especially when nothing worked, becoming really good friend.

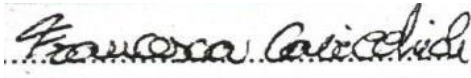
Lastly, I would like to thank my family for always being there for me.

Thank you.

Candidate's declaration

I declare that the research contained in this thesis, unless otherwise formally indicated within the text, is the original work of the author. The thesis has not been previously submitted to this or any other university for a degree, and does not incorporate any material already submitted for a degree.

Signed

A handwritten signature in black ink, reading "Francesca Cavicchioli", written over a dotted line.

(Francesca Cavicchioli)

Dated 5th June 2014

1 Introduction

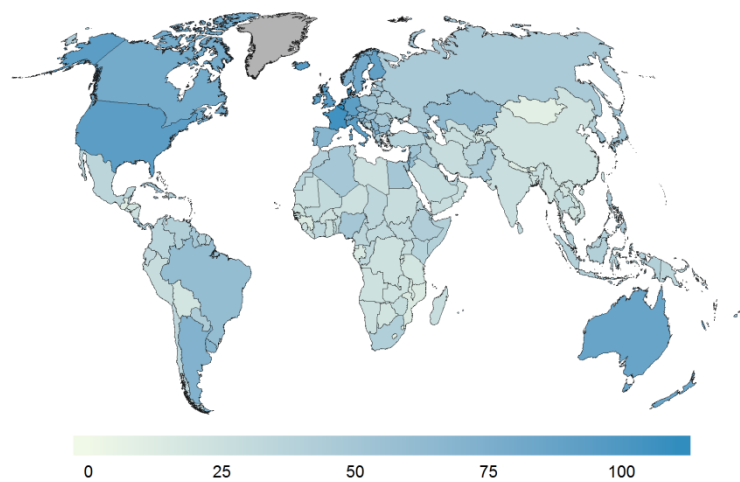
1.1 Introduction to Breast cancer

1.1.1 Breast cancer incidence and mortality

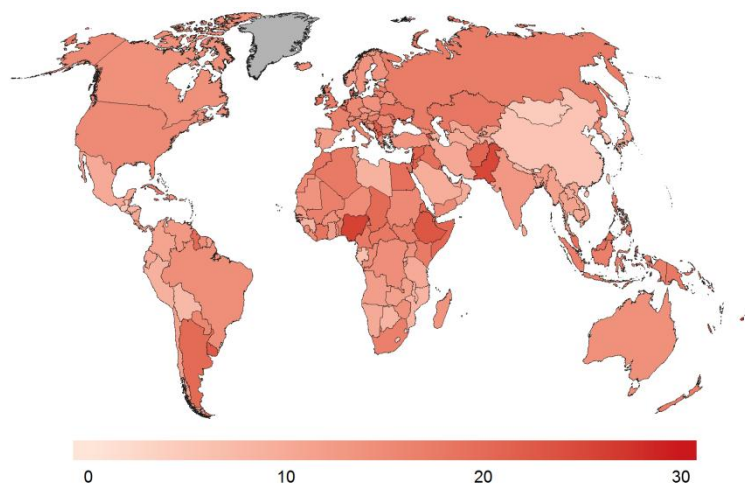
Breast cancer is the second most common type of cancer in the world accounting for 25% of all diagnosed neoplasms in 2012. 1.677 million cases have been diagnosed worldwide in 2012 making it the most frequent in the world female population (International Agency for Research on Cancer (IARC) 2014). Because of increased life expectancy, industrialization and screening programmes, breast cancer incidence remained higher in Western than developing countries (Figure 1-1 A, C). In 2012, there were over 70 per 100,000 women in developed countries compared to below 40 per 100,000 women in developing nations diagnosed with breast cancer (Figure 1-1 C) (International Agency for Research on Cancer (IARC) 2014).

Breast cancer is also the second most common cause of death after lung cancer in developed countries and the leading cause of death in developing countries (Alberg and Sigh 2001, International Agency for Research on Cancer (IARC) 2014). Breast cancer mortality in 2012 was 1.6 fold higher in Eastern than Western countries, with 0.324 and 0.198 million deaths per 100,000 respectively (Figure 1-1 B, C). These differences in mortality can be attributed to life expectancy, screening programmes that detect breast cancer at earlier stages and treatment availability in developing countries (International Agency for Research on Cancer (IARC) 2014).

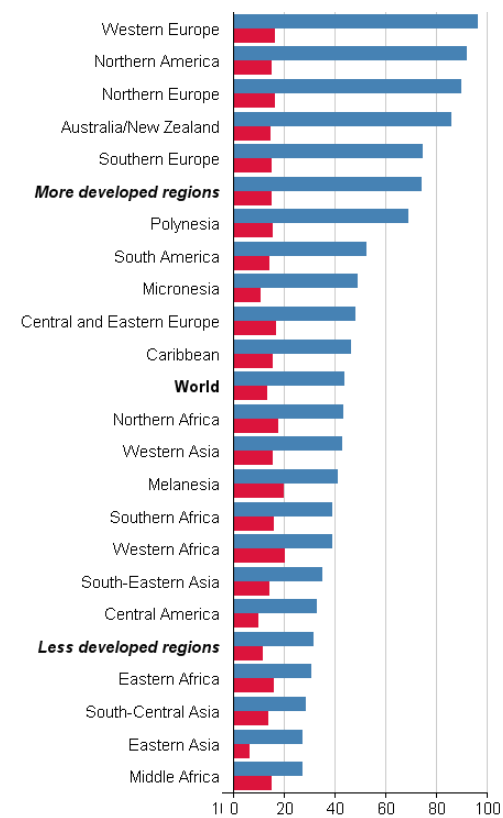
A)



B)



C)



GLOBOCAN 2012 (IARC)

■ Incidence
■ Mortality

Figure 1-1. Breast cancer incidence and mortality.

Colour-coded world-map showing estimates A) incidence and B) mortality of breast cancer. Incidence and mortality for breast cancer are shown together as bar charts (C) for each country for males and females. Increase in colour intensity in A) and B) represents an increase in incidence and mortality rate respectively in a sample of 100,000 people. The data have been age-standardised (International Agency for Research on Cancer (IARC) 2014).

1.1.2 Risk factors

Worldwide, every woman has an estimated one in eight probability of developing breast cancer in her lifetime (Lawvere et al. 2004, Ries et al. 2009). As with all types of neoplasm, breast cancer presents a multifactorial aetiology and there is a wide range of risk factors influencing the probability of developing the disease. Those include age, reproductive life-style, endogenous and exogenous hormones, diet, alcohol, smoking, obesity, physical activity, previous breast disease, genetics and family history, and epigenetic modifications on the genome (discussed later).

The predominant risk factor for breast cancer is age and the stage of the disease at diagnosis. Women over the age of 65 have a six fold greater risk (1 in 13) of developing breast cancer than those below 65 (1 in 78) (Alberg and Sigh 2001, Cancer Research 2012). The nature of the neoplasia also significantly influences mortality and risk of recurrence. It has been shown that 5-year survival rates are directly correlated with stage and advancement of the disease. Mortality rate is increased 12 fold in the most advanced pathological stages of the disease, with 60% survival when localised and 2% when un-staged (Ries et al. 2009). At the same time, women diagnosed and successfully treated for a non-invasive breast cancer have double the risk of having a second primary breast cancer or developing an invasive cancer in their life (Cancer Research 2012).

Analysis on breast cancer incidence from the 1990s demonstrates how reproductive life-style influences breast cancer development. Having fewer children, late pregnancies and abstinence from breast feeding have been associated with increased risk of breast cancer (Tavassoli and Devilee 2003, Cancer Research 2012). Those

data partly explained the lower incidence of this tumour in developing countries where women are more likely to have multiple children, starting at an early age and breastfeed. However, confounding factors, such as diet and lifestyle differences in developed and developing nations, also influence this data (Tavassoli and Devilee 2003, Cancer Research 2012).

There is an approximate increased risk of 7-12% associated with habitual drinkers (10g of alcohol intake a day) and 10-20% for smokers (Tavassoli and Devilee 2003, Cancer Research 2012). Many of the studies on alcohol and smoking have inconclusive leading to the conclusion that there is no causal relationship with breast cancer. A lot of studies have been focused on the role of diet in breast cancer incidence; most of them inconclusive. However, a clear association has been found with fat intake (13% increased risk), and with soy-based food mimic of oestrogen (15% reduced risk) (Cancer Research 2012).

Following on from this, overweight and obese women have a 10-20% higher risk of developing breast cancer, increasing to 30% for women already in menopause (Tavassoli and Devilee 2003, Cancer Research 2012). Conversely, frequent physical activity in women correlates with a reduction in developing breast cancer of 20% and 40% when already in menopause (Tavassoli and Devilee 2003, Cancer Research 2012).

Hormones, either endogenous or exogenous, play an important role in breast development and carcinogenesis. There is a trend of increased risk in women with higher levels of sex hormones, in particular oestrogen and progesterone (Tavassoli

and Devilee 2003, Cancer Research 2012). There is a clear correlation between high levels of insulin in the blood and breast cancer incidence in post-menopausal women. This effect of insulinemia has been proposed to be mediated by an increase in oestradiol production from adipocytes due to insulin stimulation (Tavassoli and Devilee 2003, Cancer Research 2012). At the same time, women using oral contraceptives or under menopausal hormonal replacement treatment have an increased risk of 81% and 66% respectively of developing the disease compared to women who have never used such compounds. The risk is temporary, returning to levels of never-users after 10 or 5 years from the last treatment for oral contraceptive and menopausal replacement therapy respectively (Tavassoli and Devilee 2003, Cancer Research 2012).

A hereditary component of breast cancer is well recognised: a woman with a first-degree relative, male or female, diagnosed with the neoplasia has double the risk of developing the same pathology. It is important to note that only 15% of women with breast cancer have a family history and of these only 85% will develop the disease (Tavassoli and Devilee 2003, Cancer Research 2012). 20% of familial breast cancer share a germ-line mutation on Breast Cancer genes 1 (BRCA1) or 2 (BRCA2) (Tavassoli and Devilee 2003, Cancer Research 2012). These genes are involved in homologous recombination, a key mechanism in DNA double break repair (Jasin 2002). Deletion or insertions of a few nucleotides and single-base substitutions are the most common mutations found in BRCA1 and BRCA2, generating a premature stop-codon and a non-functioning protein (Ewald et al. 2009). The absence of a functioning protein increases the amount of genome instability and the inefficient

DNA double-break repair promotes tumour progression (Jasin 2002, Ewald et al. 2009).

1.1.3 Breast cancer staging system

To determine the best therapy for each patient, it is necessary to have the tumour staged and classified. Clinical staging is based on the patient's first examination prior to any treatment. This includes the patient's physical status, imaging results from mammography, biopsy and/or surgical examination. The pathological staging is established based on clinical data and histological examination results from the primary tissue after surgery. The examinations from these determine tumour grade: grade 1 or lower (cancer cells are really similar to the epithelial cells they are derived from), grade 2 or intermediate (cancer cells look abnormal but they are slow growing), and grade 3 or higher (cancer cells look very different from the tissues they are derived from and are also fast growing) (Tavassoli and Devilee 2003, Kataja and Castiglione 2009).

The most widely used system is the TNM staging, where three parameters are analysed to describe the tumour: T, N and M. The tumours are assessed based on the Haematoxylin and Eosin (H&E) stained primary tissue sections. The T value represents the tumour status: tumour size, presence of invasion, oedema and inflammation. The score spans from T0 with no presence of primary tissues, to T4 when invasion is present. The N value corresponds to the lymph node status: N0 when no cancer cells are found in the regional lymph nodes to N3 when metastases are present not only in the regional, but also in the distal lymph nodes. Finally the M grade defines the metastatic status, with M0 if there are no metastases to M1 when distant metastases are present (Tavassoli and Devilee 2003).

1.1.4 Breast cancer development

Normal breast is comprised of a system of epithelial tubules, called ducts, connecting the secretory units, lobules, to the nipple, where the milk is secreted. The secretory units in each lobule are called acini. The lobules and the distal end of the duct form the terminal duct lobular unit (TDLU). Both tubules and lobules are formed by a single layer of epithelial cells (luminal cells), forming the lumen, surrounded by a layer of myo-epithelial or basal cells. The double layer structure is encircled by a basement membrane, formed of laminin and collagen. The whole system is surrounded by a layer of connective tissue and embedded into adipose tissues (Figure 1-2) (Young and Heath 2005).

Breast cancer development follows a series of steps involving the TDLU, ending in invasive breast carcinoma in the worst case scenario. The model, first described by Wellings and Jensen (Wellings and Jensen 1976), implies that breast cancer starts as a benign epithelial lesion with no atypical proliferation, but characterised by abnormal structure of the duct or lobule. By atypical proliferation this evolves into atypical hyperplasia in either duct or lobular section of the TDLU. Through accumulation of genetic and epigenetic defects in the genome, the hyperplasia grows and proliferates to become an early stage *in situ* carcinoma (Figure 1-3). The invasive breast cancer eventually derives from the *in situ* carcinoma by genome alteration, epithelial-mesenchymal transition and accumulation of cellular abnormalities driven by micro-environmental stimuli (Vargo-Gongola and Rosen 2007, Allred et al. 2008, Butcher et al. 2009, Cichon et al. 2010, Naus and Laird 2010).

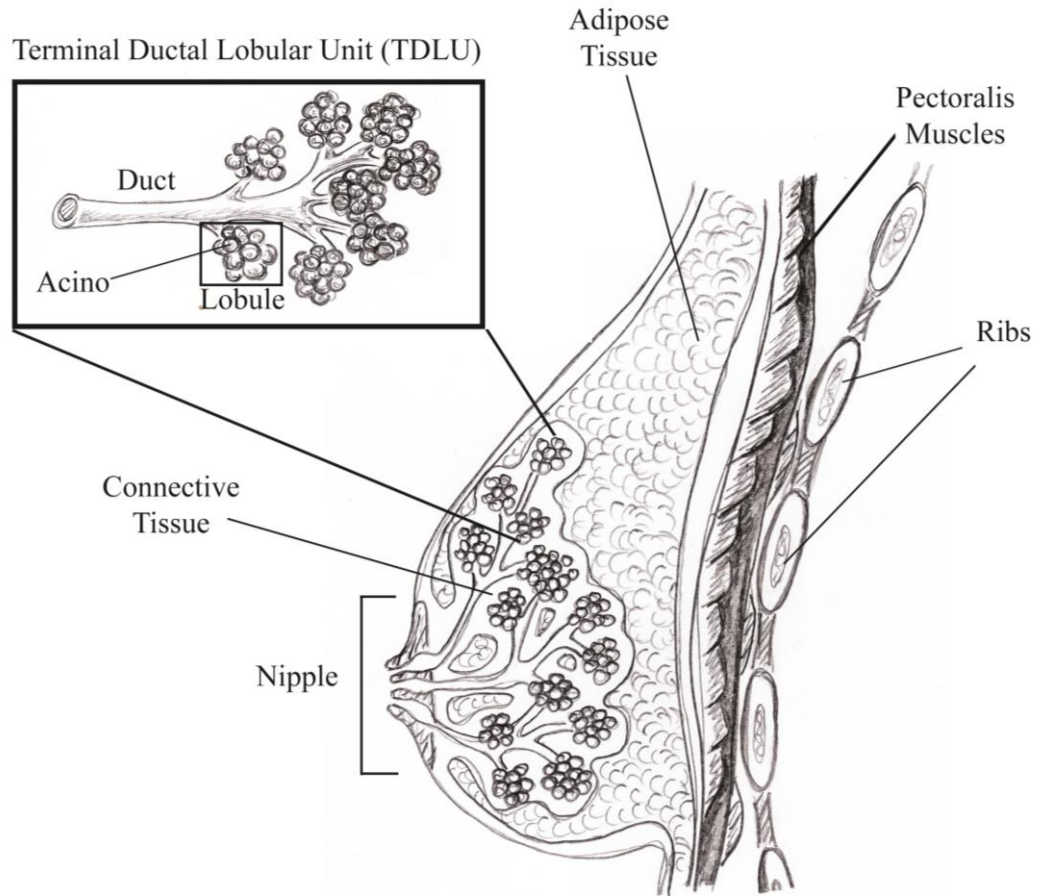


Figure 1-2. Breast anatomy.

Normal breast is comprised of a system of ducts connecting the lobules to the nipple. Lobules are formed by a group of acini, where the milk is produced. The lobules and the distal end of the duct represent the terminal duct lobular unit (TDLU). The whole system is surrounded by a layer of connective tissue and embedded by adipose tissues (Adapted from Young and Heath 2005).

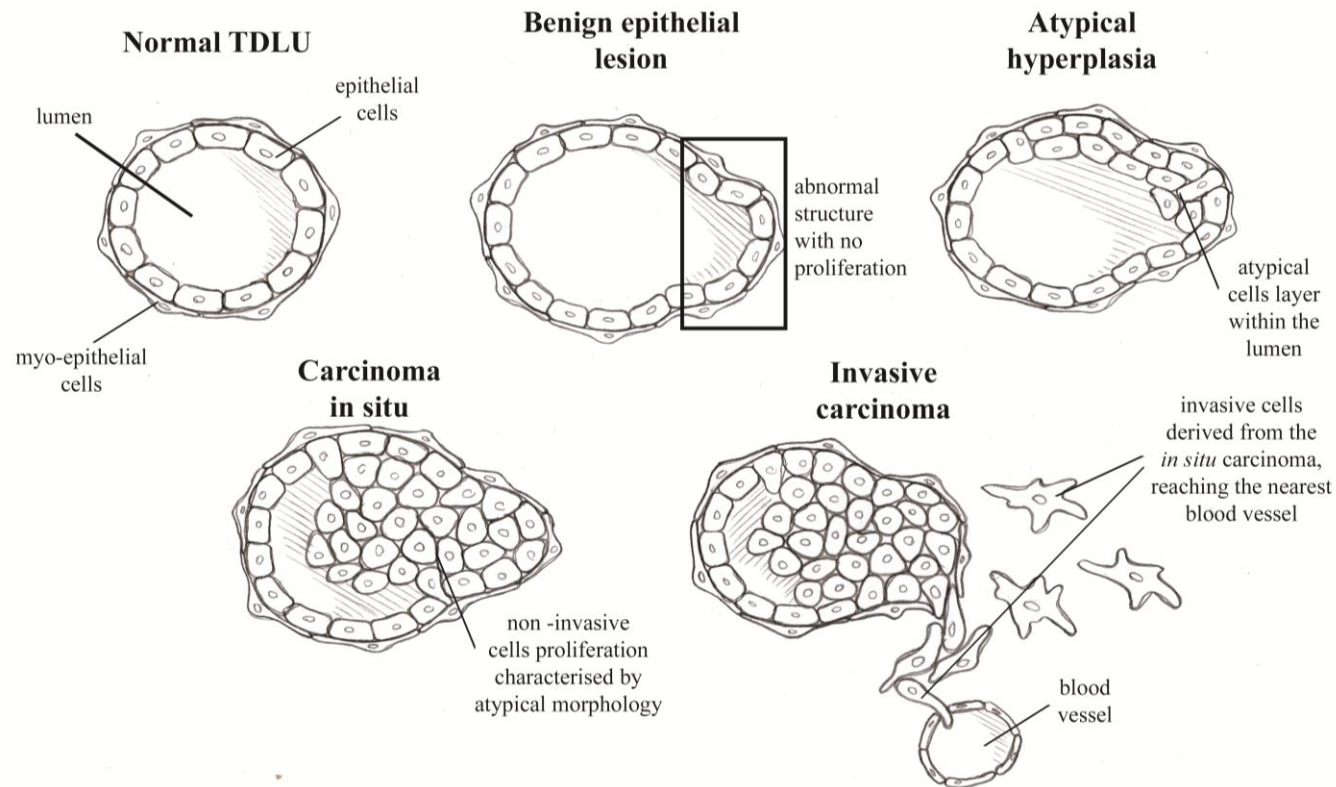


Figure 1-3. Breast cancer development.

The 5 stages of breast cancer development. Breast cancer starts as a benign epithelial lesion characterised by abnormal structure of the duct or lobule. This evolves in atypical hyperplasia with extra cell layers into the lumen. The hyperplasia grows and proliferates to become an early stage *in situ* carcinoma which develops into invasive breast cancer reaching towards the nearest blood vessels, causing metastasis formation.

1.1.5 Breast cancer classification

1.1.5.1 Atypical hyperplasia

The term ‘atypical hyperplasia’ describes a group of cells proliferating in the TDLU. In these lesions the original epithelial cells are replaced with multi-layer intraluminal proliferation. Cells in this condition are evenly distributed and morphologically identical to the native ones (Figure 1-4 A). Atypical hyperplasia is generally considered the step prior to *in situ* carcinoma (Tavassoli and Devilee 2003).

1.1.5.2 *In situ* carcinoma

Breast *in situ* carcinoma is a benign disease, characterised by an uncontrolled proliferation of small loose-cohesive cells into the lumen of ducts or lobules. The myo-epithelial cell layer and the basal membrane are usually intact. Therefore the disease is localised, making it the ideal target for excision treatment (Tavassoli 2003). The *in situ* carcinoma can be a ductal carcinoma *in situ* (DCIS) (Figure 1-4 B) or lobular carcinoma *in situ* (LCIS) (Figure 1-4 C) based on the localization in the terminal ductal lobular unit. 1% to 3.8% of all breast carcinoma are LCIS and 3.9% to 17.5% are DCIS (Tavassoli and Devilee 2003, Li et al. 2005).

Ductal carcinoma *in situ* is classified into three grades, based on the cancer cell differentiation. Grade 1 is characterised by small, differentiated cells with uniform nuclei and a low mitotic rate. Grade 3 consists of highly atypical and undifferentiated cells with multiple nucleoli and high proliferative rate, generating a mass of over 5 mm in diameter. Grade 2 represents an intermediate profile between the grade 1 and

3. 75% of DCIS are positive for oestrogen receptor (ER), 30% over-express the epidermal growth factor receptor 2 (Her2). The relative risk to develop an invasive carcinoma when diagnosed with a DCIS is 8-11 (Tavassoli and Devilee 2003).

Lobular carcinoma *in situ* can be subdivided into type A and B based on the cells present. Type A lobular carcinoma is formed by small, uniform cells with round nuclei and indistinct cell margins, while Type B consists of larger and more atypical cells with abnormal chromatin and multiple nucleoli. LCIS is oestrogen receptor (ER) and progesterone receptor (PR) positive in 60-90% of cases, and over-expression of the epidermal growth factor receptor 2 (Her2) is rare. The relative risk in developing an invasive carcinoma when diagnosed with a LCIS is 6.9-12 (Tavassoli and Devilee 2003).

1.1.5.3 Invasive carcinoma

Invasive breast carcinoma describes a group of epithelial malignant cancers characterised by invasion into the adjacent tissues and a tendency to metastasise. Invasive breast carcinoma accounts for 22% of all female cancers, with good prognosis if diagnosed at an early stage. It is classified as ductal or lobular invasive carcinoma based on the *in situ* carcinoma it is associated with (Tavassoli and Devilee 2003).

Invasive ductal breast carcinoma (IDC) is associated with focal ductal carcinoma *in situ* and represents 40-70% of all invasive carcinoma, i.e. 50-80% of all breast cancer cases. As an *in situ* carcinoma it is rare in women below 40. There are not specific macroscopic features associated with IDC due to variability in size and morphology.

The tumour edge is usually unclear and poorly defined (Figure 1-4 D). IDC has frequent mutations in BRCA1 or BRCA2, with 70-80% of ER positive cases, 60-70% PR positive and 15-30% of cases over expressing Her2 (Tavassoli and Devilee 2003).

Invasive lobular carcinoma (ILC) is composed by non-cohesive singularly dispersed cells in the presence of lobular carcinoma *in situ*. 5-15% of all invasive carcinoma are lobular. The tumour is poorly delimited, formed by proliferation of small cells that are either individually dispersed in the stroma or form linear cord around normal ducts and lobules (Figure 1-4 E). 70-95% of ILC are ER positive, 60-70% PR positive, but Her2 over-expression is lower than in IDC. In 63-87% of cases ILC presents a deletion on the long arm of chromosome 16, where the E-cadherin gene is located. This gene is involved in cell-cell adhesion and maintenance of tissue coherence, explaining the observed high tendency of ILC to metastasise. Patients diagnosed with ILC frequently develop metastases in lung, bone, gastro-intestinal tract, uterus and ovary (Tavassoli and Devilee 2003).

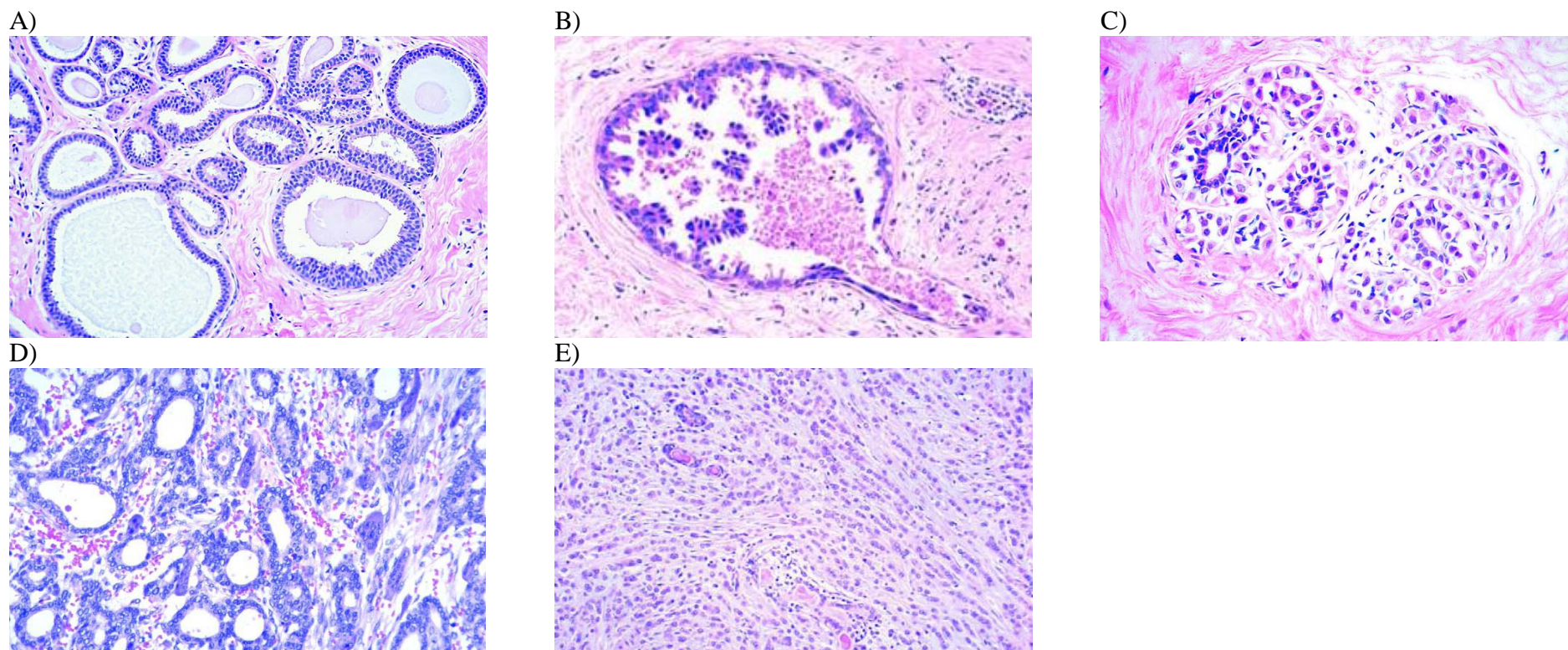


Figure 1-4. Histological images of breast cancer.

Examples of histological images from different types of breast cancer. A) Atypical hyperplasia characterised by multiple epithelial layers within the lumen. B) *In situ* ductal carcinoma with cancer cell proliferation within the duct. C) *In situ* lobular carcinoma with abnormal cell proliferation in the lobules. D) Invasive ductal carcinoma and E) Invasive lobular carcinoma with proliferating cells in the stroma surrounding ducts and lobules (Tavassoli and Devilee 2003).

1.1.6 Molecular profiling

It is now known that a histological classification is not enough to fully describe the heterogeneity of breast cancer disease. In the last ten years, high-throughput microarray-based gene expression profiling has revealed how conventional classification based on histological and molecular biomarkers was not sufficient to describe the intrinsic heterogeneity of breast cancers (Perou et al. 1999, Perou et al. 2000, Li et al. 2005, Hu et al. 2006, Van der Auwera et al. 2010, Guedj et al. 2012). This is particularly relevant when considering treatment for invasive and metastatic breast cancer, where efficient and specific therapy is necessary.

The preeminent biomarkers in breast cancer are the oestrogen receptor (ER), the progesterone receptor (PR) and the epidermal growth factor 2 (Her2/erbB2). During the histological examination, each receptor presence is routinely evaluated by immunohistochemistry (IHC) and considered in the breast cancer classification (discussed previously). The assessment of Her2 over-expression also includes a gene copy number examination by Fluorescence *in situ* hybridization (FISH) (Bertos and Park 2011). Currently, based on the presence or absence of these three markers breast cancer has been subdivided into three main groups: 1) Triple Negative (TNB) or Basal cancers when negative for all these receptors, 2) Hormone-driven when positive for either ER or PR but Her2 negative, and 3) Her-2 positive in which the Her2 gene is amplified (Guedj et al. 2012). Hyper-activation or over-expression of the protein ER, PR and Her2 has been associated with uncontrolled gene transcription and an increase in cell proliferation (Pietras and Marquez-Garban 2007, Fox et al. 2009).

Recent micro-array data have identified 5 different breast cancer subtypes: luminal, Her2-enriched, basal-like, Claudin-low and normal breast-like (Perou et al. 2000, Sorlie et al. 2003, Hu et al. 2006).

Luminal breast cancers show a very similar expression profile to the luminal epithelial cells and they can be subdivided in two groups based on ER and Her2 expression levels. The Luminal A subtype is characterised by over-expression of ER-signalling genes, under-expression of Her2 and represents 40% of all breast cancers. Luminal B is characterised by lower expression of genes regulated by ER-signalling, variable levels of Her2 and correlates with a worse clinical outcome and a higher tendency to relapse. Luminal B is less frequent than Luminal A, representing 20% of all breast cancer cases (Kittaneh et al. 2013).

The Her2-enriched subtype demonstrates over-expression of genes downstream Her2-signalling and under-expression of luminal-associated genes, such as cytokeratin. This subtype corresponds to 20-30% of all diagnosed breast cancers, with a strong association with ductal carcinoma. Tumours included in this subtype are usually negative for ER and PR expression (Kittaneh et al. 2013).

The basal-like subtype corresponds to 15% of invasive ductal carcinoma and presents a similar profile to basal myo-epithelial cells. The basal-like genes such as laminin and keratin are highly expressed in this subtype which is also negative for ER, PR and Her2 (Kittaneh et al. 2013). However cancers included in this subtypes are only a small part of the more heterogeneous group described as triple negative (Nielsen et al. 2004, Carey et al. 2007). Basal-like is also associated with a mutation in BRCA1 and a more malignant phenotype (Kittaneh et al. 2013).

The Claudin-low subgroup is part of the TNB as it includes cancers negative for ER, PR and Her2. This subtype has a gene-expression profile associated with epithelial-

mesenchymal transition (EMT). Tumours in this subtype over-express genes involved in cell communication, extracellular matrix formation, cell differentiation, migration, angiogenesis, immune-associated and stem-cell genes (Kittaneh et al. 2013).

1.1.7 Breast cancer screening, diagnosis and treatment

1.1.7.1 Breast cancer screening

The main aim of screening is to detect breast cancer at a very early stage, thereby improving the prognosis of the disease. Mammography is the main technique in use for screening and has been demonstrated to detect breast cancer at early stages, with an associated reduction in mortality rate (International Agency for Research on Cancer (IARC) 2002, Youlden et al. 2012). The mammography screening programme in most developed countries involves women between 50 and 69 years of age, who are screened by mammography every two years (Youlden et al. 2012). Screening has also been used in several developing countries since 1980s, where women over 50 are screened every two years by National Care unit (International Agency for Research on Cancer (IARC) 2002).

1.1.7.2 Breast cancer diagnosis

Breast cancer diagnosis is based on clinical examination of the breast and lymph nodes, mammography of both breasts and a core biopsy or needle aspiration examination. The physical and menopausal status is included in the examination of each patient, with personal and family cancer history. The neoplasia is evaluated and

classified using the TMN staging system based on the H&E stained biopsies, ER, PR and Her2 assessment as described previously (Kataja and Castiglione 2009, Youlden et al. 2012).

1.1.7.3 Breast cancer treatment

Carcinoma *in situ*, DCIS and LCIS, are normally treated by breast-conserving surgery. Adjuvant therapies, such as radiation and endocrine treatment, can be considered after surgery to decrease the risk of recurrence and metastases. Invasive carcinomas, IDC and ILC, are treated by mastectomy when the tumour is localised and has not spread beyond the breast and lymph nodes. Neo-adjuvant treatment can be administered to patients with late stage disease to reduce the tumour size before surgery (International Agency for Research on Cancer (IARC) 2002, Kataja and Castiglione 2009, Youlden et al. 2012).

Cancer treatment can be classified based on the period it is administered to the patient, pre- or post-surgery, or based on the target. Neo-adjuvant treatment, chemo- or endocrine therapy, is given before surgery. The aim of such treatments is usually to reduce the tumour mass to make it operable. Adjuvant treatment, radiation chemo- endocrine- Her2-targeting therapy or a combination of all of these, is administered to un-operable patients or after surgery (Kataja and Castiglione 2009). Radiotherapy is used after surgery, both breast-conservative or mastectomy, to eliminate any remaining cancer cells in the tissues surrounding the tumour. It involves irradiating the area for a number of cycles depending on the patient's tumour characteristics (Kataja and Castiglione 2009). Chemo-therapy includes drugs targeting a specific

pathway, such as endocrine or Her2-targeting treatments, and those with a broader range, such as platinum agents (Bosch et al. 2009).

Endocrine therapy is most suited for ER, PR positive tumours. It has been shown that the presence of PR has no significant contribution in endocrine therapy and clinical outcome; therefore treatments tend to have ER as the main target (Bardou et al. 2003, Patel et al. 2007, Dowsett et al. 2008, Bartlett et al. 2011). Endocrine treatment induces oestrogen deprivation by using Tamoxifen, Fulvestrant or Aromatase Inhibitors (AIs). Tamoxifen and Fulvestrant prevent the receptor from binding to the ligand, whereas AIs block oestrogen synthesis (Higgins and Baselga 2011, Wong and Chen 2012). Although endocrine therapy is efficient for the treatment of primary breast cancers, 50% of patients will relapse and develop metastases through *de novo* or acquired resistance (Higgins and Baselga 2011, Wong and Chen 2012).

Breast cancers with amplified Her2 are subjected to Her2-targeting therapy. This includes two approved drugs: Trastuzumab and Lapatinib. Trastuzumab is a monoclonal antibody against Her2 which blocks the receptor activation causing specific cytotoxicity in the cancer cells over expressing Her2 (Clynes et al. 2000, Junttila et al. 2009). Lapatinib is a Tyrosine Kinase Inhibitor (TKI) that blocks Her2 phosphorylation, therefore activation, thus repressing the downstream signalling pathway. Her2-independent activation via PI3K/AKT determines the development of resistance to the treatment (Higgins and Baselga 2011).

Triple negative cancers do not respond to endocrine or Her2-targeting treatments. Multiple approaches have been tested to treat pathways active in this breast cancer subtype (Bosch et al. 2009, Higgins and Baselga 2011). For example, Centuximab, a monoclonal antibody targeting the epidermal growth factor receptor (EGFR), present in 45-70% of TNB, has shown promising results in combination with cis-platinum (Higgins and Baselga 2011). Progress has also been made with anti-angiogenic agents, for example, Bevatuzimab and Sunitinib, which have been tested in combination with an anti-mitotic agent, Paclitaxel, and reported to increase progression-free survival in TNB (Bosch et al. 2009, Higgins and Baselga 2011). Furthermore, PARP (Poly-ADP-ribose polymerase) inhibitors have been tested in breast cancer defective in DNA-break repair mechanisms, such as TNBs mutated for BRCA1 and BRCA2. Those treatments have shown to positively enhance overall survival when in combination with drugs inducing DNA breaks, such as Fluorouracil or Mitoxantrone (Bosch et al. 2009, Higgins and Baselga 2011).

1.1.8 New biomarker for breast cancer

It is clear that breast cancer is not a homogenous entity, but comprises heterogeneous subtypes differing from each other in clinical characteristics, disease course and response to specific treatments. Understanding the molecular basis of this heterogeneity is essential to improve and personalize the use of the conventional treatment, as well as developing new therapies (Bertos and Park 2011). The importance of validating new molecular biomarkers in cancer is becoming increasingly apparent, as there is currently no available biomarker with the desired sensitivity and specificity for the detection of early stages of development in breast cancer.

Tumour biomarkers can be proteins, RNA or DNA molecules measured in serum, plasma or tumour tissue. ER, PR, Her2, BRCA1 and BRCA2 (discussed before), Ki67 antigen and p53 are used to identify individuals with increased predispositions to certain cancers, to screen for early malignancies, assist in diagnosis and to predict therapy response and prognosis (Javanovic et al. 2010). Ki67 antigen, a non-histone nuclear protein expressed only when cells are proliferating, has been shown to be a prognostic marker of treatment response in breast cancer. p53 is instead a crucial protein in cellular response to stress stimuli and genome integrity maintenance. Its mutation has been associated with poor clinical outcome (Hirata et al. 2014).

Recently, it has become clear how cancer development is intrinsically linked with accumulation of epigenetic modifications in the genome, in particular an increase in DNA methylation (Hill et al. 2011, Park et al. 2011). DNA methylation not only correlates with different stages in carcinogenesis, but also clearly discriminates between cancer and normal tissues (Christensen et al. 2010, Hill et al. 2011). This makes it a serious candidate not only as a reliable biomarker to detect cancer at early stages, but also as a target for cancer therapies (Lewandowska and Bartoszek 2011).

Therefore it is of great interest to investigate the epigenetic mechanisms involved in gene expression and their role in cancer development.

1.2 Epigenetics and cancer

Epigenetic modifications are stable changes on the genome not involving the DNA sequence but its structure. Two of the main epigenetic mechanisms will be investigated in this study: DNA methylation and histone modification. They are inherited by daughter cells and accumulate on the genome through the life of the organism. These inherited changes could provide a useful resource for therapy and as prognostic biomarkers (Qiu 2006).

1.2.1 DNA methylation

In mammalian cells, DNA methylation is a post-replication modification on the 5th position of the cytosine pyrimidine ring when located next to a guanine nucleotide. When cytosine and guanine are next to each other in a DNA sequence, they are known as CpG dinucleotide or CpG sites. Clusters of CpG dinucleotide generate a CpG island, whose length is usually between 400 and 4000 nucleotides (Bird 2002, Sandoval and Esteller 2012). CpG islands are present in over half of the promoter region of protein-coding genes, influencing their expression via cytosine methylation (Rivera and Bennett 2010, Deaton and Brid 2011).

DNA methylation plays an important role in normal cells behaviour as well as in cancer development. It is maintained by DNA methyl-transferases (DNMTs). At each replication cycle DNA methylation patterns are copied and maintained by DNMT1, whereas DNMT3a and DNMT3b are responsible for *de novo* methylation (Rivera and Bennett 2010, Park et al. 2011, Alabert and Groth 2012). DNA

methylation contributes to chromatin organization, silencing of transposable elements, X-chromatin inactivation and tissue-specific gene expression. In tumours, the physiological methylation trend is disrupted causing the inactivation of genes involved in the cell cycle, cell adherence, DNA repair and apoptosis (Costello et al. 2000, Suijkerbuijk et al. 2010, Deaton and Brid 2011, Sandoval and Esteller 2012).

In normal cells, CpG dinucleotides tend to be unmethylated in the promoter region and methylated across the rest of the genome. Cancer cells show the opposite pattern with methylated CpG islands on the promoter region and unmethylated CpG sites within the coding regions (Figure 1-5) (Javanovic et al. 2010, Suijkerbuijk et al. 2010). DNA hypo-methylation of the promoter region correlates to gene reactivation and chromosomal instability, leading to up-regulation and over-expression of the gene the promoter is related to. Promoter hyper-methylation is frequently associated with gene inactivation resulting in gene silencing (Costello et al. 2000, Javanovic et al. 2010, Suijkerbuijk et al. 2010, Deaton and Brid 2011, Park et al. 2011, Sandoval and Esteller 2012).

DNA methylation silences gene expression via two main mechanisms: by blocking transcriptional factors' via steric conformation or by protein recruitment. In the first scenario, hypo-methylated or hyper-methylated of the promoter region leads to changes in binding of transcriptional regulatory proteins which bind specifically to either unmethylated or methylated DNA (Javanovic et al. 2010). In the second scenario, DNA methylation is recognised by methyl binding proteins and repressing factors, such as the Histone Deacetylases (HDACs), mediating chromatin

conformational changes, and therefore gene silencing (Klose and Bird 2006, Deaton and Brid 2011, Park et al. 2011, Shoemaker et al. 2011).

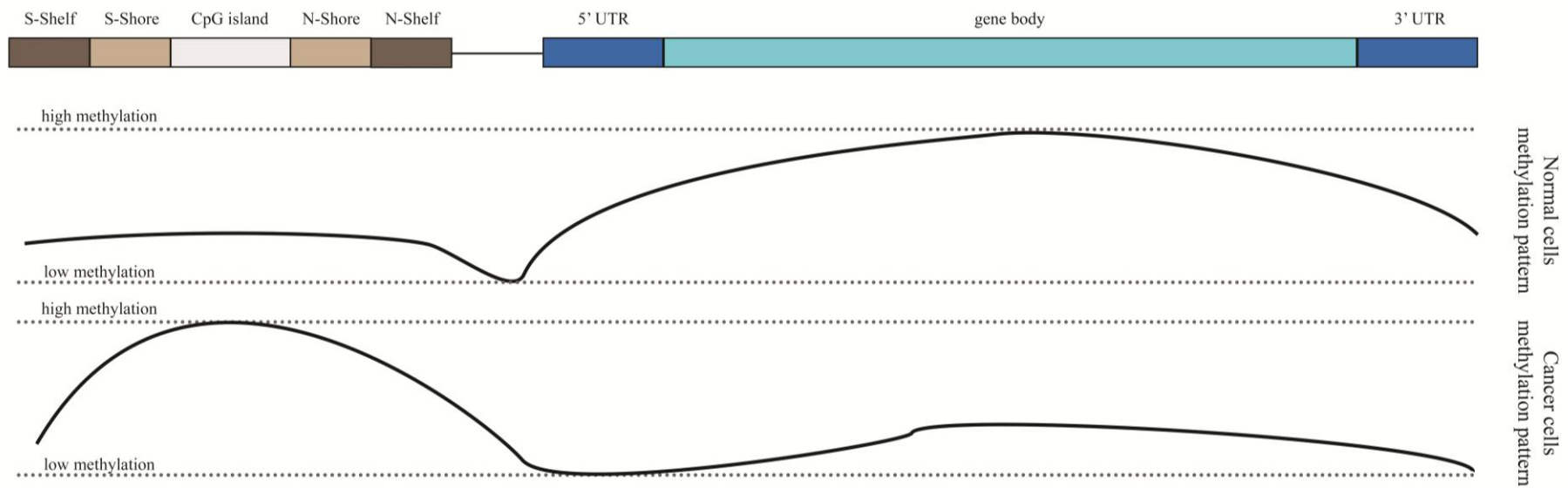


Figure 1-5. DNA methylation pattern in normal and cancer cells.

The black lines represent the levels of methylation, from low (0%) to high (100%), across different parts of the gene, including Shelf Shore CpG island regions 5' and 3' UTR and the gene body, in normal and cancer cells. This does not apply to the X-chromosome as one copy is completely inactivated.

1.2.2 Histone modifications

Histones are small proteins, ranging in size from 11-17kDa, at the base of chromatin structure. The core structure of the chromatin organization is composed by 8 histone subunits, two Histone 2A (H2A), two Histone 2B (H2B), two Histone 3 (H3) and two Histone 4 (H4). Together, they constitute a structure around which the DNA is coiled, each coil consisting of 147 bp, forming the nucleosome. Histone 1 (H1) and Histone 5 (H5) function as linkers and mediate the entry and exit of the DNA from the nucleosome (Rivera and Bennett 2010, Hassler and Egger 2012, Hatzimichael and Crook 2013). Post-transcriptional modifications on the histone tails can dynamically modify the chromatin structure, determining activation or repression of gene expression. Histone acetylation and methylation are the most common modifications and predominantly involve Histone 3 and Histone 4. Acetylation prevents methylation of the histone tails, so that the acetylation profile mirrors alternative chromatin conformations (Nakao 2001, Lakowski et al. 2006).

Histone acetylation is actively modulated by Histone Acetyl-transferase (HATs) and Histones Deacetylase (HDACs). HATs add and HDACs remove an acetyl-group on lysines 5, 8, 12, 16, 20 on the N-terminal tail of H4 and lysines 9, 14, 18, 23 of H3 (Fuchs et al. 2006, Javanovic et al. 2010). Hyper-acetylation of these residues is associated with active transcription and euchromatin conformation, whereas hypo-acetylation correlates with gene silencing and heterochromatin structure (Javanovic et al. 2010, Park et al. 2011, Lee and Lee 2012, Hatzimichael and Crook 2013).

If acetylation is associated with gene expression, histone tail methylation can be associated with active or repressed gene states depending on the residue involved.

Lysines on H3 and H4 can be mono-, di- or tri-methylated by S-adenosylmethionine dependent methyl-transferase and removed by Lysine specific histone demethylase (LSD) (Fuchs et al. 2006). Trimethylation on H3 lysine 9 and 27 and trimethylation on H4 lysine 20 correlate with gene inactivation and condensed state of the chromatin (heterochromatic). Conversely, trimethylation on H3 lysine 4 and 36 is associated with gene activation (Fuchs et al. 2006, Park et al. 2011, Sandoval and Esteller 2012).

Based on these observations, modifications of H3 and H4 are particularly relevant in this study as a marker of gene expression, in particular acetylation as a non-ambiguous marker of gene activation.

1.2.3 Chromatin structure

It has become evident that epigenetic modifications work as a whole to define the chromatin structure and alter it dynamically during cancer development and normal tissue differentiation. HDACs and DNMTs have been identified in complexes on the DNA with and without intermediate proteins (Javanovic et al. 2010). Intermediate proteins are represented by proteins containing Methyl Binding Domains (MBDs) that recognise symmetric methylated CpG site and recruit HDACs (Klose et al. 2005, Sharma et al. 2005, Ho et al. 2008). The MBDs HDACs and DNMTs have been demonstrated to initiate recruitment of repressive complexes on gene promoter regions, such as SIN3 Mi2-NuRD and CoREST-like complex, of which they are important components (Lakowski et al. 2006).

Previously published examples of gene modulation via chromatin remodelling include Claudin-6 gene silencing in breast cancer, which has been shown to be mediated by methylation via HDAC recruitment by MeCP2, leading to cell proliferation, migration and invasion (Xu et al. 2012). There is also evidence that Mi2-NuRD can inactivate gene expression via the activity of HDACs (Nakao 2001). Furthermore, ER-negative breast cancer cell lines have been found to be characterised by the co-existence of H3 and H4 hyper-acetylation and DNA hyper-methylation in presence of a repressive complex on the promoter region of the oestrogen receptor. The complex included DNMT, HDAC, LSD and MBD; absent in ER-positive breast cancer cells lines (Sharma et al. 2005).

Recent studies have emphasised the strong connection between DNA methylation and histone modifications. In ER-negative breast cancer cell lines treated with a combination of a DNMT inhibitor (5-aza-2'-deoxycytidine) and a HDAC inhibitor (Trichostatin A) there was a release of the repressing complexes from the promoter region and the subsequent re-expression of ER (Sharma et al. 2005). Following on from this, Trichostatin A has been shown to reduce the activity of LSD and consequently histone acetylation. The changes in chromatin structure have been shown to reactivate genes which have been associated with silencing via hyper-methylation in their promoter region (Huang et al. 2011). These results emphasise the role of histone modifications in stabilising the gene inactivation effect of DNA methylation, leading to the importance of evaluating both epigenetic mechanisms when studying gene epigenetic modulation.

These results place DNA methylation in a more complex mechanism of regulation, where it is not simply inducing gene repression, but also and more importantly involved in the chromatin remodelling process (Figure 1-6). Methylation has been shown to be the promoting marker for repressive complex binding; therefore DNA methylation is of great interest as potential new marker of repressed gene which could be targeted in breast cancer therapy.

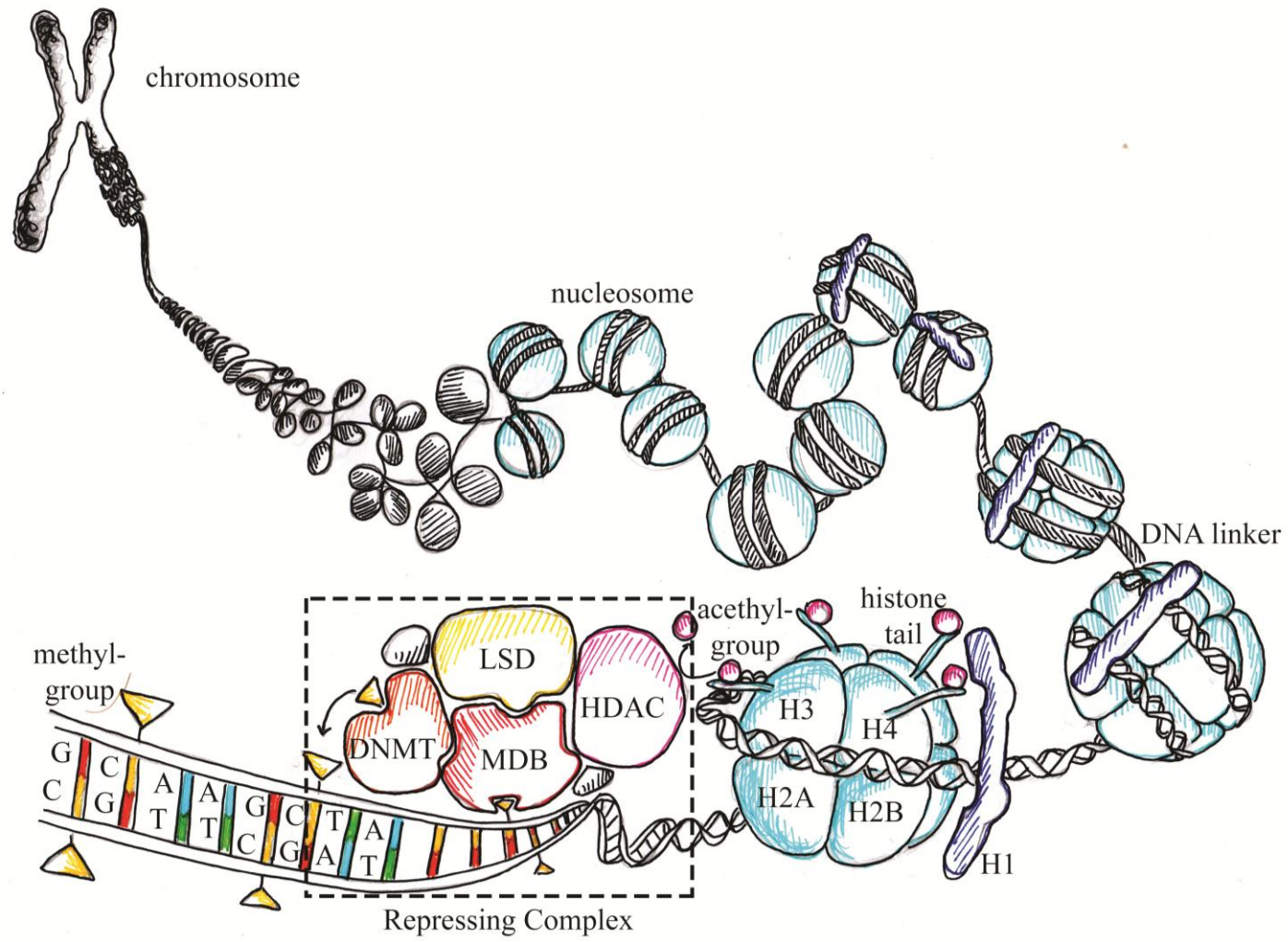


Figure 1-6. Chromatin structure.

Illustration of how chromatin conformation changes from open (bottom right) to condense into the nucleosome leading to chromosome structure. Methylated cytosines in CpG island are the binding site for MDB proteins, that recruit the repressing complex responsible for histone de-acetylation and chromatin condensation.

DNMT: DNA methyl transferase; MDB: Methyl-domain binding protein; HDAC: Histone deacetylase; LSD: Lysine specific histone demethylase; H1: Histone 1; H2A: Histone 2A; H2B: Histone 2B; H3: Histone 3; H4: Histone 4.

1.2.4 Alteration in DNA methylation as a biomarker

Hyper-methylation of the gene promoter regions has been shown to be an early event in cancer development and one of the most frequent aberration, with 600 to 1000 aberrantly methylated genes per tumour (Suijkerbuijk et al. 2010). DNA methylation is not only involved from the early stages of the tumour, but has also been shown to be tumour-specific. Within the same tumour type, methylation can be used to assign subtypes and stages (Costello et al. 2000, Lambert et al. 2011, Sproul et al. 2011, Walker et al. 2012). Methylation patterns for each tumour can also be found in the surrounding tissues, up to 4 cm from the primary neoplasm (Love and Barsky 1996). These data suggest that it may be possible to use methylation as an early marker to detect cancer development earlier than clinically detectable.

DNA methylation patterns are not reflected in the DNA sequence and they cannot be amplified by normal PCR (Laird 2010). However, bisulphite treatment deaminates unmethylated cytosines to uracil, while the methylated cytosines remain unchanged (Clark et al. 1994, Yan et al. 2006). This creates a difference in the sequence between methylated and unmethylated CpG sites that can be amplified by PCR. The sensitivity of the PCR allows us to detect little aberrations from a small amount of biological material. DNA hyper-methylation thus results in an easier detectable signal than many other genetic alterations, such as loss of heterozygosis (Javanovic et al. 2010). Hence, it is likely that PCR will provide the best opportunity for constructing multi-gene screening analysis to better characterise specific stages of cancer development (Levenson 2007).

As previously described, methylation patterns could provide a dynamic picture of carcinogenesis, while mutations or Single Nucleotide Polymorphisms (SNPs) only provide a snapshot of this process. DNA-genome wide profiling has shown a significant association between specific methylation patterns in the peripheral blood and risk-prediction of developing cancer (Teschendorff et al. 2009). Following from this, utility of DNA methylation analysis in the blood of cancer patients has already been demonstrated for the ATM (ataxia-telangiectasia mutated) gene. It has been shown to be highly methylated in peripheral blood of women with bilateral breast cancer when compared to matched controls, discriminating between normal and cancerous tissues (Flanagan et al. 2009).

Based on these results, it is clear that DNA methylation has a strong potential as diagnostic biomarker to detect and follow the tumour development from early stages.

1.3 Synthetic lethality

Genetic or epigenetic mutations can identify susceptibility in a subset of cancers that could be exploited for treatment causing synthetic lethality of the tumour cells. Synthetic lethality occurs when genetic and/or epigenetic aberrations, arisen during cancer development, cause the selective death of cancer cells. It also considered synthetic lethality when a genetic or epigenetic condition is not lethal per se but causes sensitivity to a specific drugs or micro-environmental change (Nijman 2011).

Genetic aberrations discriminating cancer from normal tissues have already been exploited in cancer treatment based on synthetic lethality (Levenson 2007, Javanovic et al. 2010), whilst epigenetic changes are now starting to be considered as potential targets for new therapies. For instance, O⁶-methylguanine DNA methyltransferase (*MGMT*), involved in DNA repair, has been shown to be repressed via methylation in glioblastoma, colorectal carcinoma and melanoma, correlating to a better response to treatment inducing DNA damages (Mikeska et al. 2012). Furthermore, *ASS1*, the rate-limiting enzyme responsible for arginine synthesis (Wu et al. 1998, Delage et al. 2010), has been found to be silenced via methylation in melanoma, hepatocellular carcinoma and prostate cancer treatment. Cancer cells lacking the enzyme via DNA methylation have been shown to be auxotrophic for arginine and have been successfully treated by arginine depletion therapy (Ensor et al. 2002, Feun et al. 2006, Szlosarek et al. 2006, Kim et al. 2009).

MGMT and *ASS1* showed how epigenetic modifications can be exploited to predict the tumour response to treatment and to develop new therapies based on the

epigenetic modifications characterising the specific tumour, respectively. Furthermore, *ASS1* is a good example of how nutrient additions to tumours can be exploited to design therapies that selectively target cancer cells. For this reason it would be of great interest to investigate the epigenetic modulation of metabolism-related genes with the aim of finding novel markers for synthetic lethality in breast cancer. Epigenetic modifications that would alter the ability of cancer cells to response to micro-environmental changes can be used to selectively treat these tumours and cause cell death in the tumour.

1.4 Cancer metabolism

It is known that cancer cells alter their metabolism compared to healthy tissues since the discovery of the Warburg effect (Warburg et al. 1927, Warburg 1956). Cancer cells have been shown to up-regulate anaerobic glycolysis and amino-acids uptake compared to normal cells in concomitance with an increase in cell proliferation and survival. This mechanism is facilitated by the increased supply of nutrients from the micro-environment (Vander Heiden et al. 2009, Ferreira et al. 2012).

In the presence of oxygen, differentiated cells metabolise glucose to pyruvate through aerobic glycolysis. Pyruvate enters the tricarboxylic acid (TCA) cycle to generate cellular energy as adenosine tri-phosphate (ATP) molecules (Ferreira et al. 2012, Schulze and Harris 2012). This metabolic flow is strictly regulated mainly by the Phospho-Inositide-3-Kinase (PI3K) and the alpha serine/threonine-protein kinase (AKT) pathway, to respond to micro-environmental changes, such as nutrients' supply and the presence of growth factors. This pathway is responsible for cell survival and production of the metabolites, such as lipids, proteins and nucleic acids, necessary for cell replication (Schulze and Harris 2012, Shanware et al. 2013). The downstream effects include the translocation of the glucose transporter to the plasma membrane increasing glucose uptake, repression of FOXO (Forkhead box O) translocation into the nucleus suppressing gene expression, and the activation of mTOR (mammalian target of Rapamycin) inhibiting autophagy. mTOR is also the cellular sensor of amino acids supply in the cell and promotes protein turn-over and amino acid recycling when necessary (Figure 1-7) (Nicklin et al. 2009, Shanware et al. 2013).

Cancer cells are characterised by the switch from aerobic to anaerobic glycolysis and increased uptake of amino acids. Research on the mechanisms behind this metabolic reprogramming is still ongoing, but an explanation could be the alteration of the main pathways involved. PI3K-AKT pathway is one of the most altered in cancer, mainly via activating mutations in PI3K and loss or inactivating mutations in PTEN (phosphatase and tensin homolog) responsible for PI3K inactivation (Jones and Schulze 2012). PI3K-AKT pathway activation up-regulates anaerobic metabolism as well as autophagy and amino-acid intake (Shanware et al. 2013). The activation of anaerobic glycolysis deprives cells of the intermediate metabolites for the synthesis of proteins and lipids (Yuneva 2008). To compensate for the loss, cancer cells increase the uptake of glutamine that would enter the TCA cycle to produce metabolic energy and supply the biosynthetic intermediates the cell needs (Jones and Schulze 2012, Moncada et al. 2012, Yabu et al. 2012, Lorin et al. 2013, Shanware et al. 2013). At the same time deprivation stimuli, such as a decrease in amino acid concentration, determine the activation of autophagy via mTOR and FOXO up-regulation (Duran et al. 2012, van der Vos et al. 2012, Syed et al. 2013). For example, low concentration of glutamine and/or arginine has been associated with modulation of the PI3K-AKT mTOR pathway and autophagy induction in cancer cells (van der Vos 2012, Duran 2012, Syed 2013). FOXO modulates the expression of metabolic genes, such as glutamine synthetase, and can inhibit the autophagy response that might cause cell death if not controlled (van der Vos et al. 2012, White 2012, Lorin et al. 2013).

The metabolic reprogramming characteristic of cancer cells is also influenced by mutation and activation of other genes in cancer cells, such as over expressing mutation of c-Myc (myelocytomatosis viral oncogene homolog) and activation of

HIF1 α (hypoxia inducible factor 1 alpha). c-Myc is a transcriptional factor over-expressed in cancer cells, whose activation leads to induction of lactate production, glutamine uptake and translocation of glucose transporter on the plasma membrane (Yuneva et al. 2007, Liu et al. 2012, Miller et al. 2012, Schulze and Harris 2012). HIF1 α is one the main transcription factors activated in the centre of the tumour in response to hypoxic conditions, but can also be induced by PI3K-AKT and c-Myc. When up-regulated, HIF1 α induces constitutive activation of anaerobic glycolysis, glucose uptake and autophagy (Thompson 2009, Jones and Schulze 2012, Lorin et al. 2013). Together, these data explain the increased intake of nutrients and the activation of anaerobic glycolysis characteristic of cancer cells (Jiang and Deberardinis 2012).

The metabolic differences between healthy and cancer cells have been recently exploited in developing new therapies, the majority still in the preclinical stage. Two main strategies are currently being tested: interfering with anaerobic glycolysis to induce cell death or blocking an over-activated PI3K-AKT pathway and the subsequent autophagy induction (Schulze and Harris 2012, Shanware et al. 2013). The first approach involves using analogues of glucose, blocking agents for glucose transporters, inhibitors for steps of the glycolysis such as glucose phosphorylation by Hexokinase 2 (HKII) and inhibitors of lactate removal from cancer cells to inhibit glycolysis. Even though some of these drugs have shown promising results, they are still under development. Cancer cells can induce compensatory mechanisms to overcome these effects, such as increasing glucose uptake after treatment with a glucose analogue. The other problem with this approach is that some of the compounds used have serious side effects, such as blockage of glucose transporters

in liver and brain (Schulze and Harris 2012, Ganapathy-Kanniappan and Geschwind 2013). The second approach consists of kinase inhibitors for PI3K-AKT-mTOR and autophagy blockers. One example is Chloroquine, used alone or in combination with chemotherapy. The clinical response has been modest and the side effects of this treatment are still under scrutiny (Jang et al. 2013, Shanware et al. 2013). Recently, loss of *ASS1* has been used for identification of tumours sensitive to arginine depletion therapy in hepatocellular carcinoma, melanoma, prostate cancer and mesothelioma (Ensor 2002, Feun 2006, Szlosarek 2006, Kim 2009). Arginine depletion treatment is based on the Mycoplasma-derived enzyme Deiminase, capable of reducing arginine in citrulline and NH_4 (Feun 2006). It is important to highlight that lack of *ASS1* expression in cancer cells is not sufficient to predict the response to arginine depletion treatment. In absence of methylation on the promoter region, cancer cells have been shown to develop resistance via *ASS1* up-regulation, whilst no resistance was found in methylated cells (Delage 2010).

Cancer metabolism has been shown to be drastically different from the physiological state and little is known about the epigenetic modulations of the pathways involved. Cancer metabolic reprogramming could potentially be a target for synthetic lethality in breast cancer, as in the case of arginine depletion treatment. Non-essential amino acid metabolism, in particular, may be a promising area of study, as healthy cells can synthesise them when necessary. Epigenetic modifications should arise during cancer development causing the gene silencing of the enzyme responsible for a non-essential amino acid synthesis, low nutrients treatment might be selectively lethal for cancer cells. Therefore, the non-essential amino-acid metabolism could be a really innovative and interesting area of investigation.

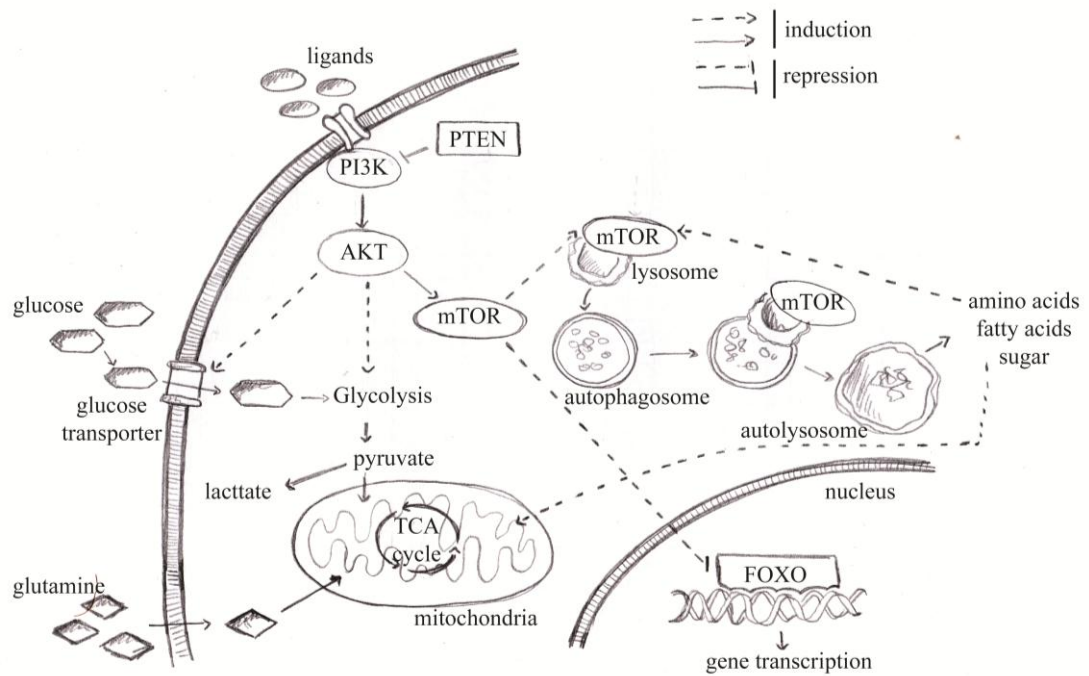


Figure 1-7. Metabolic network.

Connections between metabolic pathways, e.g. glycolysis and TCA cycle, and signalling pathways, such as PI3K-AKT, autophagy and gene expression (adapted from (Shanware et al. 2013).

PI3K: Phosphatidylinositol-3-kinases; AKT: serine/threonine-specific protein kinase; mTOR: mammalian target of Rapamycin; TCA cycle: tricarboxylic acid cycle; FOXO: forkhead box O.

2 Materials and methods

2.1 Work with immortalised cell lines

2.1.1 Cell lines and culture conditions

Human breast carcinoma cell lines were cultured in the recommended media (Sigma-Aldrich®) supplemented with Foetal Bovine Serum (FBS), 2mM of L-glutamine and 50µg/ml of Streptomycin and 0.5U/ml of Penicillin (Sigma-Aldrich®) (Table 2-1). Cell lines analysed for glutamine-deprivation were grown in 4mM L-glutamine for a minimum of one month to maximise the effect of the treatment.

The panel of 16 breast cancer cell lines used covered a range of disease types, including 7 triple negative, of those 2 basal A, 4 basal B and 1 luminal, 6 Her2-positive, and 3 ER/PR-positive (Table 2-1).

Cell line ID	Media	% FBS	Origin	subtype	ER	PR	Her2
BT549	RPMI	10	Invasive ductal carcinoma	Triple negative, basal B	-	-	-
MDA-MB-231	DMEM	10	Adeno-carcinoma	Triple negative, basal B	-	-	-
MDA-MB-436	DMEM	10	Adeno-carcinoma	Triple negative, basal B	-	-	-
Hs 578T	DMEM	10		Triple negative, basal B	-	-	-
MDA-MB-468	DMEM	10	Adeno-carcinoma	Triple negative, basal A	-	-	-
Hcc1937	RPMI	10	Primary ductal carcinoma	Triple negative, basal A	-	-	-
MDA-MB-453	DMEM	10	Metastatic luminal carcinoma	Triple negative, luminal	-	-	-
SKBR3	McCoy's 5a	10	Adeno-carcinoma	Her2 positive, luminal	-	-	+
MDA-MB-361	Leibovitz's L-15	20	Adeno-carcinoma	Her2-positive, luminal	+	-	+
JIMT1	DMEM	10	Ductal carcinoma	Her2 positive, basal B			+
BT474	RPMI	10	Invasive ductal carcinoma	Her2 positive			+
Hcc1569	RPMI	10		Her2 positive, basal A	-	-	+
Hcc1954	RPMI	10	Ductal carcinoma	Her2 positive, basal A	-	-	+
T-47D	RPMI	10		ER/PR positive, luminal	++	+	-
ZR-75-1	RPMI	10		ER/PR positive, luminal	+	-	-
MCF7	RPMI	10	Adeno-carcinoma	ER/PR positive, luminal	+	+	-

Table 2-1. Panel of Breast cancer cell lines.

The cell line panel covered a wide range of different subtypes of breast cancer. Cells were cultured in Dulbecco's Modified Eagle Medium (DMEM), Roswell Park Memorial Institute (RPMI), McCoy's 5a Medium Modified or Leibovitz's L-15 Medium. Cell lines differed by the expression of oestrogen receptor (ER), progesterone receptor (PR), epidermal growth factor receptor 2 (Her2/neu). Cells that were not expressing the receptor were considered negative ("-"), whereas positive ("+") or over-amplified ("++").

2.1.2 Glutamine deprivation

Cell lines were seeded in 24-well plate (Corning) in medium supplemented with 10% FBS, 50µg/ml of Streptomycin and 0.5U/ml of Penicillin (Sigma-Aldrich®), without L-glutamine addition and left overnight to consume any trace of L-glutamine from the serum. The next day, 4mM L-glutamine was added in the controls wells. Cells were deprived up to 8 days and survival rate analysed by MTT assay.

2.1.3 Survival analysis

Cell survival was investigated using MTT (3-(4,5-Dimethylthiazol-2-yl)-2,5-diphenyltetrazolium bromide) (Bio Basic Inc.), a yellow tetrazole which is reduced to purple formazan from metabolically active cells. Briefly, cells were seeded in 96- or 24-well plates depending on the experimental set-up, treated and the survival fraction analysed at different time points by MTT. At each time point, the medium in each well was replaced with medium containing 2mg/ml MTT. After 2 hours incubation at 37°C, MTT solution was removed from each well and replaced with DMSO (dimethyl sulfoxide, Sigma-Aldrich®). The colour intensity in each well was analysed by absorbance at 570 over 650 nm using a plate reader (Biotek Synergy HT). Optical density in each well was corrected by subtracting the background (650nm reading) caused by precipitated protein and cellular debris. The survival fraction for each treatment was determined as a ratio between the treated and untreated wells.

2.1.4 Autophagy analysis

Cells were seeded in 96-well plate with black wall and clear bottom (Corning) in absence of L-glutamine. Induction of autophagy was analysed at 2, 4 and 6 hours and every 2 days up to 8 days of L-glutamine deprivation using the Cyto-ID® Autophagy Detection Kit (Enzo Life Sciences) as per the manufacturer's instructions. Briefly, at each time point cells were washed twice in assay buffer and incubated for 30 min in 150µl of Dual detection reagent at 37°C. After the incubation step, cells were washed twice and 80µl of assay buffer added to each well. The dual detection buffer contained equal amounts of Hoechst 33342 Nuclear stain and Cyto-ID® Green Detection Reagent: the first stains the nucleus, whereas the second stains the vesicles produced during autophagy. Fluorescent emissions at 480 nm for the nuclear and at 340 nm for the vesicle staining were read using a plate reader (Biotek Synergy HT). The level of autophagy in each well was determined as the ratio between the fluorescence from the vesicle stain to the nuclear stain. The increase in autophagy level was calculated using the increase in ratio between treated and untreated cells, with the untreated samples at each time point as a reference.

2.1.5 Chloroquine treatment

Cells were seeded in 96-well plates (Corning) as described above. Medium was then replaced with increasing concentration of Chloroquine diphosphate salt (Sigma-Aldrich®), at 5, 10 or 20 µM. After 4 hours treatment with Chloroquine, L-glutamine was removed from the treated wells. After 4 hours of glutamine deprivation autophagy induction was measured using the Cyto-ID® Autophagy

Detection Kit (Enzo Life Sciences) as described above. Cell survival was analysed by MTT after 24 hours deprivation.

2.1.6 Arginine deprivation

Cell lines were seeded in 96-well plates (Corning) and left overnight to attach to the bottom of the well. The following day, each well was washed twice in Phosphate saline buffer (PBS) (Sigma-Aldrich®) and incubated for 10 days in Dulbecco's Modified Eagle's Medium (DMEM) with 1000 mg/L D-glucose, L-glutamine, sodium bicarbonate and without arginine, leucine, lysine, sodium pyruvate, and phenol red (Sigma-Aldrich®) supplemented with 10% dialysed serum (Sigma-Aldrich®), 50µg/ml of Streptomycin and 0.5U/ml of Penicillin (Sigma-Aldrich®) and MEM non-essential amino acids solution (Gibco). Cells were either grown in total absence of L-arginine (Sigma-Aldrich®) and L-citrulline (Sigma-Aldrich®) or in presence of either 1mM L-arginine or 1mM L-citrulline or both. Survival rate was analysed by MTT.

2.1.7 Arginine Deiminase (ADI-PEG20) administration

Cell lines were seeded in 96-well plates (Corning), left for 24 hours, washed twice in PBS (Sigma-Aldrich®) and medium replaced with Dulbecco's Modified Eagle's Medium with 1000 mg/L D-glucose, L-glutamine, sodium bicarbonate and without arginine, leucine, lysine, sodium pyruvate, and phenol red (Sigma-Aldrich®). 10% dialysed serum (Sigma-Aldrich®), 50µg/ml of Streptomycin and 0.5U/ml of Penicillin (Sigma-Aldrich®), MEM non-essential amino acids solution (Gibco), 1mM L-arginine and 1mM L-citrulline (Sigma-Aldrich®) were added to the medium

in all wells. Cells were treated up to 10 days with increasing concentrations of ADI-PEG20 (Polaris Group), from 0 to 10µg/ml. Survival rates were analysed by MTT.

2.1.8 De-methylation and pro-acetylation treatment

Cells were grown in appropriate medium until 80% confluent; 5µM of 5'-aza-deoxycytidine (aza) (Sigma-Aldrich®) was added and left on the cells for 5 days. In the final 16 hours 0.3nM of Trichostatin A (tsa) (Sigma-Aldrich®) was added. De-methylation on the gene of interest was confirmed by pyrosequencing analysis at the end of each experiment.

2.1.9 shRNA transfection

RNA constructs (shRNA) were designed to target Arginino-succinate synthetase (ASS1) transcripts (Table 2-2) and ligated into a pSilencer vector (Invitrogen) (Figure 2-1). Vector with and without the shRNA constructs were transfected using FuGENE® HD (Roche) in 6-well plates. Briefly, cells were seeded the day before to be 70-80% confluent when transfected. 500 ng of each shRNA was diluted in media without FBS and combined with 1µl transfection reagent at room temperature for 20 min to form complexes. The complexes were then added drop-wise to the cells and left overnight. After the incubation the complexes were removed and 500 µg/ml of Puromycin (Sigma-Aldrich®) added to select for cells expressing the constructs.

Each shRNA was optimised by testing different shRNA and FuGENE® HD concentrations and treating them with the selection drug. Cells were considered stably transfected when there were no live un-transfected cells and the clones resistant to the drug were growing at the same speed of the parental cell line.

Gene silencing was validated on stably transfected cells using real-time PCR and SDS-PAGE electro-blotting.

	shRNA sequence	Loop Sequence	Complementary sequence	Position from the TSS
shRNA1	GCCAAATAGACCCGTGTACAATC	TCTT	GAATTGTACACGGGTCTATTTG	+1587 to +1608 bp +1525 to +1546 bp
shRNA2	AGGAACAAGGCTATGACGTCATC	TCTT	GAATGACGTCATAGCCTTG TTC	+430 to +451 bp +368 to +389 bp

Table 2-2. *ASS1* shRNA constructs.

Two different shRNA oligos were designed to bind both *ASS1* transcripts (NM_000050.4, NM_054012.3). The shRNAs contained the siRNA sequence that would bind the mRNA and inhibit its expression, a loop and a complementary sequence, to generate a hairpin secondary structure. The hairpin structure allowed recognition of the construct by the cellular machinery and generate a functional siRNA. The two oligos target different positions from the transcriptional start site (TSS) on *ASS1* transcripts: the first line in each cell in the last column represents the targeted sequence position on NM_000050.4, the second on NM_054012.3.

bp: base pair.

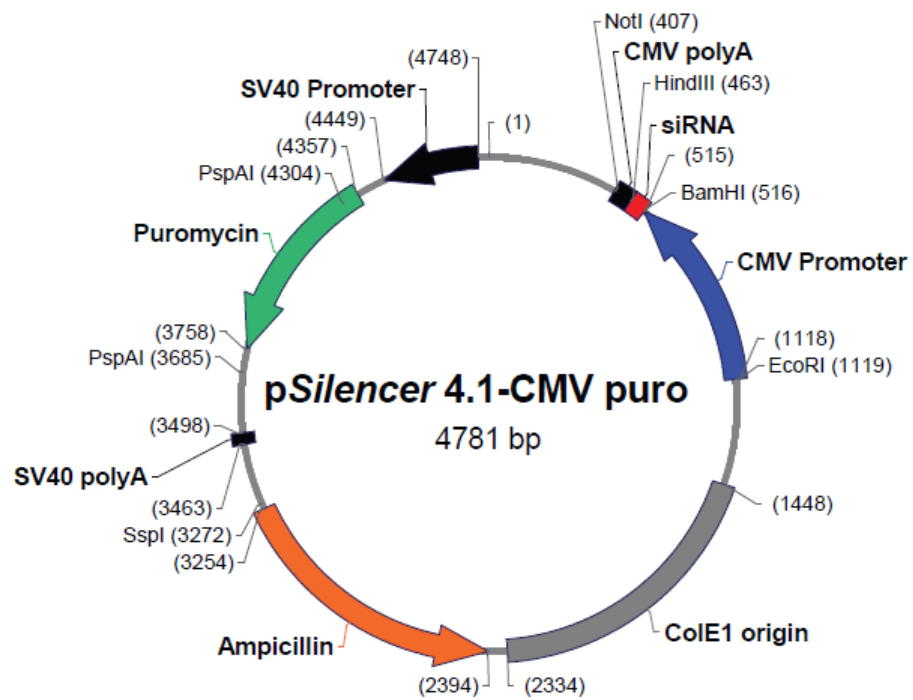


Figure 2-1. pSilencer plasmid.

shRNA:	463–515bp
CMV Promoter:	516–1118bp
CMV pA signal:	404–462bp
SV40 Promoter:	4449–4748bp
Puromycin resistance gene:	3758–4357bp
SV40 pA signal:	3463–3498bp
Ampicillin resistance gene:	2394–3254bp
ColE1 Origin:	1448–2334bp

2.1.10 Plasmid transfection

Glutamine synthetase (*GLUL*) was re-expressed using a commercially available cDNA (derived from clone MSC-19700, ATCC) covering all the complete Open reading frames (ORF). The expression vector pcDNA3.1 (+) (Invitrogen) (Figure 2-2) was used for cloning and expression. Both MSC-19700 and pcDNA3.1 were digested with BamHI and XhoI (New England Biolabs) and ligated using T4 ligase (New England Biolabs) overnight at 16°C. Vectors with and without construct were then amplified using competent *E.coli* DH5 α (Invitrogen) and purified using Plasmid Plus Maxi Kit (Qiagen) as per the manufacturer's instructions. Clones were verified for the correct sequence via sequencing.

Cells were seeded in 6-well plates to be 70-80% confluent when transfected. Briefly, for transfection: 100 ng of each plasmid were mixed with 1 μ l of X-tremeGENE HP (Roche). The mixture was left for 20 min at room temperature to form complexes. The complexes were then added drop-wise to the cells and left overnight. The following day, the complexes were removed and 500 μ g/ml of G418 (Sigma-Aldrich®) was supplemented to the medium to select cells that incorporated the constructs.

Transfected cells were selected using the same criteria as before.

Over-expression of Glutamine synthetase was confirmed by SDS-PAGE electroblotting.

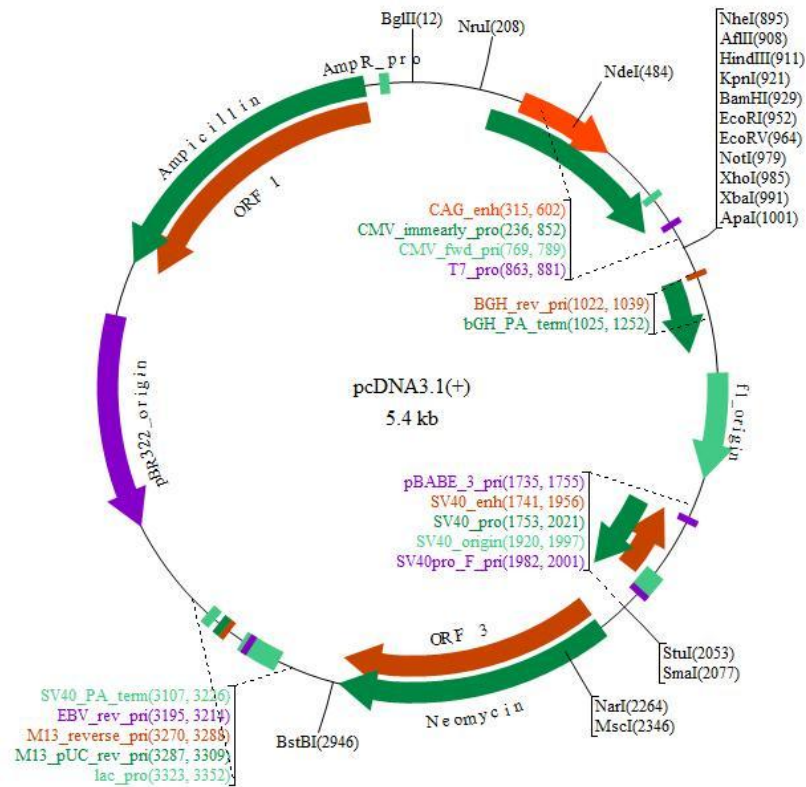


Figure 2-2. pcDNA3.1 (+) plasmid map.

CMV promoter:	232-819bp
T7 promoter/priming site:	863-882bp
Multiple cloning site:	895-1010bp
pcDNA3.1/BGH reverse priming site:	1022-1039bp
BGH polyadenylation sequence:	1028-1252bp
f1 origin:	1298-1726bp
SV40 early promoter and origin:	1731-2074bp
Neomycin resistance gene (ORF):	2136-2930bp
SV40 early polyadenylation signal:	3104-3234bp
pUC origin:	3617-4287bp (complementary strand)
Ampicillin resistance gene (Blazek and Benbough):	4432-5428bp (complementary strand)
Open reading frame (ORF):	4432-5292bp (complementary strand)
Ribosome binding site:	5300-5304bp (complementary strand)
Bla promoter (P3):	5327-5333bp (complementary strand)

2.2 DNA and RNA extraction and analysis

2.2.1 DNA extraction from formalin-fixed paraffin-embedded (FFPE) tissues and cell lines

Total DNA from cell lines was extracted using the DNeasy Blood & Tissue Kit (Qiagen) according to the manufacturer's instructions. Briefly, cell pellets were re-suspended in 200 µl of PBS and lysed by incubation with 200 µl of Lysis Buffer (Buffer AL) and 20 µl of protease (Qiagen) at 56°C for 10 min. The samples were then loaded onto the DNeasy Mini spin columns and centrifuged at 8000 rpm, allowing DNA capture on the column membrane. After two wash steps, DNA was then eluted in 100µl of water.

Genomic DNA was isolated from approximately two 10 µm sections of human formalin-fixed paraffin-embedded tissue (FFPE) using a modified high molecular weight genomic DNA extraction protocol (Sambrook 2001). Briefly, paraffin wax was removed by incubating the samples overnight in 10 ml xylene (Sigma-Aldrich®) and cleared by washing twice in 1 ml pure ethanol (Sigma-Aldrich®). Tissue was digested by incubating in 500 µl lysis buffer (Tris-HCl pH 7.5, EDTA 0.5M, 10% SDS, NaCl 3M) and 0.2mg/ml Proteinase K (Ambion®) at 55°C until completely digested. An equal volume of TE-saturated phenol (Sigma-Aldrich®) was added to the mixture. The mixture was vigorously vortexed, and then centrifuged at 4°C at 14000 rpm for 10 min to enable phase separation. The upper aqueous layer was carefully moved to a new tube, avoiding the phenol. The phenol extraction was repeated, the DNA was precipitated by adding 1.2X volume of isopropanol and centrifuged at 14000 rpm at 4°C for 20 min to form a pellet. Finally it was concentrated by precipitation at -80°C for at least an hour adding 500 µl pure

ethanol, centrifuged at 14000 rpm at 4°C for 2 min and re-suspended in 50 µl of pure water.

Nucleic acids were quantified using a spectrophotometer (Nanodrop, Thermo Scientific). DNA was considered pure when 260/280 ratio was ≥ 1.8 .

2.2.2 DNA bisulphite modification

1 µg of genomic DNA was bisulphite converted using the EZ DNA methylation kit (ZymoGenetix Ltd., Hampshire, UK). The kit is based on a three step reaction that takes place between unmethylated cytosine and sodium bisulphite: unmethylated cytosines were converted to uracil, whereas methylated cytosines remained unchanged. DNA was denatured and protonated by adding 5 µl of dilution buffer in a total volume of 50 µl and incubating at 37°C for 15 min. 100 µl of CT conversion buffer were then added and incubated overnight at 50°C to mediate DNA sulphonation. The next day, the mixture was placed into a Zymo-Spin™ IC column, DNA was washed and converted to uracil by adding desulphonation buffer, which promoted the deamination and desulphonation reaction, leading to the final conversion to uracil (Figure 2-3). Converted DNA was finally eluted in 10 µl of pure water.

Commercial methylated and unmethylated human genomes (Merck Millipore) were used as controls.

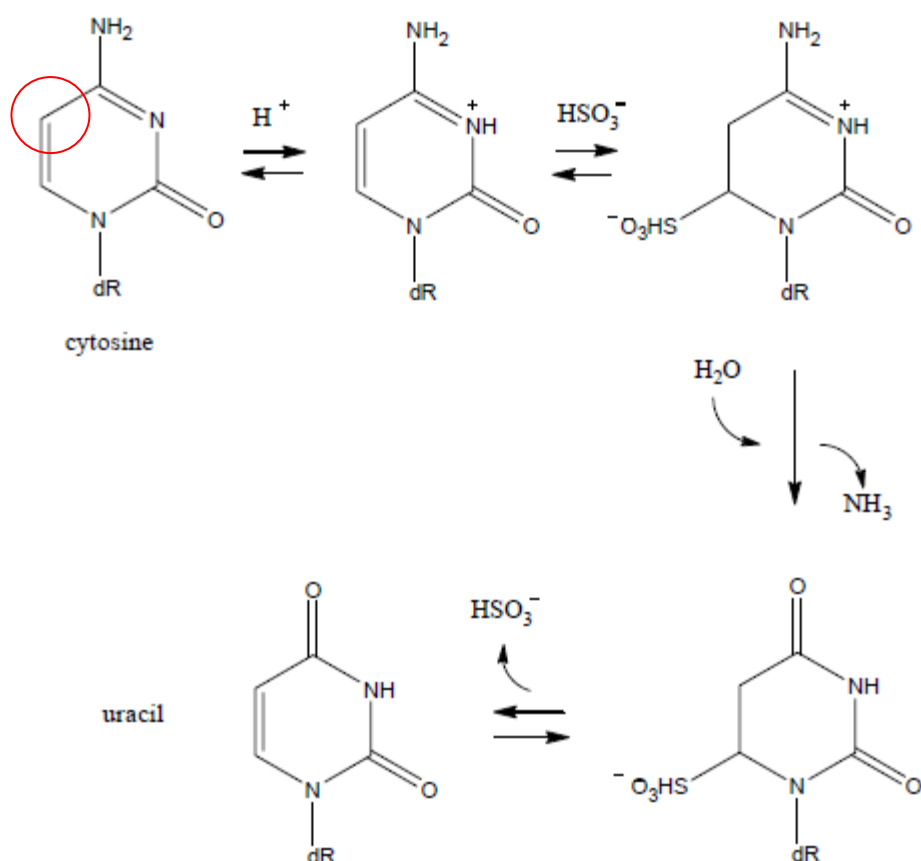


Figure 2-3. Bisulphite conversion reaction.

Bisulphite modification is based on a three step reaction that involves only the unmethylated cytosines. In the first step unmethylated cytosines (red circle highlighted the position on the benzene circle where the methyl-group would be when the cytosine is methylated) are protonated to promote the transformation of cytosine into sulphonate cytosine by bisulphite (HSO_3). During the second step, uracil sulphonate is formed by an overnight incubation. In the last step, uracil is formed by a deamination follow by desulphonation reaction. The highly selective deamination of unmethylated cytosine into uracil is due to the greater steric interference between the methyl-group and the bisulphite. At the end of the conversion reaction the unmethylated cytosine is changed to uracil, whereas the methylated remains unchanged (Biosystem 2007).

2.2.3 450k Methylation array

13 breast cancer cell lines were profiled at the Genome Centre, Barts and the London Medical School, using the Infinium Human Methylation 450 BeadChip (Illumina Inc.). 1 µg of genomic DNA from each cell line, extracted as described above, was screened according to the supplier's standard operating procedures.

The scanned data were first normalised using Genome Studio software (Illumina Inc.) to reduce the differences between the two types of probes used in the array, Infinium I and II. Infinium I probes are designed across the CpG so there are two for each CpG site, whereas the Infinium II are designed immediately adjacent to the CpG so that there is only one for each dinucleotide. After normalisation, the methylation status of each CpG site was presented as β -values, the ratio of the methylated to the total signal.

2.2.4 Bisulphite sequencing

The DNA sequence, as appears after bisulphite conversion (Figure 2-4), was analysed to design overlapping primer sets (Table 2-3) in a region without CpG sites. PCR conditions were optimised for each primer set on the methylated and unmethylated DNA (Merck Millipore) to ensure reduced bias during the amplification.

Each fragment was amplified by PCR using 0.2 µM primers and 2.5 mM MgCl₂, 0.2 mM Deoxynucleotide Triphosphates (dNTPs), 0.05 U/ml AmpliTaq Gold® 360 (Applied Biosystems) in a total volume of 50 µl. DNA was amplified in a GeneAmp® PCR System 9600 (Applied Biosystems) using the following conditions: an initial denaturation at 95°C for 15 min was followed by 95°C for 40

sec, X°C extension temperature depending on the primer set for 50 sec and 67°C for 1 min for 40 cycles, and a final extension step at 72°C for 7 min. PCR products were purified using QIAquick PCR purification kit (Qiagen) as per the manufacturer's instructions. PCR products were eluted in 30 µl of pure water and quantified using a spectrophotometer (Nanodrop, Thermo Scientific).

The purified PCR products were blunt-end ligated into a pGEM®-T Easy vector system (Promega) (Figure 2-5) and transformed into JM109 high efficiency competent cells (Promega) as per the manufacturer's instructions. Colonies were selected using 100 µg/ml ampicillin/0.5 mM IPTG/80 µg/ml X-Gal LB-agar plate (IPTG, X-Gal, agar and LB broth powder from Fisher Scientific). Using the lacZ white/blue screening, ten white colonies (gene integrated in the vector) were picked from each plate and grown separately in 15 ml tubes at 37°C, shaking in 5 ml LB broth media (Fisher Scientific) containing 100 µg/ml ampicillin (Fisher Scientific). Plasmid from each clone was purified using the QIAprep spin Miniprep kit (Qiagen) protocol, as per the manufacturer's instructions, and out-sourced for sequencing (GATC Biotech). Each CpG site in the sequence was examined. Where a cytosine was present the CpG site was considered to be methylated; when there was a thymine the CpG site was considered unmethylated.

TYGATGATTATTTTATTTTGTAGATGAGGAAATTTGGGTTTTGAAAGATTTGTTTAGGGTT
 TG**GTTAGTAGTATGAGATAGG**TTTTTAGATTTAGTTTTTTAT**YG**TTTTTTAGAATTTTTTTTG
 TAAAATTAGAGAAATAGTAY**GT**TGATTTTAAATGTGAAATGGTAGAGTTTTGTTTATTTT
 TTTAGATTTAAGAGAGT**YGGAGYGGGYG**TTTTTTTTAGGTTTTGGGAATTT**YGG**TTTTGTT
 TTTAGGTT**YGYGYGGTATTYGT**TTTTAGTTTAGGTT**YGT**TTAAAGTTTTTT**YGG**TTTT**YGYG**
 TTT**YGYG**TTTTTTTTTAAGTTAATTTTTGTT**YGT**AGGAAG**YGGGGT**YGGAGGTTTTTT**YGT**
 TAATAAAAGGTTAAAT**YGG**TTTTTTGTT**YGT**ATTTTTTTAGGGAGTTTTTT**YGTAA**
 AATTATTTTT**YGTGAAGGYGG**TAGGGTAGAGGTTAGGG**YGG**TTTTGTTGGGAGTT**YGT**
 GGATTT**YGG**TTGGGGGT**YGTGGGGYGT**ATTTGG**YAG**TTGG**YGG**TTGGG**YGGYAG**TT
YAGGTTTTTT**YGG**TTTGG**YGTAA**TT**YGT**TTTTTTGTTTTTAGTTTTTT**YGT**TTT**YGT**TTTTT
 TTTTTTTA**YGTYGT**TTTTGTTTTTTTTTA**YGT**TTTTTTTTTTTTTTTTTTTTTTTAGTT**Y**
GTTTGTTTTTATTTTAG**YGGYGT**YGT**YGG**TTTTTT**YGT**TTAATGGT**YGYGGGG**TT**YGG**
 AT**YGT**ATTAGTTGAT**YGT**TT**YGG**TTTTTGGT**YGTGGGAGTTAATTAGGGTAT**YGGGGG
YGGTTTT**YGG**TY**YGG**GATAAAGGGTG**YGGGG**TTGTTGG**YGT**TTTTGTAGAGT**YAGAGT**
GGGAGAAGAGYGGAG**YGTGTGAGTAGTATTG**YGTTTTTTTTTTTTTTTAATTT**YGT**TTT
YGYGGTTTAGTTTTATT**YGT**TT**YGT**TTTGT**YGYG**ATTAGGTAAGTTTT**YGGAYGG**TT**YGG**
 TGTTA**YGTAAGYAGG****YGYGT**YGTTTTTGTTATT**YGYGAGGYGYGT**YGTTAGTTTTTT
 TTT**YGG**TTGTTTGTTTTTTAGTTTTAGTTTTA**YGT**TTG**YGG**TTTTTT**YGT**TTATGTTGA
 GATT**YGG**TATGAGTGTTTTTTT**YGYGTGTTTTYGT**YGTGGTGGTTGGATT**YGT**YGGGGT
 TGG**YGT**TTGGTGGGG**YGYGT**TTTT**GGTTAGGTTTGGGAAGGGY**GGGTGAGTTGTTTTGA
 TTTTTTTTTTATTATTT**YGG**TYGAAG**YGT**YGTTTTTGGAGGT**YGTGGG**YGTTT**YGT**
 TTTGGGGTT**YGT**AGTGTTTGT**YGT**TTGTGGATGGAGTGG**YGG**TYGGTTTTTTGTGG
 AG**YGTAAATAAGGYGT**TTTGGTTGG**YGYGGGYGT**TTGGTTGTTTTTT**YGTGG**TGGGGTTT
 TYGGAGTAAT**YGT**TTTGGTTTGG**YGT**ATGGTTGAGAY**GT**TT**YGT**ATT**YGGYGT**GTAA**YGT**
 GTGAG**YGT**TTGTTTGGG**YGT**YGT**YGT**TTTT**YGT**TT**YGGGG**TTTT**YGGGG**TTTTTAATGTGAT
YGAATAATGGAGAGTTYGGGTT**YGGYGT**AGTTAGTGGAGAAGT**YGT**TT**YGGYGG**AG
 GTAGTAGTAG**YGYGT**AGTTTTTA**YGT**TTT**YGT**TTTTATTTTTTT**YGT**ATTTTTTAATTTT
 TYGG**YGG**TAGGGTATGGTTATTT**YGT**GAGGTTT**YGT**AGATT**YGGAYGGGGG**TT**YGT**AGGGG
 TAGGG**YGT**TTATTTTAGGGATATTTAGTGGGAAGGGGTTGTTTTTAAAGTGGATAATTA
 TAATTTTT**YGGGGGYGGGAAGYGGG**ATTTTTTTTTTAGT**YGTAA**AGTTA**YGAAGAA**AGTA
 A**YGAATGAAAATTATGAAGATAAYGAGAAGTAGATTTTTYGGG**Y**YGT**TTTTAGTTG
 TTT**YGT**TT**YGT**YGTATTATTTGTGAATTT**YGGGGAGAGATTYGT**AGTTAAGATTAAGATT
 TTAATTTATTAATTTGTTGTT**YGT**ATTTTT**YGG**TYGT**YGT**TTGTTTGTTTTTTTTTTTT
 AT**YGT**TTTTTTTTTAGAAAGTT**YGT**GTTTGGATTAGTTA**GAGTTTGAGAAAGAGGAGAG**
GYGYGAA**YGT**ATTATTTAAAAAGAGAAGGGTTAAAGAGGGTAATTTTAA**YGTATA**YGT**YGT**
 ATTTTTTGTGGTTGGGGTGAGTGAGGGGGTAGGGAGGA**YGT**ATT**YGGAG**TTGGTGGGAG
 TTGTAGAAATTGTTGAAAATTTTAGAATTTATTTTTTTA**YGTAA**ATTGGTAT**YGT**AGTA
 GTAGTAGTTGATAGAGTGGTATTAGGTTGT

Figure 2-4. *GLUL* CpG island.

Primer sets designed on the Glutamine synthetase (*GLUL*) CpG island converted sequence. All CpG site are marked in red and all the cytosines in those sites were annotated to Y as per IUPAC convention. Finally all the cytosines in the sequence that were not within a CpG site were converted to thymine (homologous to uracil in the DNA sequence). Three primer sets, identified in three different colours, were design to generate overlapping fragments and ensure complete sequence coverage.

	Forward primer	Reverse primer	Fragment length	Annealing Temperature
GLUL_1	GGTTAGGTTTTGGGAAGGG	CCTCTCTCCTCTTTCTCAAACCTC	841 bp	60°C
GLUL_2	GTTGGGAGTTAATTAGGGTAT	TCAAAACAACCTCACCCC	392 bp	56°C
GLUL_3	GGGCCC GTTAGTAGTATGAGATAGG	CCCCTCTTCTCCCACTCTC	762 bp	56°C

Table 2-3. Bisulphite sequencing PCR primer sets.

Three different sets of primers were designed to cover the *GLUL* CpG island. Commercial methylated and unmethylated DNA from human genome (Merck Millipore) was used to optimise the three primer sets (Figure 2-4) to ensure the same efficiency on different methylation status.

T annealing: annealing temperature of for each primer pair. bp: base pair number.

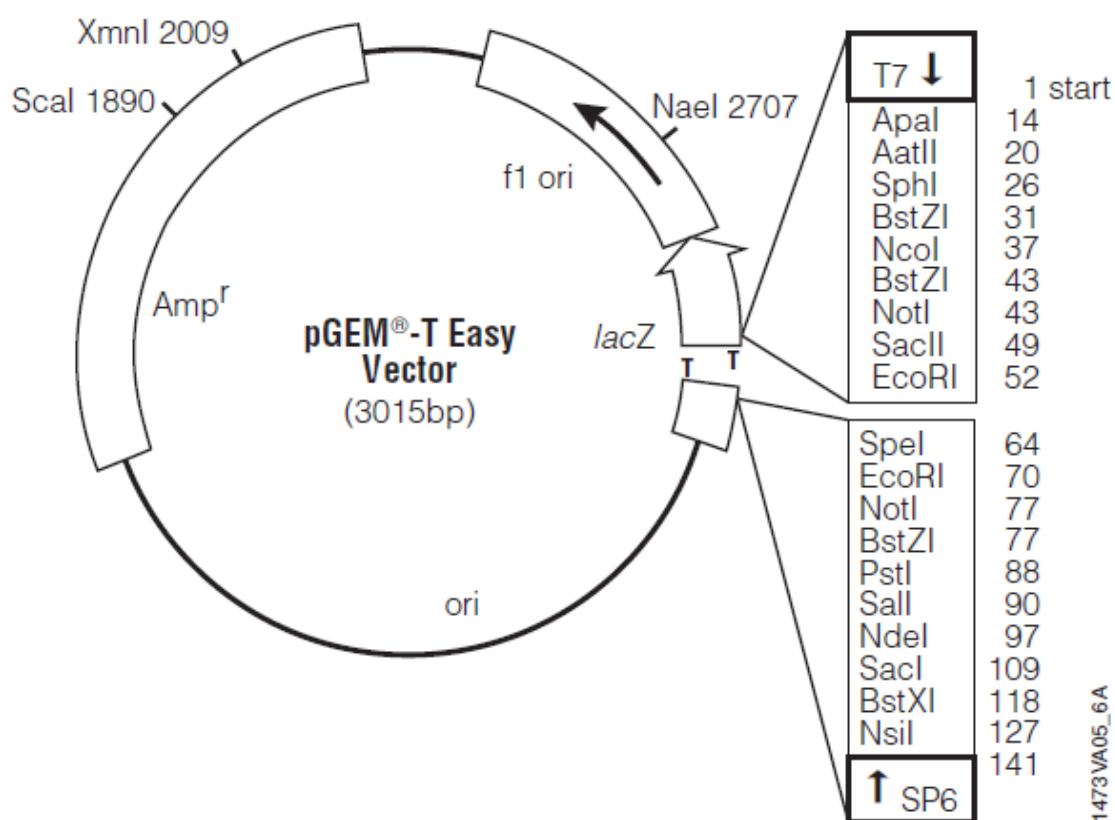


Figure 2-5. pGEM®-T vector map and reference points.

T7 RNA polymerase transcription initiation site	1
multiple cloning region	10–128
SP6 RNA polymerase promoter (↑SP6), for sequencing	(–17 to +3) 139–158
SP6 RNA polymerase transcription initiation site	141
pUC/M13 Reverse Sequencing Primer binding site	176–197
<i>lacZ</i> start codon	180
<i>lac</i> operator (LacZ), for X-gal based colour screening of the colonies	200–216
β-lactamase coding region (<i>Amp^r</i>) that confers ampicillin resistance	1337–2197
phage f1 region (<i>f1 ori</i>)	2380–2835
<i>lac</i> operon sequences	2836–2996, 166–395
pUC/M13 Forward Sequencing Primer binding site	2949–2972
T7 RNA polymerase promoter (↓T7), for sequencing	(–17 to +3) 2999–3

2.2.5 Pyrosequencing analysis

PCR primers (Table 2-4) were designed to amplify a fragment across a representative region of about 200 bp in the CpG island in each gene of interest. 200 ng of bisulphite converted DNA and 0.2 μ M primers were used during each PCR reaction in a GeneAmp® PCR System 9600 (Applied Biosystems) using a PyroMark PCR Kit (Qiagen) in a total volume of 30 μ l using the following conditions: an initial denaturation at 95°C for 15 min was followed by 94°C for 30 sec, X°C depending on the gene of interest for 30 sec and 72°C for 30 sec for 40 cycles, and a final extension at 72°C for 7 min.

PCR products were separated by electrophoresis on a 1% agarose gel to confirm presence of products and absence of contamination. PCR products were incubated and mixed with Streptavidin beads (GE Healthcare) for 15 min at 1400 rpm, binding the biotinylated primers to the immobilised streptavidin conjugates. The complexes were then washed to remove any contaminants from the PCR amplification, using PyroMark Q96 Vacuum Prep Workstation (Qiagen), and denatured for 2 min at 80°C to leave single strand sequences bound to each bead. Finally, PCR products were sequenced on a PyroMark Q96 ID (Qiagen), using the un-biotinylated primer. The pyrogram shows a sequence of peaks over a DNA sequence corresponding to the region of interest. Each peak represents the amount of the specific nucleotides incorporated into the sequence. Pyromark CpG Software (Qiagen) was used to analyse the CpG site methylation percentage by calculating the ratio between the methylated and the total methylated and unmethylated peaks (Figure 2-6).

Commercial methylated and unmethylated DNA (Merk Millipore) was used during each reaction as positive and negative controls respectively.

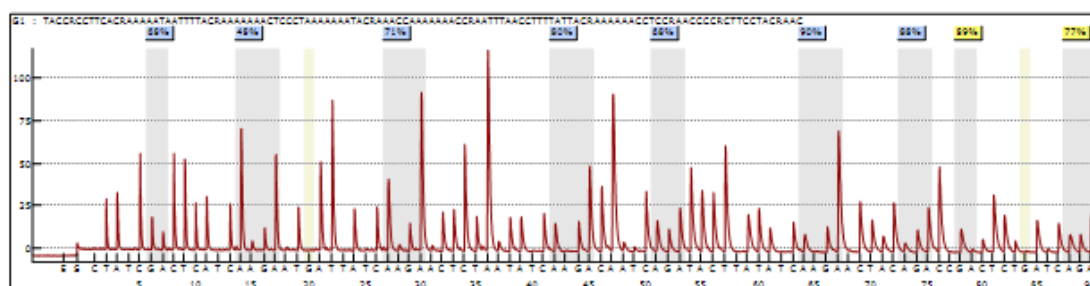
	Forward primer	Reverse primer	Fragment length	T annealing
GLUL	[BTN]GGTTTTTTTAGGTTTGGGAATTT	CCCTAAACCTCTACCC	255 bp	58°C
ASS1	[BTN]TGTGTTTATAATTTGGGATGG	CCTCCTCCTCTAAACCC	107 bp	56°C

Table 2-4. Pyrosequencing primer sets.

Representative region on Glutamine synthetase (*GLUL*) and Arginino-succinate synthetase (*ASS1*) analysed by pyrosequencing. Primers were optimised using commercial methylated and unmethylated human genome DNA (Merck Millipore) to ensure the same efficiency with different methylation status. Each primer set consisted of a biotinylated (BTN) and a un-biotinylated primer: the biotinylated primer is necessary for the binding with the streptavidin beads (GE Healthcare) and the un-biotinylated as sequencing template.

T annealing: temperature of annealing for each set of primer. bp: base pair number.

A)



B)

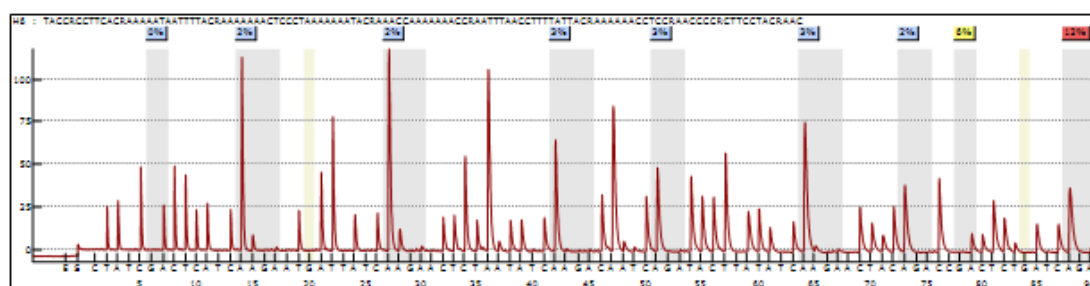


Figure 2-6. Pyrograms from methylated and unmethylated DNA.

Representative examples of pyrograms from A) methylated and B) unmethylated DNA. The pyrogram shows a sequence of peaks over a DNA sequence corresponding to the region of interest. The sequence analysed in this examples is *GLUL*. Each peak represented the amount of the specific nucleotides incorporated into the sequence. Pyromark CpG Software (Qiagen) analysed the CpG site methylation percentage over each CpG site. The software colour-codes the results based on the confidence level of the quantification and how strong the signal is over the background noise in each sequence: from blue for a high reliable quantification to red for a low reliable value.

2.2.6 Chromatin Immuno-Precipitation (ChIP)

Cells were seeded in 150 mm dishes (Corning) and detached, pelleted and washed twice in 1ml of PBS when 80-90% confluent. Pellets were incubated on ice for 20 min in 500 µl of nuclei isolation buffer (20 mM Tris-HCl pH 7.5, 10 mM NaCl, 0.2% NP-40, and 3 mM MgCl₂) and protease inhibitors (cOmplete, Mini, EDTA-free Protease Inhibitor Cocktail, Roche) to isolate the nuclei. The solution was then passed through a 25-gauge needle 10 times to break up the cell membranes and the nuclei pelleted at 3000 rpm for 10 min at 4°C. The DNA and any proteins bound to it were then fixed by incubating the nuclei in 1 ml solution of PBS and 1% formaldehyde without methanol (Polyscience, Inc.) for 8 min at room temperature. The reaction was stopped by the addition of 125 mM glycine (Sigma-Aldrich®). Nuclei were pelleted at 2000 rpm for 2 min at 4°C to remove the formaldehyde and re-suspended in 500 µl of SDS lysis buffer (50 mM HEPES pH7.5, 140 mM NaCl, 1 mM EDTA pH 8.0, 1% Triton X-100, 0.1% Sodium Deoxycholate, 0.1% SDS). The solution was sonicated for 15 cycles 30''ON 30''OFF using Bioruptor® Twin (Diagenode). Membrane debris were discarded after centrifugation at maximum speed for 20 min at 4°C and DNA-protein complexes diluted 10 fold in IP buffer (150 mM NaCl, 10 mM Tris-HCl pH 7.5, 2 mM EDTA, 0.1% NP-40 with protease and phosphatase inhibitors). 10 µl of the diluted complexes were incubated at 4°C overnight with 4 µg of anti-acetylated Histone3 (rabbit polyclonal, 06-598, Merck Millipore) antibody, anti-acetylated Histone4 (rabbit polyclonal, 06-599, Merck Millipore) antibody or anti-mouse IgG (rabbit polyclonal, ab46540, Abcam) antibody, in 500 µl of IP buffer containing 0.5% bovine serum albumin (BSA) (Sigma-Aldrich®) and 200 ng/ml of Salmon Sperm DNA (Sigma-Aldrich®). At the end of the overnight incubation, 10 µg of secondary antibody (goat anti-rabbit,

polyclonal, AP132, Merck Millipore) was added for 1 hour, followed by 1 hour incubation with 40 μ l of Magna CHIP™ Protein G Magnetic Beads (Merck Millipore). The beads bound to the Fc region of the antibodies, mediating their pull down, along with attached DNA-protein complexes. Beads and DNA-protein complexes were washed with 1 ml of IP buffer for four times at 5 min each and the cross-linker was removed by incubating the sample overnight at 65°C in 100 μ l of elution buffer (0.1% SDS, 200 mM NaCl, 100 mM NaHCO₃). The magnetic beads were then removed and the DNA purified using QIAquick PCR Purification Kit (Qiagen) according to the manufacturer's instructions, and eluted in 50 μ l of pure water.

Purified DNA was analysed by SYBR Green qPCR for enrichment at different positions on *GLUL* promoter regions and on the promoter region of positive and negative controls genes (Table 2-5). 1 μ l of eluted DNA was amplified using SYBR® Green PCR Master Mix (Applied Biosystems) as follows: an initial denaturation at 95°C for 2 min, followed by 95°C for 15 sec and 60°C for 1 min for 40 cycles, 95°C for 1 min and 65 °C to 95 °C at 2 °C / sec on a MX3000 (Stratagene, Agilent Technologies). The DNA enrichment Δ Ct was determined as the difference between the Ct from each pull-down reaction with the specific antibody, and the one from input DNA without antibody. The method was verified by ensuring that the controls, anti-IgG-mediated and negative pull-down were null compared to those obtained from the anti-Histone3 and anti-Histone4 antibodies. The specific gene enrichment was calculated as $\Delta\Delta$ Ct of the region of interest versus a non-expressed gene, Haemoglobin 2 α (H2A). *GAPDH* and *RPLP0* were analysed for DNA enrichment about 1000 bp upstream their transcriptional start site (TSS) as positive controls of the CHIP reaction, as they were constitutively expressed in the cell lines.

Assay ID	Forward primer	Reverse primer	Position to the TSS
5000	TCAACTTCTGGCTGGGTCTT	AGGAAGGCTCCCAAAGAAAA	-5128 to -4988 bp
2500	CATCTGCGCCCTAATTTTCAT	GCAGCACCATCAAGAGAACA	-2564 to -2275 bp
500	ACATTTTCCCAACCATCACG	GCAGCTGAAAGGAAATCGAG	-635 to -480 bp
GLUL	TTCCCCAGACCCAAGAGAG	GAACCAGGGAAACCGAATTT	-226 to -25 bp
GAPDH	CGGCTACGCGGTTTTTACG	AAGAAGATGCGGCTGACTGT	-1455 to -1276 bp
RPLP0	CACTGCTAACAGGGCTGACA	G TTCAGTTGGCGGATGACTT	-1608 to -1412 bp
HBA2	CTGGCAAACCATCACTTTT	GCTCTGGGTAGGGAAAGGC	-1077 to -929 bp

Table 2-5. ChIP qPCR primer set.

DNA enrichment was investigated at different positions from the transcriptional start site (TSS) on *GLUL*: approximately 5000 base pair (bp) (5000), 2500 bp (2500), 500 bp (500) upstream the TSS and on the TSS (*GLUL*). Large Ribosomal Protein p0 (*RPLP0*) and Glyceraldehyde-3-phosphate dehydrogenase (*GAPDH*) genes were used as positive control as these genes are constitutively expressed in the cells. *HBA2* was used as negative controls as this gene is not expressed in the cell lines used for this experiment. All the control assays were designed to cover a region of the promoter around 1000 bp upstream the TSS of each gene.

2.3 RNA and protein extraction and analysis

2.3.1 RNA extraction from cell lines

Total RNA from cell lines was extracted using the TRI Reagent (Ambion®) following standard laboratory protocol (Sambrook 2001). Briefly, the cells were homogenised in 1 ml of TRI Reagent, followed by 100 µl of 1-bromo-3-chloropropane (Sigma-Aldrich®). The solution was vigorously vortexed and centrifuged at 10000 rpm at 4°C for 20 min to enable phase separation. The upper aqueous layer was carefully moved in to a new tube avoiding disruption of the interphase. RNA was washed adding 1.2X volume isopropanol and concentrated with 1 ml of 75% ethanol. The RNA pellets were eluted in 50 µl of pure water.

RNAs were quantified using a spectrophotometer (Nanodrop, Thermo Scientific). RNA was considered pure when the ratio of absorbance at 260/280 was approximately 2.

2.3.2 Gene expression analysis

100 ng of RNA was reverse-transcribed into cDNA using the High Capacity cDNA Kit (Applied Biosystems) per manufacturer's instructions in a geneAmp® PCR System 9600 (Applied Biosystems) as follows: 25°C for 2 min was followed by 37°C for 2 hours and 85°C for 5 min.

Gene transcript levels were determined by semi-quantitative real-time PCR using TaqMan® gene expression assay: Hs000374213_m1 for Glutamine synthetase (*GLUL*), Hs00540723_m1 for Arginino-succinate synthetase (*ASS1*) and Hs00999901_s1 for Ribosomal Large protein p0 (*RPLP0*) (Applied Biosystems).

Each real-time reaction was repeated in assay triplicate using 1 ng of cDNA in a 10 µl reaction, using the following PCR reaction: an initial denaturation at 95°C for 2 min, followed by 95°C for 15 sec and 60°C for 1 min for 40 cycles on a MX3000 (Stratagene, Agilent Technologies). Real-time PCR results were represented by a threshold value (Ct). qPCR results were then normalised by subtracting *RPLP0* values from *GLUL* and *ASS1* results, generating the Δ Ct, followed by calculation of the antilog of the calculated Δ Ct. $\Delta\Delta$ Ct was calculated as difference between the Δ Ct between the treated and untreated cells, when available, and used to determine the fold change. The final quantifications across the three biological replicates were then averaged and the standard deviation calculated for each sample.

2.3.3 Protein analysis

2.3.3.1 SDS-PAGE electro-blotting in reducing conditions

The presence of Glutamine synthetase (GS) and Arginine-succinate synthetase (ASS1) in each sample was analysed by SDS-PAGE electro-blotting in reducing conditions using standard laboratory protocol (Abcam). Briefly, cells were lysed in 100 µl of RIPA buffer (150 nM sodium chloride, 1% Triton-X100, 0.5% sodium deoxycholate, 0.1% sodium-dodecyl-sulphate (SDS), 50 nM Tris-HCl, pH 8.0) with the addition of protease inhibitors (cOmplete, Mini, EDTA-free Protease Inhibitor Cocktail, Roche) at 4°C under agitation for 30 min. Purified proteins were quantified using the DC Protein assay (BioRad Laboratories) as per manufacturer's protocol in a 96-well plate. Briefly, each protein solution was diluted in a 96-well plate well and a mix of reagent A and S (alkaline copper tartrate solution) was added to each well prior to reagent B (dilute Folin Reagent). The assay is based on the reduction of Folin reagent by the protein treated with alkaline copper tartrate solution, leading to

colour development which is analysed by absorbance after 15 min incubation at room temperature at 750 nm in a plate reader (Biotek Synergy HT). Each sample was analysed in duplicate and concentration was determined using a standard curve of bovine serum albumin (BSA by Sigma-Aldrich®).

After protein quantification, each sample was diluted in 2X Laemmli buffer (4% SDS, 10% β -mercaptoethanol, 20% glycerol, 0.04% bromophenol blue, 0.125 M Tris-HCl) and denatured at 95°C for 15 min.

20 μ g of total protein from each sample and 4 μ l of PageRuler™ Prestained protein ladder (10-170 kDa, Thermo Scientific) were separated according to their molecular weight using a poly-acrylamide gel. Protein were firstly stacked for 10 min at 100 V in a 4% poly-acrylamide gel (0.1% SDS, 0.5 M Tris-HCl), and then resolved into a 10% gel (0.1% SDS, 1.5 M Tris-HCl) for 1 hour at 180 V.

Proteins were then transferred from the polyacrylamide gel to a PVDF membrane (GE Healthcare) by electro-blotting. The gel and the membrane were clamped together in a paper and sponge sandwich (sponge, paper, gel, membrane, paper, sponge) removing any trapped air that may interfere with the protein migration. The sandwich was submerged into a transfer buffer (25 mM Tris-base, 190 mM glycine, 20% methanol) and 300 mA was applied for 1 hour using a Bio-Rad chamber (BioRad Laboratories) to transfer the protein onto the PVDF membrane.

The membrane was incubated with 5% skimmed milk powder (Fisher Scientific) in TBS-T (0.1% Tween-20, 50 mM Tris-HCl, 150 mM NaCl up to 1 L in water, pH 7.6) for 1 hour at room temperature to block any non-specific binding in subsequent antibody incubations. The primary antibody (Table 2-6) was diluted in 5% skimmed milk solution and incubated overnight at 4°C, and then washed in TBS-T for 30 min.

The membrane was then incubated with the secondary antibody in TBS-T for 1 hour at room temperature following by washing in TBS-T for 30 min.

The detection signal was generated after 5 min incubation using ECL plus solution (GE Healthcare). A chemi-luminescence reaction between the Horseradish Peroxidase (HPX) on the secondary antibody and the substrate generates a light signal detected by G:BOX iChemi XT software (Syngene) using a G-BOX Syngene (Syngene).

In some experiments, membranes were stripped by washing in stripping solution (200 mM glycine, 3.5 mM SDS, 0.1% Tween 20 in 1 L water, pH2.2) for 30 min.

The membrane was then treated as described above.

The intensity of each band was quantified using the densitometry measurement tool Gene Tools software (Syngene) and compared to the loading control, β -actin (Cell Signalling). Blots presented in this thesis are a representative image from a minimum of three biological replicates averaged with standard deviation.

First antibody		Secondary antibody	
Antibody clone and company	dilution	Antibody company	dilution
GS 610517, BD Transduction Laboratories™	1:5000	Anti-Mouse #7076, Cell Signalling Technologies™	1:1000
ASS1 611700, BD Transduction Laboratories™	1:2500	Anti-Mouse #7076, Cell Signalling Technologies™	1:1000
β-actin 13E5, #4970, Cell Signalling Technologies™	1:2000	Anti-Rabbit #7074, Cell Signalling Technologies™	1:2000

Table 2-6. Antibodies used in SDS-PAGE electro-blotting.

Glutamine synthetase (GS) and Arginino-succinate synthetase (ASS1) levels were analysed using SDS-PAGE electro-blotting. Each signal was then compared to a loading control, β-actin, which was shown to remain stable regardless of treatment.

2.3.3.2 Native gel separation

Proteins were analysed in their native form by Native gel using the Abcam protocol (Abcam). Cells were lysed and proteins quantified as previously described. After protein quantification, each sample was diluted in non-reducing 2X Laemmli buffer (25% glycerol, 1% bromo-phenol blue, 62.5 mM Tris-HCl pH6.8).

40 µg of total proteins from each sample and 10 µl of HiMark™ Prestained HMW protein standard (31-460 kDa, Invitrogen) were separated in 1X Novex® Tris-Glycine Native Running Buffer (Life Technologies) according to their molecular weight using the Novex® NativePAGE™ Bis-Tris Gel System (Life Technologies) for 4 hour at 80 V. Proteins were then transferred to a PVDF membrane (GE Healthcare) and analysed as described before.

2.4 Clinical samples

2.4.1 Cuneo's cohort

151 primary breast cancer and 20 samples of normal breast tissues were obtained as paraffin-embedded tissues, after informed patient consent and local ethics committee approval, from S.Croce-Carle Hospital (Cuneo, Italy). DNA from slices of paraffin-embedded tissue blocks was extracted and analysed by pyrosequencing as described above.

2.4.2 Tissue Micro-Array

89 paraffin embedded tissues from Cuneo's Tissue bank, were used as starting material to generate a Tissue Micro-Array (TMA) at Basel University Hospital, Switzerland. TMAs in an agarose block were generated according to the supplier's standard protocols.

Tissue Micro-array were stained and scored for Glutamine synthetase expression at Barts Cancer Institute (Queen Mary University of London) using the anti-Glutamine synthetase antibody used previously in SDS-PAGE electro-blotting (610517, BD Transduction Laboratories™).

2.4.3 In silico dataset

523 primary breast cancer patients' methylation and clinical data were available and downloaded from The Cancer Genome Atlas (TCGA) Data Portal (<https://tcga-data.nci.nih.gov/tcga/>). Primary breast cancer tissues were analysed using 450k

methylation array (Illumina Inc.) as described previously. No normal tissues were included in the cohort.

2.5 Statistical analysis

2.5.1 Survival analysis

Difference in methylation status between normal and tumour samples were analysed using Receiver Operating Characteristics (ROC) curves on SPSS (IBM Software). In the ROC curve the straight line represents the null hypothesis that there is no difference between the two datasets. The other line shows the distribution of the experimental data as sensitivity (ability to recognise true positive) and 1-specificity (ability to recognise false positive). The area between the two lines represents how accurate the test is to discriminate between the two populations examined: the closer to 1 the better the test is. Methylation cut-off was determined using the mean methylation of the normal tissue plus three standard deviations. Tumour samples were therefore divided into hyper-methylated and hypo-methylated. Methylation was analysed statistically as scale variable by non-parametrical Wilcoxon-Mann-Whitney (two variables) or Kruskal-Wallis One-way ANOVA (for more than two variables) test for age, ER and PR expression, Her2 expression, grade, tumour size and nodal status.

Overall survival was defined as the period between surgery and death or the last time the patient was recorded. Differences in survival between hyper- and hypo-methylated patients were investigated using Kaplan-Meier survival curve and compared by means by log-rank test on SPSS (PASW Statistic 18 for PC). Significance was reached when the p-value was less than 0.05. When the survival analysis were significant, the COX progression-hazards regression model was used to determine the Hazard-Ratio (HR) and to investigate the possible confounding effects, such as age, ER-PR expression, Her2 expression, tumour size and nodal

status. The HR represents the risk of the event to occur in one of the population versus the other, with 95% probability to vary into the confidence interval (C.I.).

2.5.2 *In vitro* data statistical analysis

In vitro experiments were analysed as biological triplicates by One-way or Two-way ANOVA based on the experimental set-up using Prism 6.0 (Graph Pad).

Sensitivity or resistance to a specific drug was determined using Inhibitory Concentration 50 (IC₅₀) analysis on Prism 6.0 (Graph Pad) by determining the concentration at which half-maximum effect is obtained. Briefly, different drug concentrations were Log₁₀ transformed and the Optical Density (OD) from the survival analysis normalised to set the highest value as 100% and an OD reading of zero as 0%. Non-linear regression for normalised dose-response-inhibition was then applied to obtain the IC₅₀ values for each dataset. IC₅₀ from biological replicates were then averaged and the standard deviation determined. Statistical significance between IC₅₀ values at specific time points were tested using the non-parametric Mann-Whitney test.

3 Glutamine synthetase

3.1 Introduction

Glutamine (gln) is the most abundant amino acid in serum, in which it plays a role as carrier of ammonia. Its major role within the cell is as a substrate for the TCA cycle and macromolecule intermediate for nucleic acids and protein synthesis (Fuchs and Bode 2006, Yuneva 2008, DeBernardis and Cheng 2010). The observation that immortalised cells are unable to grow in glutamine limited conditions first emphasised the relevance of this amino acid in cancer biology (Warburg 1956, Yuneva et al. 2007). Recently, glutamine limitation has been shown to inhibit cell growth and invasion in prostate cancer (Fu et al. 2011) and in breast cancer, in a subtype-dependent manner (Kung et al. 2011).

Lack of glutamine in cancer cells activates autophagy via the mTOR and glutamine synthesis by up-regulation of Glutamine synthetase (Wang and Watford 2007, Chiu et al. 2012). The two pathways co-operate to restore glutamine concentration to normal levels (van der Vos et al. 2012). mTOR, once activated, translocates onto the lysosome surface and increases autophagy flux to replace metabolic intermediates and any amino acids that are in short supply (Eng and Abraham 2010, Gomes et al. 2011, van der Vos et al. 2012). The pathway is then inhibited via glutamine when the concentration returns to normal levels (Duran et al. 2012) (Figure 1-7). Glutamine absence also promotes the PI3K-AKT pathway activation causing FOXO3A

translocation into the nucleus. FOXO3A binds to the Glutamine synthetase promoter region and up-regulates the gene (*GLUL*) (van der Vos et al. 2012).

Glutamine synthetase (GS) is the only enzyme in human cells that can synthesise glutamine using glutamate and ammonia as substrates (Dang 2010). This role places it in a perfect position as target of synthetic lethality under glutamine deprivation conditions. Glutamine synthetase level has already been shown to correlate with tumour grade and to influence the response to treatment, although the mechanisms involved are still poorly understood (Reinert et al. 2006, Di Tommaso et al. 2009, Dal Bello et al. 2010). Glutamine synthetase (GS) protein levels have been correlated to hepatocellular carcinoma patients' response to specific treatments, such as Radiofrequency Thermal Ablation (RFTA) (Dal Bello et al. 2010) and L-asparaginase administration (Reinert et al. 2006). High level of the enzyme correlates with a decrease in progression-free survival after RFTA treatment (Dal Bello et al. 2010) and development of resistance to L-asparaginase therapy (Reinert et al. 2006). GS is not only linked with response to treatment, but has also been validated as a marker of highly malignant hepatocellular carcinoma (Di Tommaso et al. 2009, Dal Bello et al. 2010).

Although Glutamine synthetase (*GLUL*) gene has been shown to be differentially expressed in breast cancer sub-types (Kung et al. 2011) and proven to be induced in cancer cells via multiple pathways (Medina 2001, Haghighat 2005, Liu et al. 2012, Miller et al. 2012, van der Vos et al. 2012), its epigenetic regulation has not been investigated.

The aim of this section of the thesis was to evaluate the epigenetic modulation of Glutamine synthetase, primarily via DNA methylation, and the presence of a subset of breast cancer characterised by *GLUL* silencing. Epigenetic silencing of *GLUL* would make cancer cells unable to up-regulate the gene in minimal glutamine conditions. Glutamine depletion would be therefore lethal for these cells but not for healthy cells, therefore leading to synthetic lethality. Should the hypothesis be confirmed, Glutamine synthetase would be a potential predictive biomarker of sensitivity to glutamine-depletion treatment in breast cancer.

3.2 Epigenetic regulation

3.2.1 Methylation analysis

3.2.1.1 450k methylation array

Large scale methylation screening was used to identify novel targets of synthetic lethality in breast cancer. 13 breast cancer cell lines were screened using the 450k Methylation array to identify aberrant methylated region(s). The array is designed to analyse different regulatory regions covering more than 485,000 CpG sites in the human genome. The probes are distributed mainly to cover CpG islands but they also include the Shore (2.5 kb up- and down-stream each CpG Island) and Shelf regions (2.5 kb up- and down-stream the Shore), 5'UTRs, gene bodies and 3'UTRs (Illumina 2012).

Based on the 450k Methylation array screening, Glutamine synthetase (*GLUL*) was identified as highly methylated in a subset of breast cancer cell lines (4/12). As shown in Figure 3-1, a highly variable region of methylation was found within the *GLUL* CpG island. Based on the methylation status of the seven probes in this region, breast cancer cell lines can be divided into *GLUL* highly methylated and *GLUL* unmethylated. *GLUL* methylation was found between 46% and 98% in the highly methylated cells and between 1.5% and 11% in the unmethylated cells. Highly methylated cells were found to be predominantly Her2 positive, the only exception was the MDA-MB-468 triple negative cell line. It is worth noting that no significant variation was found in the S-Shore, N-Shore, N-shelf and gene body. The

methylation was limited to 57-95% in the S-Shore, 7-15% in the N-Shore, 71-83% in the N-Shelf and 54-97% in the gene body.

The variation seen in *GLUL* CpG island places it in a very interesting position as an epigenetic-regulated gene. If it is true, high level of methylation in the gene regulatory region should cause the gene silencing, and highly methylated cancer cells would have null gene expression and translational level.

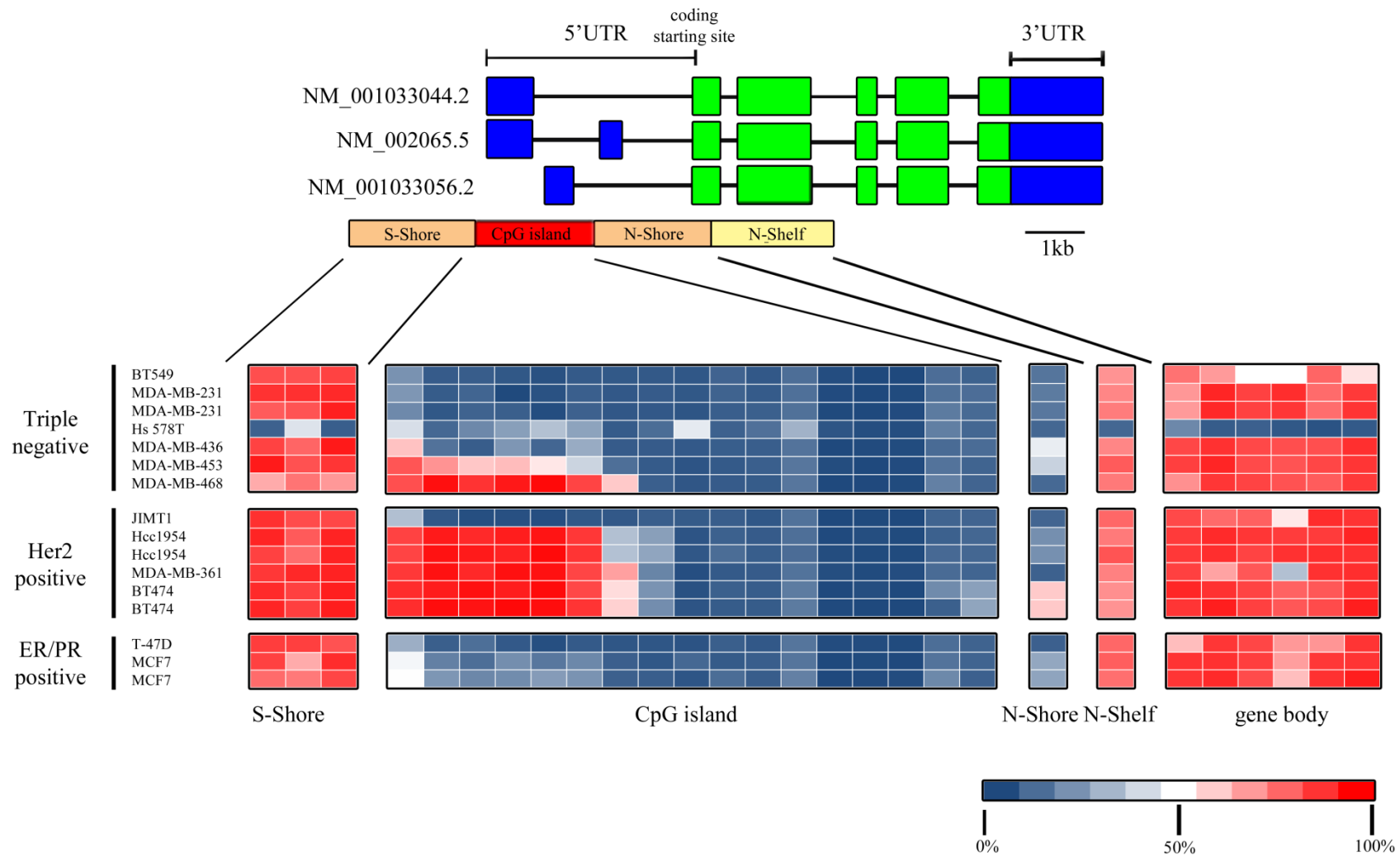


Figure 3-1. Methylation array analysis for Glutamine synthetase.

GLUL is located on chromosome1 q23 and includes three different transcripts (NM_001033044.2, NM_002065.5, NM_001033056.2) encoding the same protein. Exons are in green, 3'UTR and 5'UTR in blue, CpG island in red, S-Shore and N-Shore in orange, N-Shelf in yellow.

The transcripts share the same coding region, composed of 5 exons and the same 3'UTR, but differ in the 5'UTR. NM_001033044.2 and NM_002065.5 has the same transcriptional start site (TSS) and the same first exon but the second has an extra exon in the 5'UTR. NM_001033056.2 has a different transcriptional start site downstream the others with only one exon in the 5'UTR.

The panel of cell lines was divided into subtypes: 6 triple negative, 4 Her2-positive and 3 Her2-negative ER/PR-positive cells. The results are colour-coded based on the β -value: red corresponds to high methylation (100%) and blue to low methylation (0%).

3.2.1.2 Bisulphite sequencing validation

Based on the 450k Methylation array data, a region at the 5'UTR of Glutamine synthetase CpG island was identified as highly variable across the panel. To verify this result, the *GLUL* CpG island was analysed in a selection of cell lines using bisulphite sequencing.

One cell line per subtype was included in the analysis: MDA-MB-231 (Triple negative), JIMT1 (Her2-positive), MCF7 (hormone-receptor positive), and Hs 578T as it is unmethylated across all the probes in the 450k Methylation array (Figure 3-1). As shown in Figure 3-2, bisulphite sequencing confirmed the most variable region of methylation status as covering the first 26 CpG sites, ranging from 5% in MDA-MB-231 to 75% in the JIMT1. This region corresponded to the sequence covered by the first seven probes in the 450k Methylation array analysis (Figure 3-1). Furthermore, the sequencing results confirmed the status of MDA-MB-231 and MCF7 as unmethylated and Hs 578T as poorly methylated (Figure 3-2). However, JIMT1 was highly methylated (Figure 3-2) in contrast with the 450k Methylation array data (Figure 3-1).

Results demonstrated the 5' UTR of *GLUL* CpG island was established as the most variable region in methylation status, by which methylated and unmethylated breast cancer cell lines could be differentiated. This led to the design of a pyrosequencing-based assay to screen a larger panel of breast cancer cell lines.

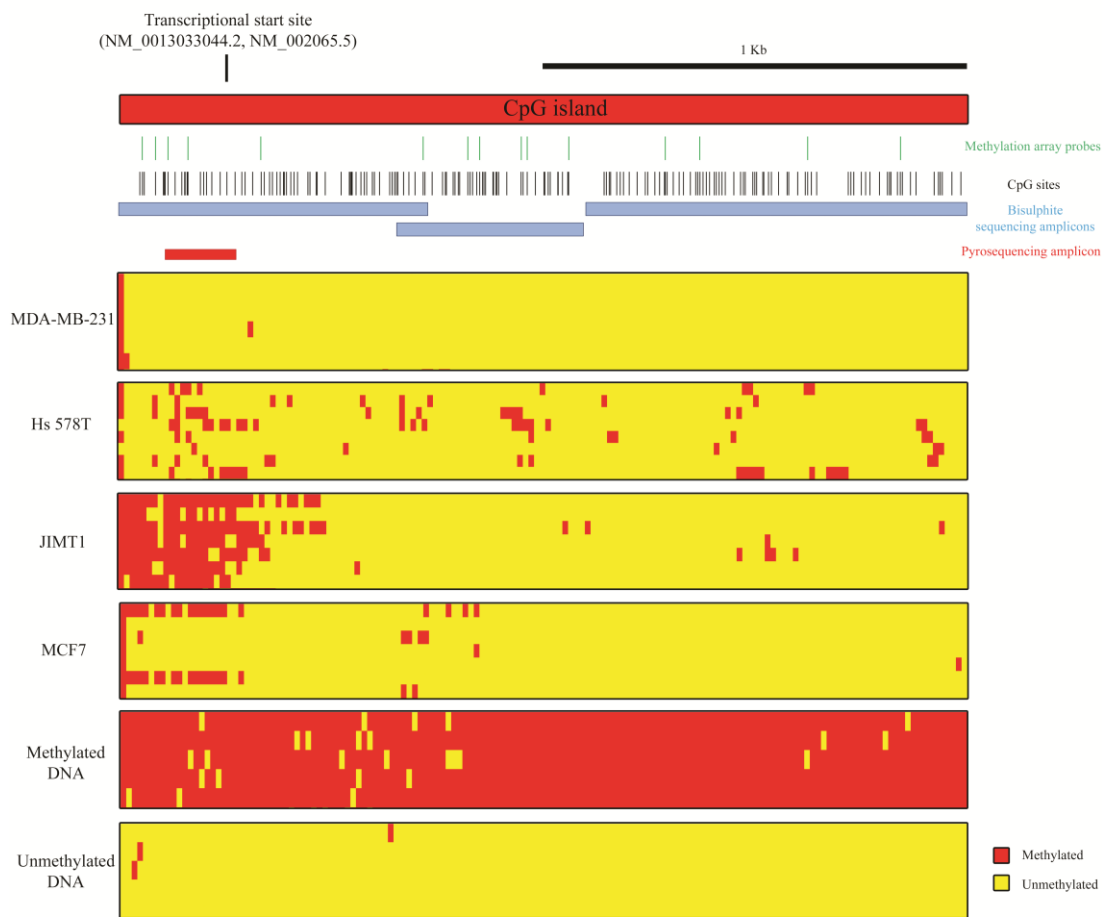


Figure 3-2. *GLUL* CpG Island bisulphite sequencing.

Glutamine synthetase CpG island overlaps the first exons of all three transcripts. The transcriptional start site (TSS) of the longest transcripts (NM_001303304.2 and NM_002065.5) is shown in the figure. The 450k Methylation Array probes location is represented by green lines, and the CpG sites by black lines. Three primer sets were designed within the CpG island (blue rectangles; see details on sequences in Table 2-3). CpG sites that appeared to be methylated from the analysis of 10 clones for each cell line are red, unmethylated sites yellow. Pyrosequencing primers were designed in the region that was most highly methylated (red rectangle).

3.2.1.3 Pyrosequencing analysis

The pyrosequencing assay was designed to investigate the methylation status of 9 CpG sites in the region identified as the most variable from the 450k Methylation array and the bisulphite sequencing analysis.

This extended panel of 16 cell lines included 7 triple negative cell lines of which only MDA-MB-468 was found to be methylated in the region of interest. A cell line was considered to be highly methylated when the methylation percentage across the pyrosequencing assay was above 60%. Of the 6 Her2 positive cell lines in the panel, 4 were methylated (MDA-MB-361, Hcc1954, BT474 and JIMT1). Of 3 ER/PR expressing cell lines, none were methylated. As expected, the pyrosequencing data correlated very closely with the bisulphite sequencing results. JIMT1 was methylated by 75% and 72%, MDA-MB-231 5% and 5% by bisulphite sequencing and pyrosequencing respectively.

The pyrosequencing results identified 37.5% highly methylated (average methylation over 60%), 12.5% intermediately methylated (with an average methylation ranged from 15% to 60%) and 50% unmethylated (average methylation below 15%) from a panel of 16 breast cancer cell lines. The influence of methylation in modulating the expression levels of the gene will be discussed in section 3.2.2.

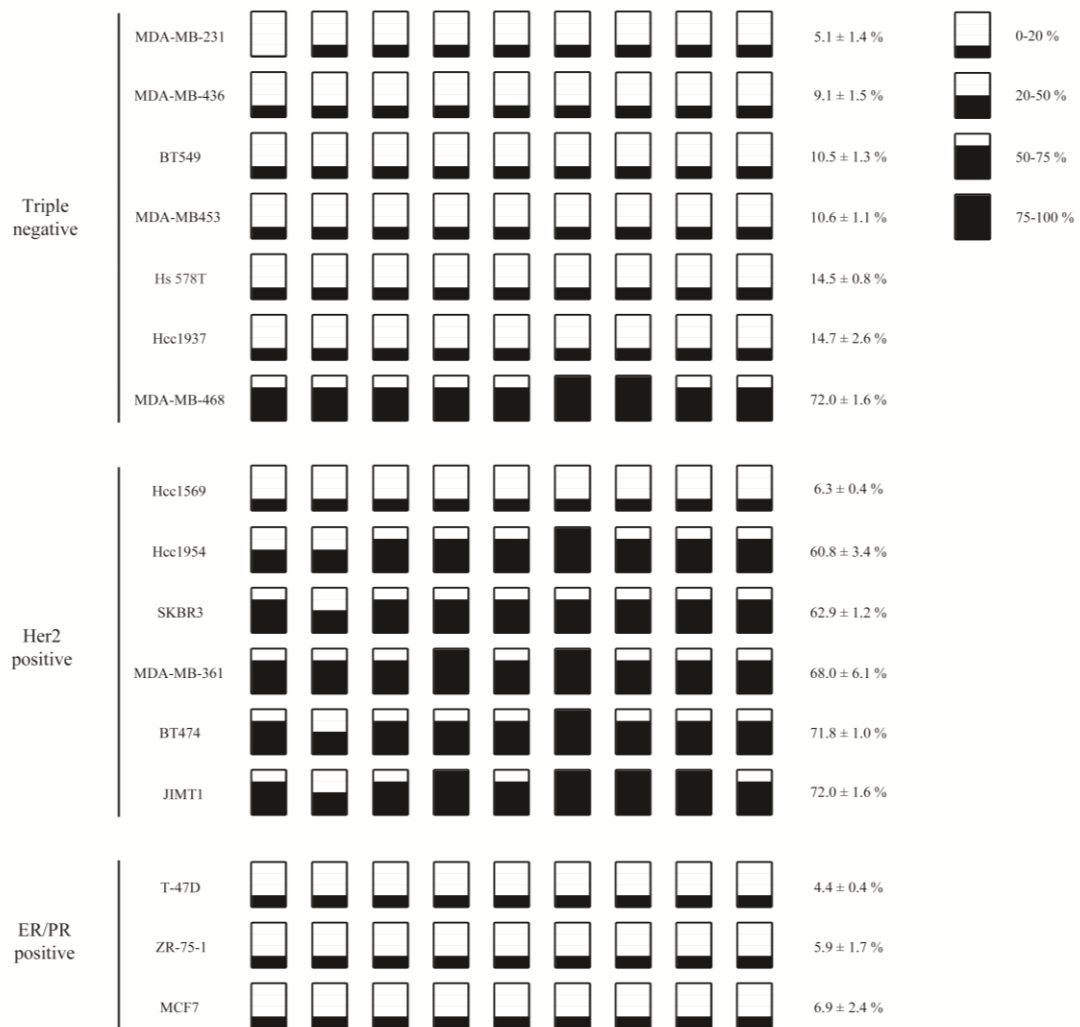


Figure 3-3. Screening of cell lines for *GLUL* by pyrosequencing.

9 CpG sites, each represented by a square in the figure, on *GLUL* CpG island were analysed in biological triplicates by pyrosequencing across the breast cancer cell line panel. The proportion of black in each square shows the average of methylation in each CpG site (see legend on the top right). The methylation status across the panel was calculated as the mean from the 9 CpG sites for each cell line. The biological triplicates were then averaged and the standard deviation generated to obtain the methylation status for each cell line (values on the right).

3.2.2 Expression analysis

3.2.2.1 *GLUL* expression level in breast cancer cell lines

Based on the methylation analysis, the region at the 5' UTR of *GLUL* CpG island was established to be the most variable, enabling discrimination of methylated or unmethylated cells. To investigate the role of methylation in modulating the gene, it was crucial to analyse its expression and translation level across the panel.

GLUL consists of three transcripts, NM_001033044.2, NM_002065.5 and NM_001033056.2, encoding the same protein (Figure 3-1). The real-time PCR (qPCR) was designed to detect the expression of all transcripts as the primer set covers a shared coding region (between the first and second coding exon). As shown in Figure 3-4, the cell line panel was divided based on breast cancer subtype to evaluate the possibility of different expression level within them. Within each subtype a wide range of expression was found (Figure 3-4). Triple negative cells showed the most variation in *GLUL* expression level with a 252 fold change between the lowest (Hs 578T) and the highest expressing (MDA-MB-468). Conversely, the hormone-positive lines were the least variable, with a 7 fold change between the T-47D and the ZR-75-1. It is worth noting that Hs 578T and MDA-MB-361, the lowest and the highest expressing respectively with a 526 fold difference, were both found methylated in the previous analysis (Figure 3-3).

Based on expression level, none of the breast cancer subtypes correlates with a high or low *GLUL* expression profile, all showing a wide range of expression. However, complete characterisation of our breast cancer cell line panel requires examination of

not only the expression level of *GLUL* but also the protein levels, which will be discussed in the following chapter.

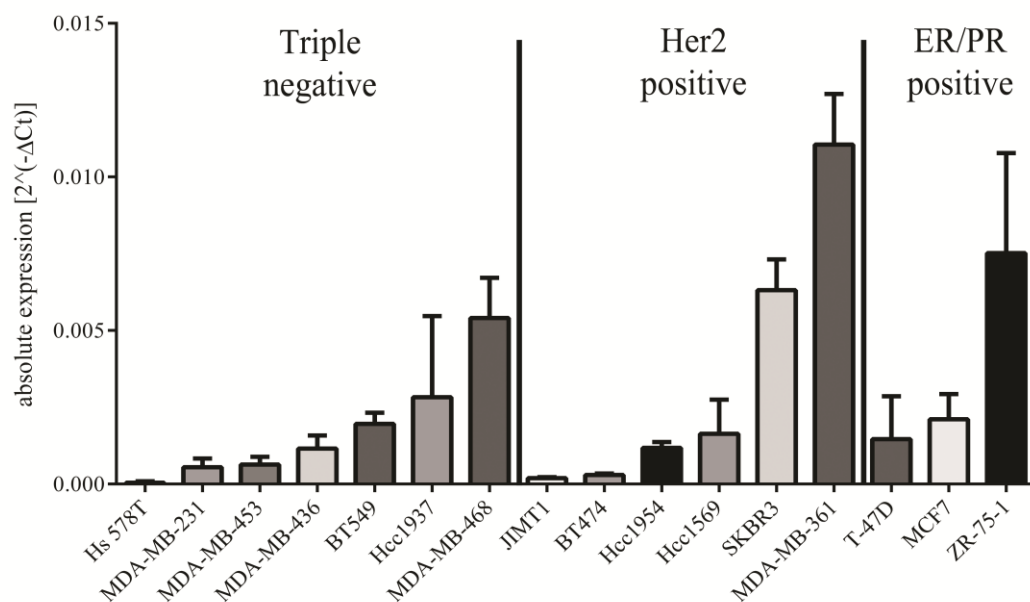


Figure 3-4. *GLUL* expression level analysis.

Glutamine synthetase expression was investigated in the breast cancer cell lines panel by real-time PCR. The cells were organised by breast cancer subtype and ordered by increasing gene expression values by qPCR. Each value was expressed as average with standard deviation among biological triplicates.

3.2.2.2 Glutamine synthetase protein (GS) level in breast cancer cell lines

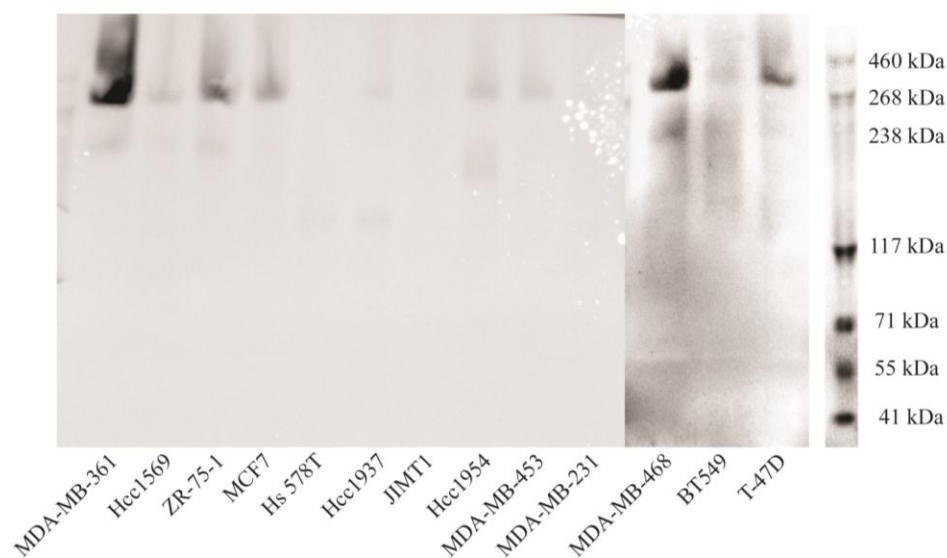
Our breast cancer cell line panel was screened by SDS-PAGE electro-blotting to complete the characterisation of Glutamine synthetase. The Glutamine synthetase enzyme is formed by two symmetrical rings of 4 monomers (GS), each encoded by *GLUL*. The quaternary structure is stabilised by hydrophobic interaction and hydrogen bonds between monomers mirroring each other from the two rings (Eisenberg et al. 2000).

To investigate the specificity of the antibody used in these experiments, lysates from a selection of cell lines were analysed by native electro-blotting. Only one band was found in each cell line, between 268 kDa and 460 kDa, as shown in Figure 3-5 A. The band was located at 440 kDa as predicted (each monomer is 42 kDa, the enzyme was expected to be around 440 kDa), and thus established the reliability of the antibody to specifically recognise the protein of interest. However, native gel can not be used to quantify the protein level due to lack of loading controls. Therefore GS level were routinely analysed using denaturing SDS-PAGE electro-blotting from this point onwards.

The bonding of the dimers, which stabilises the quaternary structure, was found to be extremely difficult to disrupt. Thus GS was detected as monomer (42 kDa) and dimer (about 80 kDa) form when analysed after denaturation in reducing condition (Figure 3-5 B). The fold change in total GS was determined across the whole panel, and was calculated by determining a densitometric value for both GS bands in each cell line. A 24.7 fold change from Hs 578T to MDA-MB-361 was observed, for the lowest and the highest Glutamine synthetase protein (GS) level respectively. These

are the same two cell lines found to be the lowest and the highest for *GLUL* expression respectively in the previous analysis (see chapter 3.2.2.1). It is worth noting that triple negative cell lines showed the least variation with a 2.5 fold change between the lowest and the highest protein level, Hs 578T and Hcc1937 respectively. The widest variation was found across the Her2-positive cell lines with a 24.6 fold change between the lowest level in JIMT1 and the highest level in MDA-MB-361. However, the fold-change between Hs 578T and MDA-MB-361 observed by SDS-PAGE electro-blotting is 10-times less than the mRNA level detected. This is due to the different nature of the samples, cDNA and protein, and the detecting methods, fluorescent intensity and densitometry respectively. Real-time PCR used to study mRNA level is more sensitive and reproducible, while SDS-PAGE electro-blotting results are more variable and less sensitive. The analysis demonstrated triple negative cell lines as generally expressing lower amounts of GS.

A)



B)

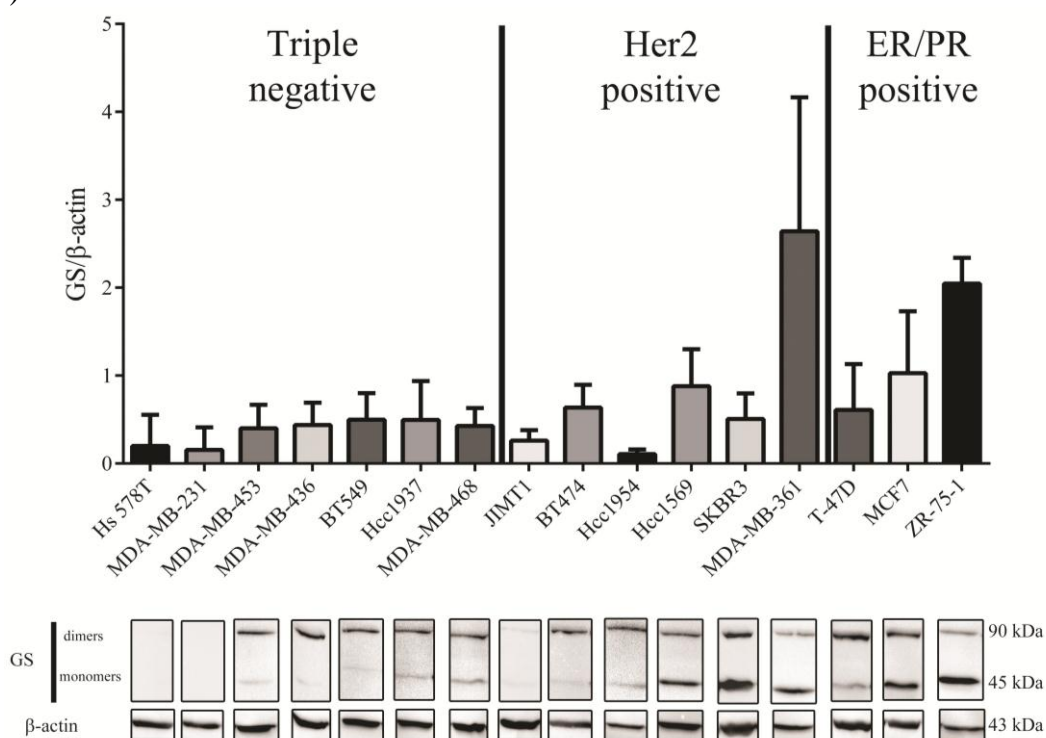


Figure 3-5. Glutamine synthetase protein analysis.

Glutamine synthetase expression was investigated in the breast cancer cell line panel by A) native gel or B) SDS-PAGE followed by electro-blotting. The cells were divided by breast cancer subtype and ordered by increasing expression by qPCR. The expression level was expressed as the average \pm standard deviation of biological triplicates. Densitometry analysis was used to determine the quantity of Glutamine synthetase in each experiment and was calculated using the ratio between the

densitometry values of GS, i.e. the sum of the two bands, representing monomer and dimer, to the loading control.

3.2.2.3 Correlation between methylation gene expression and protein level

To evaluate the role of methylation in modulating the expression and translation of *GLUL*, correlation analysis across the three variables were crucial. The hypothesis was that highly methylated cells have low to non-existent expression of the gene.

Based on the DNA methylation and *GLUL* expression analysis, no correlation was found between methylation status and mRNA level (R: 0.301, p-value: 0.258) (Figure 3-6, Figure 7-2 B). As described in the previously (sections 3.2.2.1 and 3.2.2.2), methylated cell lines included both the lowest (Hs 578T) and the highest (MDA-MB-361) expressing cells across the panel. While no clear association was found between methylation status and gene expression, there was a strong correlation between mRNA and protein level (R: 0.818, p-value<0.001) (Figure 3-6, Figure 7-2 A). It was observed no evident role for DNA methylation on *GLUL* silencing thus far. However, one group of breast cancer cell lines (Hs 578T and JIMT1) in which methylation correlated to no expression of GS. Therefore, it may be possible that DNA methylation plays a role in *GLUL* modulation, but requires complementary mechanisms to be fully functional. The hypothesis will be investigated in the chapters 3.2.3 and 3.2.4.

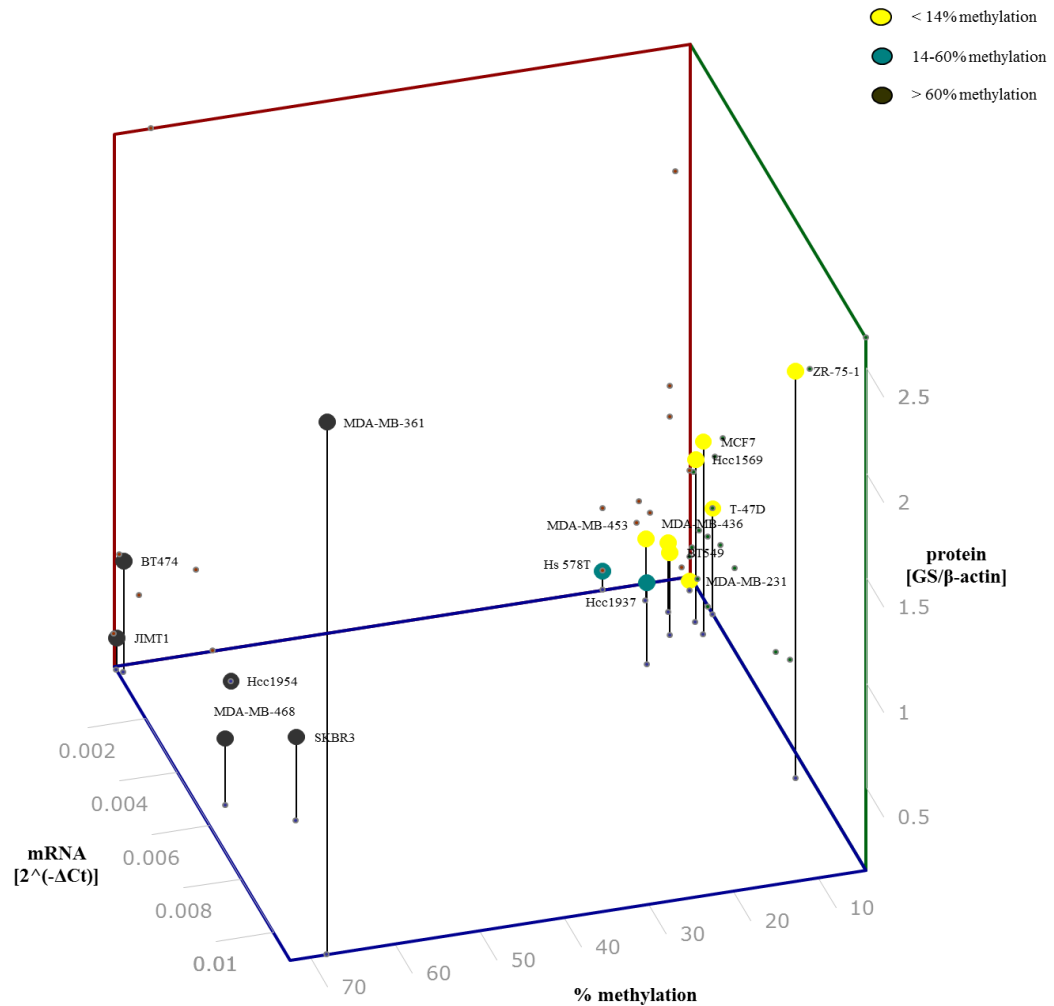


Figure 3-6. 3D scatter blot of *GLUL* methylation and expression levels.

The methylation data obtained by pyrosequencing analysis were correlated with the expression and protein level. Each dot represents a cell line characterised by three different values: the average methylation, expressed as a percentage, on the X axis (blue); the *GLUL* gene expression level by qPCR on the y axis (red) and the protein level by SDS-PAGE electro-blotting on the z axis (green). A grey line connects each 3D dot with the corresponding methylation value onto the corresponding 2D plane to make easier positioning each cell lines in the 3 dimensional space. Cell lines panel are colour-coded based on methylation results by pyro-sequencing.

3.2.3 De-methylation effects on *GLUL* expression

Previous analysis demonstrated the existence of a group of breast cancer cell lines characterised by high *GLUL* DNA methylation and no baseline expression, suggesting a role for methylation in modulating the expression of the *GLUL* gene. Therefore a selection of cell lines with different methylation status and baseline expression was tested by whole genome de-methylation and pro-acetylation treatments.

To discern if *GLUL* could be epigenetically modulated, the gene expression and translational levels were investigated in a selection of cell lines after widespread genome de-methylation and pro-acetylation treatment. Widespread de-methylation was obtained by aza (5-aza-deoxycytidine), a cytosine homologue binding to methyl-transferase in proliferating cells, while pro-acetylation of histones was caused by tsa (Trichostatin A), a HDAC inhibitor that reduces chromatin condensation. Genes repressed mainly via DNA-methylation were up-regulated after aza treatment, whilst those whose repression involved histone pro-acetylation were up-regulated after tsa treatment.

As shown in Figure 3-7, wide-spread de-methylation had no effect on *GLUL* expression in unmethylated cell lines (MDA-MB-231, MCF7 and T-47D), even though the basal level across the three cell lines was different. In addition, there was no variation in the methylation status in response to aza treatment (Table 3-1), confirming the hypothesis that no epigenetic modulation was present in this group of breast cancer cell lines.

All methylated cell lines showed a decrease in the promoter region methylation of about 30% in response to de-methylation treatment (Table 3-1), with JIMT1 showing the strongest difference while Hs 578T showed the smallest difference. There was a 9.5 fold change difference between the methylation status of JIMT1 and Hs 578T when treated with aza. However, up-regulation of the *GLUL* gene was observed only in cells with no *GLUL* baseline expression (Hs 578T and JIMT1) (Figure 3-7) after de-methylation treatment. As shown in Figure 3-7, in this subset of cells pro-acetylation treatment enhanced the effect of de-methylation on *GLUL* gene. *GLUL* expression changed from a maximum increase of 8.4 fold in JIMT1 when treated with aza to 15.5 fold when in combination with tsa. It is worth noting that tsa treatment on its own did not up-regulate *GLUL* expression (Figure 3-7). No *GLUL* modulation was found in methylated *GLUL* expressing cells in response to any of the epigenetic treatments (Figure 3-7), in contrast with a de-methylation of approximately 30 % with aza (Table 3-1).

These results delineated two groups of methylated cell lines based on their *GLUL* expression baseline level: methylated *GLUL* expressing or methylated *GLUL* non expressing, i.e. silenced. *GLUL* up-regulation after de-methylation treatment in methylated *GLUL* non expressing cells confirmed a role of DNA methylation in modulating the gene expression. However, the null effect of epigenetic treatment on methylated *GLUL* expressing cells and the synergetic effect of de-methylation and pro-acetylation treatments in methylated *GLUL* non expressing cells demonstrated a co-operation between DNA methylation and histone acetylation. Therefore it was important to understand the effect of the histone acetylation status on the activity of the Glutamine synthetase promoter region.

	MDA-MB-231	MCF7	T-47D	Hcc1954	MDA-MB-468	MDA-MB-361	Hs 578T	JIMT1
ct	4.7 ± 2.1	3.7 ± 2.1	5.0 ± 1.0	75.4 ± 6.0	63.3 ± 12.7	73.7 ± 5.1	18.3 ± 1.2	74.3 ± 2.1
aza	3.7 ± 1.5	3.3 ± 0.6	4.0 ± 0.1	40.7 ± 9.6	30.7 ± 21.2	49.0 ± 7.9	14.0 ± 2.6	36.3 ± 4.9
aza+tsa	11.0 ± 3.6	12.3 ± 4.7	7.3 ± 3.2	37.7 ± 7.5	36.7 ± 16.7	55.0 ± 7.0	14.7 ± 2.3	37.7 ± 5.1
tsa	11.0 ± 5.0	9.3 ± 2.1	5.3 ± 2.1	68.7 ± 8.1	65.0 ± 5.0	73.3 ± 4.5	18.0 ± 3.2	67.7 ± 6.7

Table 3-1. Methylation status of the *GLUL* promoter region after the epigenetic treatments.

Levels of *GLUL* methylation were checked after aza and tsa treatments by pyrosequencing. The average and standard deviation between the biological triplicates are shown in the table. Cell lines are colour-coded based on their methylation and gene expression status: unmethylated in white, methylated *GLUL* expressing in light grey and methylated *GLUL* non expressing in dark grey.

ct: untreated. aza: 5 days administration of 5-aza-deoxycytidine. aza+tsa: 5 days with 5-aza-deoxycytidine and 16 h incubation with Trichostatin A before harvesting. tsa: 16 h incubation with Trichostatin A before harvesting.

Figure 3-7. *GLUL* re-expression analysis.

Cell lines were divided into three groups based on their methylation and expression status: unmethylated cells (MDA-MB-231, MCF7 and T-47D), methylated *GLUL* expressing (Hcc1954, MDA-MB-468 and MDA-MB-3) and methylated *GLUL*-silenced (Hs 578T and JIMT1) cells.

The histogram represents the qPCR average and standard deviation across biological triplicates. Gene modulation is expressed as fold change. One-way ANOVA on Prism 6.0 (Graph Pad) was used to analyse the statistical significance of any *GLUL* modulation after treatments. Statistical significance for the survival is shown as stars (*: p-value 0.05, **: p-value 0.01, ***: p-value 0.001, ****: p-value <0.001). A representative image showing GS modulation by SDS-PAGE electro-blotting after each treatment and the loading control, β -actin, is given for each cell line.

ct: untreated. aza: 5 days with 5-aza-deoxycytidine. aza+tsa: 5 days with 5-aza-deoxycytidine and 16 h incubation with Trichostatin A before harvesting. tsa: 16 h incubation with Trichostatin A before harvesting. GS: Glutamine synthetase.

3.2.4 Histone acetylation analysis

Two groups of methylated cells were defined during previous analysis based on *GLUL* baseline and response to epigenetic modulating treatments. The results led to the hypothesis that both DNA methylation and histone acetylation could have a role on *GLUL* expression. To verify the role of histone modification, histone acetylation status of Histone4 (H4) and Histone3 (H3) was analysed by Chromatin Immuno-Precipitation (ChIP) in the same cell lines tested previously.

To validate histone acetylation as a marker of gene expression and determine the acetylation threshold corresponding to gene expression, the baseline status of reference genes, *GAPDH* and *RPLP0*, known to be constitutively expressed in our cell lines panel, were determined. *HB2A*, a gene not expressed across the panel, was used as reference of background level. As shown in Figure 3-8 A, both genes were enriched for histone acetylation across the panel. *GAPDH* enrichment ranged from 2.3 to 8.1 fold for H4 and from 3.8 to 17.8 fold for H3. *RPLP0* enrichment was in the range 2.3 to 8.1 fold in H4 and from 3.7 to 17.9 fold in H3. Therefore enrichment values in the range of *GAPDH* and *RPLP0* and over should be considered to be involved in promoting gene expression.

As evident from Figure 3-8 B and C, methylated *GLUL* expressing cell lines can be characterised by a specific peak of histone acetylation enrichment 2500 bp upstream of the gene TSS. H3 acetylation ranged from a minimum of 5.8 fold to a maximum of 10.2 fold and H4 from 11.9 to 19.9 fold. However, no enrichment was seen in methylated cells non expressing *GLUL*, ranging from 0.5 to 3.1 fold for H4 and from 0.2 to 3.2 for H3. Furthermore, MDA-MB-361 cells showed a significant enrichment

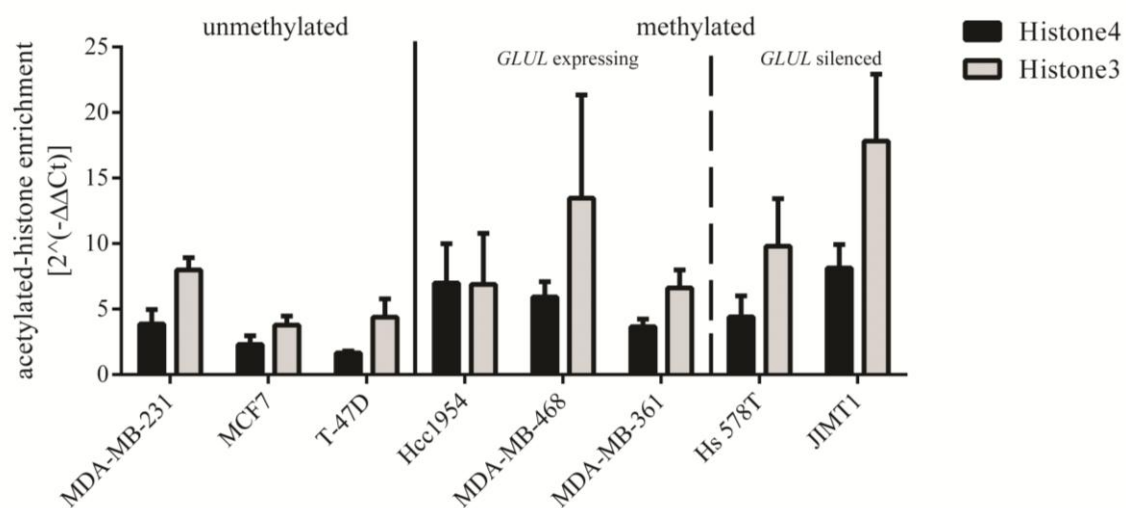
across all regions analysed on the *GLUL* promoter region (Figure 3-8 B), correlating with the highest GS expressing cell line in our panel (Figure 3-4).

It is worth noting that histone acetylation status at 2500 bp upstream of the *GLUL* TSS (Figure 3-8 B) correlated closely with baseline expression (Figure 3-4) across the breast cancer cell lines. The cell line JIMT1 which showed poor enrichment (0.5 fold on H4 and 0.2 fold on H3) had no expression of *GLUL*, while significant enrichment in MDA-MB-468 cells (5.8 fold on H4 and 19.9 fold on H3) was associated with high *GLUL* baseline expression.

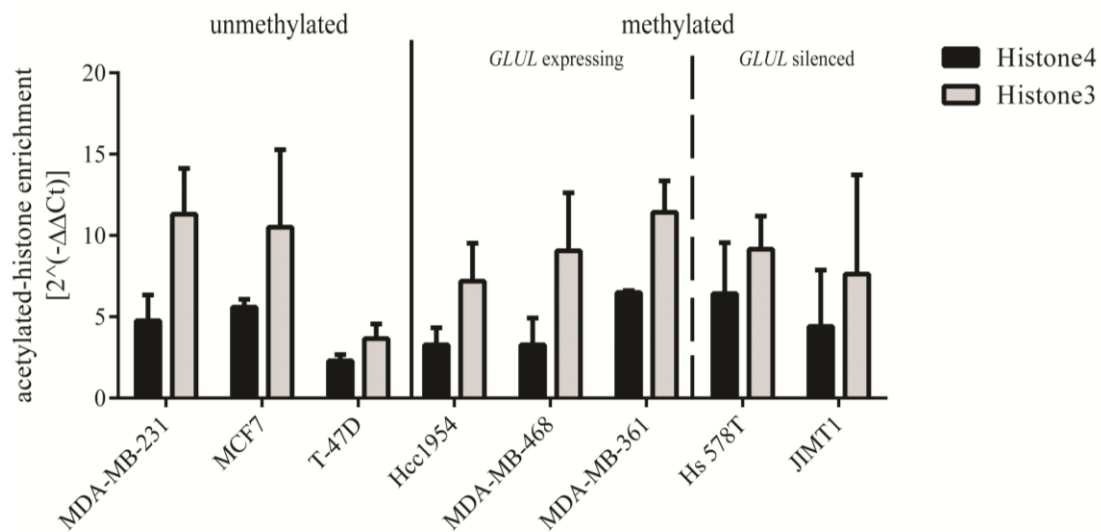
Histone acetylation analysis confirmed the presence of two subsets of methylated cell lines. Methylated *GLUL* expressing cell lines showed a specific peak of histone acetylation at 2500 bp upstream of the gene TSS. This result correlates with the null effect of epigenetic treatment on methylated *GLUL* expressing cells and the synergistic effect of tsa on aza treatment in methylated *GLUL* non expressing cells (Figure 3-7).

A)

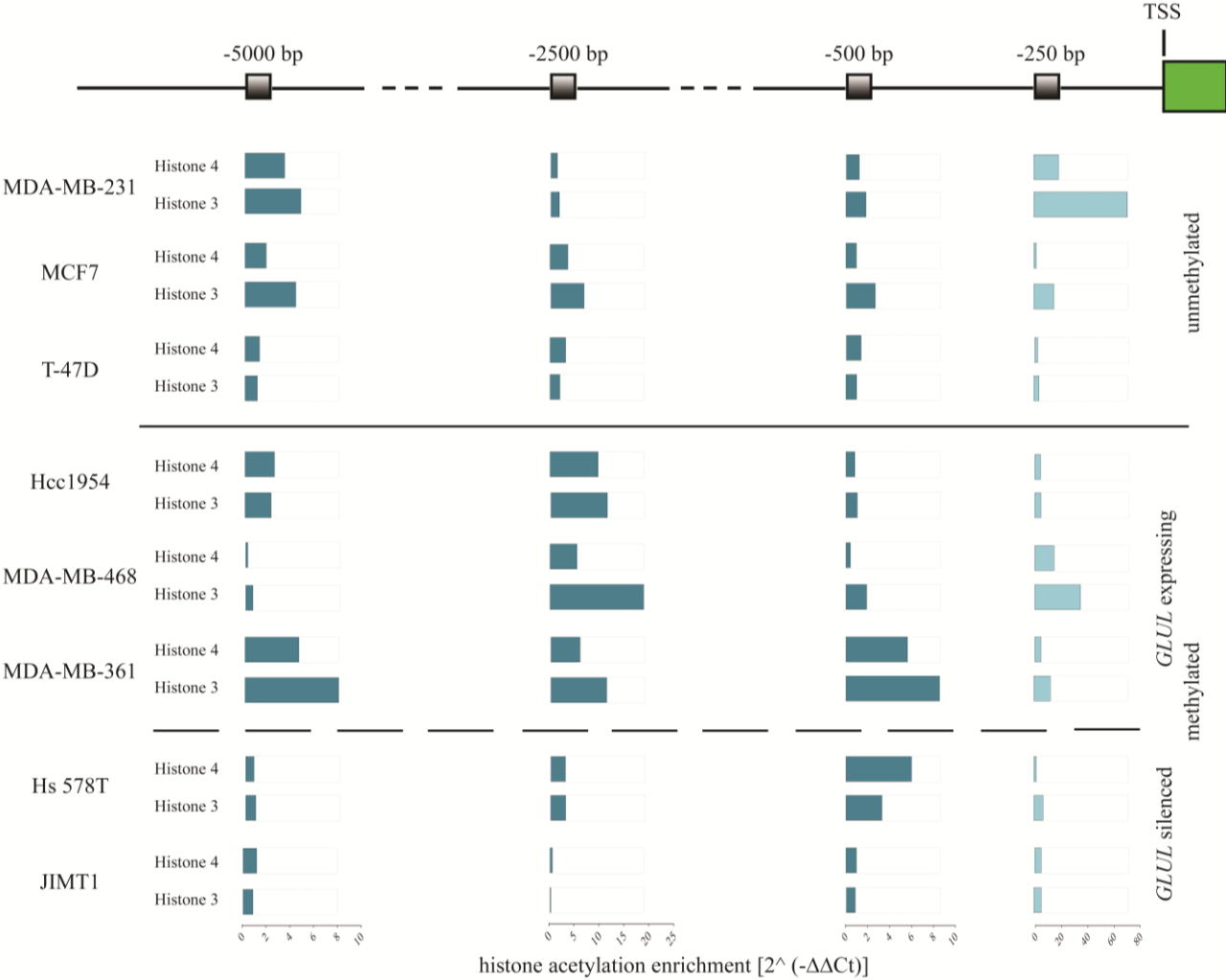
GAPDH



RPLP0



B)



C)

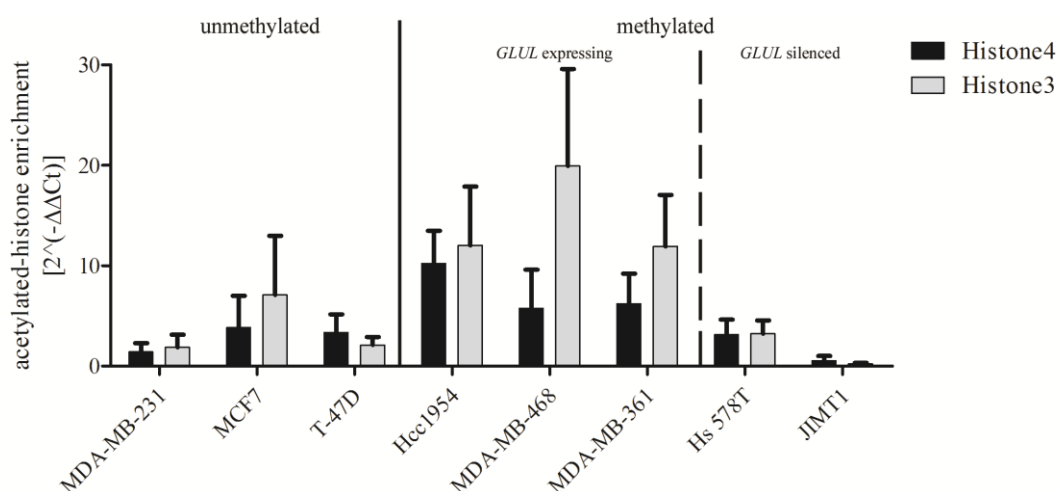


Figure 3-8. Histone acetylation analysis by ChIP.

Enrichment in H3 and H4 acetylation was analysed in unmethylated (MDA-MB-231, MCF7 and T-47D), methylated *GLUL* expressing (Hcc1954, MDA-MB-468 and MDA-MB-361), and methylated *GLUL* non expressing (Hs 578T and JIMT1) cell lines.

A) *GAPDH* and *RPLP0* were analysed for DNA enrichment approximately 1000 bp upstream of their TSS as positive controls.

B) Dark blue bars show the enrichment in histone acetylation at 5000 bp (-5000bp in the figure) 2500 bp (-2500bp) and 500 bp (-500bp) upstream of the transcriptional start site (TSS). Light blue bars show the same analysis at 25 0bp upstream of the TSS, the region where high level of methylation was found in *GLUL* CpG island.

C) DNA enrichment at 2500bp upstream of *GLUL* Transcriptional start site.

3.3 Functional analysis of Glutamine synthetase

3.3.1 Glutamine deprivation

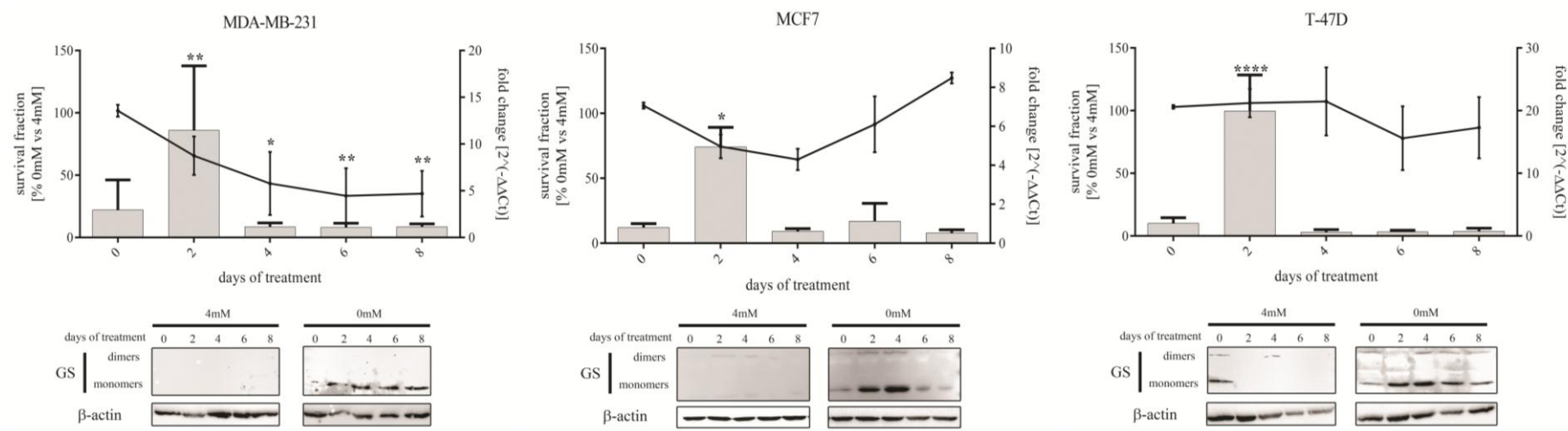
A selection of breast cancer cell lines were deprived of glutamine (gln) to evaluate the epigenetic modulation of *GLUL* as a marker for susceptibility to synthetic lethality. Gene expression as well as translation levels were analysed during treatment. Untreated cells were cultured in 4 mM gln, whilst deprived cells in medium without gln. The cell lines tested were representative of the three subtypes established in the epigenetic analysis: unmethylated, methylated *GLUL*- expressing and methylated *GLUL* non expressing.

As expected, cell lines responded to treatment based on their baseline expression of *GLUL*. As shown in Figure 3-9, cells with baseline expression of *GLUL* were not sensitive to glutamine deprivation and their survival rate was independent of the corresponding methylation status. Unmethylated and methylated *GLUL* expressing cells up-regulated the gene in response to glutamine deprivation (Figure 3-9 A, B). This was the case also for the unmethylated MDA-MB-231 cells, where gln deprivation caused 64% cell death (Figure 3-9 A). Nonetheless, the gene up-regulation response in the unmethylated cell lines was faster than in the methylated *GLUL* expressing subset of cells. As shown in Figure 3-9 A, unmethylated cells showed a maximum increase in *GLUL* expression on day 2 (up to 20 fold). Methylated *GLUL* expressing cell lines slowly increased the level of *GLUL* expression reaching maximal expression from day 6 of deprivation (up to 18 fold) (Figure 3-9 B). In contrast, breast cancer cells with no baseline expression had

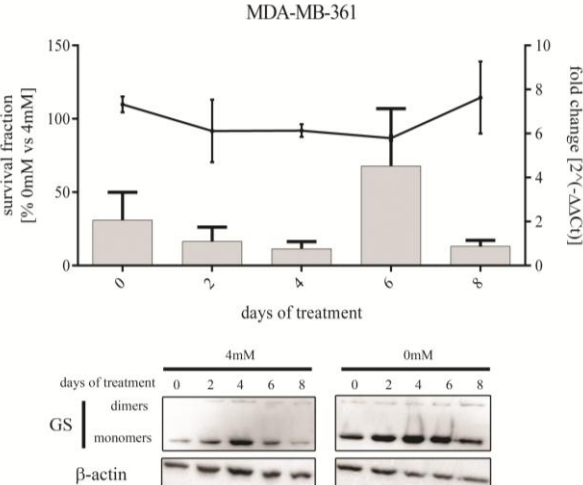
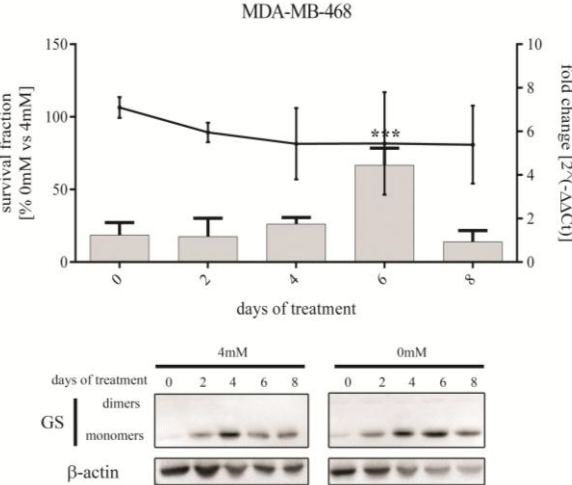
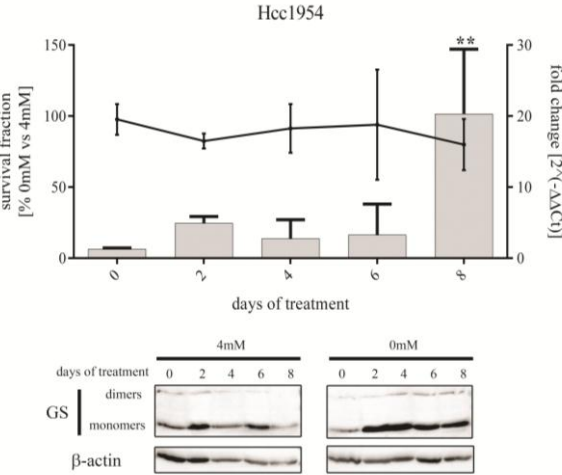
markedly reduced survival with up to 78% cell death. As before, this was independent of their methylation status. However, cells with methylated *GLUL* and no expression (Hs 578T and JIMT1; Figure 3-9 C), were unable to modulate *GLUL* gene expression and GS protein level in response to glutamine deprivation.

Based on the effect of glutamine deprivation on the panel of breast cancer cell lines tested, *GLUL* silencing by epigenetic modulation appeared to cause sensitivity to the treatment. Concurrently in methylated *GLUL* expressing cells, DNA methylation appeared to delay the gene up- during the depletion treatment. This suggests an induction of a compensatory mechanism in methylated *GLUL* expressing cells to overcome the initial stages of glutamine deprivation which will be described in the section 3.3.2.

A)



B)



C)

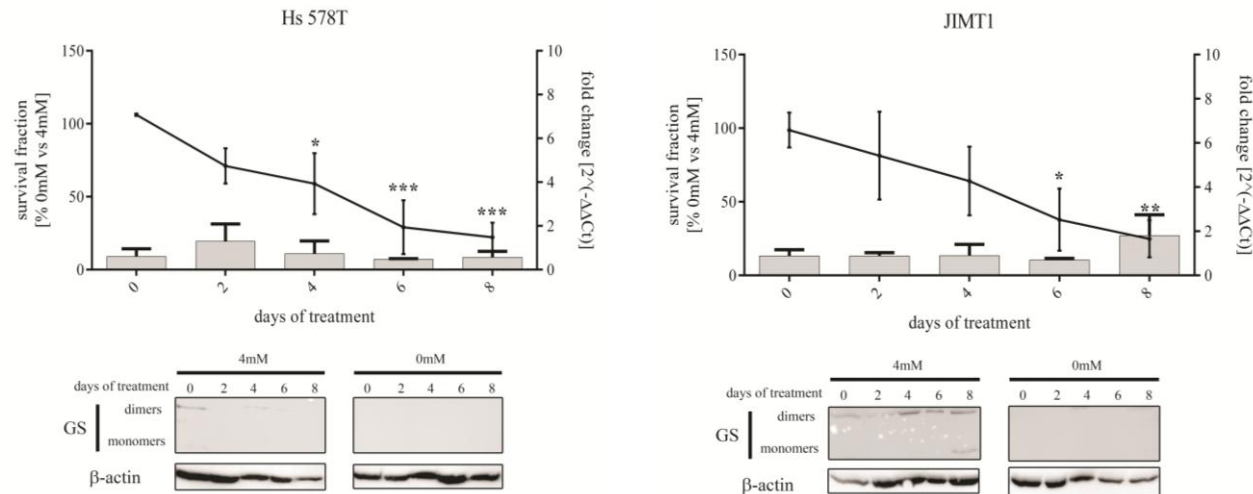


Figure 3-9. Effects of Gln deprivation on breast cancer cell lines.

A) Unmethylated (MDA-MB-231, MCF7 and T-47D), B) methylated *GLUL* expressing (Hcc1954, MDA-MB-468 and MDA-MB-361), C) methylated *GLUL*-silenced (JIMT1 and Hs 578T) cell lines survival was analysed by MTT (black line), gene expression levels by qPCR (histogram) and protein levels by SDS-PAGE electro-blotting during gln deprivation. The survival fraction was calculated as percentage of live cells in the treated (grown in absence of gln) compared to the untreated cells (grown in 4mM gln) on each day. During each experiment RNA was collected for analysis by qPCR. *GLUL* regulation during gln deprivation was expressed as fold change. Protein level was analysed together with survival and gene expression in both treated (0mM) and untreated cell (4mM). The experiment was repeated in biological triplicates and the results are shown as average and standard deviation for each cell line. One-way ANOVA on Prism 6.0 (Graph Pad) was used to analyse the statistical significance of each day versus day0. Statistical significance for the survival is shown as stars (*: p-value 0.05, **: p-value 0.01, ***: p-value 0.001, ****: p-value <0.001).

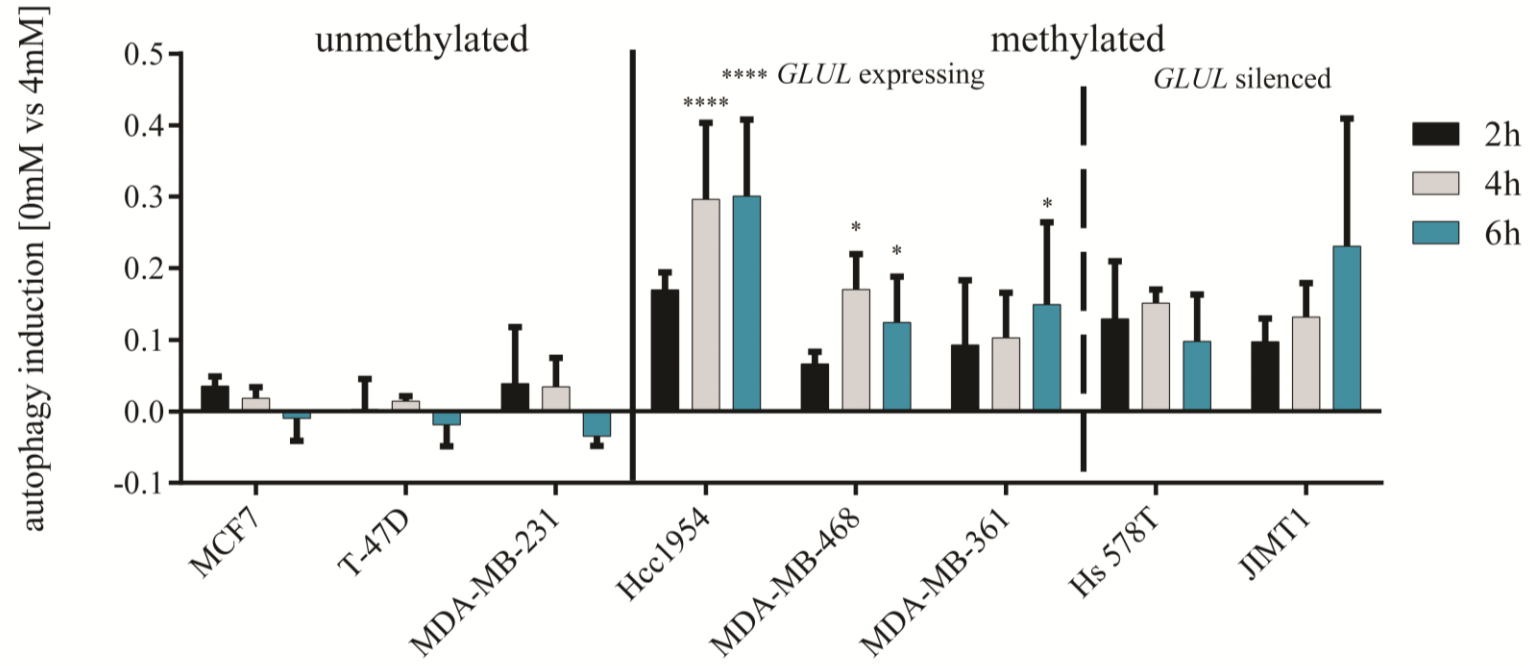
3.3.2 Autophagy induction

3.3.2.1 Autophagy response to gln deprivation

As described in the introduction, autophagy is induced in low amino acid condition in the micro-environment (Nicklin et al. 2009, Yabu et al. 2012, Lorin et al. 2013, Shanware et al. 2013). To validate the role of autophagy as a compensatory mechanism in promoting resistance to gln deprivation in methylated *GLUL* expressing cells, autophagy induction was monitored during treatment in the selection of cell lines tested previously.

As expected no autophagy induction was detected in unmethylated cells when subjected to glutamine deprivation (Figure 3-10). In contrast, all methylated cells presented an autophagy response within the hour immediately after removing gln (Figure 3-10 A). This induction increased up to 30% (Hcc1954) over background at 4 hours post-starvation. However only methylated *GLUL* silenced cells sustained the autophagy response until the end of the deprivation treatment reaching 82% and 71% on day 8 in Hs 578T and JIMT1 respectively, as shown in Figure 3-10 B. Methylated *GLUL* expressing cells decreased the autophagy response back to pre-treatment levels on day 2 (Figure 3-10 B), confirming its role as a compensatory mechanism. The autophagy response is maintained in methylated *GLUL* silenced cells that are unable to up-regulate Glutamine synthetase and have a poor survival rate following deprivation (Figure 3-9 C).

A)



B)

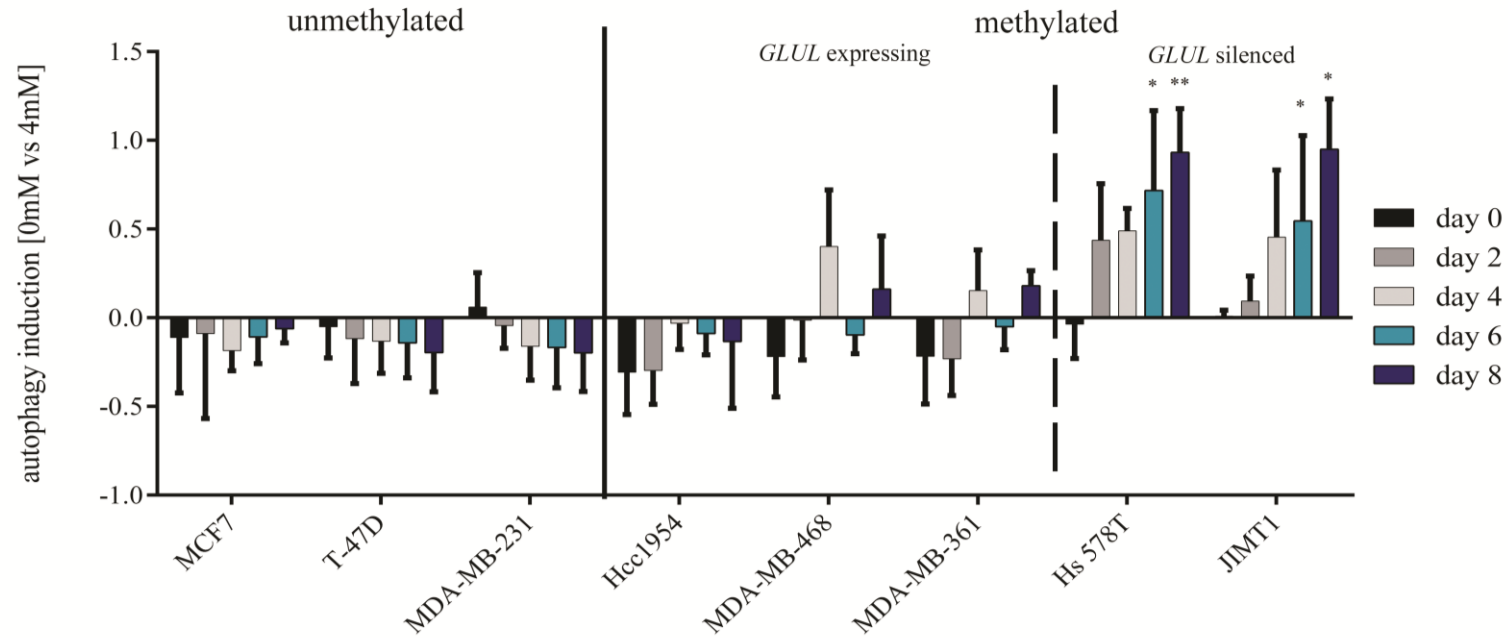


Figure 3-10. Induction of autophagy in response to gln deprivation.

Autophagy induction was analysed during gln deprivation in unmethylated (MCF7, T-47D and MDA-MB-231), methylated *GLUL* expressing (Hcc1954, MDA-MB-468 and MDA-MB-361), and methylated *GLUL* silenced (JIMT1 and Hs 578T) cell lines. Autophagy induction was analysed from A) the early hours of treatment up to B) 8 days of treatment. The induction was expressed as average with standard deviation over background (4mM) from biological triplicates. Two-way ANOVA on Prism 6.0 (Graph Pad) was used to analyse the statistical significance of each day versus every other cell lines at different time-points. Statistical significance is represented by stars (*: p-value 0.05, **: p-value 0.01, ***: p-value 0.001, ****: p-value <0.001).

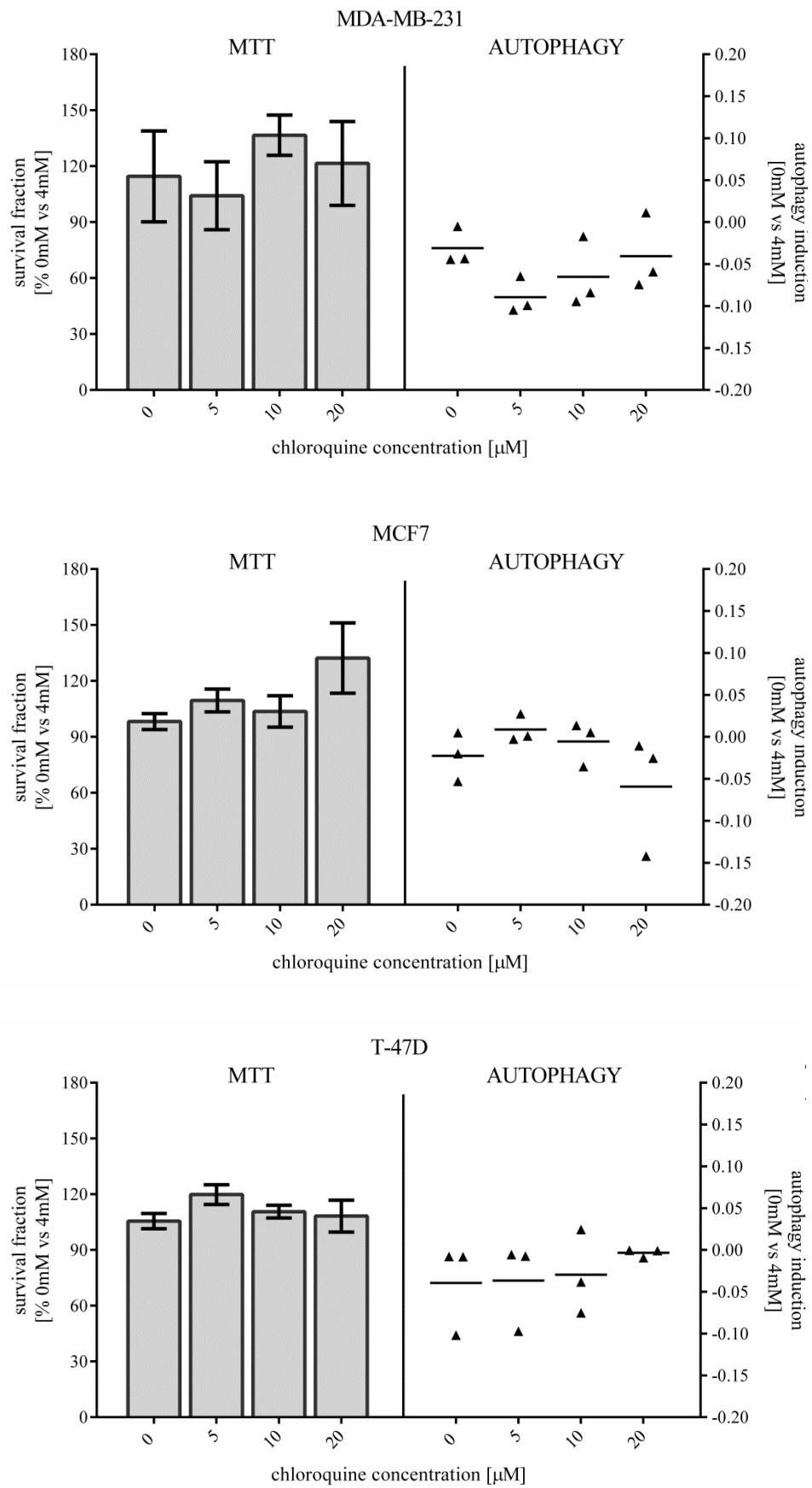
3.3.2.2 Autophagy repression effects on glutamine deprivation

Previous analysis demonstrated how methylated *GLUL* expressing cell lines induced autophagy in response to glutamine deprivation before up-regulating Glutamine synthetase expression. Autophagy induction was blocked by Chloroquine (CQ) administration to evaluate the contribution of autophagy to resistance to glutamine deprivation.

As shown in Figure 3-11 and in concordance with the previous analysis, only methylated *GLUL* expressing cells induced autophagy in response to glutamine deprivation. In this subset of breast cancer cell lines the autophagy response was inhibited with minimal Chloroquine concentration (Figure 3-11 B) and did not rise above background levels. Methylated *GLUL* expressing cells were sensitive to glutamine deprivation causing up to 60.4% cell death in MDA-MB-468 when the autophagy response was blocked (Figure 3-11 B). It is worth noting that whereas CQ blocked the autophagy response at minimal concentration (5 μ M), effects on survival rate were seen only at the maximal concentration tested (20 μ M) (Figure 3-11 B).

The results shown here indicate that the autophagy response is a compensatory mechanism enabling methylated *GLUL* expressing cells to survive the initial stages of glutamine deprivation. When autophagy is blocked, sensitivity to the gln deprivation is restored in this subset of breast cancer cell lines.

A)



B)

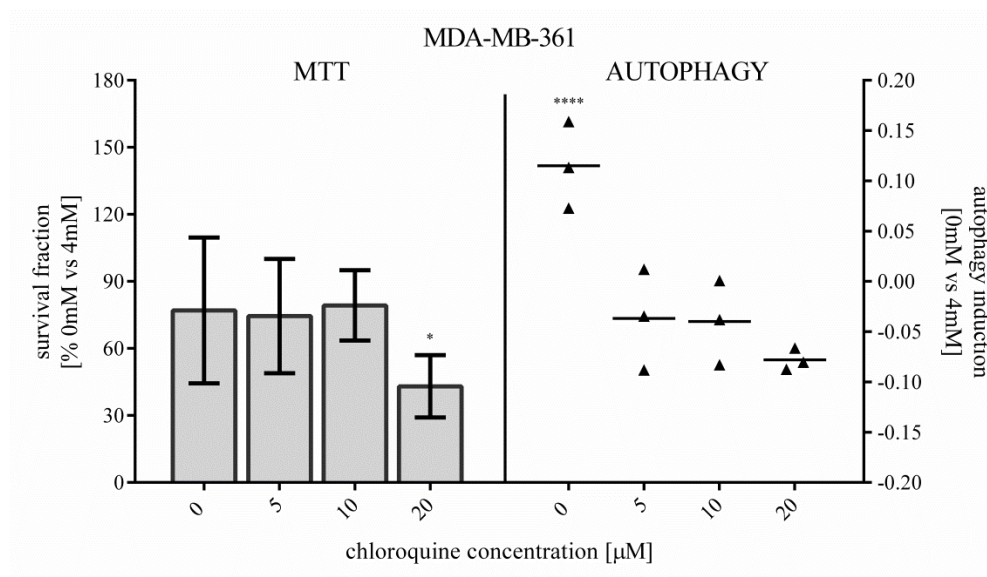
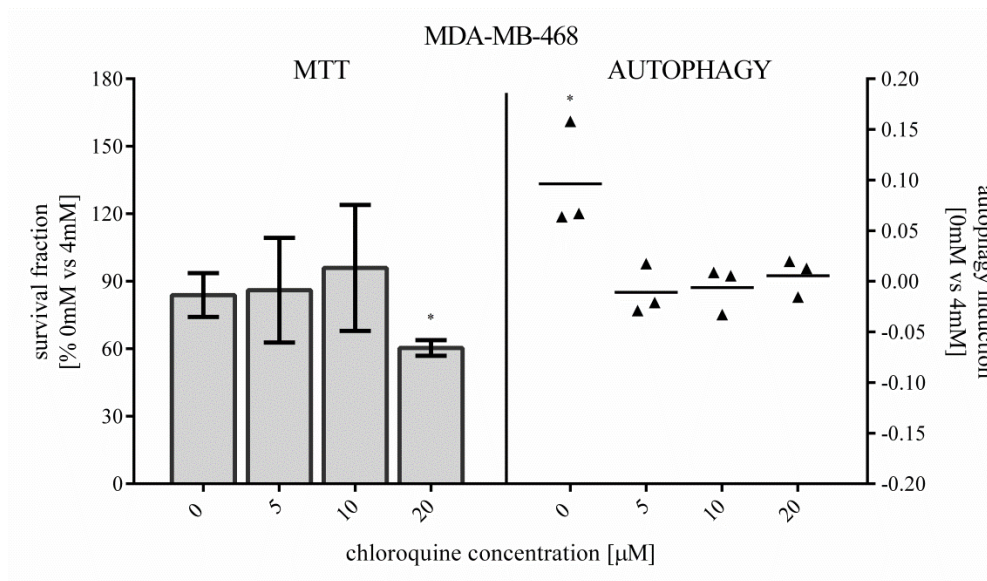
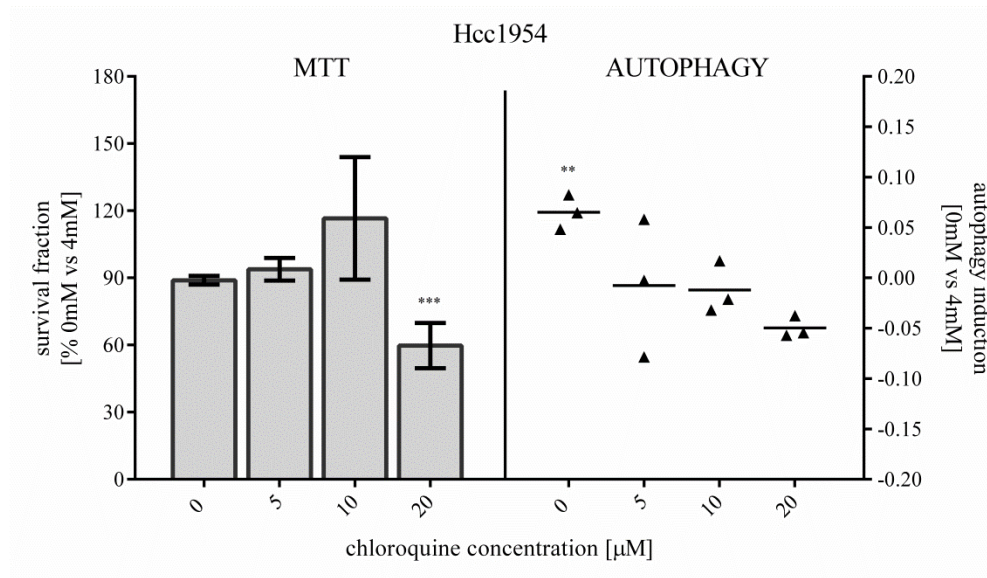


Figure 3-11. Effect of Chloroquine administration on survival and autophagy induction during gln deprivation.

The effect of Chloroquine administration on gln deprivation survival rate and autophagy induction was analysed in A) unmethylated (MDA-MB-231, MCF7 and T-47D) and B) methylated *GLUL* expressing (Hcc1954, MDA-MB-468 and MDA-MB-361) cell lines. The survival rate was analysed as described in Materials and methods after 24 hour of gln deprivation, autophagy induction after 4h of gln deprivation. The data are expressed as average with standard deviation from biological triplicates. One-way ANOVA on Prism 6.0 (Graph Pad) was used to analyse the statistical significance over the untreated control. Statistical significance was showed as stars (*: p-value 0.05, **: p-value 0.01, ***: p-value 0.001, ****: p-value <0.001).

3.3.3 GLUL re-expression

Results (above) established glutamine deprivation sensitivity as primarily associated with Glutamine synthetase baseline expression and the ability to quickly modulate expression under stress stimuli. To evaluate the importance of *GLUL* in response to starvation treatment, the gene was stably re-expressed in methylated *GLUL* silenced cells, JIMT1 and Hs 578T.

As shown in Figure 3-12, *GLUL* re-expression was sufficient to restore resistance to glutamine deprivation in JIMT1, methylated and *GLUL*-silenced cells. Glutamine deprivation had no effect in JIMT1 cells over-expressing *GLUL* (GLUL), whilst the treatment caused a decrease of 44.7% in survival in the same cell line non expressing the gene (VEC) (Figure 3-12).

The results from this experiment suggested GS presence as the primary marker of resistance to glutamine deprivation, emphasising the relevance of the gene repression by epigenetic modulation in synthetic lethality.

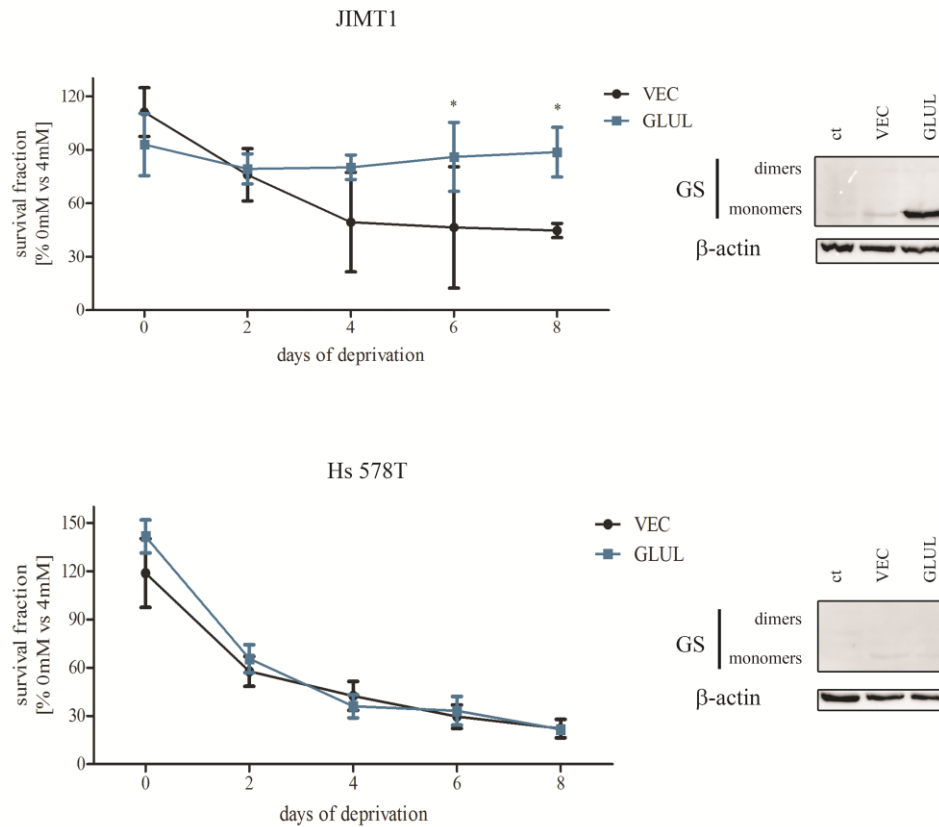


Figure 3-12. *GLUL* re-expression and gln deprivation.

JIMT1 and Hs 578T were stably transfected with a Glutamine synthetase (*GLUL*) or an empty pcDNA3.1 vector (VEC). Transfected cells were gln deprived up to 8 days. Survival fraction was calculated as described in Materials and Methods. The experiment was repeated in biological triplicates and the results are shown as average with standard deviation. GS levels were investigated by SDS-PAGE electro-blotting after each experiment. Two-way ANOVA on Prism 6.0 (Graph Pad) was used to analyse the statistical significance of each day. Statistical significance was shown as stars (*: p-value 0.05, **: p-value 0.01, ***: p-value 0.001, ****: p-value <0.001).

3.4 Methylation analysis of *GLUL* in primary breast cancer tissues

3.4.1 Primary tissue cohort

3.4.1.1 Methylation analysis

Epigenetic and functional analysis on Glutamine synthetase established DNA methylation as marker of repression of gene expression. To evaluate the *GLUL* methylation influence on overall survival in primary breast cancer patients, primary breast cancer tissues and normal breast samples were screened by pyrosequencing (Figure 3-2).

Initial experiments involved evaluation of the potential of DNA methylation to distinguish normal from primary breast cancer tissues. As shown in Figure 3-13, no *GLUL* methylation was found in normal tissues, characterised by a methylation median of 5.8% ranging from 2.5% to 9%. Median methylation was 18.22% in tumour samples, ranging from 1% to 93.33% (Figure 3-14 A). The validation of methylation as a test to discriminate the two populations was confirmed using ROC-curve analysis (area: 0.916, p-value <0.001) (Figure 3-14 B). Therefore, the normal tissue methylation mean with three standard deviations was used as cut-off to classify the tumour samples.

Tumour tissues were divided into hyper- and hypo-methylated using 11.5% as cut-off, generated based on *GLUL* methylation in normal tissues (Table 3-2). Univariate COX regression analysis showed nodal status and methylation status as the only significant prognostic factors for overall survival. However, a worse outcome was

expected to be associated with an increase in the lymph nodes status (HR: 0.25, C.I.: 0.08-0.76, p-value: 0.014). After nodal status, methylation was the only other significant prognostic factor for overall survival in breast cancer patients (HR: 0.53, C.I.: 0.29-0.97, p-value: 0.039). Patients with hypo-methylated tumour are therefore associated with a 47% higher risk of a worse prognosis compared to patients with hyper-methylated cancers. Multivariate COX regression analysis showed that the effect of *GLUL* methylation on overall survival did not change when adjusted for age, the main confounding factor in death analysis. Stepwise COX regression proportional hazards model showed that after methylation the subsequent influential factor was ER status (p-value: 0.158). However when adjusted for ER status, methylation was no longer significant (HR: 0.57, C.I.: 0.29-0.97, p-value: 0.07).

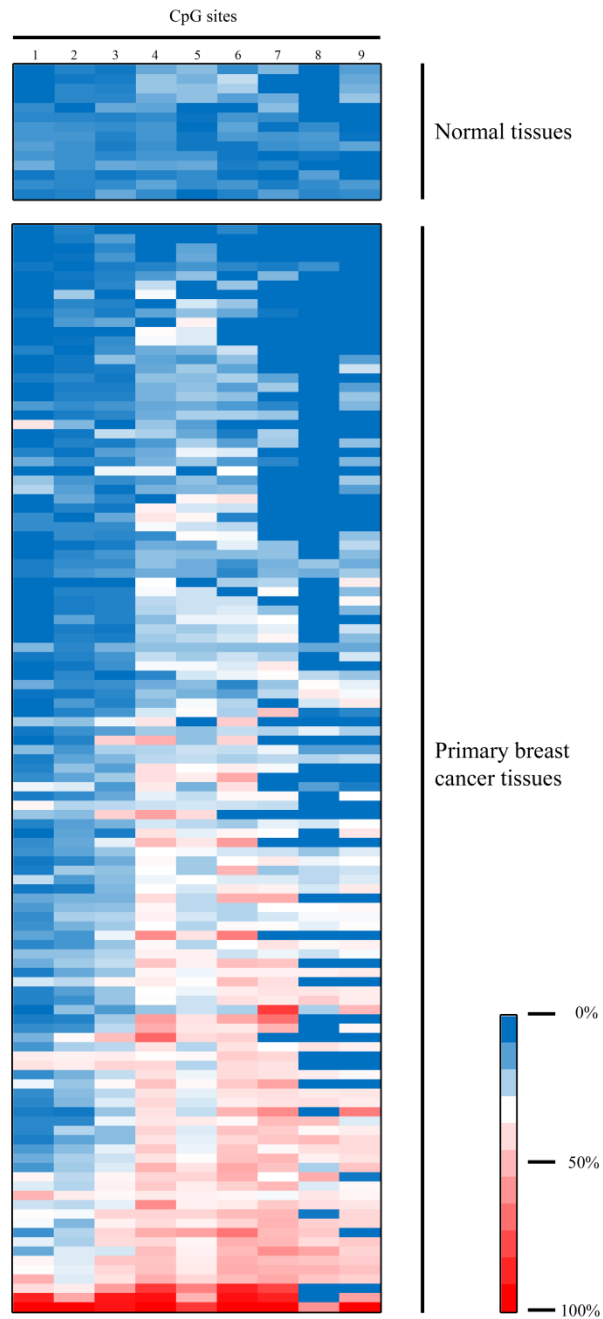


Figure 3-13. Pyrosequencing analysis of *GLUL* promoter region of primary tissue cohort.

The *GLUL* CpG island was analysed in 115 breast primary cancer and 20 normal formalin-embedded tissues by pyrosequencing. The data are shown as percentage methylation, generated from the Pyromark CpG Software (Qiagen). The results are colour-coded based on the methylation values, from red when hyper-methylated (100%) to blue when hypo-methylated (0%). Each row represents a sample.

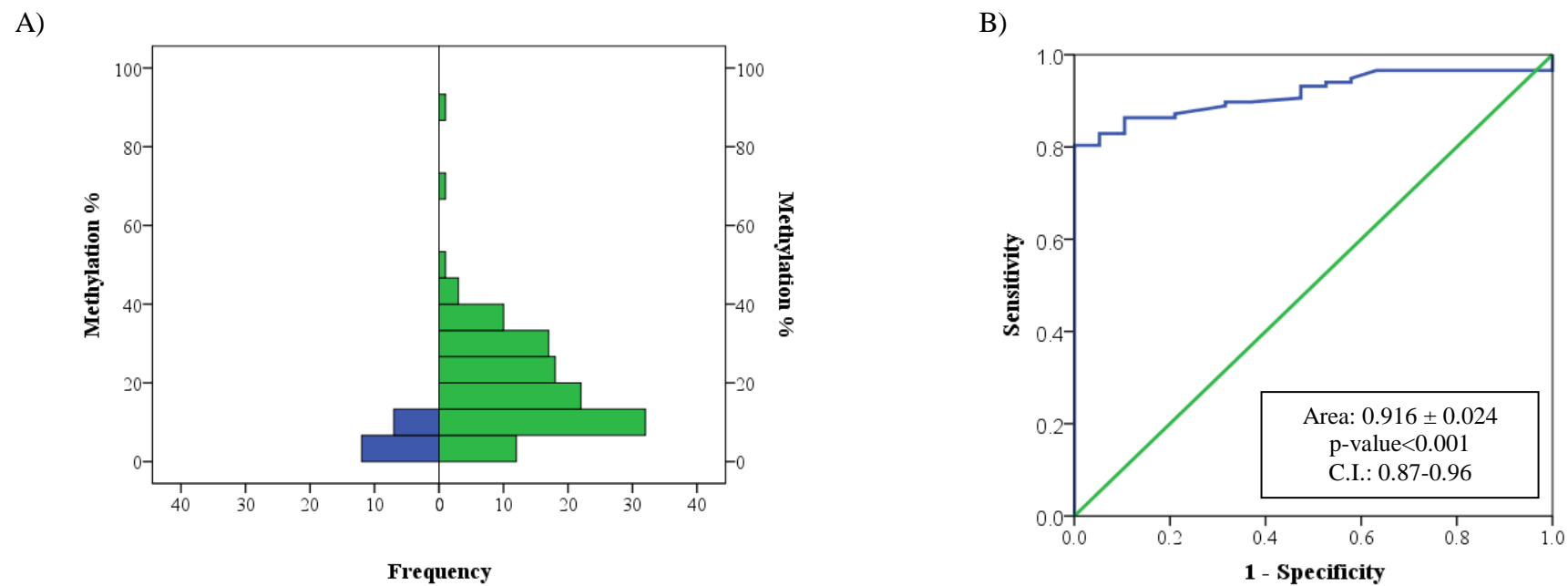


Figure 3-14. Methylation analysis of normal and tumour samples.

DNA methylation distribution was compared between normal and tumour samples using SPSS (IBM Software) either by frequencies (A), with normal samples in blue and tumour samples in green) or by Receiver Operating Characteristic (ROC) curves (B).

Tumour samples			
	Hypo-methylated	Hyper-methylated	p-value
Number of samples	37 (32%)	78 (68%)	
Age [median (min-max)]	71 [46-95]	73.5 [47-96]	0.402
Hormone-receptor status			0.046
ER+	36 (23.8%)	68 (45.0%)	
ER & PR+	30 (28.8% of ER+)	53 (65.4% of ER+)	
ER & PR-	6 (5.8% of ER+)	15 (14.4% of ER+)	
ER-	1 (0.7%)	10 (6.7%)	
Her2 status			0.833
Positive	4 (2.6%)	8 (5.2%)	
negative	33 (21.9%)	70 (46.4%)	
Triple negative	1 (0.7%)	9 (5.9%)	0.031
Tumour Grade			0.194
Grade 1	5 (3.3%)	6 (4.0%)	
Grade 2	25 (16.6%)	64 (42.4%)	
Grade 3	5 (3.3%)	8 (5.2%)	
Tumour Size			0.386
T1	19 (12.6%)	43 (28.5%)	
T2	11 (7.3%)	27 (17.9%)	
T3/4	7 (4.6%)	8 (5.2%)	
Nodal status			0.865
N0	28 (18.4%)	61(40.4%)	
N1	8 (5.2%)	16 (10.6%)	
N2/3	1 (0.7%)	1(0.7%)	
Median F/U [years]	6	7	0.976

Table 3-2. Clinical characteristics of hypo- and hyper-methylated primary breast cancer tissue samples.

Tumour samples were divided into hypo- and hyper-methylated for *GLUL* promoter region and screened for age, follow-up period (F/U), oestrogen receptor (ER), progesterone receptor (PR) and Human Epidermal Growth Factor Receptor 2 (Her2) status. Distributions between the two population were tested by non-parametrical Wilcoxon-Mann-Whitney test (two variables) or Kruskal-Wallis One-way ANOVA (for more than two variables) using SPSS (IBM Software). Tumours were histologically analysed using the TMN staging system.

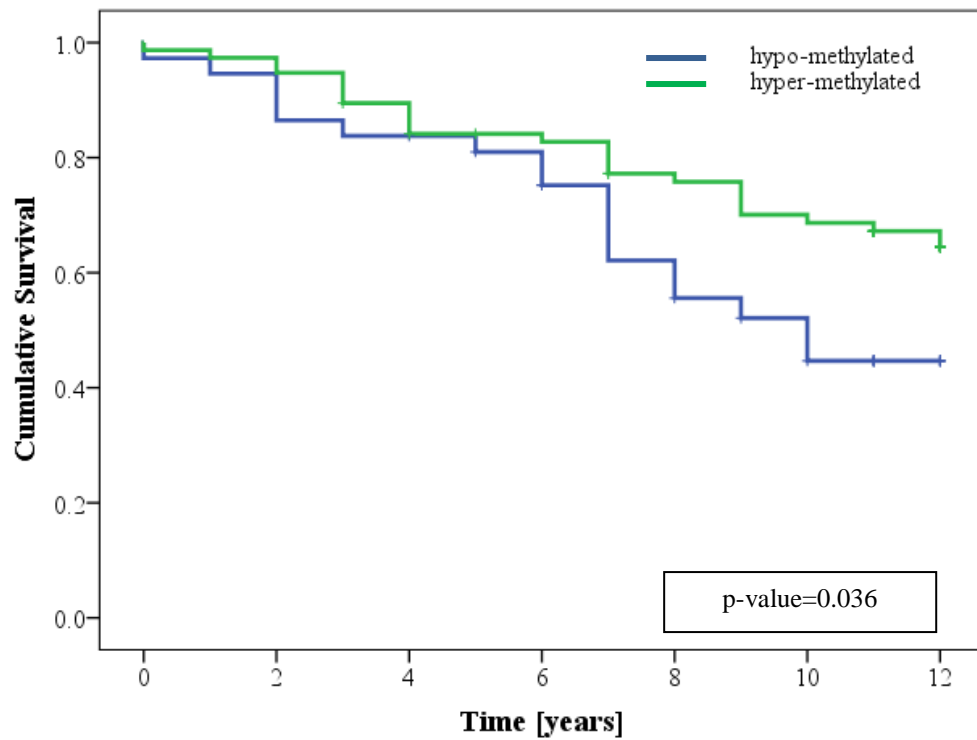


Figure 3-15. Overall survival of primary tissue cohort based on methylation status.

Overall survival of primary breast cancer patients (in years) was analysed using COX-regression in SPSS (IBM Software). Patients' data were divided into hypo- (blue) and hyper-methylated (green) for *GLUL* promoter region during the analysis. Kaplan-Meier plot and Hazard Ratio (HR) were generated by COX-regression analysis using SPSS (IBM Software).

3.4.1.2 Tissue Micro-Array analysis

Glutamine synthetase epigenetic and functional analysis established the expression and protein level as primary markers for sensitivity to glutamine deprivation treatment, therefore breast cancer tissues were screened for GS by TMA.

Tumour samples were scored from 0, when no stain was detectable, up to 3 for increasing GS-staining by a pathologist from Barts Cancer Institute (Queen Mary University of London). For the purpose of this study breast cancer tissues were divided into GS-negative when scored 0 and GS-positive otherwise (Table 3-3). Univariate COX regression showed that none of the variables tested, including GS level (p-value 0.124), were prognostic factor for overall survival in the breast cancer patients cohort (Figure 3-16).

Tumour samples			
	GS-positive	GS-negative	p-value
Number of samples	55	28	
Age [median (min-max)]	73.0 [26-89]	75.5 [48-87]	0.146
Hormone-receptor status			0.712
ER+	52 (63.9%)	26 (31.3%)	
ER & PR+	42 (53.8% of ER+)	19 (24.4% of ER+)	
ER & PR-	10 (12.8% of ER+)	7 (8.9% of ER+)	
ER-	3 (3.6%)	2 (2.4%)	
Her2 status			0.461
Positive	38 (45.8%)	18 (21.7%)	
negative	16 (19.3%)	10 (12.1%)	
Triple negative	0 (0%)	0 (0%)	
Tumour Grade			0.508
Grade 1	3 (3.6%)	1 (1.2%)	
Grade 2	41 (44.4%)	23 (27.7%)	
Grade 3	9 (10.8%)	4 (4.8%)	
Tumour Size			0.657
T1	23 (27.7%)	13 (15.7%)	
T2	19 (22.9%)	13 (15.7%)	
T3/4	12 (14.5%)	2 (2.4%)	
Nodal status			0.517
N0	38 (45.8%)	22 (26.5%)	
N1	13 (15.7%)	6 (7.2%)	
N2/3	1 (1.2%)	0 (0%)	
Median F/U [years]	6	7.5	0.088

Table 3-3. Clinical characteristics of GS-positive and GS-negative primary breast cancer tissue samples.

Tumour samples were divided into GS-positive and GS-negative based on the pathology staining score. Each group was screened and statistically tested for age, F/U, ER, PR and Her2 status by non-parametrical Wilcoxon-Mann-Whitney test (two variables) or Kruskal-Wallis One-way ANOVA (for more than two variables) using SPSS (IBM Software). Tumours were histologically analysed using the TMN staging system.

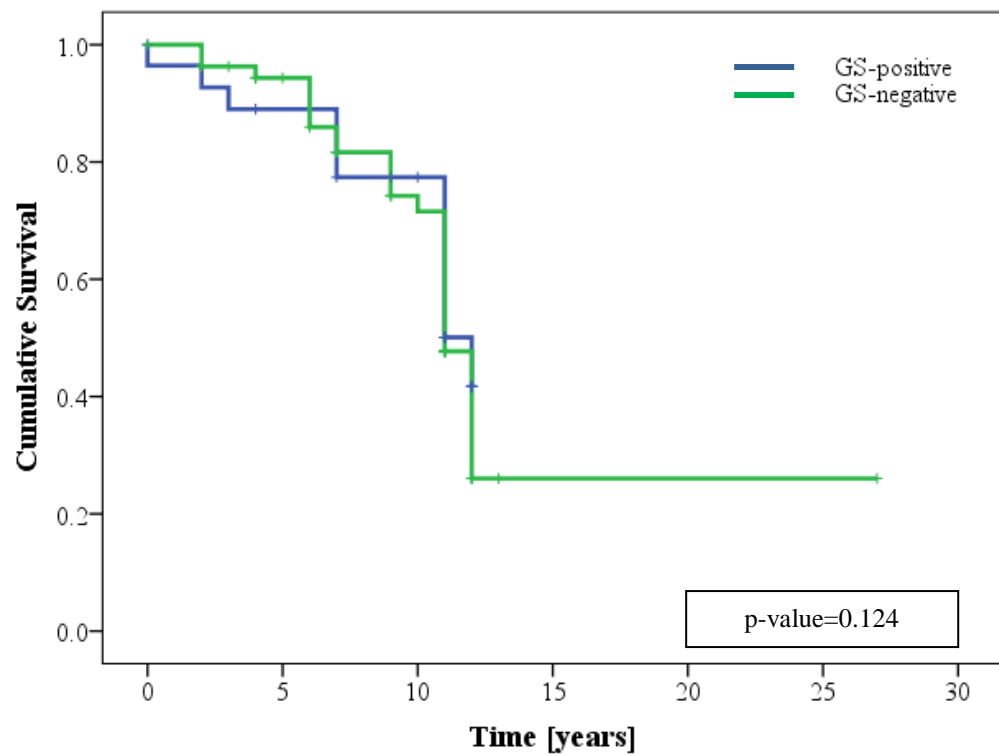


Figure 3-16. Primary tissue cohort survival based on TMA analysis.

Overall survival in years in primary breast cancer patients was analysed using Kaplan-Meier curve on SPSS (IBM Software). Patients' data was divided into GS-positive (blue) and GS-negative (green).

3.4.1.3 TMA and methylation combined analysis

In vitro analysis identified *GLUL* methylated breast cancer cell lines with no baseline gene expression as the main target for synthetic lethality. Therefore DNA methylation and TMA screening results were combined to investigate the correlation between overall survival and *GLUL*-related tumour subtypes.

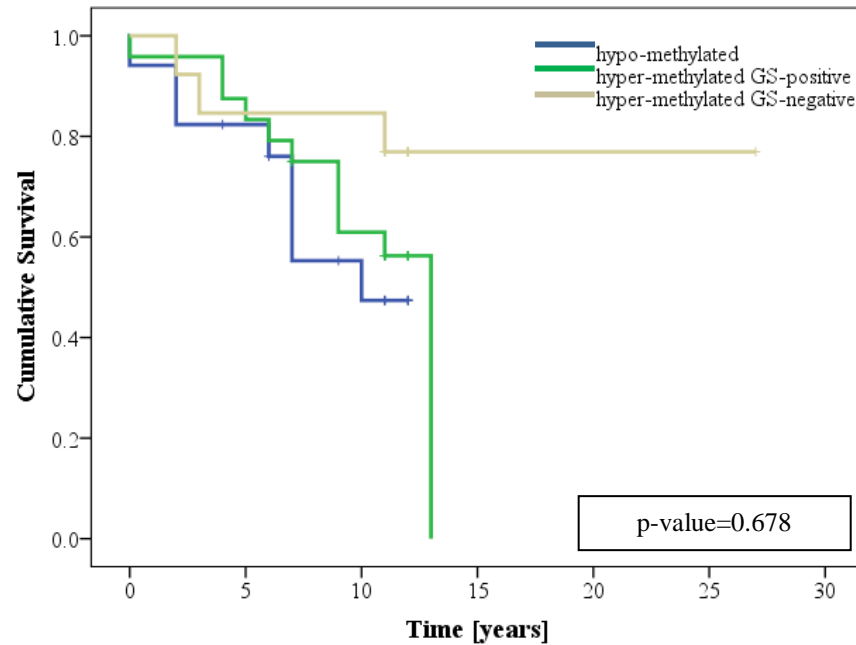
Tumour patients were thus divided into three groups: unmethylated, methylated GS-positive and methylated GS-negative (Table 3-4). Univariate COX regression analysis showed that none of the variables tested, including *GLUL*-related subtypes (p-value 0.678), was a prognostic factor for overall survival in this cohort of breast cancer patients (Figure 3-17 A). However, the survival plot showed a trend of better survival in patients with methylated tumours non-expressing Glutamine synthetase (Figure 3-17 A). When patients with methylated GS-negative tumours were isolated and compared with the remaining patients, *GLUL*-silencing was very close to statistical significance as a prognostic factor in univariate COX regression analysis (HR: 0.39, C.I.: 0.11-1.33, p-value 0.093) (Figure 3-17 B), whilst the other variables were non-significant.

Tumour samples			
	Hypo-methylated	Hyper-methylated GS-positive	Hyper-methylated GS-negative p-value
Number of samples	17 (31.5%)	24 (44.4%)	13 (24.1%)
Age [median (min-max)]	74 [36-87]	68 [26-89]	67 [58-87] 0.312
Hormone-receptor status			0.077
ER+	17 (31.5%)	22 (40.7 %)	11 (20.4%)
ER & PR+	14 (28% of ER+)	17 (34% of ER+)	7 (14% of ER+)
ER & PR-	2 (4% of ER+)	5 (10% of ER+)	4 (8% of ER+)
ER-	0(0%)	2 (3.7%)	2 (3.7%)
Her2 status			0.326
Positive	9 (16.7%)	4 (7.4%)	9 (16.7%)
negative	8 (14.8%)	20 (37.0%)	4 (7.4%)
Tumour Grade			0.452
Grade 1	1 (1.9%)	2 (8.3%)	1 (1.9%)
Grade 2	14 (25.9%)	21 (38.9%)	8 (14.8%)
Grade 3	2 (3.7%)	1 (1.9%)	4 (7.4%)
Tumour Size			0.469
T1	7 (12.9%)	11 (20.4%)	5 (9.3%)
T2	6 (11.1%)	11 (20.4%)	6 (11.1%)
T3/4	4 (7.4%)	2 (3.7%)	2 (3.7%)
Nodal status			0.379
N0	12 (22.2%)	17 (31.5%)	12 (22.2%)
N1	5 (9.3%)	6 (11.1%)	1 (1.9%)
N2/3	0 (0%)	1 (1.9%)	0 (0%)
Median F/U [years]	7	6	10 0.297

Table 3-4. Clinical characteristics of hypo-methylated, hyper-methylated GS-positive and hyper-methylated GS-negative primary breast cancer tissue samples.

Tumour samples were divided into hypo-methylated, hyper-methylated GS-positive and hyper-methylated GS-negative. Each group was screened and statistically tested using SPSS (IBM Software) as described before for Hormone-receptor status, Her2 status, tumour size, nodal status. Each sample was histologically graded using the TMN staging system.

A)



B)

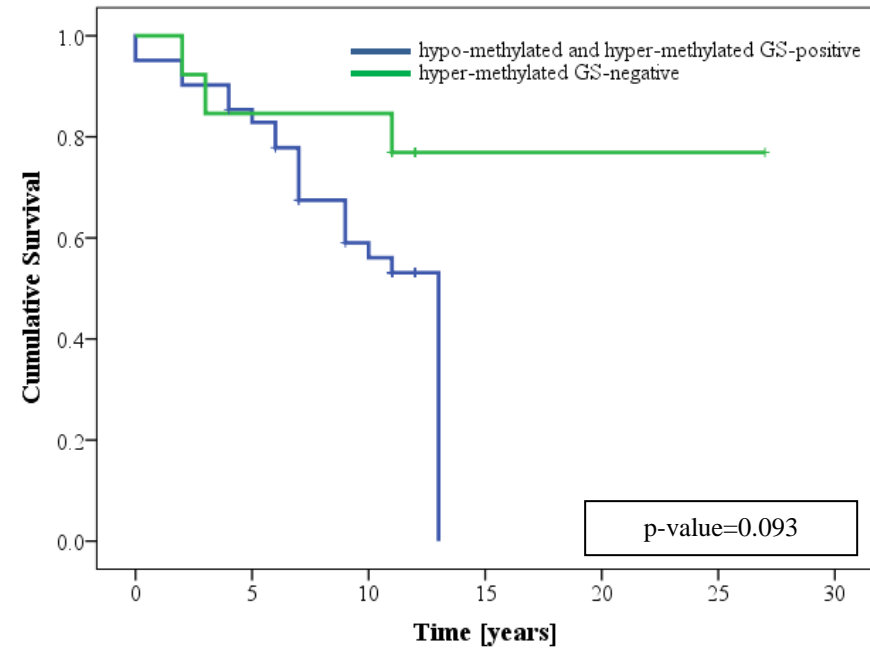


Figure 3-17. Survival analysis on primary tissue cohort based on TMA and methylation status.

Overall survival in years was analysed in primary breast cancer patients by COX regression. Overall survival was investigated dividing patients into A) hypo-methylated (blue), hyper-methylated GS-positive (green) and hyper-methylated GS-negative (grey) and B) combining unmethylated and methylated GS-positive (blue) versus methylated GS-negative (green).

3.4.2 TCGA dataset

523 primary breast cancer patients' methylation and clinical data were downloaded from The Cancer Genome Atlas (TCGA) Data Portal as a second cohort to test DNA methylation as a marker for overall survival.

The 450k Methylation array results showed less global methylation (Figure 3-18) than the primary breast cancer tissue cohort (Figure 3-13). Unfortunately, two out of the four CpG sites screened by pyrosequencing in the primary tissues cohort (section 3.4.1.1) were missing from the dataset (Figure 3-18), as they were covering Single Nucleotide Polymorphisms (SNPs). For this reason, this cohort could not be used to validate the influence of *GLUL* methylation on overall survival in breast cancer.

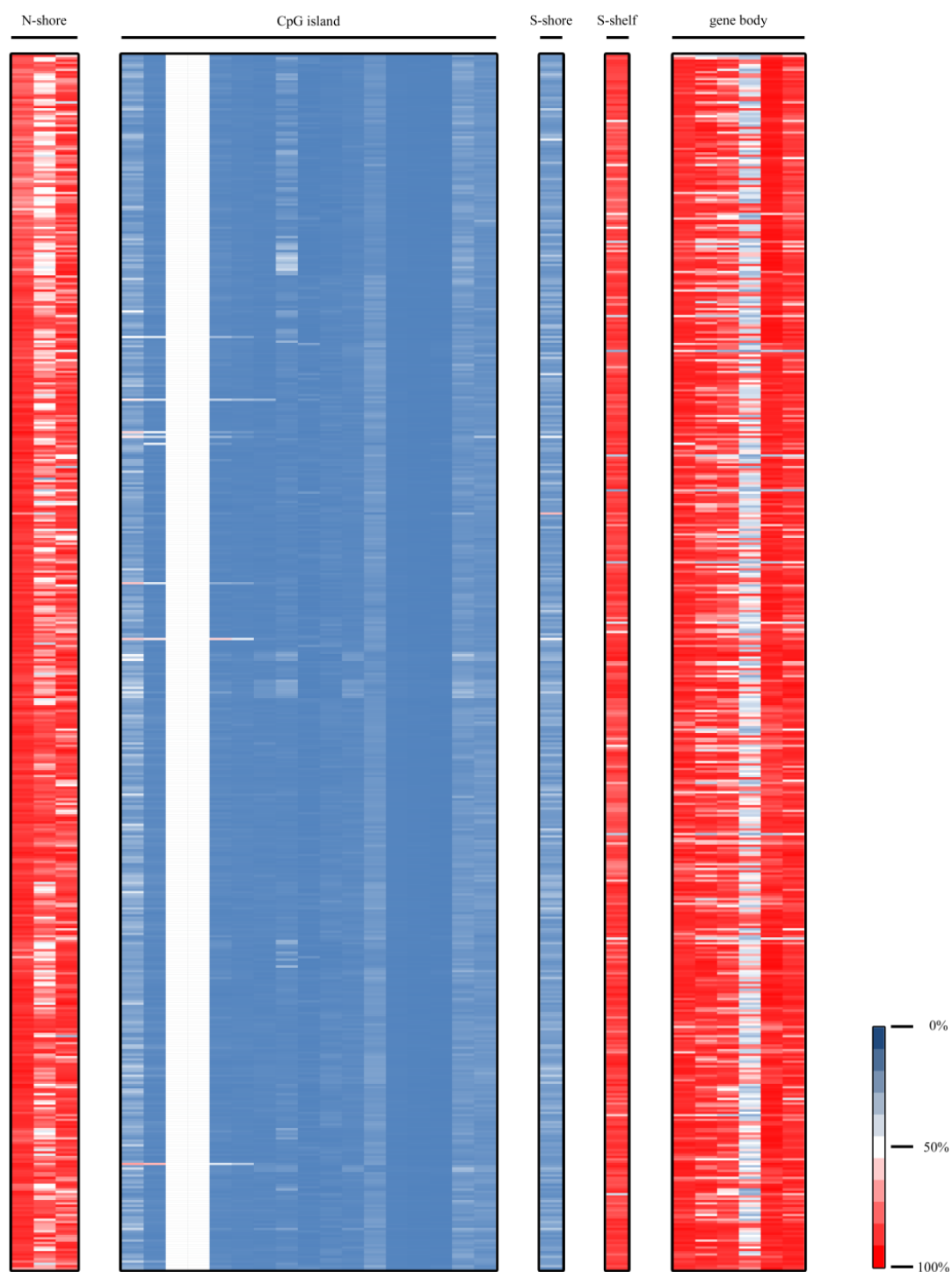


Figure 3-18. Array analysis of the methylation status of the TCGA dataset.

523 frozen primary breast tissues were analysed using 450k Methylation array from the Cancer Genome Atlas (TCGA). The data are shown as β -value and colour-coded based on the methylation status, where red corresponds to a highly methylated (100%) and blue to an unmethylated (0%) CpG site.

3.5 Discussion

Glutamine synthetase (*GLUL*) was identified as highly methylated in breast cancer cell lines by 450k Methylation array (Illumina Inc.) screening. This gene is demonstrated to be epigenetically regulated via DNA methylation and histone acetylation. Based on the epigenetic modifications *GLUL* is subjected to, and the consequent effect on the gene expression levels, three main breast cancer subtypes have been identified in the panel of cell lines tested: unmethylated, methylated *GLUL* expressing and methylated *GLUL*-silenced. Methylated *GLUL*-silenced cells lost the ability to synthesise glutamine and were found to be sensitive to gln deprivation treatment. Methylated cells with baseline *GLUL* expression induced autophagy to compensate for the delay in the gene up-regulation. Blocking autophagy was sufficient to restore sensitivity to the deprivation treatment.

The *in vitro* analysis established *GLUL* as biomarker of synthetic lethality in breast cancer. Epigenetic regulation of Glutamine synthetase, particularly via DNA methylation of the promoter region, determines the cellular response in low glutamine conditions. These results led to further investigations in patient data. Although, COX regression analysis did not show any significant correlation between *GLUL* silencing and overall survival in primary breast cancer patients, a subgroup population with methylated *GLUL* promoter and no detectable GS might be treatable by glutamine depletion therapy.

3.5.1 *GLUL* promoter region is epigenetically silenced in breast cancer cell lines

This is the first study investigating the epigenetic regulation of Glutamine Synthetase gene, and in particular, DNA methylation and histone acetylation in breast cancer cell lines and primary breast cancer tissues.

An important issue to be considered before addressing the DNA methylation role in the gene expression regulation is the identification of the region of most variability. The region most variable in methylation status was first identified by 450k Methylation array and then validated by bisulphite sequencing and pyrosequencing. It is not unusual for differences in methylation status to be found between an array and any validation methods (Bediaga et al. 2010, Roessler et al. 2012, Shen et al. 2012). This is also the case of the validation results in this study; whilst the location of the most variable region within the gene promoter region was confirmed by the validation methods, in some cases the methylation status seen in the array has not been confirmed by the validation methods (Roessler et al. 2012, Shen et al. 2012). However, since the data have been validated with the most accurate method for methylation analysis of bisulphite sequencing, the validation results are robust and the 5'UTR of *GLUL* CpG island confidently identified as the most variable in methylation status.

GLUL promoter hyper-methylation was confirmed in 44% of breast cancer cell lines. It is worth noting that from the analysis of breast cancer cell lines used in this study, highly methylated cells are predominantly Her2 positive with the exception of Triple negative MDA-MB-468. However, a screen on a larger panel of breast cancer cell lines (from Genentech Inc., San Francisco, USA) showed no association between

GLUL methylation and any breast cancer subtypes (Figure 7-1). Therefore, *GLUL* methylation can be concluded not to be associated with any breast cancer subtypes.

Although *GLUL* is highly methylated in approximately 44% of the breast cancer cell lines tested, the Glutamine synthetase gene is not detectable in 12.5% of methylated cell lines by gene expression and translational analysis. Linear regression analysis confirmed no correlation between *GLUL* expression and methylation status (R : 0.301, p -value: 0.258), whilst emphasised a high correlation between gene expression and translational levels (R : 0.818, p -value<0.001), concluding that gene expression determines protein levels. It is worth noting that translational analysis depend on the specificity of the antibody in use: since the anti- Glutamine synthetase antibody specificity was address by native gel, the two bands in the SDS-PAGE electro-blotting analysis were confidently identified as monomers and dimers. This is not the first time Glutamine synthetase appeared in both monomers and dimers in SDS-PAGE electro-blotting analysis (Allodi et al. 2006). Dimers are usually associated with the protein in its active state, as in the case of eNOS, where the ratio between dimers over monomers determines the amount of enzyme active in the cell (Terasaka et al. 2008, Sabri et al. 2011). Unfortunately this was not the case for GS, where the active form is an octamer and the inactive a tetramer (Llorca et al. 2006). The dimers band in this study is probably due to the GS complex quaternary structure: the enzyme consists of eight monomers forming two symmetrical tetramer rings facing each other in the active form of the enzyme. The whole enzyme is stabilised by hydrophobic and hydrogen bonds between mirroring monomers, and the intersection of the C-terminal of one monomer into the hydrophobic region of the adjacent monomer within each ring (Eisenberg et al. 2000, Krajewski et al. 2009).

This tight bond between monomers would explain the difficulties in disrupting it during the denaturation procedure for SDS-PAGE without losing some protein (data not shown). As the main aim of the SDS-PAGE electro-blotting was to compare relative protein levels across the cell line panel, the densitometry from monomers and dimers were combined during the quantification analysis.

Based on the gene expression and translational analysis, DNA methylation is not sufficient to determine *GLUL* silencing in breast cancer cells. However, the presence of a subset of cells highly methylated with no gene expression and no detectable protein led to the hypothesis that a more complex regulatory mechanism was involved in the gene regulation. DNA methylation has been shown to either determine gene silencing on gene expression by itself (Buchholtz et al. 2014, Yang and Zheng 2014), or to work by a set of mechanisms that do not necessarily correlate with gene silencing. In these models DNA methylation would act not by direct silencing, but as a starting marker for chromatin remodelling activation which will cause the gene silencing (Mossman and Scott 2011, Jones 2012, Al-Rayyan et al. 2014, Vallot et al. 2014). Genes involved in cancer development have been demonstrated to be silenced by the co-occurrence of DNA methylation and histone modifications (Mossman and Scott 2011, Al-Rayyan et al. 2014, Liu et al. 2014). DNA methylation has been shown to recruit MeCP2 (methyl CpG binding protein 2)-SIN3 repressive complex (as described in the Introduction) and to promote nucleosome formation on gene promoter regions. This leads to chromatin condensation and gene silencing (Cannuyer et al. 2013, Piazza et al. 2013, Portela et al. 2013). The proposed model not only explains the presence of baseline expression in methylated cell lines, but also their lack of response to de-methylation and pro-

acetylation treatments, and the enhancing effect of pro-acetylation on de-methylation treatment in methylated cells with no baseline expression. If DNA methylation requires condensed chromatin structure to effectively repress gene expression, the gene promoter region would be in an open state in methylated *GLUL* expressing cells and in a condensed state in methylated *GLUL*-silenced cells. Histone acetylation enrichment at 2500 bp upstream *GLUL* TSS confirmed this model, differentiating methylated *GLUL* expressing cells from either unmethylated or methylated *GLUL* non expressing cells (Figure 7-3), being acetylated H3 and H4 markers of gene expression (Nakao 2001, Fuchs et al. 2006, Lee and Lee 2012, Sandoval and Esteller 2012). Consistent with the proposed model, little to no H3 and H4 acetylation was found in JIMT1 and Hs 578T, characterised by high methylation and no baseline expression. Furthermore, histone acetylation levels in these cell lines were inversely proportional to their methylation status: the least amount of acetylation enrichment was found in the highest methylated JIMT1. This result confirms DNA methylation leading to gene silencing by recruiting repressive complexes, which stabilise the chromatin structure removing the acetyl groups from the histone tails (Lakowski et al. 2006, Lee and Lee 2012). Furthermore, the specific position of acetylation enrichment on *GLUL* promoter region is of great interest as it is located on a region of consensus sequences for transcriptional factors such as FOXO3A and β -catenin. Both the transcriptional factors have been associated with a regulatory binding site at 2500 bp upstream *GLUL* transcriptional start site, inducing an increase in the enzyme level within the cell (Kruithof-de Julio et al. 2005, van der Vos et al. 2012).

It is worth noting the interesting profile of the methylated MDA-MB-361 cell lines as the whole promoter region was characterised by an enrichment in histone

acetylation, explaining its very high expression level relative to other breast cancer cell lines.

3.5.2 *GLUL* methylation influences response to glutamine deprivation treatment

The main relevance of Glutamine synthetase epigenetic silencing is its role in cellular response to glutamine deprivation. Glutamine synthetase has been shown to be one of the main genes up-regulated in response to lack of the amino acid in the micro-environment (Wang and Watford 2007). Different transcription factors and pathways have been proposed to regulate *GLUL* under conditions of starvation. For instance, GATA3 (GATA-Binding Factor 3) has been proposed to regulate GS level mainly in luminal breast cancer cells, suggesting a symbiotic mechanism between luminal and basal breast cancer cells. In the proposed model luminal cells up-regulate Glutamine synthetase via GATA3 stimulation, synthesising glutamine for basal cells that are not expressing the enzyme (Kung et al. 2011). Likewise, c-Myc and oestrogen have been shown to modulate glutamine metabolism in cancer cells via down-regulation of microRNA 23a (mir23a) targeting GLS1 (glutaminase, enzyme responsible for glutamine degradation) or by inducing *GLUL* up-regulation and GS increase (Haghighat 2005, Rathore et al. 2012). More interestingly, FOXO3A and β -catenin transcription factors have been shown to bind directly onto *GLUL* promoter region and induce up-regulation of the gene and subsequently of the enzyme (Kruithof-de Julio et al. 2005, van der Vos et al. 2012). Their relevance lies in the co-existence of a regulatory binding site for each of these transcription factors and a peak of histone acetylation on the same region on *GLUL* promoter in cell lines expressing the gene of interest. This would explain the different effect of gln deprivation on *GLUL* expression and survival in methylated breast cancer cells. In

methyated *GLUL*-silenced cells, the condensed state of *GLUL* promoter region doesn't allow the binding of those transcription factors and the gene modulation in response to gln deprivation, determining cell death. Consistent with these results, *GLUL* re-expression in these cells, restored resistance to glutamine deprivation treatment. In contrast, in methyated *GLUL* expressing cell lines an open state of the chromatin in the region of interest, enables the binding of the transcription factors and GS up-regulation. These cells survived the glutamine deprivation treatment.

Interestingly, although methyated *GLUL* expressing cells were not sensitive to glutamine deprivation treatment, Glutamine synthetase up-regulation was delayed compared to unmethyated cell lines in response to low glutamine conditions (Figure 7-4). To supply the amino acid in the early stages of glutamine starvation, these cells induce autophagy. While this is the first study associating autophagy induction to *GLUL* methylation status, published studies has shown cancer cells' induction of autophagy to overcome the need for nutrients and low amino acid conditions (Nicklin et al. 2009, Vander Heiden et al. 2009, Boukhettala et al. 2010, Ferreira et al. 2012, Lorin et al. 2013, Shanware et al. 2013). For instance, arginine deprivation treatment has been associated with an increase in autophagy in different types of cancer (Savaraj et al. 2010, García-Navas et al. 2012, You et al. 2013). Arginine, as glutamine, is a non-essential amino acid normally derived from the blood stream, but it can be synthesised when required (Wu and Morris 1998). Consistent with data shown for *GLUL* in this study, methylation of the enzyme responsible for arginine synthesis (Arginino-succinate synthetase, *ASSI*) has been demonstrated not only to be the primary cause of the autophagy response during the amino acid deprivation treatment, but also to be associated with treatment resistance (Delage et al. 2010,

Syed et al. 2013). When autophagy induction was blocked by Chloroquine administration, sensitivity to arginine deprivation treatment was restored (Syed 2013). Consistent with this study, methylated *GLUL* expressing cells were found to be sensitive to glutamine deprivation when treated with Chloroquine, while no difference was seen in survival in unmethylated cells.

In conclusion, this study demonstrated for the first time that Glutamine synthetase (*GLUL*) gene is subjected to epigenetic modulation via DNA methylation and histone modification. The epigenetic profile determines the cellular response in low glutamine conditions. Whilst unmethylated cells up-regulate the gene as an immediate response to glutamine deprivation, methylated cells induce autophagy. The autophagy response is then repressed once *GLUL* is up-regulated. In the event that the gene up-regulation is not possible, autophagy is maintained causing cell death. Therefore methylated *GLUL*-silenced cells are sensitive to glutamine deprivation, whereas methylated *GLUL* expressing are not. For this reason, breast cancers with high methylation on *GLUL* promoter region and no baseline expression/protein level are the perfect target for synthetic lethality via low glutamine conditions (Figure 3-19). The data obtained in this study suggested PI3K-AKT pathway as the main mechanism inducing Glutamine synthetase up-regulation and autophagy in glutamine low conditions. Indeed, in response to glutamine starvation the pathways have been shown to determine autophagy induction via mTOR and *GLUL* up-regulation via translocation of FOXO3A into the nucleus (van der Vos et al. 2012). The pathway perfectly fits in the response described for methylated breast cancer cell lines and the methylated *GLUL* expressing cells ability

to overcome the repressive effect of DNA methylation by histone acetylation at 2500 bp upstream the gene TSS, where a binding sequence for FOXO3A is located.

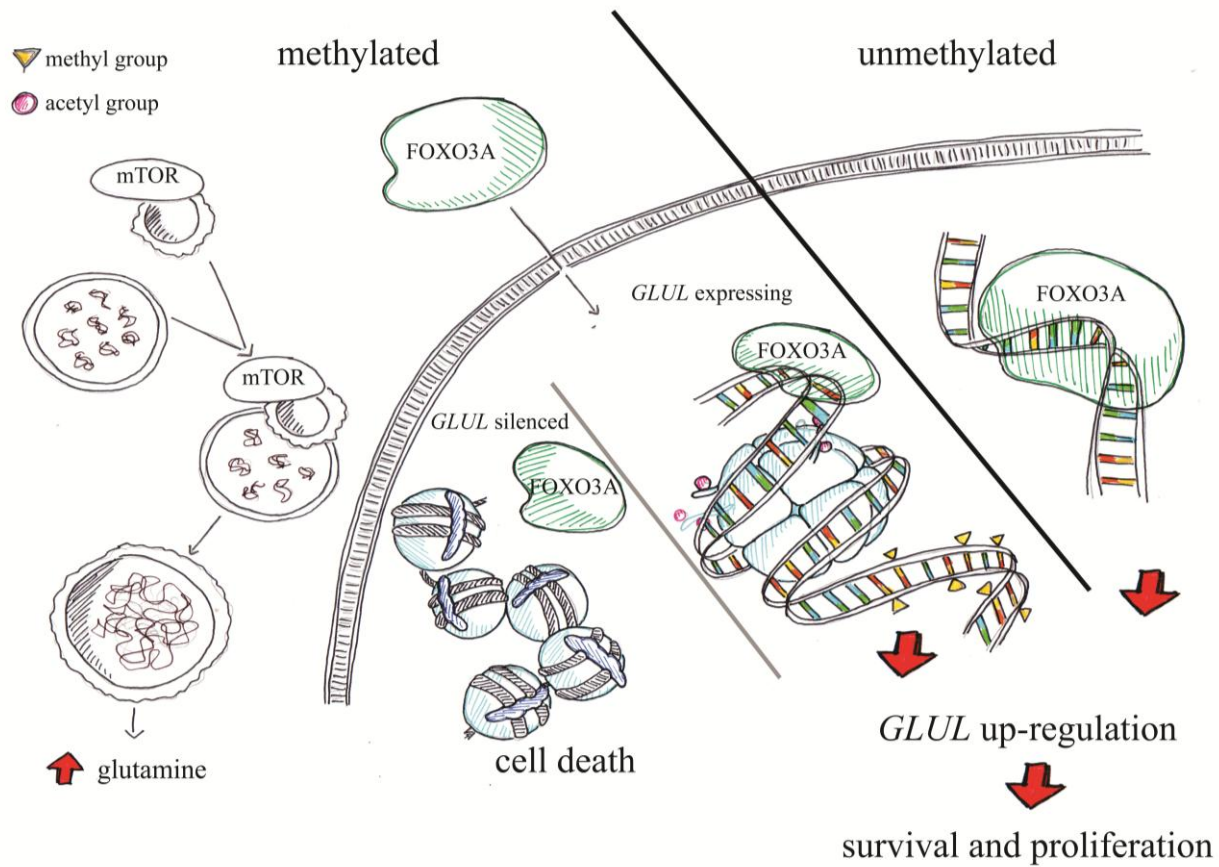


Figure 3-19. *GLUL* modulation in low glutamine conditions.

GLUL unmethylated cells up-regulate Glutamine synthetase in response to gln deprivation. Methylated cells induce autophagy and *GLUL* up-regulation when possible. Cells enable to up-regulate *GLUL* survive the treatment, whilst *GLUL* silenced cells unable to do so do not.

3.5.3 Glutamine synthetase epigenetic regulation and breast cancer patients

In the analysed primary breast cancer cohort, 68% of breast cancer tissues were found highly methylated for Glutamine synthetase. Furthermore, patients with hypo-methylated breast cancer showed to have 47% higher risk of a worst outcome compared to the hyper-methylated (HR: 0.53, C.I.: 0.29-0.97, p-value: 0.039). DNA methylation has already been used as biomarker in other types of cancer: e.g. *MGMT* has been identified and validated as a positive prognostic marker for overall survival and *ASS1* as predictive biomarker for arginine deprivation therapy (Delage et al. 2010, Shen et al. 2010, Delage et al. 2012, Quillien et al. 2014, Zhang et al. 2014). However, in these studies DNA methylation resulted in the gene silencing, which is not the case for Glutamine synthetase. Based on the *in vitro* analysis, only methylated breast cancer with no detectable GS would be sensitive to glutamine deprivation, resulting in the importance of correlating the DNA methylation data with the protein level in each tumour sample.

An important issue that needs to be addressed before discussing data any further is methylation cut-off. The cut-off determination is extremely important in defining which population has to be considered hyper-methylated and which hypo-methylated and the consequent evaluation of gene methylation as biomarker in overall survival. There are no golden standard to determine a cut-off value DNA methylation as large-scale analysis has only recently been possible. In published studies, methylation cut-off has been determined by ROC-curve analysis; value, above the median value of tumour tissues is identified as hyper-methylated, or, when available, using the mean or median of normal tissues methylation distribution with or without standard deviation (Shen et al. 2010, Bihl et al. 2012, Chen et al. 2013, Oberstadt et al. 2013,

Suzuki et al. 2013, Quillien et al. 2014). Since normal tissues methylation distribution is the most informative in defining a non-malignant profile, the cut-off was calculated as mean of methylation in normal tissues with three standard deviations, taken into account the higher margin of error due to FFPE samples.

In the primary breast cancer tissues cohort, 24.1% of the population was hyper-methylated for *GLUL* with no detectable GS, yet no significant association with overall survival was observed. Interestingly, the proportion of hypo- and hyper-methylated samples remained the same across the analysis, suggesting a relevance of *GLUL* methylation in breast cancer patients' outcome. Unfortunately, only 36% (54/151) of the primary breast cancer samples were analysed for both *GLUL* methylation and GS level. It would be of great interest to reproduce the same analysis on a larger cohort of samples.

Although, *GLUL* epigenetic modulation does not significantly correlate with overall survival, its main relevance resides in its potential as therapeutic indicator. *GLUL* epigenetic silencing can be exploited for synthetic lethality in breast cancer in the same way arginine depletion has already been used in tumours lacking *ASS1* via methylation (Scott et al. 2000, Ensor et al. 2002, Feun and Savaraj 2006, Szlosarek et al. 2006, Kim et al. 2009, Delage et al. 2010, Kobayashi et al. 2010, Kuo et al. 2010). Indeed, the *in vitro* analysis identified a subset of cells characterised by high DNA methylation, no protein and high sensitivity to glutamine deprivation treatment. It would be of great interest to validate the model *in vivo*, which would emphasise the clinical relevance of *GLUL*-silencing as predictive biomarker in breast cancer. An *in vivo* model would enable evaluation to the response of normal and

tumour tissues to glutamine deprivation with and without *GLUL*-silencing, as well as the side-effect of such a therapy in a whole organism. While this was beyond the scope of the current study, such experiments are planned to the immediate future.

Recently an available drug, Erwinase, has been shown to be active in glutamine depletion in a different type of cancer (Willems et al. 2013). The drug has been approved in 2011 as an orphan drug, designed to treat to treat patients with acute lymphoblastic leukaemia (ALL), a disease affecting less than 200,000 people (FDA 2014). It was first design to reduce the level of asparagine, a non-essential amino acid important for leukaemia cells proliferation (Agrawal et al. 2013). The glutamine-depletion activity increased changing the bacteria the drug was produced in. The bacteria strand was changed to contrast the allergic side effect patients develop to the E.coli-derived asparaginase-based drug (Emadi et al. 2014, FDA 2014). Indeed Erwinase has been shown to reduce the serum glutamine concentration, and correlated with complete remission in leukaemia patients (Agrawal et al. 2013, Willems et al. 2013). Consistent with the response described for breast cancer cells in this study, myeloma cells have been shown to respond to glutamine depletion by *GLUL* up-regulation and autophagy induction (Willems et al. 2013). Furthermore, in these cells *GLUL* up-regulation and autophagy induction during Erwinase administration have been associated with the development of a resistant phenotype (Willems et al. 2013), in the same way breast cancer cells have being shown to develop resistance to glutamine depletion treatment in this study. Therefore, it would be of great interest as an extension of this project to evaluate Erwinase treatment as potential therapy in *GLUL*-epigenetic modulated breast cancer. Based on the *in vitro* data discussed in this study, *GLUL*-silenced breast

cancer cells and consequently patients with *GLUL*-silenced breast carcinoma would be sensitive to glutamine deprivation treatment via Erwinase administration. *GLUL*-silenced cancer cells would be unable to up-regulate the gene in low glutamine condition, inducing autophagy that would lead to selective death of cancer cells. Normal tissues would up-regulate *GLUL* without any effect on survival. Based on the current results, it would also be of great interest to validate Erwinase treatment in *in vivo* model to validate it as treatment in *GLUL*-silenced breast cancer.

4 Arginino-succinate synthetase

4.1 Introduction

Preliminary data within our group have identified *ASS1* as highly methylated in a selection of primary breast cancer patients. *ASS1* is the rate-limiting enzyme in the arginine-NO-citrulline cycle and synthesis of arginine (Delage et al. 2010). Tumours lacking *ASS1* expression via methylation-mediated silencing have been shown to be sensitive to synthetic lethality via arginine reduction (Ensor et al. 2002, Feun and Savaraj 2006, Kim et al. 2009, Kobayashi et al. 2010, Kuo et al. 2010). *ASS1* silencing has not been associated with any other mechanisms other than DNA methylation.

Human cells normally derive arginine from the blood stream, but it can be synthesised via the urea cycle when required (Delage et al. 2010). Various tumour cell lines are auxotrophic for arginine and incapable of survival in amino acid reduced conditions (Scott et al. 2000). The corresponding tumours, including melanoma, hepatocellular carcinoma, mesothelioma and prostate cancer, are associated with high chemo-resistance and poor clinical outcome (Ensor et al. 2002, Dillon et al. 2004, Szlosarek et al. 2006, Kim et al. 2009, Nicholson et al. 2009).

Arginine-targeting therapy has been shown to be effective in cancers such as melanoma, prostate cancer and glioblastoma (Ensor et al. 2002, Feun and Savaraj 2006, Kim et al. 2009, Kobayashi et al. 2010, Kuo et al. 2010). The treatment is based on a recombinant form of the Arginine Deiminase (ADI-PEG20), a

Mycoplasma-derived enzyme capable of degrading arginine (Ensor et al. 2002, Kuo et al. 2010). Tumours with low to non-existent *ASS1* have been shown to be more sensitive to ADI-PEG20 treatment (Szlosarek et al. 2006, Kim et al. 2009). However in the absence of *ASS1* methylation-mediated repression cancer cells reactivate the gene developing a resistant phenotype (Feun and Savaraj 2006). In contrast, tumours with *ASS1* methylation are unable to transcriptionally up-regulate the gene and have not been associated with any resistant phenotype (Nicholson et al. 2009).

This study aims to examine *ASS1* silencing via methylation and evaluate the possibility of using this as a predictive biomarker for synthetic lethality in breast cancer.

4.2 Epigenetic regulation

4.2.1 Methylation analysis

4.2.1.1 450k methylation array

The breast cancer cell lines panel was screened using the 450k Methylation array (Illumina), as previously described.

As shown in Figure 4-1, the N-shore, the S-Shelf and 6 probes in the gene body were found to be highly methylated, while the S-Shore and 2 probes in the gene body showed little to no methylation. Highly methylated region ranged from 58% to 92%, whilst low methylated between 3.5% and 46%. It is worth noting that the CpG island was the only region showing variability in methylation across the panel, ranging from 3.2% to 79%. However, no methylation was found in the region that has been correlated with silencing of gene expression (Nicholson et al. 2009, Syed 2013) (the second probe in the CpG island in Figure 4-1).

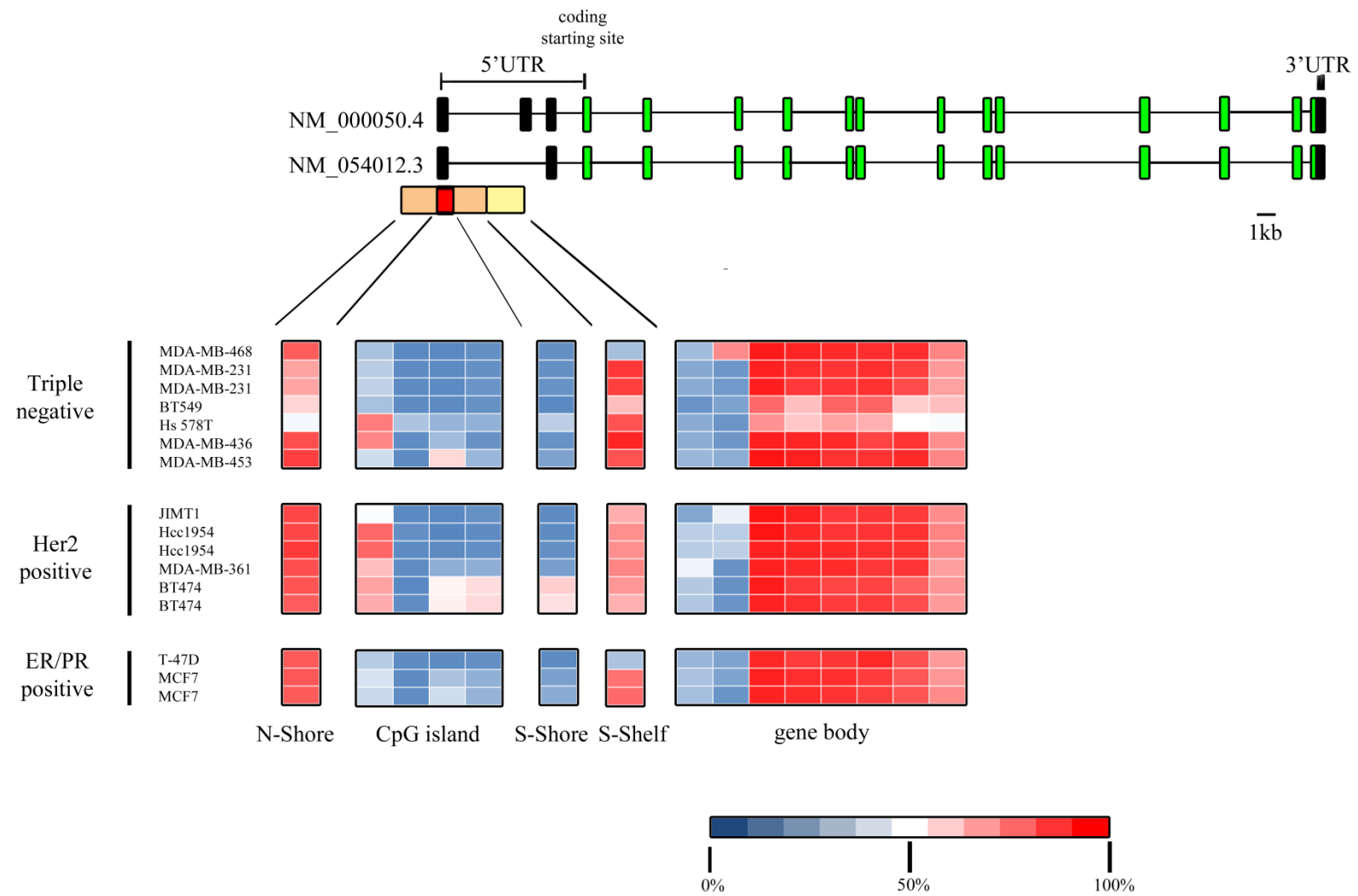


Figure 4-1. Results of 450k Methylation array for Arginino-succinate synthetase.

Breast cancer cell lines were analysed using the 450k Methylation array (Illumina). Cells were divided based on subtypes: 6 Triple negative, 4 Her2-positive and 3 hormone-positive. The CpG island starts 230 bp upstream the transcriptional start site (TSS). *ASS1* is located on chromosome 9q43 and includes two transcripts, NM_000050.4 and NM_054012.3. The transcripts share the same coding region, composed of 13 exons (in green) and the same 3'UTR (in blue), but differ in the 5'UTR. NM_000050.4 has an extra exon in the 5'UTR. The CpG Island includes the first intron, while the S-Shore and S-Shelf cover from the first intron until the beginning of the NM_000050.4 second exon.

4 probes covers the *ASS1* CpG island, 1 the S-Shore region, 1 the N-shore, 1 the S-Shelf and 8 the gene body. The results are colour-coded based on the β -value, where red corresponds to high methylation (100%) and blue to low (0%).

ER: oestrogen receptor; PR: progesterone receptor; Her2: human epidermal growth factor receptor 2.

4.2.1.2 Pyrosequencing analysis

Our breast cancer cell line panel was screened by pyrosequencing based on published data (Nicholson et al. 2009, Syed 2013).

As shown in Figure 4-2, no methylation was found in any of the cell lines by pyrosequencing, confirming the results of the 450k Methylation array (Figure 4-1). In all the cell lines tested, there was little to no methylation (lower than 10%) on every CpG site was observed. It is worth noting that in some cell lines, such as Hcc1569, JIMT1 or MDA-MB-361, one of the CpG sites showed a higher methylation status, up to a maximum of 12.3% in JIMT1. However this percentage of methylation in one single CpG site was unlikely to have any effect on gene expression level.

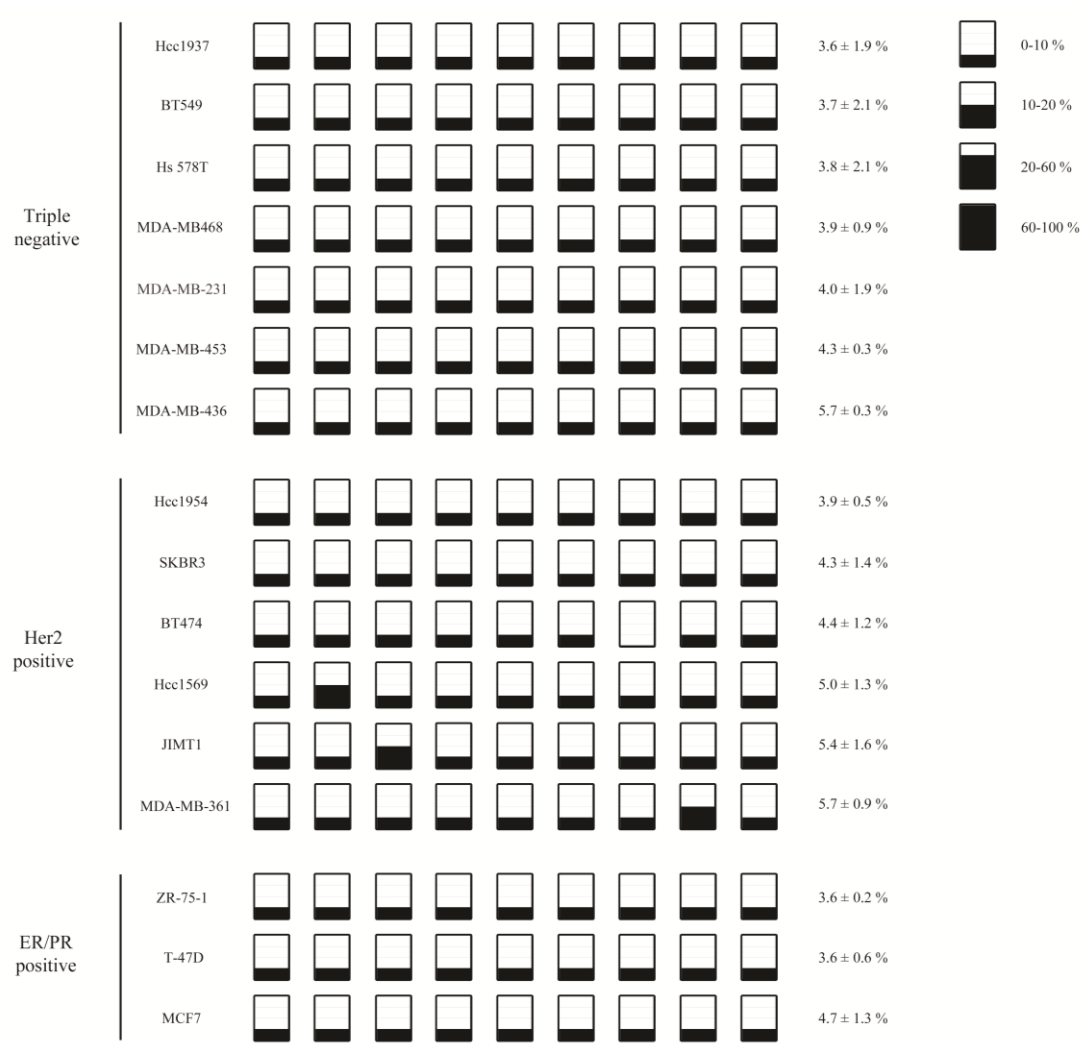


Figure 4-2. Pyrosequencing analysis of *ASS1* in breast cancer cell lines.

9 CpG sites were analysed in *ASS1* CpG island by pyrosequencing. Each CpG site is represented by a square in the figure. The proportion of black in each square shows the average of methylation in each CpG site (see legend on the top right). The methylation status across the panel was calculated as mean across the CpG sites. The biological triplicates were then averaged and the standard deviation generated (values on the right).

4.2.2 Gene expression analysis

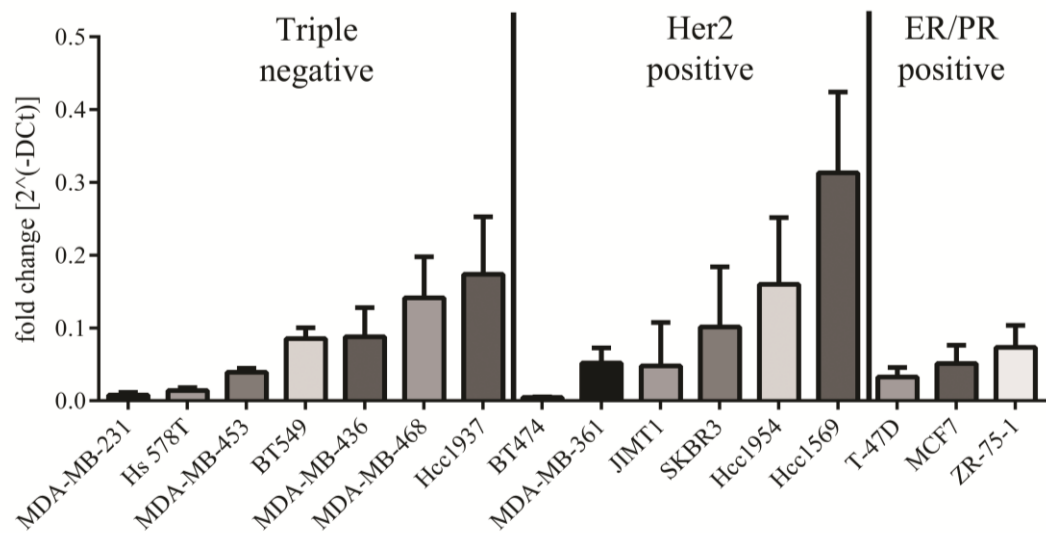
In order to complete their characterisation, *ASS1* expression and protein level were screened in the panel of breast cancer cell lines. As part of the analysis, cells were divided into groups to evaluate subtype-specific expression pattern.

ASS1 consists of two transcripts, NM_000054.2 and NM_054012.3 (Figure 4-1), coding for the same protein. The real-time PCR (qPCR) allowed analysis of the expression of both transcripts as the primer set covered a shared coding region (between the first and second exon). As shown in Figure 4-3 A, the panel of cell lines was categorised based on breast cancer subtypes, all demonstrating a wide range of expression. Her2-positive cells exhibited the most variable expression with a 61 fold change between the lowest (MDA-MB-231) and the highest expressing (Hcc1937) cells. The hormone-positive cells were the least variable with 2.3 fold change between T-47D and ZR-75-1. It is worth noting that even the lowest expressing cell line showed a significant level of *ASS1* mRNA, with an average Ct value of 29.16.

Characterisation of the cell lines was completed by SDS-PAGE electro-blotting analysis on *ASS1* protein levels. Consistent with the mRNA analysis, each breast cancer subtype showed a wide range of protein levels (Figure 4-3 B). Her2-positive cells were the most variable with a 7.9 fold range between the cells showing the lowest (JIMT1) and the highest (SKBR3) amount of protein. Triple negative cells were the least variable with 2.3 fold change between MDA-MB-231 and BT549.

No correlation was found between Arginino-succinate synthetase and any breast cancer subtypes; by qPCR or SDS-PAGE electro-blotting. Moreover, no correlation was found between mRNA and protein levels by linear regression analysis (R : 0.036, p -value: 0.515) (Figure 7-6). As no significant methylation was found in any of the cell lines tested, no further analysis were possible.

A)



B)

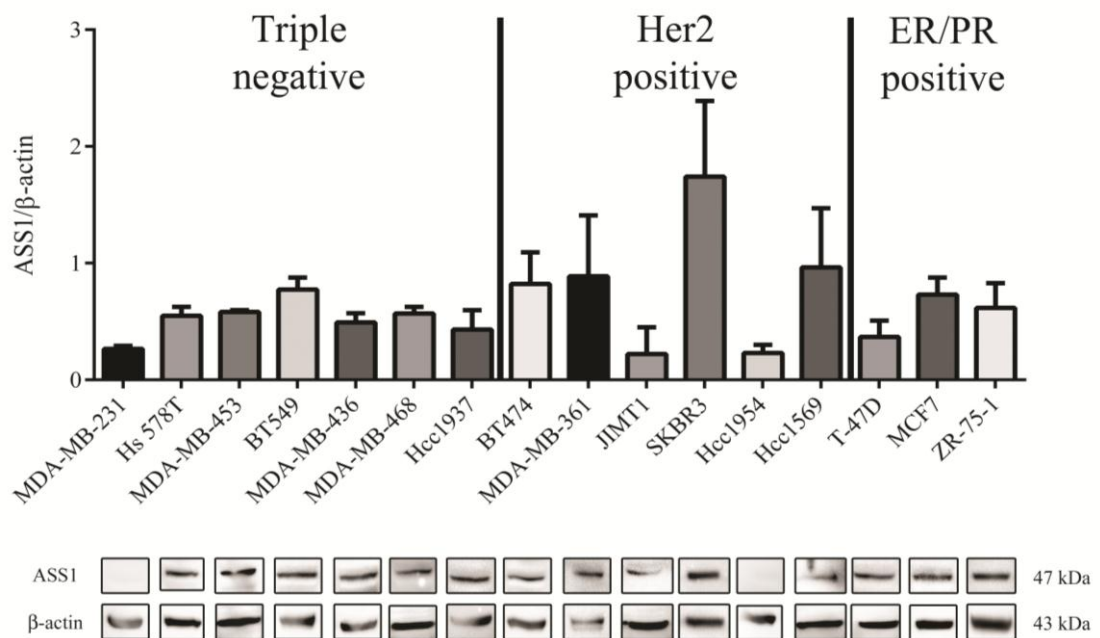


Figure 4-3. Analysis of Arginino-succinate synthetase expression in breast cancer cell lines.

Arginino-succinate synthetase expression was investigated in the breast cancer cell line panel by real-time PCR (A) and SDS-PAGE electro-blotting (B) as described in Materials and Methods. Cells were divided into breast cancer subtypes and ordered by increasing absolute expression. mRNA and protein levels are expressed as average with standard deviation among biological triplicates.

4.3 Functional analysis of *ASS1*

The aim of the previous analysis was to identify a group of breast cancer cell lines in which *ASS1* was silenced via methylation. Although, none of the cells in our panel showed any methylation in the region modulating *ASS1* expression, published data in other cancers supports the hypothesis that this gene silencing might have a role in arginine depletion therapy sensitivity (Szlosarek et al. 2006, Nicholson et al. 2009, Delage et al. 2012, Syed et al. 2013). Thus, shRNA constructs (Table 2-2) were used to mimic the silencing due to methylation and evaluate the response to arginine deprivation and ADI-PEG20 treatment in breast cancer.

Two cell lines were selected for testing the effects of silencing by shRNA, based on their *ASS1* baseline: SKBR3 was the highest expressing by SDS-PAGE electroblotting and Hs 578T had an intermediate expression profile (Figure 4-3 B). *ASS1* was stably reduced by 50% by shRNA2 in Hs 578T and 48% by shRNA1 in SKBR3 (Figure 4-4).

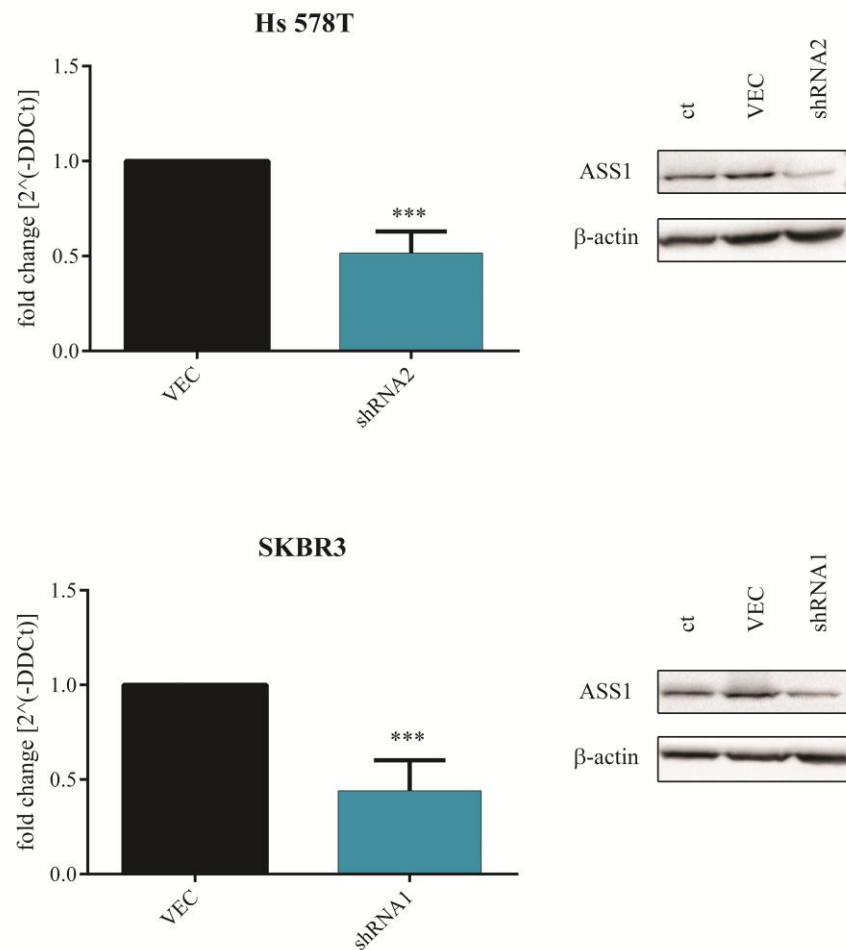


Figure 4-4. *ASS1* silencing by shRNA in Hs 578T and SKBR3.

Hs 578T and SKBR3 were stably transfected with either a shRNA against *ASS1* (shRNA1 and shRNA2) or an empty pSilencer vector (VEC). Cell pellets were collected during each experiment and tested for *ASS1* silencing by SDS-PAGE electro-blotting (a representative image is shown on the right). The results are shown as average and standard deviation for each sample. T-student on Prism 6.0 (Graph Pad) was used to analyse the statistical significance. Statistical significance is shown as stars (*: p-value 0.05, **: p-value 0.01, ***: p-value 0.001, ****: p-value <0.001).

4.3.1 Arginine deprivation

To test the hypothesis that ASS1 silencing would sensitise breast cancer cells to arginine deprivation, stably transfected Hs 578T and SKBR3 with *ASS1*-targeting shRNA were arginine deprived. To further test the relevance of *ASS1* in the survival rate, cells were deprived not only of the ASS1-mediated enzymatic reaction final product, arginine, but also its substrate, citrulline.

As shown in Figure 4-5 for Hs 578T and Figure 4-6 for SKBR3, absence of arginine and citrulline had no effect on cells expressing the empty vector (VEC). When ASS1 was down-regulated (shRNA), arginine deprivation was responsible for a 30% reduction in survival when compared to cells grown in complete media. This was replicated when the cells were deprived of citrulline. Adding arginine into the medium restored cells expressing the shRNA resistance to arginine deprivation, while no effect was seen when citrulline was added (Figure 4-5, Figure 4-6).

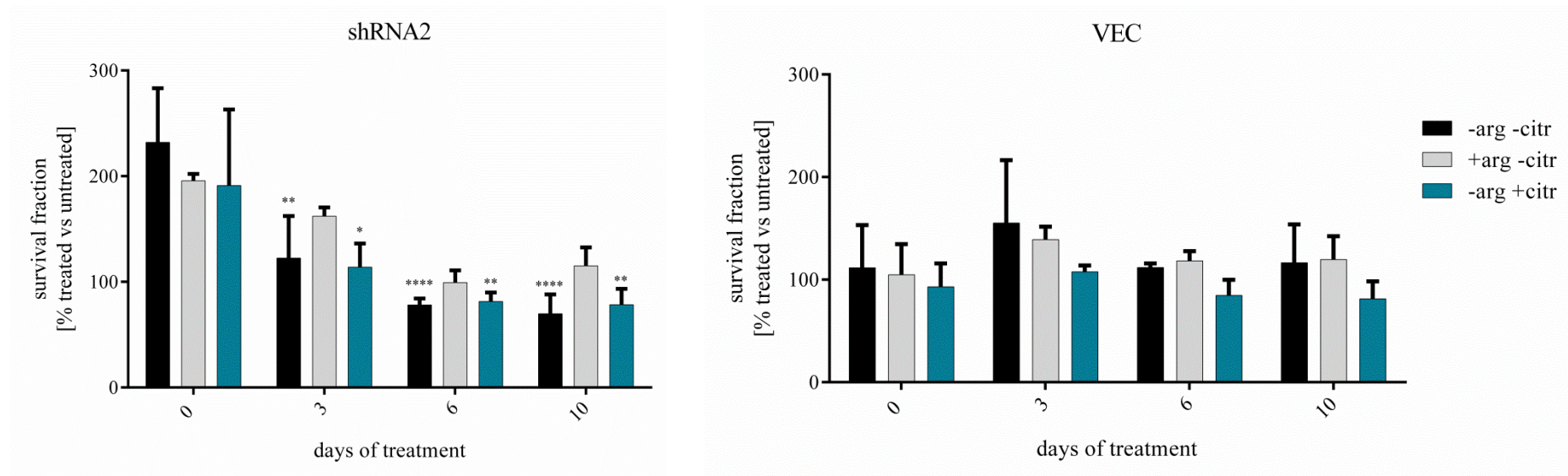


Figure 4-5. Effects of ASS1 knock-down on arginine deprivation in Hs 578T.

Hs 578T transfected with a pSilencer vector with (shRNA2) and without (VEC) the shRNA construct targeting *ASS1*, were arginine deprived up to 10 days. Cells were grown in absence of either L-arginine (arg) or L-citrulline (citr). Survival fraction was calculated as percentage of remaining live treated cells over untreated on each day (cultured in complete media). Statistical significance was calculated against day 0 using One-way ANOVA on Prism 6.0 (Graph Pad) and shown as stars (*: p-value 0.05, **: p-value 0.01, ***: p-value 0.001, ****: p-value <0.001).

-arg-citr: both L-arginine and L-citrulline absent in the media; +arg-citr: only L-arginine present in the media; -arg+citr: only L-citrulline present in the media.

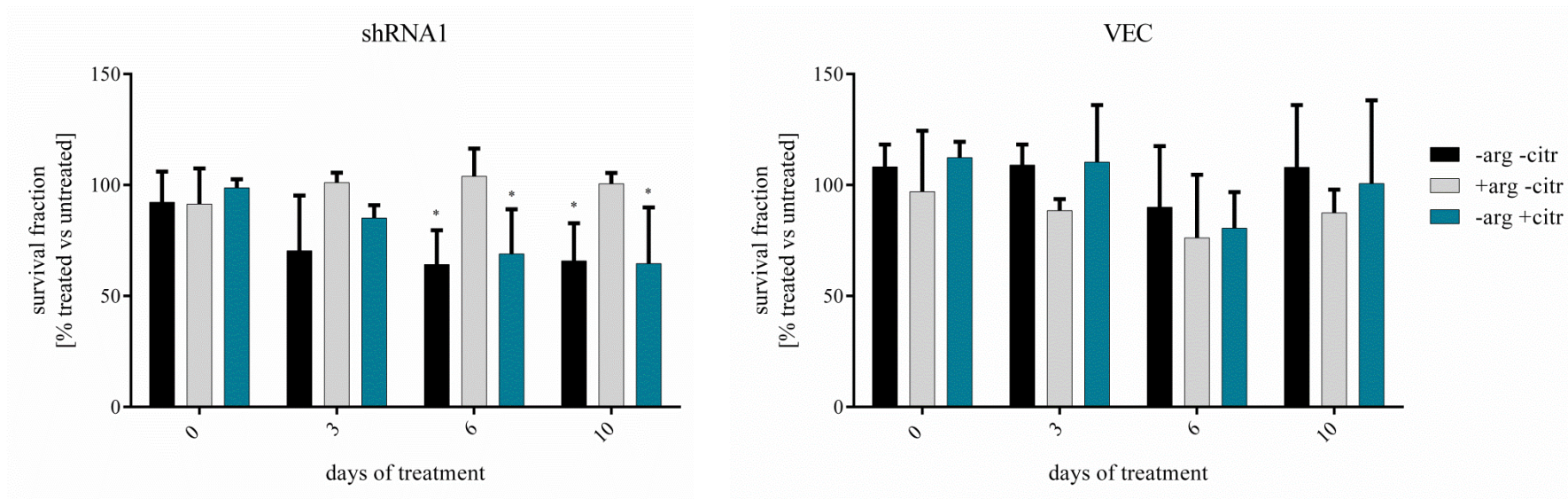


Figure 4-6. Effects of ASS1 knock-down on arginine deprivation in SKBR3.

SKBR3 were transfected with a pSilencer vector with (shRNA1) and without (VEC) the construct targeting *ASS1*. Cells were arginine deprived up to 10 days. Cells were grown in absence of either L-arginine (arg) or L-citrulline (citr). Survival fraction was calculated as percentage of remaining live treated cells over untreated on each day (cultured in complete media). Statistical significance was calculated against day 0 using One-way ANOVA on Prism 6.0 (Graph Pad) and shown as stars (*: p-value 0.05, **: p-value 0.01, ***: p-value 0.001, ****: p-value <0.001).

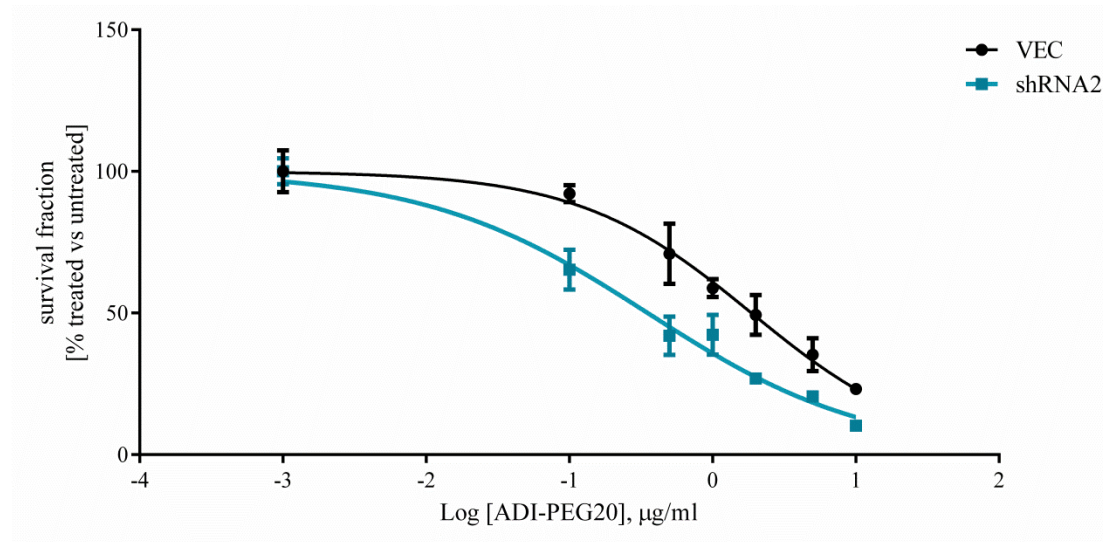
-arg-citr: both L-arginine and L-citrulline absent in the media; +arg-citr: only L-arginine present in the media; -arg+citr: only L-citrulline present in the media.

4.3.2 ADI-PEG20 administration

Having shown that ASS1 silencing resulted in arginine dependence for 2 of the breast cancer cell lines, the same cell lines were tested using Arginine Deiminase (ADI-PEG20), a drug capable of removing arginine from the media and currently used in clinic.

As shown in Figure 4-7 and Figure 4-8, ASS1 silencing caused a shift in the drug-response curve and a reduction in IC_{50} in both cell lines. The IC_{50} was reduced by 6 fold in the Hs 578T (from 0.74 $\mu\text{g/ml}$ to 0.12 $\mu\text{g/ml}$) (Figure 4-7 B). SKBR3 became sensitive to the treatment, with an IC_{50} of 1.2 $\mu\text{g/ml}$ (Figure 4-8 B).

A)



B)

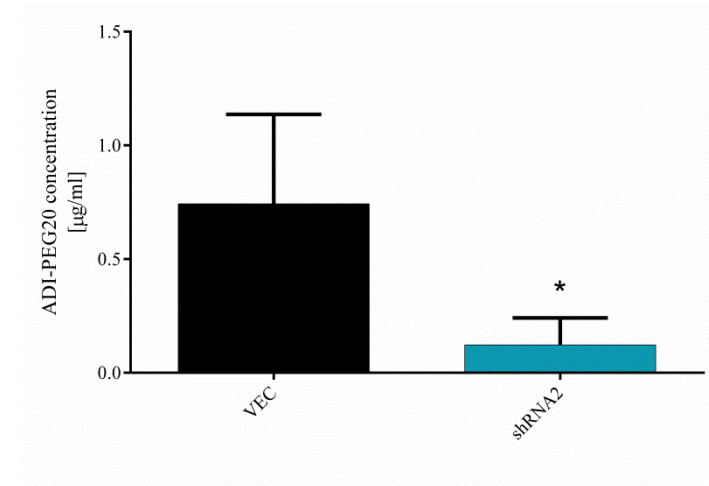
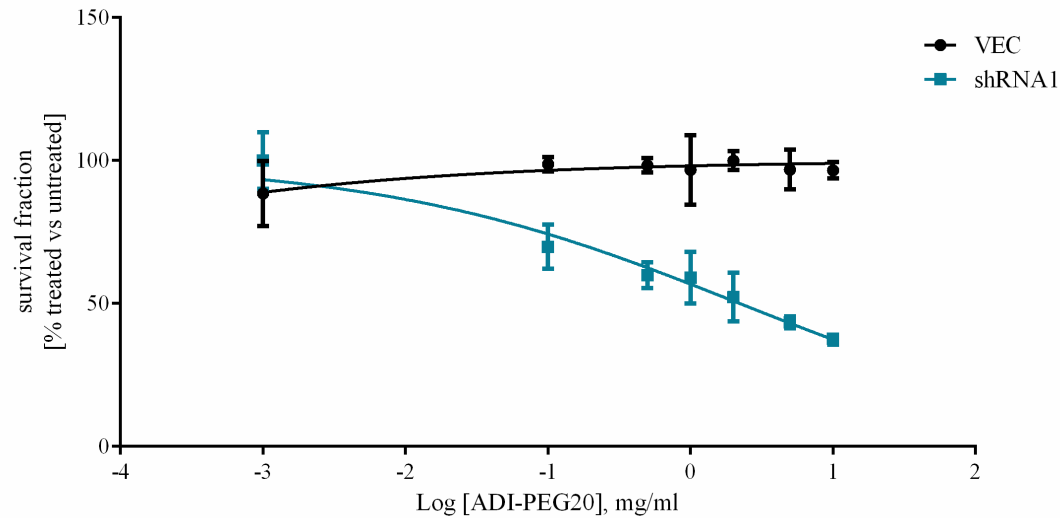


Figure 4-7. IC₅₀ analysis in shRNA transfected Hs 578T.

Hs 578T were transfected with a pSilencer vector with (shRNA2) or without (VEC) the construct targeting *ASS1*. Cells were treated with increasing concentrations of ADI-PEG20, up to 10 µg/ml. Half maximal inhibitory concentration (IC₅₀) was calculated after 6 days of treatment using Prism 6.0 (Graph Pad). A) The graph shows a representative replicate of the drug-response curve of cells expressing (shRNA2) and not expressing (VEC) the construct. B) IC₅₀ results from biological triplicate were averaged with standard deviation. Statistical significance was calculated using Mann-Whitney test on Prism 6.0 (Graph Pad) and shown as stars (*: p-value 0.05, **: p-value 0.01, ***: p-value 0.001, ****: p-value <0.001).

A)



B)

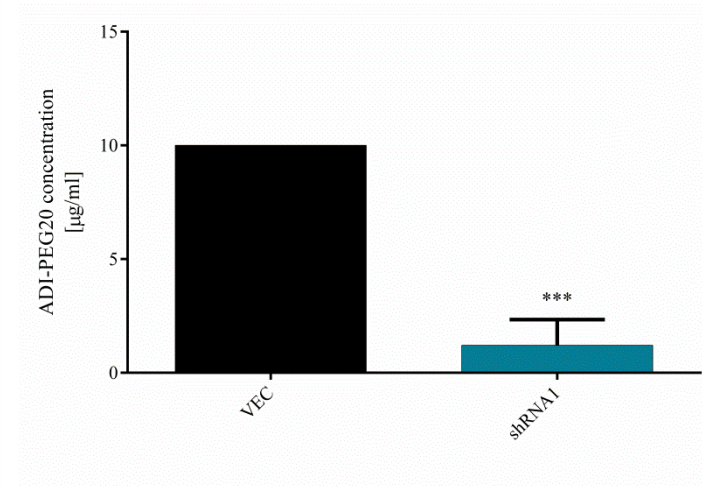


Figure 4-8. IC₅₀ analysis in shRNA transfected SKBR3.

SKBR3 were transfected with a pSilencer vector containing (shRNA1) or not (VEC) the construct. They were treated with increasing concentrations of ADI-PEG20, from 0 up to 10 µg/ml. Half maximal inhibitory concentration (IC₅₀) was calculated after 8 days of treatment using Prism 6.0 (Graph Pad). A) The graph shows a representative replicate of the drug-response curve between cells expressing (shRNA1) and not expressing (VEC) the construct. B) IC₅₀ average with standard deviation was calculated across biological triplicates. Statistical significance was calculated using Mann-Whitney test on Prism 6.0 (Graph Pad) and shown as stars (*: p-value 0.05, **: p-value 0.01, ***: p-value 0.001, ****: p-value <0.001).

4.4 Methylation analysis of *ASS1* in primary breast cancer tissues

4.4.1 Cuneo's cohort

Primary breast cancer tissues and normal breast tissues were screened for Arginino-succinate synthetase methylation in the region identified as regulating the gene of interest (Nicholson et al. 2009, Syed 2013).

To validate *ASS1* methylation status as a marker to distinguish tumour from normal tissues, the methylation distribution was compared between the two datasets (Figure 4-9). Methylation in the normal population ranged between 2.2% and 9.3% with median at 5.6%, whereas tumour samples between 1% and 24.9% with median at 9.22% (Figure 4-10 A). ROC-curve analysis demonstrated the reliability of *ASS1* methylation in discriminating tumour from normal samples (area: 0.761, p-value <0.001).

Once established that tumour and normal tissues were statistically different, methylation cut-off was set at 13.36%, calculated as mean and three standard deviations of methylation in normal tissues. Tumour samples were, as previously, divided into hypo- and hyper-methylated groups as determined by the cut-off value (Table 4-1). Univariate COX-regression analysis showed that none of the tested variable, including *ASS1* methylation status, correlated with overall survival in this cohort of breast cancer primary tissues (Figure 4-11).

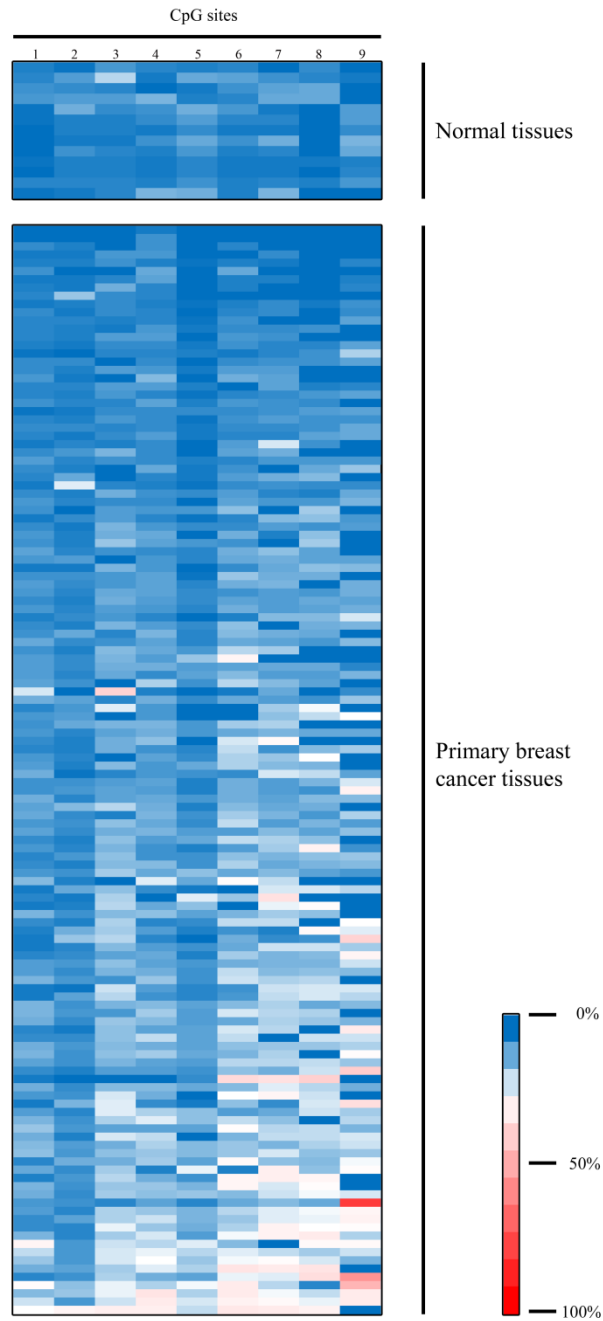
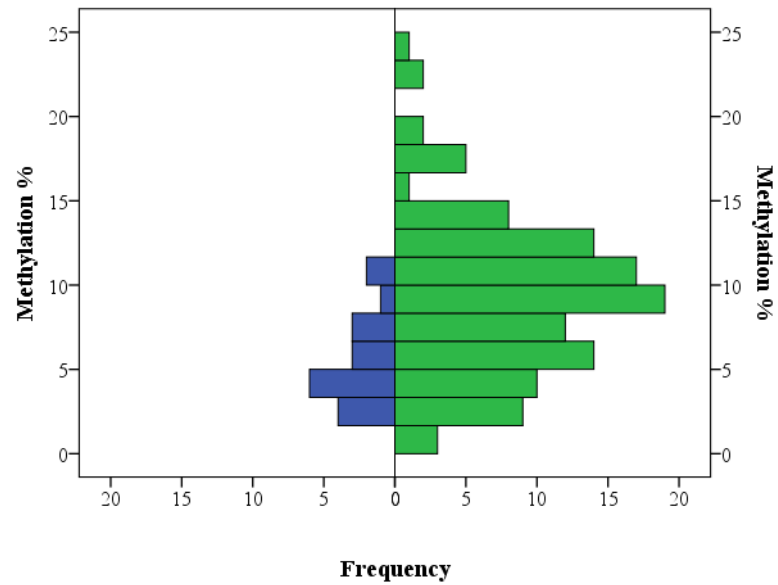


Figure 4-9. Pyrosequencing analysis of *ASS1* promoter region in primary breast cancer cohort.

9 CpG sites on *ASS1* CpG island were analysed in 150 breast primary cancer and 20 normal formalin-embedded tissues by pyrosequencing. The data are shown as percentage methylation, generated from the Pyromark CpG Software (Qiagen). Each row represents a tumour sample. The results are colour-coded based on the methylation values, where red corresponds to high methylated (100%) and blue to low methylated (0%).

A)



B)

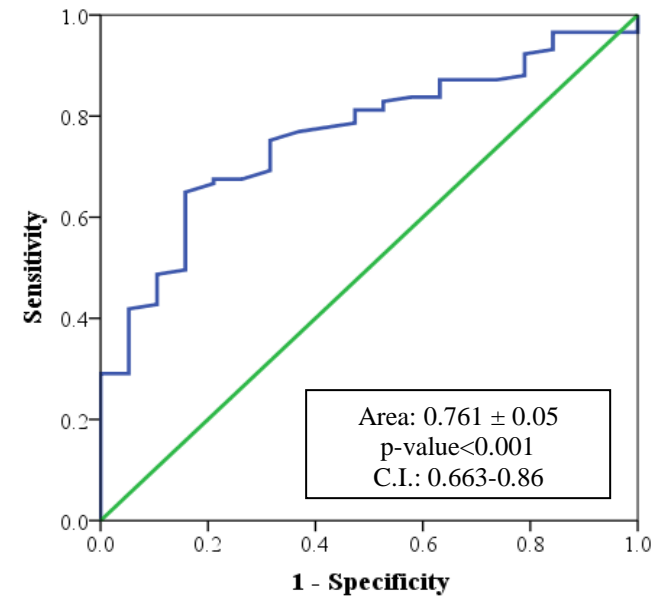


Figure 4-10. Methylation analysis of normal and tumour samples.

DNA methylation values were compared between normal and tumour samples using SPSS (IBM Software). Methylation distributions in the two dataset were compared either by A) frequencies (normal samples in blue and tumour samples in green) or B) by Receiver Operating Characteristic (ROC) curve.

Tumour samples			
	Hypo-methylated	Hyper-methylated	p-value
Number of samples	118 (78.7%)	32 (21.3%)	
Age [median (min-max)]	71.4 [45.8-94.8]	74.4 [23.6-96.3]	0.844
Hormone-receptor status			0.517
ER+	109 (72.7%)	24 (16%)	
ER & PR+	81(60.1% of ER+)	24 (18.0% of ER+)	
ER & PR-	28 (21.1% of ER+)	0 (0% of ER+)	
ER-	9 (6%)	8 (5.3%)	
Her2 status			0.384
Positive	29 (19.3%)	8 (5.3%)	
negative	83 (55.3%)	21 (14%)	
Triple negative	4 (2.7%)	0 (0%)	0.692
Tumour Grade			0.150
Grade 1	5 (3.3%)	3 (2%)	
Grade 2	95 (63.3%)	21 (14%)	
Grade 3	13 (8.7%)	3 (2%)	
Tumour Size			0.075
T1	59 (39.3%)	15 (10%)	
T2	40 (26.7%)	9 (6%)	
T3/4	14 (9.3%)	6 (4%)	
Nodal status			0.678
N0	65 (43.3%)	17 (11.3%)	
N1	33 (22%)	7 (4.7%)	
N2/3	12 (8%)	4 (2.7%)	
Median F/U [years]	7	6	0.544

Table 4-1. Clinical characteristics of hypo- and hyper-methylated primary breast cancer tissue samples.

Tumour samples were divided into hypo- and hyper-methylated based on the cut-off. Each group was then investigated for clinical characteristics: age expressed as median, follow up period (F/U), oestrogen receptor (ER), progesterone receptor (PR) and Human Epidermal Growth Factor Receptor 2 (Her2) status and tested by non-parametrical Wilcoxon-Mann-Whitney test (two variables) or Kruskal-Wallis One-way ANOVA (for more than two variables). Tumours were histologically analysed using the TMN staging system.

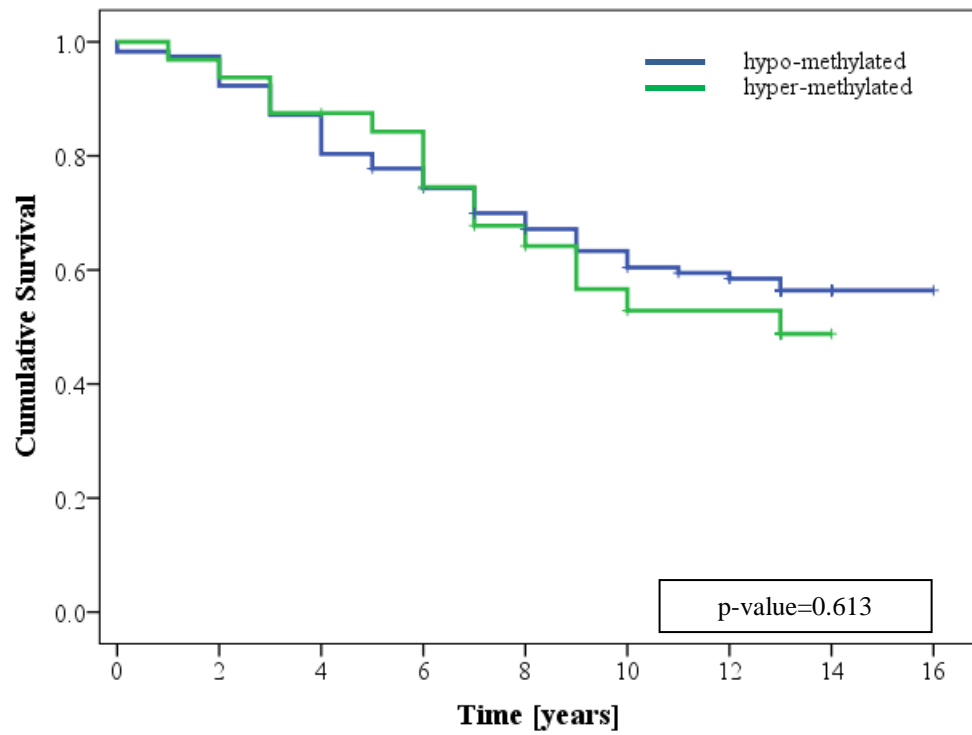


Figure 4-11. Survival of primary tissue cohort based on methylation status.

Overall survival in years was analysed in primary breast cancer patients using Kaplan-Meier curve and COX-regression analysis (SPSS, IBM Software). Patients' data were divided into hypo- (in blue) and hyper-methylated (in green) during the analysis.

4.4.2 TCGA dataset

To confirm the results obtained previously from the primary breast cancer cohort, 523 primary breast cancer patients' methylation data (Figure 4-12) with the corresponding clinical data were downloaded from The Cancer Genome Atlas (TCGA) Data Portal and used as a second cohort.

In order to compare this new dataset with the one previously described, only methylation values from the second probe in the CpG island were taken into consideration for analysis. It is the only probe covered by the pyrosequencing assay used to analyse the Cuneo's primary breast cancer cohort (section 4.4.1).

No methylation data on normal tissues were available in the TCGA Data Portal, therefore it was not possible to define the methylation cut-off as previously described. The median was used to calculate the cut-off, set at 10.4%. The cut-off was generated as median and three standard deviations and then used to divide tumour samples into hypo- and hyper-methylated (Table 4-2).

N-status (p-value <0.001), PR-status (p-value <0.001), ER-status (p-value: 0.009), grade (p-value: 0.009) and age (p-value 0.014) were found as prognostic markers for overall survival by univariate COX-regression analysis. However, *ASS1* methylation did not determine a difference in overall survival in this cohort of breast cancer primary tissues (Figure 4-13). This result was consistent with the data from the previous cohort.

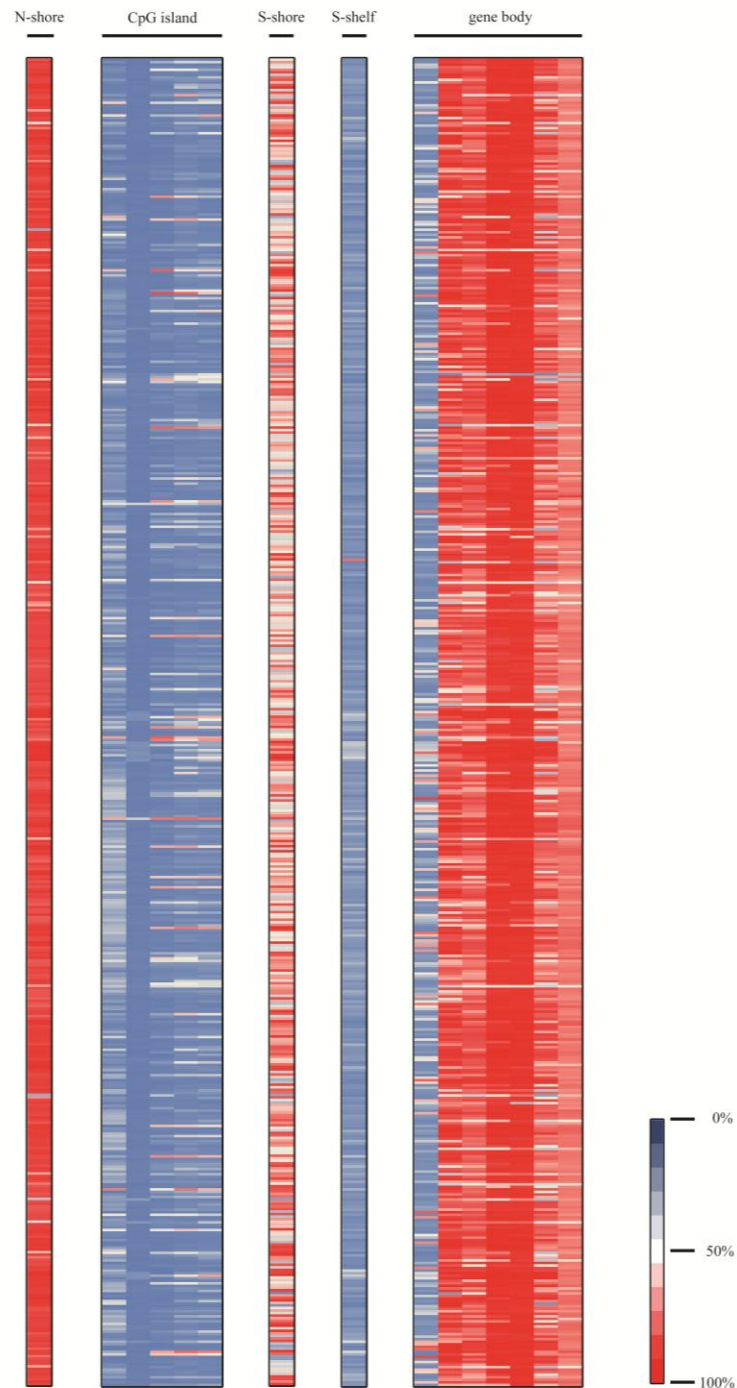


Figure 4-12. 450k Methylation array analysis of TCGA's dataset.

523 frozen primary breast tissue were analysed using 450k Methylation array from the Cancer Genome Atlas (TCGA). Each row represents a tumour sample. The data are shown as β -value and colour-coded in red when highly methylated (100%) and in blue when low methylated (0%).

Tumour samples			
	Hypo-methylated	Hyper-methylated	p-value
Number of samples	504 (96.4%)	19 (3.6%)	
Age [median (min-max)]	58 [26-90]	62 [32-90]	0.926
Hormone-receptor status			<0.001
ER+	362 (69.2%)	11 (2.1%)	
ER & PR+	214 (536.4% of ER+)	5 (1.3% of ER+)	
ER & PR-	148 (39.7% of ER+)	6 (1.6% of ER+)	
ER-	113 (21.6%)	2 (0.4%)	
Her2 status			0.001
Positive	57 (10.9%)	5 (0.1%)	
negative	260 (49.7%)	4 (0.8%)	
Triple negative	52 (9.9%)	1 (0.2%)	0.063
Tumour Grade			0.747
Grade 1	82 (15.7%)	3 (0.6%)	
Grade 2	292 (55.8%)	10 (1.9%)	
Grade 3	125 (23.9%)	6 (1.2%)	
Tumour Size			0.268
T1	134 (25.6%)	4 (0.8%)	
T2	295 (56.4%)	14 (2.7%)	
T3/4	74 (14.1%)	1 (0.2%)	
Nodal status			0.178
N0	224 (42.8%)	10 (1.9%)	
N1	181 (34.6%)	2 (0.4%)	
N2/3	94 (17.9%)	7 (1.4%)	

Table 4-2. Clinical characteristics of hypo- and hyper-methylated in the TCGA dataset.

Tumour samples were divided into hypo- and hyper-methylated based on the cut-off. Each group was then investigated for clinical characteristics: age expressed as median, follow up period (F/U), oestrogen receptor (ER), progesterone receptor (PR) and Human Epidermal Growth Factor Receptor 2 (Her2) status and tested by non-parametrical Wilcoxon-Mann-Whitney test (two variables) or Kruskal-Wallis One-way ANOVA (for more than two variables). Tumours were histologically analysed using the TMN staging system.

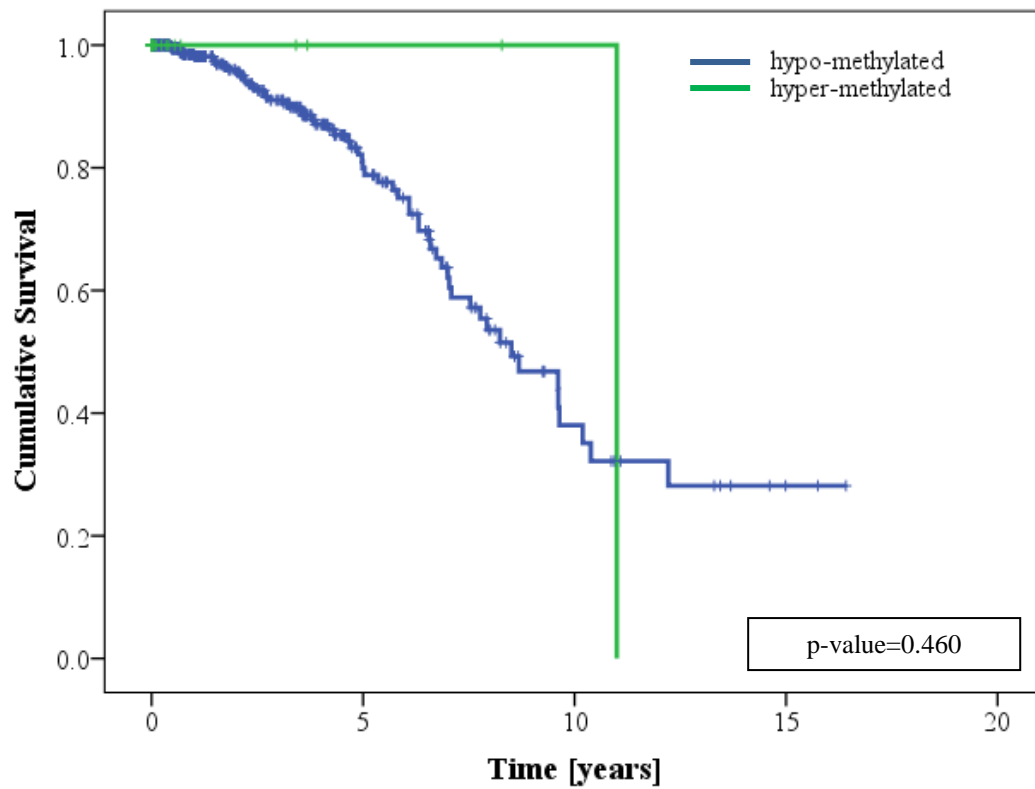


Figure 4-13. TCGA cohort survival based on methylation status.

Overall survival in years in primary of breast cancer patients was analysed using Kaplan-Meier curve and COX-regression analysis (SPSS, IBM Software). Patients' data were divided into hypo- (blue) and hyper-methylated (green line) during the analysis.

4.5 Discussion

Preliminary data within our group identified Arginino-succinate synthetase (*ASS1*) as highly methylated in a primary breast cancer cohort. Although the data could not be verified in breast cancer cell lines, *ASS1* methylation was evident in a significant proportion of primary breast cancer samples. In two independent cohorts, aberrant methylation of *ASS1* was detected in 21.3% and 3.6% of primary breast cancers. No significant association with outcome was found.

ASS1 repression via methylation has been replicated by knock-down in a selection of breast cancer cell lines, causing an increase in sensitivity to arginine depletion and ADI-PEG20 treatment.

Based on the functional analysis, *ASS1* methylated breast cancers can be considered as potential target for arginine depletion treatment.

4.5.1 ASS1 is not methylated in the breast cancer cell line panel

This is the first study investigating *ASS1* regulation in breast cancer. The gene is known to be silenced via methylation in other types of cancer, such as melanoma, lymphoma, mesothelioma and glioblastoma (Szlosarek et al. 2006, Nicholson et al. 2009, Delage et al. 2012, Syed et al. 2013). A subset of breast cancers has been identified as *ASS1* negative and therefore as a potential target for arginine depletion therapy, but this has not been correlated to any methylation information or functional data (Dillon et al. 2004). Tumour cells lacking *ASS1*, gene encoding for the rate-limiting enzyme responsible for arginine synthesis (Wu and Morris 1998, Delage et al. 2010), are auxotrophic for arginine and can be a target of synthetic lethality via arginine depletion treatment (Ensor et al. 2002, Feun and Savaraj 2006, Szlosarek et al. 2006, Kim et al. 2009).

Although the presence of some methylation within *ASS1* CpG island by 450k Methylation array was observed in both breast cancer cell lines and in the TCGA cohort, no methylation was found in the region known to regulate gene expression (Nicholson et al. 2009, Delage et al. 2012, Syed et al. 2013). This was not surprising as the percentage of hyper-methylated tissues observed in the preliminary data was very low (below 10%, data not shown), justifying the absence of methylation in a panel of 13 breast cancer cell lines. Consistent with these results, gene expression and translation analysis showed a wide range of expression levels across the panel of cell lines. Since *ASS1* protein has been demonstrated to be post-translational modified by S-Nitrosylation (Hao et al. 2004) and by phosphorylation (Corbin et al. 2008), it is not surprising that there was no correlation between gene expression and translational levels (R: 0.036, p-value: 0.515).

In the primary breast cancer cohorts, 21.3% of the primary breast cancer tissues and 3.6% of the TCGA cohort samples showed an *ASS1* methylation level above the cut-off value. The cut-off was determined as the mean with three standard deviations of *ASS1* methylation distribution in normal tissues in the primary breast cancer cohort, and median and three standard deviations of *ASS1* methylation across the dataset in the TCGA cohort. When no normal tissues is available, as the case for the TCGA dataset, published studies have determined the methylation cut-off using different methods, including the median with or without standard deviation or by testing different cut-off values and choosing the most significant by ROC-curve analysis (Cerne et al. 2012, Suzuki et al. 2013, Quillien et al. 2014). The cut-off based on the median of the samples was chosen for this analysis as considered the most informative.

It appears that the proportion of hyper-methylated population in the two primary tissue cohorts was quite different, although the methylation cut-offs are very similar. This discrepancy can be due to multiple factors differentiating the two cohorts of samples, including the sample number, the method to store the tissues and to quantify the methylation levels. The TCGA cohort was represented by 3.4 times more samples than the primary breast cancer cohort and was analysed using 450k Methylation array while the primary breast cancer cohort by pyrosequencing. While pyrosequencing allows the analysis of the methylation status of each CpG site in a sequence of interest, 450k Methylation array gives a picture of the whole CpG island testing some CpG sites within the gene promoter region. Therefore pyrosequencing analysis could be considered more informative of the methylation status of the region of interest. Another consideration for the differences between the two primary tissue

cohorts would be the way tissue were stored. While the primary breast cancer tissues cohort consist of Formalin-embedded tissues (FFPE), the TCGA dataset of fresh-frozen tissues. Formalin-embedded tissues (FFPE) are subjected to different steps that can influence the DNA quality and level of detected DNA methylation. These range from the paraffin preparation and tissue inclusion procedures to the paraffin block sectioning and DNA extraction (Leong 2013). While methylation analysis of fresh frozen tissues are highly reliable and reproducible, DNA from FFPE tends to generate higher levels of methylation that are not highly reproducible (Tournier et al. 2012, Kelemen et al. 2013). This could result in a high discordance between samples stored frozen and FFPEs (Jasmine et al. 2012), and may explain the differences seen in *ASS1* methylation in the two breast cancer cohorts in this study.

4.5.2 *ASS1* hyper-methylation relevance in breast cancer

No significant correlation was found between *ASS1* hyper-methylation and overall survival in the two primary breast cancer tissue cohorts. While no clinical variants influenced overall survival in the primary breast cancer cohort, N-status, grade, age, PR and ER were found statistically significant in the TCGA dataset. This is not surprising as age is the main confounding factor in survival analysis especially in a big cohort of samples, and grade and N-status are easily associated with a decrease in survival, corresponding to more malignant stages of the neoplasia. The little amount of ER-negative samples in the TCGA cohort also greatly influenced the ER and PR status impact on overall survival. Indeed, only 10 (1.9% of all samples) were PR-positive and only 12 (2.2%) ER negative in the 3.6% of samples found hyper-methylated, making their distribution very dissimilar to the other subgroup.

Although no association with overall survival was identified, the main relevance of *ASS1* methylation remained its potential as therapeutic biomarker, identifying a subset of breast cancers sensitive to arginine depletion treatment. For the first time in this study, functional analysis address *ASS1* reduction determining sensitivity to arginine depletion treatment in breast cancer cell lines. Loss of *ASS1* has already been used in synthetic lethality in cancers, such as hepatocellular carcinoma, melanoma, prostate cancer and mesothelioma (Ensor et al. 2002, Feun and Savaraj 2006, Szlosarek et al. 2006, Kim et al. 2009). The treatment is based on the use of a recombinant form of the Mycoplasma-derived enzyme Deiminase, capable of reducing arginine in citrulline and NH_4 (Feun and Savaraj 2006). Resistance to the treatment has been observed via *ASS1* up-regulation in absence of *ASS1* promoter methylation and via autophagy induction in *ASS1* methylated glioblastoma (Delage et al. 2010, Syed 2013). Consistent with the observations and based on the functional data described in this study, breast cancer characterised by *ASS1* silenced via DNA methylation should be selectively responsive to ADI-PEG20 treatment, whilst normal tissue should not. Therefore patients with breast cancer hyper-methylated for *ASS1* are potential target for synthetic lethality via arginine depletion therapy.

5 Final remarks

A proportion of cancer cells have been found to be unable to synthesise non-essential amino acids because of epigenetic silencing of the gene responsible for their synthesis. Cancer cells lacking Glutamine synthetase (*GLUL*) and Arginine-succinate synthetase (*ASS1*) are auxotrophic for glutamine and arginine respectively.

GLUL and *ASS1* are characterised by high DNA methylation on their promoter region, which play a role in repressing their transcription. This has been shown to be particularly relevant in low amino acid conditions when cancer cells need to restore the concentration of these amino acids to physiological concentrations. Cells epigenetically silenced for *GLUL/ASS1* have been shown to be sensitive to glutamine/arginine deprivation respectively. *GLUL* methylated cells with baseline expression induce autophagy during glutamine depletion therapy, developing a resistant phenotype. The same reaction has been shown in *ASS1* methylated glioblastoma when exposed to arginine deprivation (Syed 2013). The inhibition of autophagy induction by Chloroquine administration restores the sensitivity to glutamine/arginine depletion therapy in methylated cells.

Primary breast cancer tissues confirmed the presence of a proportion of tumours lacking either *GLUL* or *ASS1* via epigenetic modulation. Based on the functional results showed in this thesis, a subset of breast cancer patients could be candidates for therapy via amino acid depletion synthetic lethality. A drug to remove arginine from the blood stream is already available, ADI-PEG20, but no drug has been used to deplete glutamine as a cancer treatment yet. However, Erwinase has been shown

to deplete glutamine from the blood stream and generates a response in leukaemia cells identical to the one described for breast cancer cell lines. Therefore this could be a potential candidate for glutamine depletion treatment in breast cancer.

In conclusion the research described in this thesis has demonstrated epigenetic modulation of metabolic-related genes in breast cancer. The silencing of *GLUL* and *ASS1* causes cancer cells to be auxotrophic for the specific amino acid that can be exploited for amino acid depletion treatment.

6 References

Agrawal, V., Woo, J. H., Borthakur, G., and Kantarjian, H. (2013). "Red blood cell-encapsulated L-asparaginase: potential therapy of patients with asparagine synthetase deficient acute myeloid leukemia." Protein and peptide letter **20** (4): 5.

Al-Rayyan, N., Litchfield, L. M., Ivanova, M. M., Radde, B. N., Cheng, A., Elbedewy, A., and Klinge, C. M. (2014). "5-Aza-2-deoxycytidine and trichostatin A increase COUP-TFII expression in antiestrogen-resistant breast cancer cell lines." Cancer Letters.

Alabert, C. and Groth, A. (2012). "Chromatin replication and epigenome maintenance." Nature Reviews, Molecular Cell Biology **13**: 15.

Alberg, A. J. and Sigh, S. (2001). "Epidemiology of breast cancer in older women: Implication for future healthcare." Drugs and Aging **18** (10): 12.

Allodi, S., Bressan, C. M., Carvalho, S. L., and Cavalcante, L. A. (2006). "Regionally specific distribution of the binding of anti-glutamine synthetase and anti-S100 antibodies and of Datura stramonium lectin in glial domains of the optic lobe of the giant prawn." Glia **56** (6): 9.

Allred, D. C., Wu, Y., Mao, S., Nagtegaal, I. D., Lee, S., Perou, C. M., Mohsin, S. K., O'Connell, P., Tsimelzon, A., and Medina, D. (2008). "Ductal Carcinoma In situ and the Emergence of Diversity during Breast Cancer Evolution." Human Cancer Biology **14**: 8.

Bardou, V. J., Arpino, G., Elledge, R. M., Osborne, C. K., and Clark, G. M. (2003). "Progesterone receptor status significantly improves outcome prediction over estrogen receptor status alone pf adjuvant endocrine therapy in two large breast cancer database." J Clin Oncol. **75**(3): 6.

Bartlett, J. M., Brookes, C. L., Robson, T., van de Velde, C. J., Billingham, L. J., Campbell, F. M., Grant, M., Hasenburg, A., Hille, E. T., Kay, C., Kieback, D. G., Putter, H., Markopoulos, C., Kranenbarg, E. M., Mallon, E. A., Dirix, L., Seynaeve, C., and Rea, D. (2011). "Estrogen receptor and progesterone receptor as predictive biomarker of response to endocrine therapy: a prospectively powered pathology study in the Tamoxifen and Exemestane Adjuvant Multinational trail." J Clin Oncol. **29**(12): 7.

Bediaga, N. G., Acha-Sagredo, A., Guerra, I., Viguri, A., Albaina, C., Diaz, I. R., Rezola, R., Alberdi, M. J., Dopazo, J., Montaner, D., de Renobales, M., Fernández, A. F., Field, J. K., Fraga, M. F., Liloglou, T., and de Pancorbo, M. M. (2010). "DNA methylation epigenotypes in breast cancer molecular subtypes." Breast Cancer Research **12**(5): 12.

Bertos, N. R. and Park, M. (2011). "Breast cancer-one term, many entities?" J.Clini Invest. **121** (10): 7.

Bihl, M. P., Foerster, A., Lugli, A. and Zlobec, I. (2012). "Characterization of CDKN2A(p16) methylation and impact in colorectal cancer: systematic analysis using pyrosequencing." Journa of Translational Research: 10.

Biosystem, A., Ed. (2007). Methylation Analysis by Bisulfite Sequencing: Chemistry, Products and Protocols from Applied Biosystems.

Bird, A. (2002). "DNA methylation patterns and epigenetic memory." Genetics Development **16 (1)**: 15.

Blazek, R. and Benbough, J. E. (1981). "Improvement in the persistence of microbial asparaginase and glutaminase in the circulation of the rat by chemical modifications." Biochim Biophys Acta **677(2)**: 220-224.

Bosch, A., Eroles, P., Zaragoza, R., Vina, J. R. and Lluch, A. (2009). "Triple-Negative breast cancer: Molecular features, pathogenesis, treatment and current lines of research." Cancer Treatment Reviews **36**: 9.

Boukhattala, N., Claeysens, S., Bensifi, M., Maurer, B., Abed, J., Lavoinnie, A., Dechelotte, P. and Coeffier, M. (2010). "Effects of essential amino acids or glutamine deprivation on intestinal permeability and protein synthesis in HTC-8 cells: involvement of GCN2 and mTOR pathways." Springer.

Buchholtz, M. L., Brüning, A., Mylonas, I. and Jückstock, J. (2014). "Epigenetic silencing of the LDOC1 tumor suppressor gene in ovarian cancer cells." Archives of gynecology and obstetrics.

Butcher, D. T., Alliston, T. and Weaver, V. M. (2009). "A tense situation: forcing tumour progression." Nature reviews, Cancer **9**: 15.

Cancer Research, U. (2012). "Breast cancer risk factors." from <http://www.cancerresearchuk.org/cancer-info/cancerstats/types/breast/riskfactors/breast-cancer-risk-factors>.

Cannuyer, J., Loriot, A., Parvizi, G. K. and De Smet, C. (2013). "Epigenetic Hierarchy within the MAGEA1 Cancer-Germline Gene: Promoter DNA Methylation Dictates Local Histone Modifications." PlosONE **8** (3).

Carey, L. A., Dees, E. C., Sawyer, L., Gatti, L., Moore, D. T., Collichio, F., Ollila, D. W., Sartor, C. I., Graham, M. L. and Perou, C. M. (2007). "The triple negative paradox: primary tumor chemosensitivity of breast cancer subtypes." Clin Cancer Res. **13** (8): 5.

Cerne, J. Z., Zong, L., Jelinek, J., Hilsenbeck, S. G., Wang, T., Oesterreich, S. and McGuire, S. E. (2012). "BRCA1 promoter methylation status does not predict response to tamoxifen in sporadic breast cancer patients." Breast Cancer Res Treat **135**: 9.

Chen, J., Zhang, X., Zhang, H., Lin, J., Zhang, C., Wu, Q. and Ding, X. (2013). "Elevated Klotho promoter methylation is associated with severity of chronic kidney disease." PlosONE **8**(11).

Chiu, M., Tardito, S., Barilli, A., Bianchi, M. G., Dall'Asta, V. and Bussolati, O. (2012). "Glutamine stimulates mTORC1 independent of the cell content of essential amino acids." Amino Acids **43**: 7.

Christensen, B. C., Kelsey, K. T., Zheng, S., Houseman, E. A., Marsit, C. J., Wrensch, M. R., Wiemels, J. L., Nelson, H. H., Karagas, M. R., Kushi, L. H., Kwan, M. L. and Wiencke, J. K. (2010). "Breast cancer DNA methylation profiles are associated with tumour size and alcohol and folate intake." Plos Genetics **6** (7): 10.

Cichon, M. A., Degnim, A. C., Visscher, D. W. and Radisky, D. C. (2010). "Microenvironmental Influences that Drive Progression from Benign Breast Disease to Invasive Breast Cancer." J Mammary Gland Biol Neoplasia **15**: 8.

Clark, S. J., Harrison, J., Paul, C. L. and Frommer, M. (1994). "High sensitivity mapping of methylated cytosines." Nucleic Acids Res **22** (15): 7.

Clynes, R. A., Towers, T. L., Presta, L. G. and Ravetch, J. V. (2000). "Inhibitory Fc receptors modulate in vivo cytotoxicity against tumour targets." Nat Med. **6**(4): 3.

Corbin, K. D., Pendleton, L. C., Solomonson, L. P. and Eichler, D. C. (2008). "Phosphorylation of argininosuccinate synthase by protein kinase A." Biochemical and Biophysical Research Communications **377**: 4.

Costello, J. F., Fruhwald, M. C., Smiraglia, D. J., Rush, L. J., Robertson, G. P., Gao, X., Wright, F. A., Feramisco, J. D., Peltomaki, P., Lang, J. C., Schuller, D. E., Yu, L., Bloomfield, C. D., Caligiuri, M. A., Yates, A., Nishikawa, R., Su Huang, H., Petrelli, N. J., Zhang, X., O'Dorisio, M. S., Cavenee, M. S., Held, W. A. and Plass, C. (2000). "Aberrant CpG-island methylation has non-random and tumour-type-specific patterns." Nature Genetics **24** (2): 7.

Dal Bello, B., Rosa, L., Campanini, N., Tinelli, C., Torello Viera, F., D'Ambrosio, G., Rossi, S. and Silini, E. M. (2010). "Glutamine synthetase immunostaining correlates with pathologic features on hepatocellular carcinoma and better survival after radiofrequency thermal ablation." Clinical Cancer Research **16**: 9.

Dang, C. V. (2010). "Glutaminolysis, supplying carbon or nitrogen or both for cancer cells?" Cell Cycle **9**(19): 2.

Deaton, A. M. and Bird, A. (2011). "CpG island and the regulation of transcription." Genes & Development **25**: 12.

DeBernardis, R. J. and Cheng, T. (2010). "Q's next: the diverse functions of glutamine in metabolism, cell biology and cancer." Oncogene **29**: 11.

Delage, B., Fennell, D. A., Nicholson, L., McNeish, I., Lemoine, N. R., Crook, T. and Szlosarek, P. W. (2010). "Arginine deprivation and argininosuccinate synthetase expression in the treatment of cancer." Internal Journal of Cancer **126**: 11.

Delage, B., Luong, P., Maharaj, L., O'Riain, C., Syed, N., Crook, T., Hatzimichael, E., Papoudou-Bai, A., Mitchell, T. J., Whittaker, S. J., Cerio, R., Gribben, J., Lemoine, N., Bomalaski, J., Li, C. F., Joel, S., Fitzgibbon, J., Chen, L. T. and Szlosarek, P. W. (2012). "Promoter methylation of argininosuccinate synthetase-1 sensitises lymphomas to arginine deiminase treatment, autophagy and caspase-dependent apoptosis." Cell Death and Disease **5**(3).

Di Tommaso, L., Destro, A., Yeon Seok, J. B. E., Terraciano, L., Sangiovanni, A., Iavarone, M., Colombo, M., June Jang, J., Yu, E., Young Jin, S., Morenghi, E., Nyun Park, Y. and Roncalli, M. (2009). "The application of markers (HSP70 GPC3 and GS) in liver biopsies is useful for detection of hepatocellular carcinoma." Journal of Hepatology **50**: 9.

Dillon, B. J., Prieto, V. G., Curley, S. A., Ensor, C. M., Holtsberg, F. W., Bomalaski, J. S. and Clark, M. A. (2004). "Incidence and distribution of Argininosuccinate Synthetase Deficiency in Human Cancers." American cancer society **100**: 8.

Dowsett, M., Allred, C., Knox, J., Quinn, E., Salter, J., Wale, C., Cuzick, J., Houghton, J., Williams, N., Mallon, E., Bishop, H., Ellis, I., Larsimont, D., Sasano, H., Carder, P., Cussac, A. L., Knox, F., Speirs, V., Forbes, J. and Buzdar, A. (2008). "Relationship between quantitative estrogen and progesterone receptor expression and human epidermal growth factor receptor 2 (HER-2) status with recurrence in the Arimidex, Tamoxifen, Alone or in Combination trial." J Clin Oncol. **26**(7): 6.

Duran, R. V., Oppliger, W., Robitaille, A. M., Heiserich, L., Skendaj, R., Gottlieb, E. and Hall, M. N. (2012). "Glutaminolysis activates Rag-mTORC1 signalling." Molecular Cell **47**: 10.

Eisenberg, D., Gill, H. S., Pfluegl, G. M. and Rotstein, S. H. (2000). "Structure-function relationships of glutamine synthetases." Biochimica et Biophysica Acta **1477**(1-2): 24.

Emadi, A., Zokaee, H. and Sausville, E. A. (2014). "Asparaginase in the treatment of non-ALL hematologic malignancies." Cancer Chemotherapy and Pharmacology.

Eng, C. H. and Abraham, R. T. (2010). "Gltaminolysis yields a metabolic by-product that stimulates autophagy." Autophagy **6**(7): 3.

Ensor, C. M., Holstberg, F. W., Bomalaski, J. and Clark, M. A. (2002). "Pegylated arginine deiminase (ADI-SS PEG_{20,000} mw) inhibits human melanomas and hepatocellular carcinomas in vitro and in vivo." Cancer Research **62**: 8.

Ewald, E. P., Ribeiro, P. L. I., Palmero, E. I., Cossio, S. L., Giugliani, R. and Ashton-Prolla, P. (2009). "Genomic rearrangements in BRCA1 and BRCA2: A literature review." Genetics and Molecular Biology **32**(3): 9.

FDA. (2014). "U.S. Food and Drug Administration." from <http://www.fda.gov/NewsEvents/Newsroom/PressAnnouncements/ucm280525.htm>.

Ferreira, L. M. R., Hebrant, A. and Dumont, J. E. (2012). "Metabolic reprogramming of the tumour." Oncogene **31**: 12.

Feun, L. and Savaraj, N. (2006). "Pegylated arginine deiminase: a novel anticancer enzyme agent." Expert Opinion on Investigated Drugs **15** (7): 8.

Flanagan, J. M., Munoz-Alegre, M., Henderson, S., Tang, T., Sun, P., Johnson, N., Fletcher, O., dos Santos Silva, I., Peto, J., Boshoff, C., Narod, S. and Petronis, A.

(2009). "Gene-body hypermethylation of ATM in peripheral blood DNA of bilateral breast cancer patients." Human Molecular Genetics **18** (7): 11.

Fox, E. M., Andrade, J. and Shupnik, M. A. (2009). "Novel actions of estrogen to promote proliferation: integration of cytoplasmic and nuclear pathways." Steroids **74** (7): 5.

Fu, Y. M., Yu, Z. Y., Li, Y. Q., Ge, X., Sanchez, P. J., Fu, X. and Meadows, G. G. (2011). "Specific amino acid dependency regulates invasiveness and viability of androgen-independent prostate cancer cells." Nutrition and Cancer **45** (1): 13.

Fuchs, B. C. and Bode, B. P. (2006). "Stressing out the over survival: glutamine as an apoptotic modulator." Journal of surgical research **131**: 14.

Fuchs, J., Demidov, D., Houben, A. and Schubert, I. (2006). "Chromosomal histone modification patterns-from conservation to diversity." TRENDS in Plant Sciences **11**(4): 10.

Ganapathy-Kanniappan, S. and Geschwind, G.-F. H. (2013). "Tumor glycolysis as a target for cancer therapy: progress and prospects." Molecular Cancer **12**: 11.

García-Navas, R., Munder, M. and Mollinedo, F. (2012). "Depletion of L-arginine induces autophagy as a cytoprotective response to endoplasmic reticulum stress in human T lymphocytes." Autophagy **8** (11): 19.

Gomes, L. C., Di Benedetto, G. and Scorrano, L. (2011). "Essential amino acids and glutamine regulate induction of mitochondrial elongation during autophagy." Cell Cycle **10**(16): 5.

Guedj, M., Marisa, L., de Reynies, A., Orsetti, B., Schiappa, R., Bibeau, F., MacGrogan, G., Lerebours, F., Finetti, P., Longy, M., Bertheau, P., Bertrand, F., Bonnet, F., Martin, A. L., Feugeas, J. P., Bièche, I., Lehmann-Che, J., Lidereau, R., Birnbaum, D., Bertucci, F., de Thé, H. and Theillet, C. (2012). "A refined molecular taxonomy of breast cancer." Oncogene **31** (9): 10.

Haghighat, N. (2005). "Estrogen (17 β -estradiol) enhances glutamine synthetase activity in C6-glioma cells." Neurochemical Research **30** (5): 6.

Hao, G., Xie, L. and Gross, S. S. (2004). "Argininosuccinate Synthetase is Reversibly Inactivated by S-Nitrosylation in Vitro and in Vivo." the Journal of Biological Chemistry **279**: 8.

Hassler, M. R. and Egger, G. (2012). "Epigenomic of cancer-emerging new concepts." Biochemie **30**: 12.

Hatzimichael, E. and Crook, T. (2013). "Cancer Epigenetics: New Therapies and New Challenges." Journal of Drug Delivery: 9.

Higgins, m. J. and Baselga, J. (2011). "Targeted therapies for breast cancer." The Journal of Clinical Investigation **121** (10): 7.

Hill, V. K., Ricketts, C., Bieche, I., Vacher, S., Gentle, D., Lewis, C., Macher, E. R. and Latif, F. (2011). "Genome-wide DNA methylation profiling of CpG islands in breast cancer identifies novel genes associated with tumorigenicity." Cancer Research **71** (8): 11.

Hirata, B. K. B., Oda, J. M. M., Guembarovski, R. L., Ariza, C. B., de Oliveira, C. E. C. and Watanabe, M. A. E. (2014). "Molecular Markers for Breast Cancer: Prediction on Tumor Behavior." Disease Markers: 12.

Ho, K. L., McNae, I. W., Schmiedeberg, L., Klose, R. J., Bird, A. P. and Walkinshaw, M. D. (2008). "MeCP2 binding to DNA depends upon hydration at methyl-CpG." Molecular Cell **29**: 6.

Hu, Z., Fan, C., Oh, D. S., Marron, J. S., He, X., Qaqish, B. F., Livasy, C., Carey, L. A., Reynolds, E., Dressler, L., Nobel, A., Parker, J., Ewend, M. G., Sawyer, L. R., Wu, J., Liu, Y., Nanda, R., Tretiakova, M., Ruiz Orrico, A., Dreher, D., Palazzo, J. P., Perreard, L., Nelson, E., Mone, M., Hansen, H., Mullins, M., Quackenbush, J. F., Ellis, M. J., Olopade, O. I., Bernard, P. S. and Perou, C. M. (2006). "The molecular portraits of breast tumors are conserved across microarray platforms." BMC Genomics **96**.

Huang, Y., Vasilatos, S. N., Boric, L., Shaw, P. G. and Davidson, N. E. (2011). "Inhibitors of histone de-methylation and histone deacetylation cooperate in regulating gene expression and inhibiting growth in human breast cancer cells." Breast Cancer Research treatment **11**: 8.

Illumina, I. (2012). "Infinium Human methylation450 BeadChip."

International Agency for Research on Cancer (IARC), W. H. O. (2002). Breast Cancer Screening. IARC Handbooks of Cancer Prevention. H. Vainio, & Bianchini, F. Lyon, IARC Press. 7.

International Agency for Research on Cancer (IARC), W. H. O. (2014). GLOBOCAN 2012: Estimated Cancer Incidence, Mortality and Prevalence Worldwide in 2012.

Jang, K., Paranandi, K. S., Sridharan, S. and Basu, A. (2013). "Autophagy in breast cancer and its implication for therapy." American Journal of Cancer Research 3(3): 14.

Jasin, M. (2002). "Homologous repair of DNA damage and tumorigenesis: the BRCA connection." Oncogene 21: 12.

Jasmine, F., Rahaman, R., Roy, S., Raza, M., Paul, R., Rakibuz-Zaman, M., Paul-Brutus, R., Dodsworth, C., Kamal, M., Ahsan, H. and Kibriya, M. G. (2012). "Interpretation of genome-wide infinium methylation data from ligated DNA in formalin-fixed, paraffin-embedded paired tumor and normal tissue." BMC Research Notes: 5.

Javanovic, J., Ronneberg, J. A., Tost, J. and Kristensen, V. (2010). "The epigenetics of breast cancer." Molecular Oncology 4: 12.

Jiang, L. and Deberardinis, R. J. (2012). "When more is less." Nature **489**: 2.

Jones, N. P. and Schulze, A. (2012). "Targeting cancer metabolism-aiming at the tumour's sweet-spot." Drug discovery today **17**(5/6): 10.

Jones, P. A. (2012). "Functions of DNA methylation: islands, start sites, gene bodies and beyond." Nature Reviews, Genetics **13**(7): 7.

Junttila, T. T., Akita, R. W., Parsons, K., Fields, C., Lewis Phillips, G. D., Friedman, L. S., Sampath, D. and Sliwkowski, M. X. (2009). "Ligand-independent HER2/HER3/PI3K complex is disrupted by trastuzumab and is effectively inhibited by the PI3K inhibitor GDC-0941." Cancer Cell **15**(5): 11.

Kataja, V. and Castiglione, M. (2009). "Primary breast cancer: ESMO Clinical Recommendations for diagnosis, treatment and follow-up." Annals of Oncology **20**: 5.

Kelemen, L. E., Köbel, M., Chan, A., Taghaddos, S. and Dinu, I. (2013). "Differentially Methylated Loci Distinguish Ovarian Carcinoma Histological Types: Evaluation of a DNA Methylation Assay in FFPE Tissue." BioMed Research International: 11.

Kim, R. H., Coates, J. M., Bowles, T. L., McNerney, G. P., Sutcliffe, J., Jung, J. U., Gandour-Edwards, R., Chuang, F. Y. S., Bold, R. J. and Kung, H.J. (2009). "Arginine deiminase as a novel therapy for prostate cancer induces autophagy and caspase-independent apoptosis " Cancer Research **69** (2): 9.

Kittaneh, M., Montero, A. J. and Glück, S. (2013). "Molecular Profiling for Breast Cancer: A Comprehensive Review." Biomarkers Cancer **5**: 10.

Klose, R. J. and Bird, A. P. (2006). "Genomic DNA methylation: the mark and its mediators." TRENDS in Biochemical Sciences **31** (2): 9.

Klose, R. J., Sarraf, S. A., Schmiedeberg, L., McDermott, S. M., Stancheva, I. and Bird, A. P. (2005). "DNA binding selectivity of MeCP2 due to a requirement for A/T sequences adjacent to methyl-CpG." Molecular Cell **19**: 11.

Kobayashi, E., Masuda, M., Nakayama, R., Ichikawa, H., Satow, R., Shitashige, M., Honda, K., Yamaguchi, U., Shoji, A., Tochigi, N., Morioka, H., Toyama, Y., Hirohashi, S. and Yamada, T. (2010). "Reduced argininosuccinate synthetase is a predictive biomarker for the development of pulmonary metastasis in patients with osteosarcoma." Molecular Cancer Therapy **9**: 10.

Krajewski, W. W., Collins, R., Holmberg-Schiavone, L., Jones, T. A., Karlberg, T. and Mowbray, S. L. (2009). "Crystal Structures of Mammalian Glutamine Synthetases Illustrate Substrate-Induced Conformational Changes and Provide Opportunities for Drug and Herbicide Design." Journal of Molecular Biology **375**: 12.

Kruithof-de Julio, M., Labruyere, W. T., Ruijter, J. M., Vermeulen, J. L. M., Stanulovic, V., Stallen, J. M. P., Baldysiak-Figiel, A., Gebhardt, R., Lamers, W. H. and Hakvoort, T. B. M. (2005). "The RL-ET-14 cell line mediates expression of

glutamine synthetase through the upstream enhancer/promoter region." Journal of Hepatology **43**: 6.

Kung, H. N., Marks, J. R. and Chi, J. T. (2011). "Glutamine synthetase is a genetic determinant of cell type-specific glutamine independence in breast epithelia." PLOS genetics **7**(8): 15.

Kuo, M. T., Savaraj, N. and Feun, L. G. (2010). "Targeted cellular metabolism for cancer chemotherapy with recombinant arginine-degrading enzyme." Oncotarget **1** (4): 6.

Laird, P. W. (2010). "Principles and challenges of genome-wide DNA methylation analysis." Nature Reviews, Genetics **11**: 13.

Lakowski, B., Roelens, I. and Jacob, S. (2006). "CoREST-like complexes regulate chromatin modification and neuronal gene expression." Journal of Molecular Neuroscience **29**: 13.

Lambert, M. P., Paliwal, A., Vaissiere, T., Chemin, I., Zoulim, F., Tommasino, M., Hainaut, B., Scoazec, J. Y., Tost, J. and Herceg, Z. (2011). "Aberrant CpG methylation distinguishes hepatocellular carcinoma associated with HBV and HCV infection and alcohol intake." Journal of Hepatology **54**: 11.

Lawvere, S., Mahoney, M. C., Symons, A., Englert, J.J., Klein, S. B. and Mirand, A. L. (2004). "Approaches of breast cancer screening among nurse practitioners." Journal of the American Academy of Nurse Practitioners **16** (1): 6.

Lee, J. Y. and Lee, T. H. (2012). "Effects of histone acetylation and CpG methylation on the structure of nucleosome." Biochimica et Biophysica Acta **1824**: 8.

Leong, K. J., James, J., Wen, K., Tanieri, P., Morton, D.G., Bach, S.P., Matthews, G.M. (2013). "Impact of tissue processing, archiving and enrichment techniques on DNA methylation yield in rectal carcinoma." Experimental and Molecular Pathology **95**(3): 7.

Levenson, V. V. (2007). "Biomarkers for early detection of breast cancer: what, when, and where?" Biochimica and Biophysical Acta **1770** (6): 10.

Lewandowska, J. and Bartoszek, A. (2011). "DNA methylation in cancer development, diagnosis and therapy-multiple opportunities for genotoxic agents to act as methylome disruptors and remediators." Mutagenesis **26** (4): 12.

Li, C. I., Uribe, D. J. and Daling, J. R. (2005). "Clinical characteristics of different histological types of breast cancer." British J Cancer **95** (3): 6.

Liu, J., X. Zhu, X. Xu and D. Dai (2014). "DNA promoter and histone H3 methylation downregulate NGX6 in gastric cancer cells." Medical oncology **31** (1).

Liu, W., Le, A., Hancock, C., Lane, A. N., Dang, C. V., Fan, T. W.M. and Phang, J. M. (2012). "Reprogramming of proline and glutamine metabolism contributes to the proliferative and metabolic responses regulated by oncogenic transcription factor c-MYC." PNAS **109** (23): 5.

Llorca, O., Betti, M., González, J. M., Valencia, A., Márquez, A. J. and Valpuesta, J. M. (2006). "The three-dimensional structure of an eukaryotic glutamine synthetase: functional implications of its oligomeric structure." Journal of Structural Biology **156** (3): 11.

Lorin, S., Hamai, A., Mehrpour, M. and Codogno, P. (2013). "Autophagy regulation and its role in cancer." Seminars in Cancer Biology **23**: 18.

Love, S. M. and Barsky, S. H. (1996). "Breast-duct endoscopy to study stages of cancerous breast disease." Lancet **348**: 3.

Medina, M. A. (2001). "Glutamine and cancer." Journal of Nutrition **131**: 4.

Mikeska, T., Bock, C., Do, H. and Dobrovic, A. (2012). "DNA methylation biomarkers in cancer: progress towards clinical implementation." Exper Reviews on Molecular Diagnosis **12** (5): 14.

Miller, D. M., Thomas, S. D., Islam, A., Muench, D. and Sedoris, K. (2012). "c-Myc and Cancer Metabolism." Clin Cancer Res. **18**: 7.

Moncada, S., Higgs, E. A. and Colombo, S. L. (2012). "Fulfilling the metabolic requirements for cell proliferation." Biochem J **446**: 7.

Mossman, D. and Scott, R. J. (2011). "Long Term Transcriptional Reactivation of Epigenetically Silenced Genes in Colorectal Cancer Cells Requires DNA Hypomethylation and Histone Acetylation." PlosONE **6** (8): 9.

Nakao, M. (2001). "Epigenetics: interaction of DNA methylation and chromatin." Gene **278**: 6.

Naus, C. C. and Laird, D. W. (2010). "Implications and challenges of connexin connections to cancer." Nature reviews, Cancer **10**: 7.

Nicholson, L. J., Smith, P. R., Hiller, L., Szlosarek, P. W., Kimberley, C., Seholi, J., Koensgen, D., Mustea, A., Schmid, P. and Crook, T. (2009). "Epigenetic silencing of argininosuccinate synthetase confers resistance to platinum-induced cell death but collateral sensitivity to arginine auxotrophy in ovarian cancer." Internal Journal of Cancer **125**: 10.

Nicklin, P., Bergman, P., Zhang, B., Triantafellow, E., Wang, H., Nyfeler, B., Yang, H., Hild, M., Kung, C., Wilson, C., Myer, V. E., MacKeigan, J. P., Porter, J. A., Wang, Y. K., Cantley, L. C., Finan, P. M. and Murphy, L. O. (2009). "Bidirectional transport of amino acids regulates mTOR and autophagy." Cell **136** (3): 13.

Nielsen, T. O., Hsu, F. D., Jensen, K., Cheang, M., Karaca, G., Hu, Z., Hernandez-Boussard, T., Livasy, C., Cowan, D., Dressler, L., Akslen, L. A., Ragaz, J., Gown, A. M., Gilks, C. B., van de Rijn, M. and Perou, C. M. (2004). "Immunohistochemical and clinical characterization of the basal-like subtype of invasive breast carcinoma." Clin Cancer Res. **10** (16): 7.

Nijman, S. M. B. (2011). "Synthetic lethality: General principles, utility and detection using genetic screens in human cells." FEBS Letters **585**: 6.

Oberstadt, M. C., Bien-Möller, S., Weitmann, K., Herzog, S., Hentschel, K., Rimmbach, C., Vogelgesang, S., Balz, E., Fink, M., Michael, H., Zeden, J. P., Bruckmüller, H., Werk, A. N., Cascorbi, I., Hoffmann, W., Roskopf, D., Schroeder, H. W. and Kroemer, H. K. (2013). "Epigenetic modulation of the drug resistance genes MGMT, ABCB1 and ABCG2 in glioblastoma multiforme." BMC cancer: 13.

Park, Y. J., Claus, R., Weichenhan, D. and Plass, C. (2011). "Genome-wide epigenetic modifications in cancer." Progress in Drug Research: 24.

Patel, R. R., Sharma, C. G. and Jordan, V. C. (2007). "Optimizing the antihormonal treatment and prevention of breast cancer." Breast Cancer **14** (2): 9.

Perou, C. M., Jeffrey, S. S., van de Rijn, M., Rees, C. A., Eisen, M. B., Ross, D. T., Pergamenschikov, A., Williams, C. F., Zhu, S. X., Lee, J. C., Lashkari, D., Shalon, D., Brown, P. O. and Botstein, D. (1999). "Distinctive gene expression patterns in human mammary epithelial cells and breast cancers." Proc Natl Acad Sci USA **96** (16): 5.

Perou, C. M., Sørli, T., Eisen, M. B., van de Rijn, M., Jeffrey, S. S., Rees, C. A., Pollack, J. R., Ross, D. T., Johnsen, H., Akslen, L. A., Fluge, O., Pergamenschikov, A., Williams, C., Zhu, S. X., Lønning, P. E., Børresen-Dale, A. L., Brown, P. O. and Botstein, D. (2000). "Molecular portraits of human breast tumours." Nature **406** (6797): 5.

Piazza, R., Magistroni, V., Mogavero, A., Andreoni, F., Ambrogio, C., Chiarle, R., Mologni, L., Bachmann, P. S., Lock, R. B., Collini, P., Pelosi, G. and Gambacorti-

Passerini, C. (2013). "Epigenetic Silencing of the Proapoptotic Gene BIM in Anaplastic Large Cell Lymphoma through an MeCP2/SIN3a Deacetylating Complex." Neoplasia **15** (5): 12.

Pietras, R. J. and Marquez-Garban, D. C. (2007). "Membrane-Associated Estrogen Receptor Signaling Pathways in Human Cancers." Clinical Cancer Research **13** (16): 6.

Portela, A., Liz, J., Nogales, V., Setie', F., Villanueva, A. and Esteller, M. (2013). "DNA methylation determines nucleosome occupancy in the 5'-CpG islands of tumor suppressor genes." Oncogene **32**: 8.

Qiu, J. (2006). "Unfinished symphony." Nature **44**: 3.

Quillien, V., Lavenu, A., Sanson, M., Legrain, M., Dubus, P., Karayan-Tapon, L., Mosser, J., Ichimura, K. and Figarella-Branger, D. (2014). "Outcome-based determination of optimal pyrosequencing assay for MGMT methylation detection in glioblastoma patients." Journal of Neuro-oncology **113** (3): 10.

Rathore, M. G., Saumet, A., Rossi, J.-F., de Bettignies, C., Tempe', D., Lecellier, C. H. and Villalba, M. (2012). "The NF-kB membre pf p65 controls glutamine metabolism via mir-23a." The International Journal of Biochemistry & Cell Biology **44**: 7.

Reinert, R. B., Oberle, L. M., Wek, S. A., Bunpo, P., Wang, X. P., Mileva, I., Goowin, L. O., Aldrich, C. J., Durden, D. L., McNurlan, M. A., Wek, R. C. and

Anthony, T. G. (2006). "Role of glutamine depletion in directing tissue-specific nutrient stress responses to L-Asparaginase." Journal of Biological Chemistry **281** (42): 10.

Ries, L. A. G., Melbert, D., Krapcho, M., Stinchcomb, D. G., Howlader, N. and Horner, M. J. (2009) "SEER cancer statistics review, 1975-2006, National Cancer Institute."

Rivera, R. M. and Bennett, L. B. (2010). "Epigenetics in humans: an overview." current Opinion in Endocrinology, Diabetes and Obesity **17**: 6.

Roessler, J., Ammerpohl, O., Gutwein, J., Hasemeier, B., Anwar, S. L., Kreipe, H. and Lehmann, U. (2012). "Quantitative cross-validation and content analysis of the 450k DNA methylation array from Illumina, Inc." BMC Research Notes **5**: 7.

Sabri, M., Ai, J., Marsden, P. A. and Macdonald, R. L. (2011). "Simvastatin Re-Couples Dysfunctional Endothelial Nitric Oxide Synthase in Experimental Subarachnoid Hemorrhage." PlosONE **6** (2): 13.

Sambrook, J., Russel, D.W., Ed. (2001). Molecular cloning; a laboratory manual. New York, Cold Spring Harbor Laboratory Press.

Sandoval, J. and Esteller, M. (2012). "Cancer epigenomics: beyond genomics." Genetics and Development **22**: 5.

Savaraj, N., You, M., Wu, C., Wangpaichitr, M., Kuo, M. T. and Feun, L. G. (2010). "Arginine deprivation, autophagy, apoptosis (AAA) for the treatment of melanoma." Current Molecular Medicine **10** (4): 8.

Schulze, A. and Harris, A. L. (2012). "How cancer metabolism is tuned for proliferation and vulnerable to disruption." Nature **491**: 10.

Scott, L., Lamb, J., Smith, S. and Wheatley, D. N. (2000). "Single amino acid (arginine) deprivation: rapid and selective death of cultured transformed and malignant cells." British Journal of Cancer **83** (6): 11.

Shanware, N. P., and Bray, K. (2013). "The PI3K, metabolic, and autophagy network: interactive partners in cellular health and disease." Annual Review of Pharmacology and Toxyxology **53**: 17.

Sharma, D., Blum, J., Yang, X., Beaulieu, N., Nacleod, A. R. and Davidson, N. E. (2005). "Release of methyl CpG binding proteins and histone deacetylase 1 from the estrogen receptor a (ER) promoter upon reactivation in ER-negative human breast cancer cells." Molecular endocrinology **19** (7): 11.

Shen, J., Wang, S., Zhang, Y.J., Kappil, M., Wu, H.C., Kibriya, M. G., Wang, Q., Jasmine, F., Ahsan, H., Lee, P.-H., Yu, M.-W., Chen, C.J. and Santella, R. M. (2012). "Genome-wide DNA Methylation Profiles in Hepatocellular Carcinoma." Hepatology **55** (6): 19.

Shen, L., Kantarjian, H., Guo, Y., Lin, E., Shan, J., Huang, X., Berry, D., Ahmed, S., Zhu, W., Pierce, S., Kondo, Y., Oki, Y., Jelinek, J., Saba, H., Estey, E. and Issa, J. P. (2010). "DNA methylation predicts survival and response to therapy in patients with myelodysplastic syndromes." Journal of Clinical Oncology **28** (4): 9.

Shoemaker, R., Wang, W. and Zhang, K. (2011). "Mediators and dynamics of DNA methylation." WIREs System Biology and Medicine **3**: 17.

Sorlie, T., Tibshirani, R., Parker, J., Hastie, T., Marron, J. S., Nobel, A., Deng, S., Johnsen, H., Pesich, R., Geisler, S., Demeter, J., Perou, C. M., Lønning, P. E., Brown, P. O., Børresen-Dale, A. L. and Botstein, D. (2003). "Repeated observation of breast tumor subtypes in independent gene expression data sets." Proc Natl Acad Sci USA **100** (14): 5.

Sproul, D., Nestor, C., Culley, J., Dickson, J. H., Dixon, J. M., Harrison, D. J., Meehan, R. R., Sims, A. H. and Ramsahoye, B. H. (2011). "Transcriptionally repressed genes become aberrantly methylated and distinguish tumours of different lineages in breast cancer." PNAS **108** (11): 5.

Suijkerbuijk, K. P. M., van Diest, P. J. and van der Wall, E. (2010). "Improving early breast cancer detection: focus on methylation." Annals of Oncology **22**: 5.

Suzuki, M., Shiraishi, K., Eguchi, A., Ikeda, K., Mori, T., Yoshimoto, K., Ohba, Y., Yamada, T., Ito, T., Baba, Y. and Baba, H. (2013). "Aberrant methylation of LINE-1, SLIT2, MAL and IGFBP7 in non-small cell lung cancer." Oncology reports **29** (4): 7.

Syed, N., Langer, L., Janczar, K., Singh, P., Lo Nigro, C., Lattanzio, L., Coley, H.M., Hatzimichael, E., Bomalaski, J., Szlosarek, P., Awad, M., O'Neil, K., Roncaroli, F., Crook, T. (2013). "Epigenetic status of argininosuccinate synthetase and arginosuccinate lyase modulates autophagy and cell death in glioblastoma." Cell Death and Disease **4** (4): 11.

Szlosarek, P. W., Klabatsa, A., Pallaska, A., Sheaff, M., Smith, P., Crook, T., Grimshaw, M. J., Steele, J. P., Rudd, R. M., Balkwill, F. R. and Fennell, D. A. (2006). "In vivo loss of expression of argininosuccinate synthetase in malignant pleural mesothelioma is a biomarker for susceptibility to arginine depletion." Clinical Cancer Research **12** (23): 6.

Tavassoli, F. A. and Devilee, P. (2003). Pathology and Genetics of Tumours of the Breast and Female Genital Organs. Lyon, IARC Press.

Terasaka, N., Yu, S., Yvan-Charvet, L., Wang, N., Mzhavia, N., Langlois, R., Pagler, T., Li, R., Welch, R. L., Goldberg, R. J. and Tall, A. L. (2008). "ABCG1 and HDL protect against endothelial dysfunction in mice fed a high-cholesterol diet." The Journal of Clinical Investigation **118** (11): 13.

Teschendorff, A. E., Menon, U., Gentry-Maharaj, A., Ramus, S. J., Gayther, S. A., Apostolidou, S., Jones, A., Lechner, M., Beck, S., Jacobs, I. J. and Widschwendter, M. (2009). "An epigenetic signature in peripheral blood predicts active ovarian cancer." PlosOne **4** (12): 12.

Thompson, G. B. (2009). "Metabolic enzymes as oncogenes or tumour suppressor." The New England Journal of Medicine **360** (8): 3.

Tournier, B., Chapusot, C., Courcet, E., Martin, L., Lepage, C., Faivre, J. and Piard, F. (2012). "Why do results conflict regarding the prognostic value of the methylation status in colon cancers? The role of the preservation method." BMC cancer **12** (12): 12.

Vallot, C., Hérault, A., Boyle, S., Bickmore, W. A. and Radvanyi, F. (2014). "PRC2-independent chromatin compaction and transcriptional repression in cancer." Oncogene.

Van der Auwera, I., Yu, W., Suo, L., Van Neste, L., van Dam, P., Van Marck, E. A., Pauwels, P., Vermeulen, P. B., Dirix, L. Y. and Van Laere, S. J. (2010). "Array-Based DNA Methylation Profiling for Breast Cancer Subtype Discrimination." PlosONE **5** (9): 10.

van der Vos, K. E., Eliasson, P., Proikas-Cezanne, T., Vervoort, S. J., van Boxtel, R., Putker, M., van Zutphen, I. J., Mauthe, M., Zellmer, S., Pals, C., Verhagen, L. P., Groot Koerkamp, M. J. A., Braat, A. C., Dansen, T. B., Holstege, F. C., Gebhardt, R., Burgering, B. M. and Coffey, P. J. (2012). "Modulation of glutamine metabolism by the PI(3)K-PKB-FOXO network regulates autophagy." Nature Cell Biology **14** (8): 8.

Vander Heiden, M. G., Cantley, L. C. and Thompson, C. B. (2009). "Understanding the Warburg Effect: The Metabolic Requirements of Cell Proliferation." Science **324** (5930): 4.

Vargo-Gongola, T. and Rosen, J. M. (2007). "Modelling breast cancer: one size does not fit all." Nature reviews, Cancer **7**: 14.

Walker, B. A., Wardell, C. P., Chiecchio, L., Smith, E. M., Boyd, K. D., Neri, A., Davies, F. E., Ross, F. M. and Morgan, G. J. (2012). "Aberrant global methylation patterns affect the molecular pathogenesis and prognosis of multiple myeloma." Blood **117**: 9.

Wang, Y. and Watford, M. (2007). "Glutamine, insulin and glucocorticoids regulate glutamine synthetase expression in C2C12 myotubes, Hep G2 hepatoma cells and 3T3 L1 adipocytes." Biochim Biophys Acta **1770** (4): 7.

Warburg, O. (1956). "On the origin of cancer cells." Science **123**: 5.

Warburg, O., Wind, F. and Negelein, E. (1927). "The metabolism of tumour in the body." The journal of general physiology **7** (8): 11.

Wellings, S. R. and Jensen, H. M. (1976). "On the origin and progression of ductal carcinoma in the human breast." J Natl Cancer Inst. **50**(5): 7.

White, E. (2012). "Deconvoluting the context-dependent role for autophagy in cancer." Nature reviews, Cancer **12**: 10.

Willems, L., Jacque, N., Jacquet, A., Neveux, N., Maciel, T. T., Lambert, M., Schmitt, A., Poulain, L., Green, A. S., Uzunov, M., Kosmider, O., Radford-Weiss, I., Moura, I. C., Auberger, P., Ifrah, N., Bardet, V., Chapuis, N., Lacombe, C., Mayeux, P., Tamburini, J. and Bouscary, D. (2013). "Inhibiting glutamine uptake represents an attractive new strategy for treating acute myeloid leukemia." Blood **122** (20): 12.

Wong, C. and Chen, S. (2012). "The development, application and limitations of breast cancer cell lines to study tamoxifen and aromatase inhibitor resistance." Journal of Steroid Biochemistry and Molecular Biology **131** (9): 83.

Wu, G. and Morris, S. M. (1998). "Arginine metabolism: nitric oxide and beyond." Biochemistry Journal **336** (1): 18.

Xu, X., Jin, H., Liu, Y., Liu, L., Wu, Q., Guo, Y., Yu, L., Liu, Z., Zhang, T., Zhang, X., Dong, X. and Quan, C. (2012). "The expression patterns and correlations of claudin-6, methy-CpG binding protein 2, DNA methyltransferase 1, histone deacetylase 1, acetyl-histone H3 and acetyl-histone H4 and their clinicopathological significance in breast invasive ductal carcinomas." Daign Pathol **29** (7).

Yabu, T., Imamura, S., Mizusawa, N., Touhata, K. and Yamashita, M. (2012). "Induction of autophagy by amino acid starvation in fish cells." Marine Biotechnology **14**: 10.

Yan, P. S., Venkataramu, C., Ibrahim, A., Liu, J. C., Shen, R. Z., Diaz, N. M., Centeno, B., Weber, F., Leu, Y. W., Shapiro, C. L., Eng, C., Yeatman, T. J. and

Huang, T. H. M. (2006). "Applying geographic zones of cancer risk with epigenetic biomarkers in normal breast tissue." Human Cancer Biology **12** (22): 10.

Yang, W. T. and Zheng, P. S. (2014). "Promoter Hypermethylation of KLF4 Inactivates Its Tumor Suppressor Function in Cervical Carcinogenesis." PlosONE **9**(2): 10.

You, M., Savaraj, N., Kuo, M. T., Wangpaichitr, M., Varona-Santos, J., Wu, C., Nguyen, D. M. and Feun, L. (2013). "TRAIL induces autophagic protein cleavage through caspase activation in melanoma cell lines under arginine deprivation." Molecular and cellular biochemistry **374**(1-2): 10.

Youliden, D. R., Cramb, S. M., Dunn, N. A. M., Muller, J. M., Pyke, C. M. and Baade, P. D. (2012). "The descriptive epidemiology of female breast cancer: An international comparison of screening, incidence, survival and mortality." Cancer Epidemiology **37**: 12.

Young, B. and Heath, J. W. (2005). Histology and microscopical anatomy. Milan, Casa editrice Ambrosiana.

Yuneva, M. (2008). "Finding an "Achilles' heel" of cancer." Cell Cycle **7**(14): 6.

Yuneva, M., Zamboni, N., Oefner, P., Sachidanandam, R. and Lazebnik, Y. (2007). "Deficiency in glutamine but not glucose induces MYC-dependent apoptosis in human cells." The Journal of Cell Biology **178** (1): 12.

Zhang, Y., Yang, R., Burwinkel, B., Breitling, L. P., Holleczech, B., Schöttker, B. and Brenner, H. (2014). "F2RL3 methylation in blood DNA is a strong predictor of mortality." International Journal of Epidemiology.

7 Supplementary tables and figures

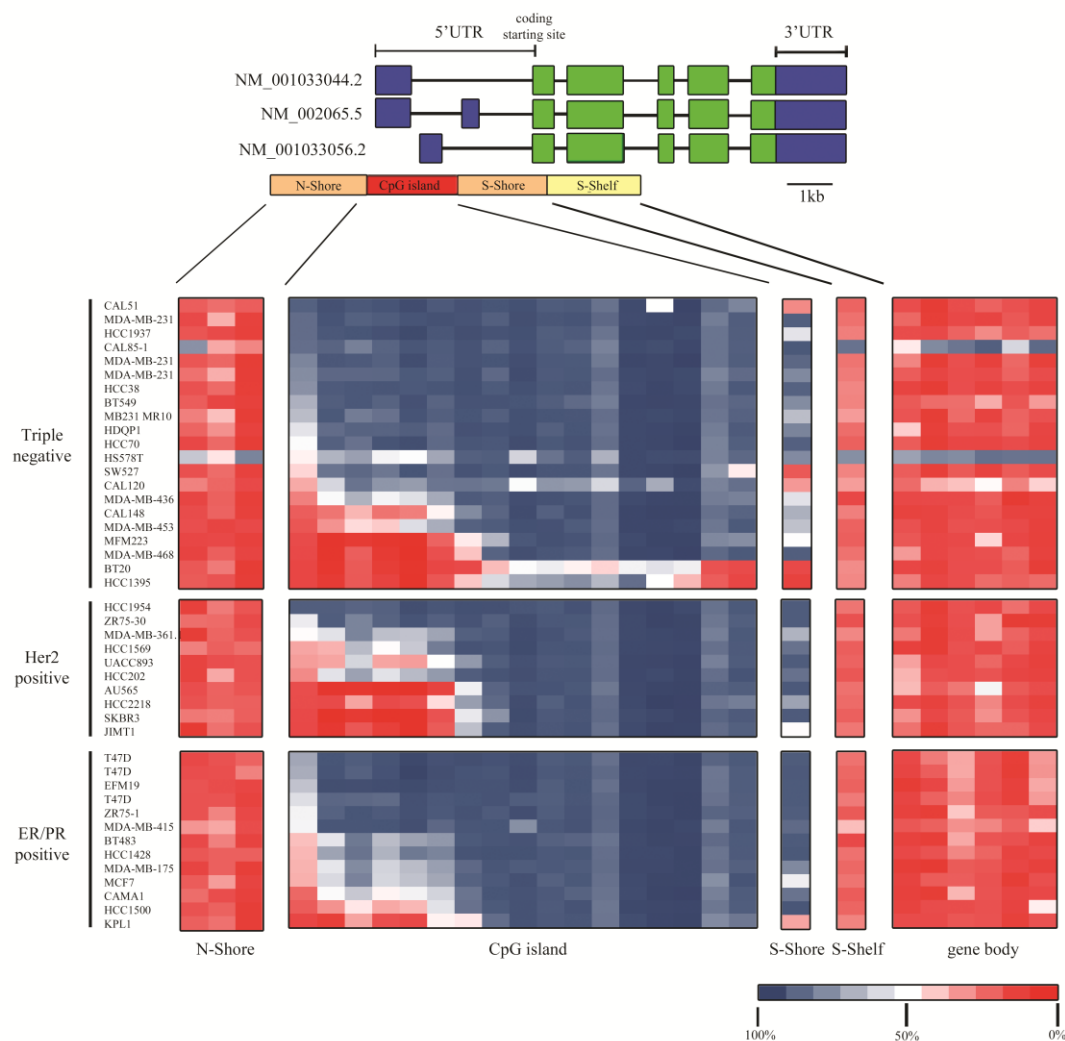
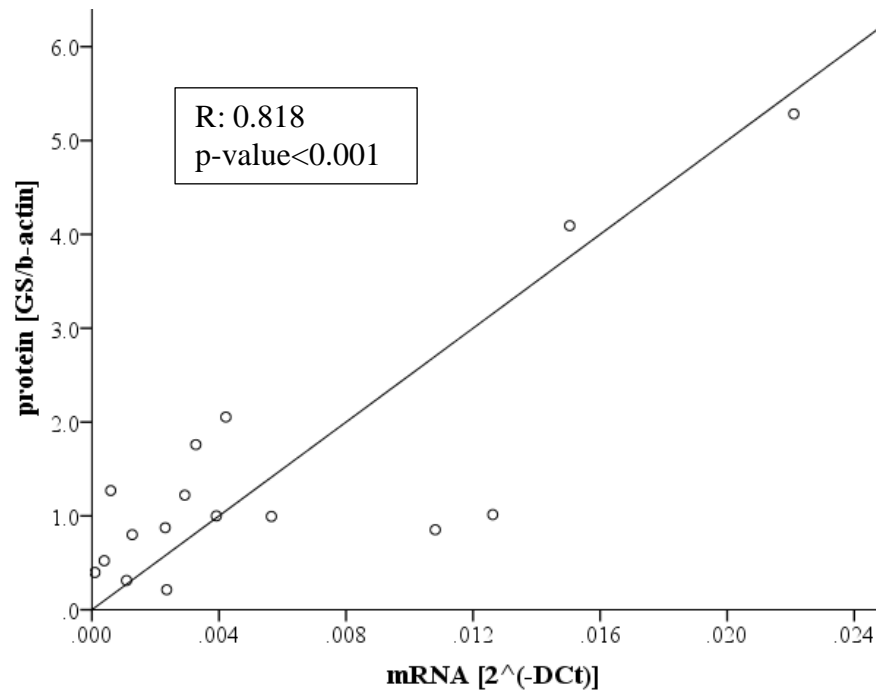


Figure 7-1. *GLUL* methylation array in a bigger breast cancer cell line panel.

GLUL was located on chromosome1q23 and included three different transcripts (NM_001033044.2, NM_002065.5, NM_001033056.2) encoding the same protein. Exons are in green, 3'UTR and 5'UTR in blue, CpG island in red, N-Shore and S-Shore in orange, S-Shelf in yellow in the figure.

The cell lines panel was divided into subtypes: 18 triple negative, 10 Her2-positive, 11 Her2-negative ER/PR-positive. The results were colour-coded based on the β -value; red when totally methylated (100%) and blue completely unmethylated (0%).

A)



B)

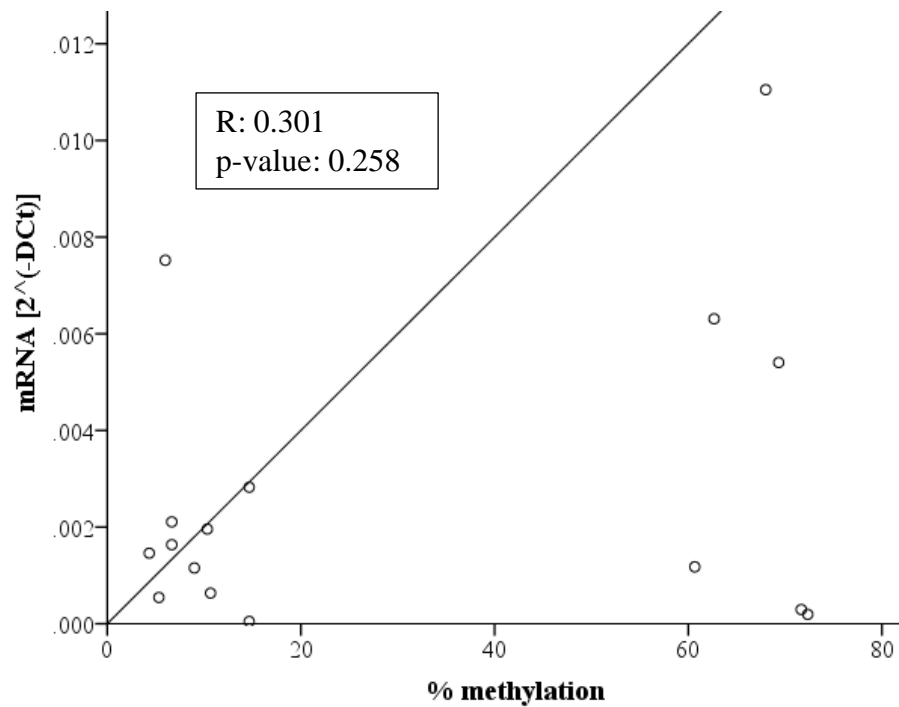
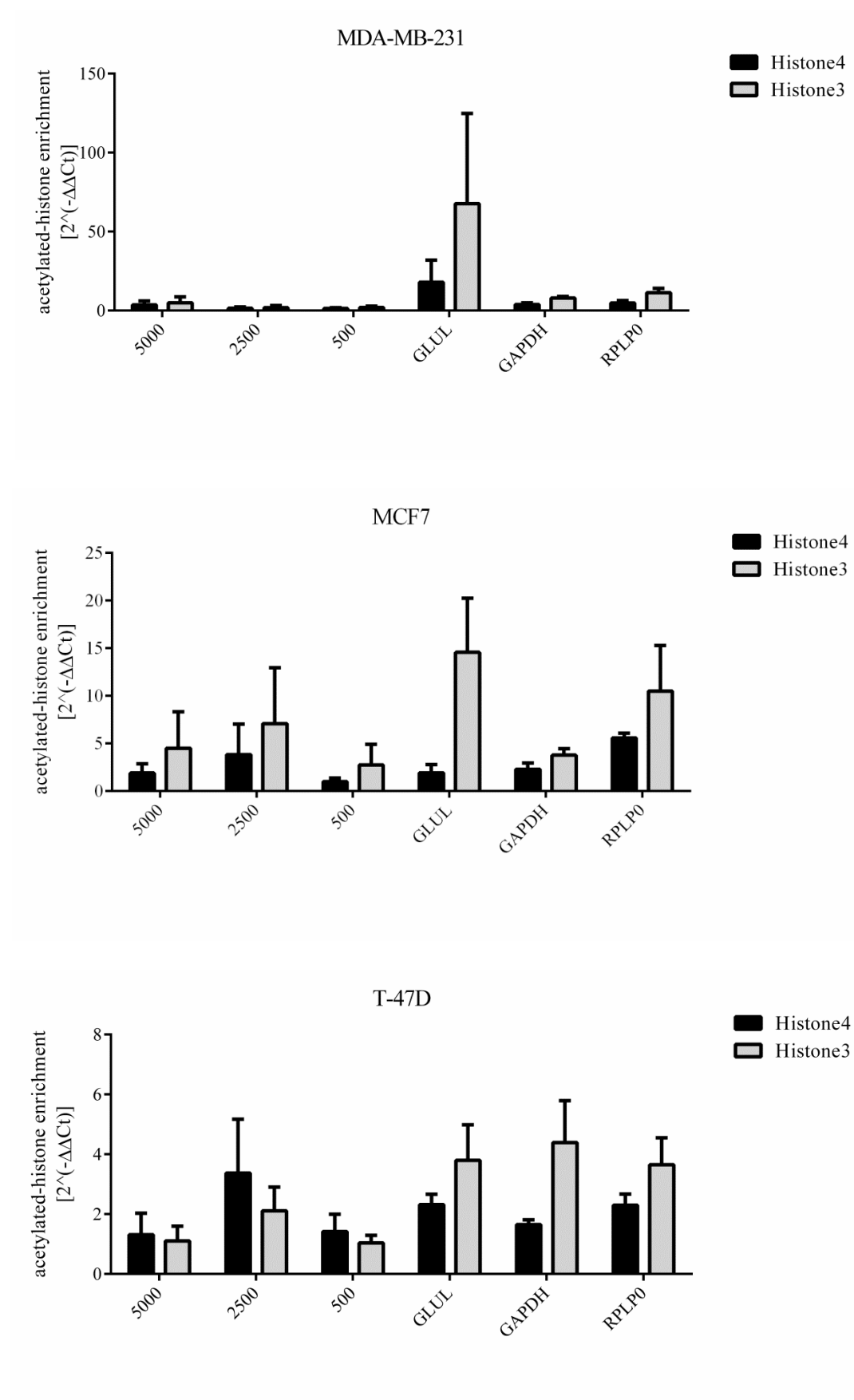


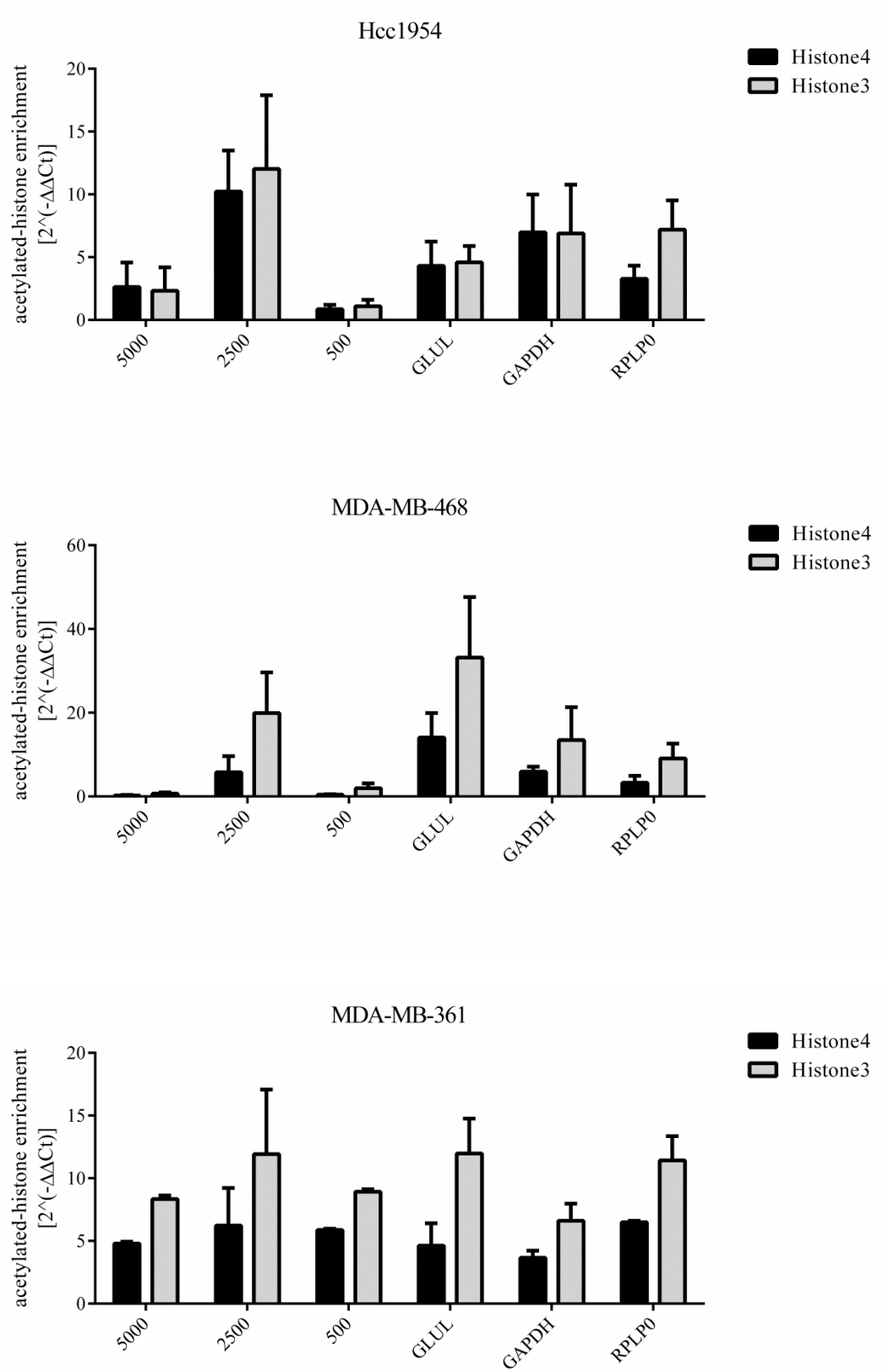
Figure 7-2. Correlation of mRNA, protein and methylation level for Glutamine synthetase.

Glutamine synthetase mRNA, protein level and methylation status were correlated by linear regression analysis using SPSS (IBM Software). R value represents how good the correlation is: the nearer to 1 the better the correlation.

A)



B)



C)

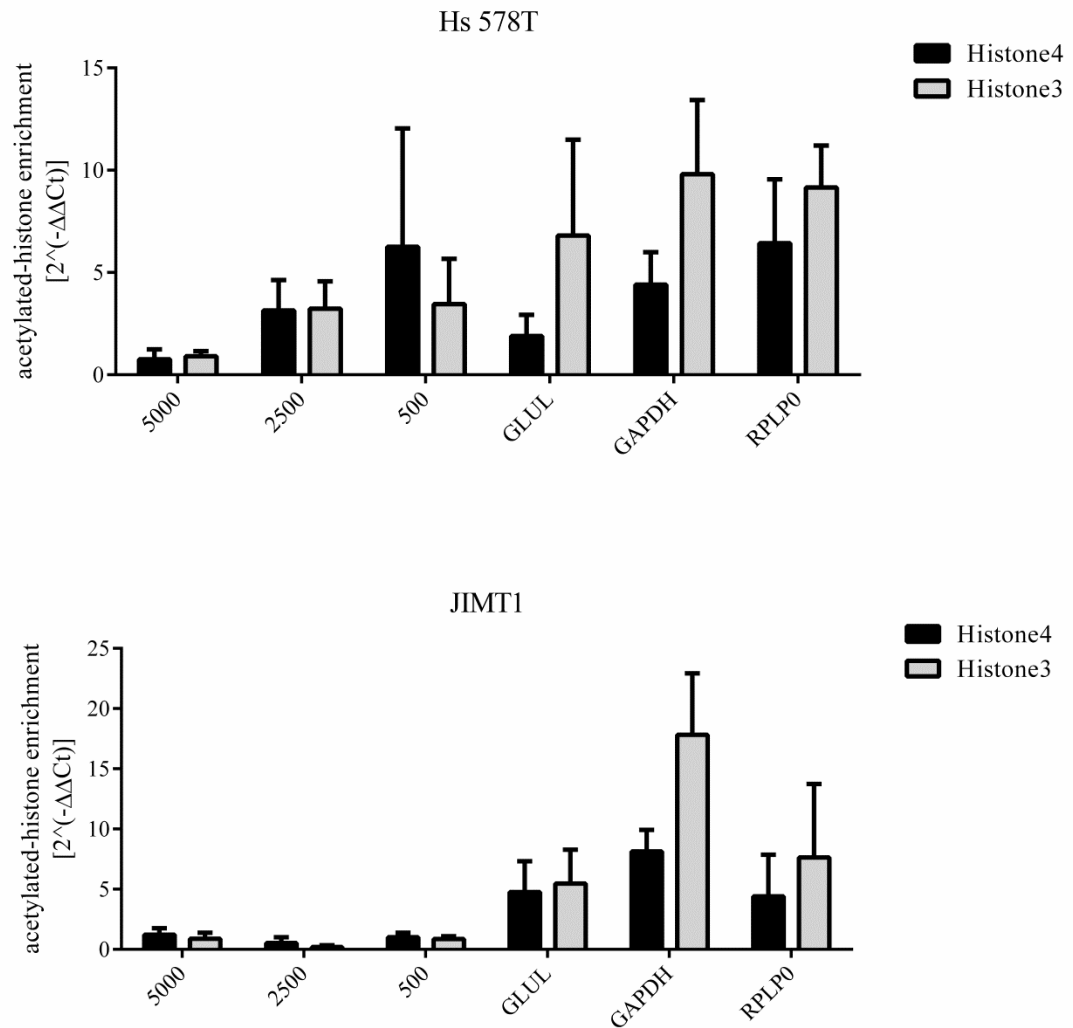


Figure 7-3. Enrichment of acetylated Histone3 and Histone4 across each tested gene promoter region in various cell lines.

Enrichment of acetylated Histone3 and Histone4 on *GLUL* promoter regions was analysed in the three groups of breast cancer cell lines: A) unmethylated, MDA-MB-231 MCF7 and T-47D, B) methylated *GLUL* expressing, Hcc1954 MDA-MB-468 and MDA-MB-361, and C) methylated *GLUL*-silenced, Hs 578T and JIMT1. The DNA pulled down was investigated by real-time PCR for different positions on *GLUL* promoter region, 5000 bp (5000) 2500 bp (2500) 500 bp (500) 250 bp (GLUL) upstream the TSS, and positive controls, GAPDH and RPLP0, as expressed genes. ΔCt was determined as the difference between the DNA amplified after each immuno-precipitation, with the two histone-specific antibodies, and the input. The enrichment was calculated as $\Delta\Delta Ct$ of the region of interest versus a not-expressed gene, Haemoglobin 2 α (H2A).

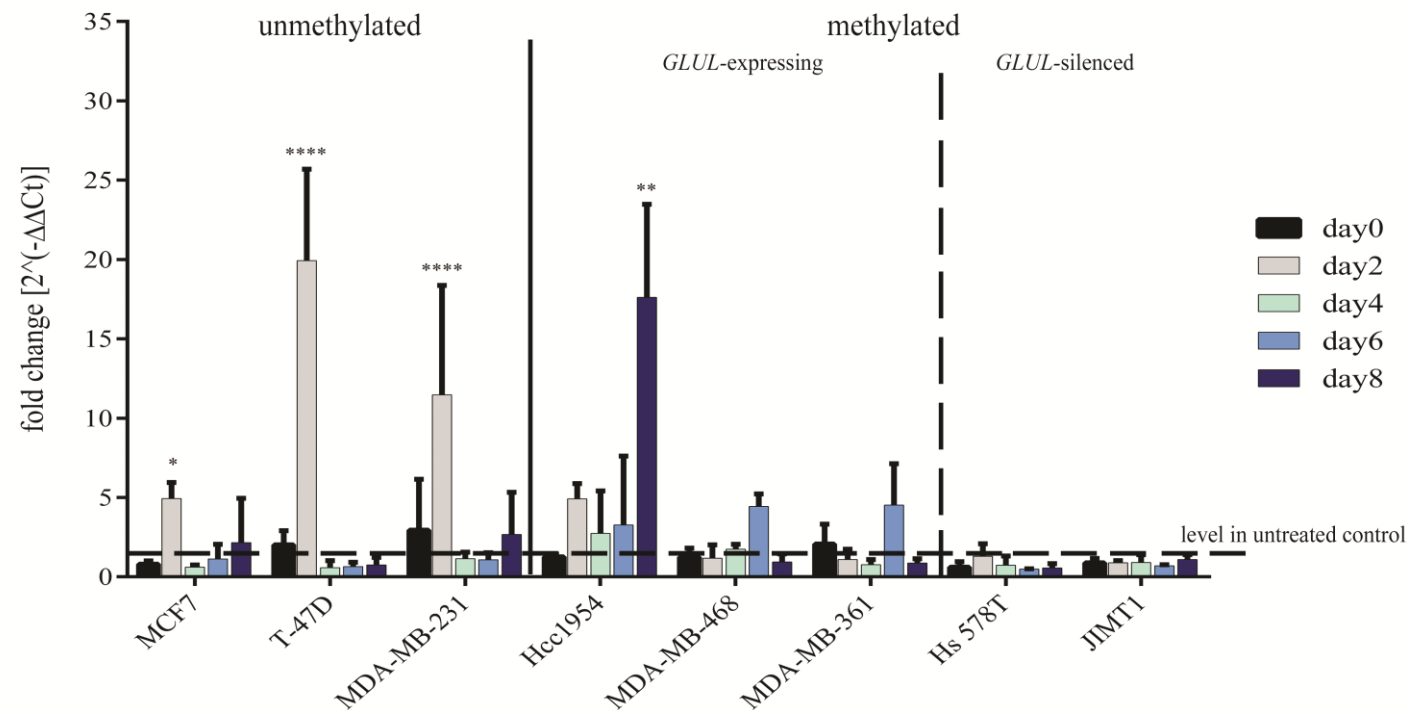
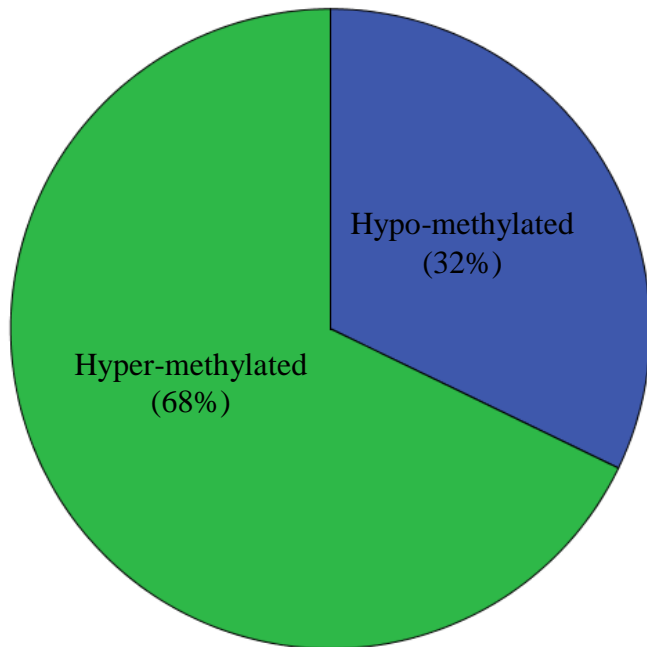


Figure 7-4. Modulation of *GLUL* during glutamine deprivation treatment.

Unmethylated cell lines MDA-MB-231 MCF7 and T-47D, methylated *GLUL* expressing, Hcc1954 MDA-MB-468 and MDA-MB-361, and methylated *GLUL*-silenced JIMT1 and Hs 578T, were analysed for gene expression by qPCR during gln deprivation. *GLUL* regulation was expressed as fold change, generated as second power of minus $\Delta\Delta Ct$. One-way ANOVA on Prism 6.0 (Graph Pad) was used to analyse the statistical significance of each day versus day0. Statistical significance is shown as stars (*: p-value 0.05, **: p-value 0.01, ***: p-value 0.001, ****: p-value <0.001) above the standard deviation bar.

A)



B)

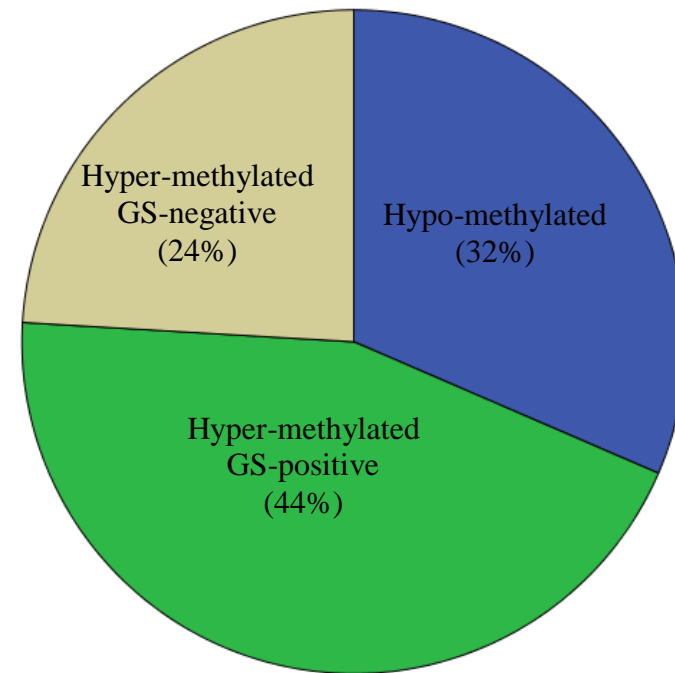


Figure 7-5. Percentage of samples in each subset of primary breast cancer tissues.

The frequencies of samples in subset based on methylation (A) or methylation and GS level (B) was analysed using SPSS (IBM Software).

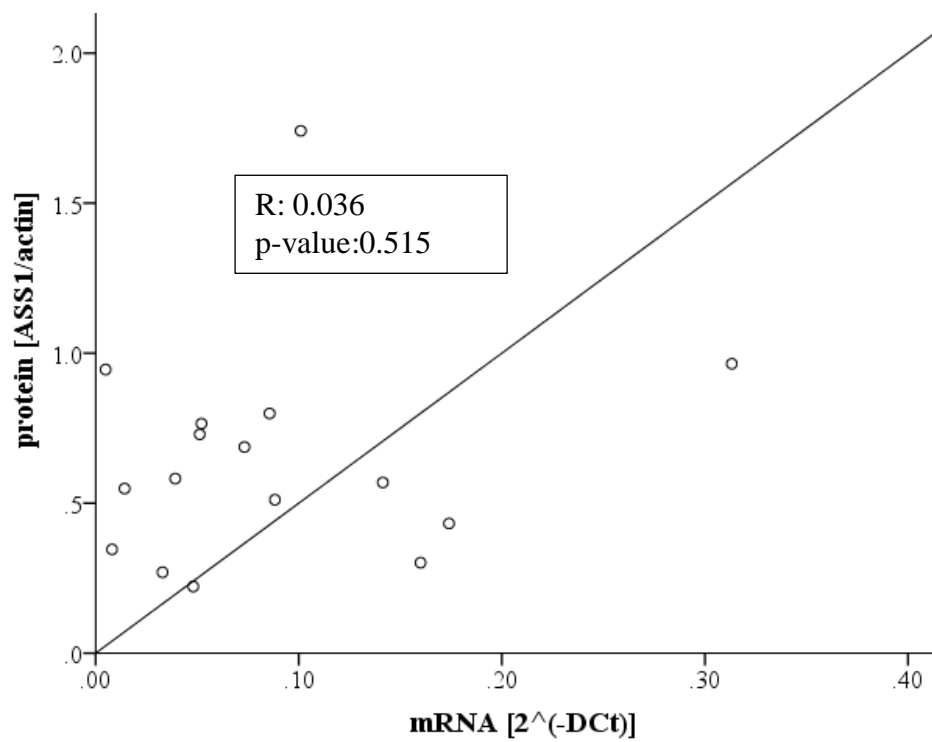
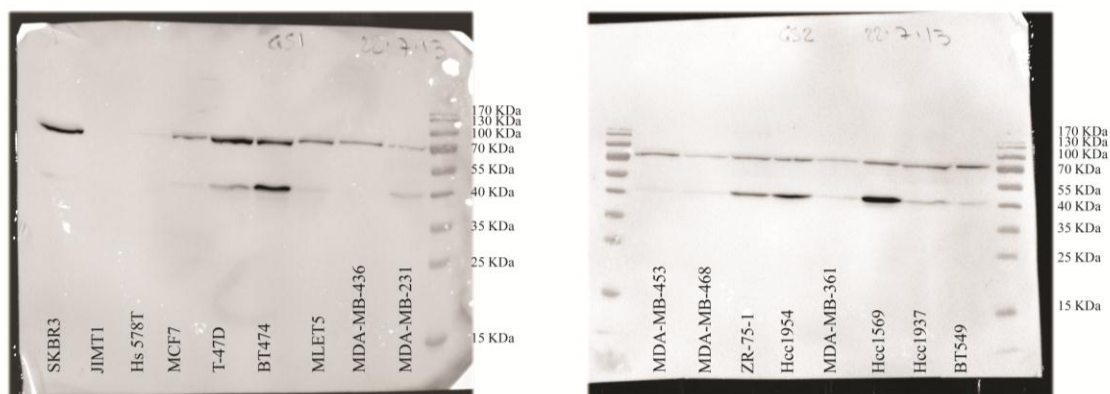


Figure 7-6. Liner regression between Arginino-succinate mRNA and protein level.

Arginino-succinate mRNA and protein level were correlated by linear regression analysis using SPSS (IBM Software). R value represents how good the correlation is: the near it is to 1 the better the correlation.

Glutamine synthetase:



β -actin:

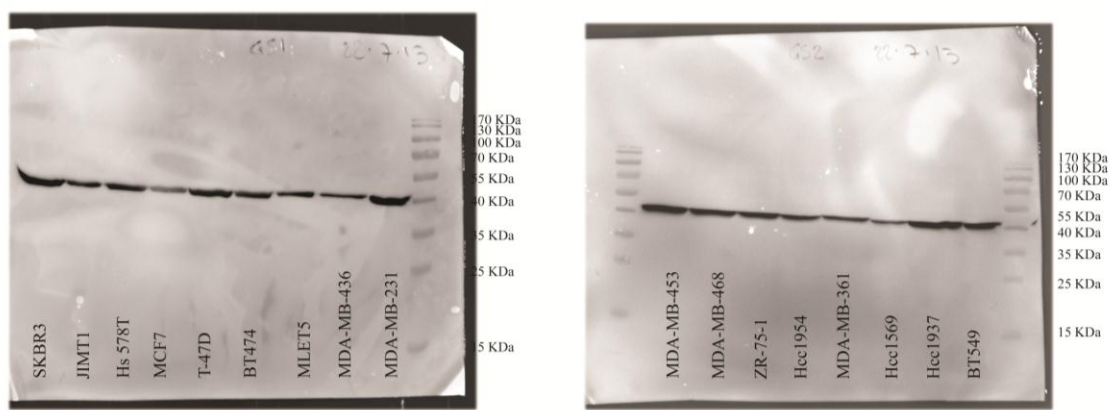
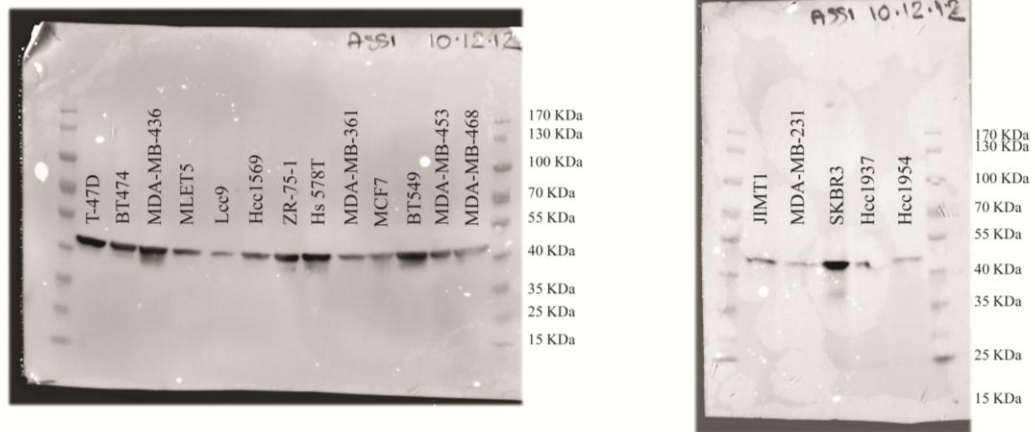


Figure 7-7. Example images of SDS-PAGE electro-blotting analysis of Glutamine synthetase.

The breast cancer cell lines panel was screened by SDS-PAGE electro-blotting to analyse the translational profile of the Glutamine synthetase as described in Materials and Methods.

Arginino-succinate synthetase:



β -actin:

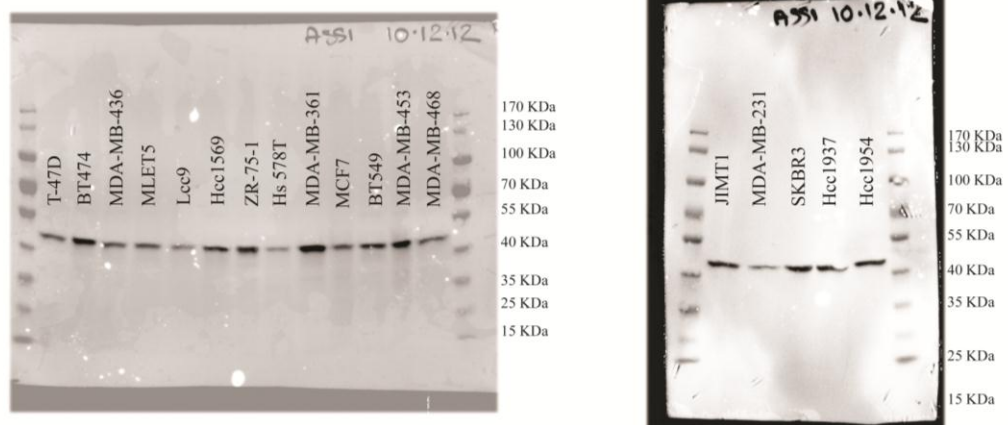


Figure 7-8. Example images of SDS-PAGE analysis of Arginino-succinate synthetase.

The breast cancer cell lines panel was screened by SDS-PAGE electro-blotting to analyse the translational profile of the Arginino-succinate synthetase as described in Materials and Methods.